

# **Controls on Thaumasite in Buried Concrete: Effect of Clay Composition and Cement Type**



A thesis submitted for the degree of Doctor of Philosophy in  
The Faculty of Engineering of the University of Sheffield

By

**Farhat Abubaker**  
**(BSc Structural Eng., MSc Concrete Eng.)**

Department of Civil and Structural Engineering  
The University of Sheffield

June 2014

## **ACKNOWLEDGEMENTS**

First, I would like to express my gratitude to Dr John Cripps and Dr Cyril Lynsdale for supervising this work. My main acknowledgement is for their constant encouragement, valuable and accurate scientific advice, discussions and rising of important questions. Their enthusiasm, commitment and patience provided a good basis for presenting this thesis. Without their support this work would not have started and certainly would not have finished. This thesis surely became reality only through their support.

I would like to acknowledge with gratitude the support of the Ministry of Higher Education, Libya, for funding this project.

I would like to thank the technicians of the Structures Laboratory, Geotechnical Laboratory and Groundwater Protection Laboratory for their continuous and excellent help during the experimental work. Especially, I would like to thank Kieran Nash, Paul Blackburn, Andy Fairburn, Paul Osborne and Mark Foster.

I am grateful to the University of Sheffield for the opportunity to be a student of one of best UK universities and one which is highly ranked and recognised throughout the world.

Finally, special thanks are due to my brothers and sisters and my wife. I would like to thank them for their valuable support and encouragement during my study and hard moments; without their support it would have been impossible to finish this work. I would like to express my deep and sincere gratitude to them.

## ABSTRACT

Problems due to the thaumasite form of sulfate attack (TSA), which has a significant influence on the strength and durability of buried concrete, have been extensively reported in the UK and worldwide. Thaumasite forms as a result of the presence of high levels of sulfate in pore waters in the ground surrounding concrete, particularly where sulfate is formed by the oxidation of pyrite and the ground temperature is less than about 12°C. In spite of this association with pyrite-bearing ground, an extensive literature search revealed that most previous research, including studies on which current concrete design recommendations are based, was carried out by exposing test specimens to sulfate-rich solutions rather than to natural ground materials. In fact, the present study appears to be the first extensive investigation of TSA in which various concretes have been tested in simulated field conditions. The changes in chemistry of different clays and clay pore solutions were also investigated.

The work includes the long-term exposure (nine years) of Portland cement (PC), Portland limestone cement (PLC), sulfate-resisting Portland cement (SRPC) and Portland cement blended with 25% pulverized - fuel ash to slightly weathered Lower Lias Clay of sulfate design class DS-2 at 5°C. Parts of the exposed concrete were coated with bitumen to test the performance of this method of protection. The study also includes an investigation into the influence of clay composition (weathered and slightly weathered Lower Lias Clay and Coal Measures mudstone) on the severity of TSA in various concretes made with CEM I, CEM I blended with 10% limestone filler (LF), CEMI - 50% PFA and CEMI - 70% GGBS; this was complemented by parallel studies which assessed the performance of specimens of the same concretes, placed in sulfate solutions equivalent to DS-2 and DS-4 and simulated pore waters at the same temperatures.

The performance of the different concretes in these tests was assessed by means of visual observation, supported by X-ray diffraction (XRD), infra-red scanning (IR) and scanning electron microscopy with energy dispersive X-ray analysis (SEM-EDX) to identify the deterioration products. The change in the chemistry of clay was assessed by the determination of water- and acid-soluble sulfate, total sulfur, rate of pyrite oxidation and change in carbonate content. Where applicable, the compositions of the different clays and clay pore solutions were also investigated.

It was found that deterioration due to the thaumasite form of sulfate attack occurred in all four concretes exposed for nine years to slightly weathered Lower Lias Clay. PLC concrete was the worst affected, with complete loss of binding of up to 47 mm thickness of concrete, but PC-25% PFA replacement and SRPC concretes were also badly deteriorated. The degree of attack decreased with increasing burial depth, probably as a result of reduced access to air. The bitumen coating proved to be effective at preventing deterioration in all concretes. Exposure to clay of design sulfate class DS-2 was found to cause similar or greater deterioration than that in case of exposure to DS-4 sulfate solution, so the aggressivity of clay may be under-estimated if only the total potential sulfate (TPS) value currently used for aggressivity classification is considered. X-ray diffraction analysis revealed that gypsum and thaumasite were the main products in the concrete exposed to solutions, whilst thaumasite and carbonate were formed in the samples exposed to clay, suggesting that the more complex chemistry of clay results in a different chemical interaction. Replacement of CEM I with 50% PFA and 70 % GGBS revealed a very good performance, as no deterioration was observed after two years in any of the exposure conditions, including DS-4 solution and pyritic clays. However, thaumasite solid solution was detected in both concretes exposed to pyritic clay at 5°C, which suggests that even these binders may be susceptible to thaumasite formation and TSA with time.

Changes to the clays confirmed that pyrite oxidation resulted in elevated sulfate levels, and the generation of sulfuric acid, which reacted with calcite and clay minerals in the clays. It is concluded from this that the carbonate content of the clay affects its aggressivity, although current standards do not take this into account.

# TABLE OF CONTENTS

## List of Figures

## List of Table

## List of Symbols and Abbreviations

<b>1. Introduction</b> .....	1
1.1 Background.....	1
1.2 Aims and objectives.....	4
1.3 Structure of the thesis .....	5
<b>2. Literature Review</b> .....	7
2.1 Introduction.....	7
2.2 Conventional form of sulfate attack.....	8
2.3 Thaumasite form of sulfate attack.....	9
2.3.1 Formation of Thaumasite.....	11
2.4 Thaumasite in buried concrete exposed to pyritic ground.....	14
2.4.1 Sulfate and sulfide in aggressive ground.....	15
2.4.2.1 Weathering of pyrite.....	16
2.4.2 The role of sulfuric acid produced as a result of pyrite oxidation in TSA.....	17
2.4.3 The presence of Mobile ground water.....	20
2.5 Factors controlling thaumasite formation and TSA.....	21
2.5.1 The role of pH on formation and stability of thaumasite.....	21
2.5.2 The role of magnesium.....	22
2.5.3 The effect of sulfate solution concentration.....	22
2.5.4 The effect of temperature.....	23
2.5.5 The role of chloride in thaumasite form of sulfate attack.....	24
2.5.6 Relative resistance of cement and cement binder.....	26
I. Limestone filler .....	26
II. Pulverised fuel ash (PFA).....	27
III. Ground Granulated Blastfurance Slag (GGBS). .....	28
VI. Sulfate Resistant Portland cement (SRPC)	29
2.5.7 Surface Coating.....	30
2.6 UK guidance of the assessment of aggressive ground condition.....	32



<b>3. Methodology .....</b>	<b>34</b>
3.1 Introduction.....	34
3.2 Experimental Design and Programme.....	34
3.2.1 Long-term study (9 years) of concrete- Lower Lias Clay interaction.....	35
3.2.2 The influence of clay compositions on severity of TSA.....	35
3.3 Experimental Details.....	37
3.3.1 Long-term study (9 years) of concrete- Lower Lias Clay interaction.....	37
3.3.1.1 Cementitious binders and concrete mixes.....	37
3.3.1.2 Lower Lias Clay.....	38
3.3.1.3 Specimen preparation and exposure.....	38
3.3.2 The influence of clay compositions on severity of TSA (series II).....	40
3.3.2.1 Materials.....	40
I.Cementitious binders.....	40
II.Aggregate.....	41
III.Clay.....	41
3.3.2.2 Water and Solutions.....	44
3.3.2.3 Concrete Mixes and Casting.....	45
3.3.2.4Curing.....	46
I.Initial curing.....	46
II.Long- term exposures to solutions and pyritic clay.....	46
3.4 Test Methods.....	48
3.4.1 Sampling.....	48
3.4.2 Concrete Cores.....	49
3.4.3 Concrete Testing.....	49
3.4.3.1 Visual observation.....	49
3.4.3.2 Deterioration thickness .....	49
3.4.3.2 Chemical Analysis.....	50
I.Determination of sulfate content .....	50
II. Determination of pH.....	50
III.Carbonate content profile.....	51
3.4.3.4 Mineralogical and microstructure of concrete.....	51
I.X-Ray Diffraction (XRD).....	51
II.Fourier Transform Infrared Spectrometry (FTIR).....	51
III.Scanning Electron Microscopy (SEM).....	52
3.4.4 pH changes of exposure solutions .....	52
3.4.5 Clay Samples.....	53
3.4.5.1 Sample preparation.....	53
3.4.5.2 Chemical analysis of clay.....	53
3.4.5.3 Clay mineralogical.....	54
3.4.6 Clay pore solutions analysis.....	54
<b>4- The Influence of Long Term Interaction of Concrete - Lower Lias Clay</b>	<b>55</b>
4-1 Long-Term Durability of Buried Concrete Exposed to Lower Lias Clay.....	55

4-1-1 Visual observation.....	55
I.Portland cement concrete column.....	56
II.Portland limestone concrete column.....	56
III.SRPC concrete column.....	58
IV.PC-PFA concrete column.....	58
V.Overall comparison.....	60
4.1.2 Deterioration thickness and rating of attack.....	60
4.1.3 Mineralogy of deteriorated products: X-Ray Diffraction (XRD).....	63
4.1.4 FTIR results.....	67
4.1.5 Microstructural analysis of concrete: SEM observations.....	69
I. Portland cement concrete.....	69
II. Portland limestone concrete.....	71
III. SRPC concrete.....	73
IV. PC- PFA concrete.....	75
4.2Changes in concrete chemistry due to long-exposure to Lower Lias Clay.....	77
4.2.1 pH profile.....	77
4.2.2 Sulfate profile.....	80
4.2.3 Carbonate profile.....	82
4.3 Chemistry of the clay.....	84
4.3.1 pH change.....	84
4.3.2 Water soluble sulfate.....	87
4.3.3 Water soluble species.....	89
4.3.4 Acid Soluble Sulfate in the clay.....	91
4.3.5 Total sulfur and pyrite oxidation.....	92
4.3.6 Carbonate content.....	95
4.4 Summary.....	97
<b>5- The Influence of Chemical Composition of Clay on the Extent of TSA</b>	<b>103</b>
5.1 Introduction.....	103
5.2 Visual assessment.....	104
5.2.1 CEM I concrete in sulfate solutions, clays and simulated pore solutions at 5 and 20°C.	104
5.2.2 CEM I –LF concrete in sulfate solutions, clays and simulated pore solutions at 5 and 20°C.	106
5.2.3 CEMI–PFA concrete in sulfate solutions, clays and simulated pore solutions at 5 and 20°C.	108
5.2.4 CEMI-GGBS concrete in sulfate solutions, clays and simulated pore solutions at 5 and 20°C.	109
5.2.5 Overall comparison of different concretes performance in different exposure conditions	110
5.3 pH Values.....	111
5.3.1 CEMI in different exposure conditions at 5 and 20°C.....	112
5.3.2 CEMI - LF in different exposure conditions at 5 and 20°C.....	114

5.3.3 CEMI - PFA in different exposure conditions at 5 and 20°C.....	117
5.3.4 CEMI - GGBS in different exposure conditions at 5 and 20°C.....	118
5.3.5 Overall Comparison.....	119
5.4 Mineralogy of the deterioration products: X-ray Diffraction (XRD).....	120
5.4.1 XRD analysis of CEMI concrete exposed to different conditions at 5 and 20°C	120
5.4.2 XRD Analysis of CEMI-LF exposed to different conditions at 5°C and 20°C...	124
5.4.3 XRD analysis of CEMI-PFA concrete exposed to different conditions at 5 and 20°C	127
5.4.4 XRD analysis of CEMI-GGBS concrete exposed to different conditions at 5 and 20°C	130
5.4.5 Overall comparison .....	132
5.5 FTIR Results analysis.....	132
5.5.1 IR Analysis of CEMI Concrete Exposed to Different Conditions at 5 and 20°C...	132
5.5.2 IR analysis of CEMI- LF concrete exposed to different conditions at 5 and 20°C	135
5.5.3 IR analysis of CEMI- PFA concrete exposed to different conditions at 5 and 20°C	138
5.5.4 IR analysis of CEMI- GGBS concrete exposed to different conditions at 5 and 20°C	140
5.6 Microstructural analysis of concrete by SEM.....	142
5.6.1 CEMI concrete.....	143
5.6.2 CEMI - LF concrete .....	148
5.6.3 CEMI - PFA concrete.....	152
5.6.4 CEMI - GGBS concrete.....	156
5.7 Summary .....	163
<b>6- Changes in Clays and Ground water Chemistry during interaction with Concrete</b>	<b>168</b>
6.1 Introduction.....	168
6.2 Chemistry Changes of Clay .....	169
6.2.1 pH changes.....	169
6.2.2 Water Soluble Sulfate.....	171
6.2.3 Acid Soluble Sulfate.....	176
6.2.4 Total Sulfur .....	180
6.2.5 Pyrite Oxidation in Different Conditions .....	182
6.2.6 Carbonate Content.....	183
6.3 Microstructural analysis of concrete.....	186
6.3.1 Weathered Lower Lias Clay (W-LLC).....	186
6.3.2 Slightly Weathered Lower Lias Clay (PW-LLC).....	188
6.3.3 Coal Measures mudstone (CM).....	190
6.4 Chemistry Change of Simulated Ground Water.....	192
6.4.1 pH change.....	192
6.4.2 Water Soluble Sulfate.....	193

6.4.3 Water Soluble Species.....	195
6.5 Summary.....	200
<b>7. Overall Discussion on The Influence of Chemical Composition of Clay on Extent of TSA in Buried Concrete</b>	<b>207</b>
7.1 Introduction.....	207
7.2 Aggressivity due to changes in the chemistry of pyritic clays. ....	207
7.3 Thaumasite formation in different conditions.....	2131
7.3 UK guidance on assessment of aggressive ground .....	218
<b>8. Conclusions and Recommendations for Future Work .....</b>	<b>223</b>
8.1 Overall Conclusions.....	223
8.1.1 Long- term concrete-clay interaction.....	224
8.1.2 Influence of clay aggressivity on extent of TSA of different concrete.....	225
8.1.3 The chemistry change of clay.....	226
8.2 Implications of Results for Research and Engineering.....	228
8.3 Recommendation for further work.....	229
<b>References.....</b>	<b>231</b>

## LIST OF FIGURES

Figure 2.1 Example of thaumasite sulfate attack in highway bridge sub-structure	10
Figure 2.2 Stages in thaumasite formations	13
Figure 2.3 The formation of thaumasite in OPC mortar	19
Figure 2.4 shows the mitigation role of chloride on TSA	26
Figure 3.1 Concrete column in disturbed Lower Lias Clay	39
Figure 3.2: Locations of used clay	42
Figure 3.3: visual appearance of used clay	42
Figure 3.4 Elevation which explain the depth of weather Lower Lias Clay	43
Figure 3.5 The long –term curing in tanks	47
Figure 3.6 controlled temperature tanks and exposure of concrete to clay	47
Figure 3.7 Modified penetrometer fitted with a thick needle attached to plunger	50
Figure 4.1: Appearance of PC concrete	57
Figure 4.2: Appearance of PLC concrete	57
Figure 4.3: Appearance of SRPC concrete	59
Figure 4.4: Appearance of PC- PFA concrete	59
Figure 4.5: Deterioration thickness of different concretes due to TSA after 9 years	61
Figure 4.6 XRD results for the surface samples of the four concrete types	64
Figure 4.7 XRD results for the interior samples of the four concrete types	64
Figure 4.8 FTIR results for deteriorated (surface) materials for the different concretes	68
Figure 4.9 FTIR results for core samples for different concretes	69
Figure 4.10: Microstructure of PC concrete	70
Figure 4.11: Microstructural analysis of PC core concrete	71
Figure 4.12: Microstructure of PLC concrete (Surface)	72
Figure 4.13: Microstructure of PLC concrete core	73
Figure 4.14: Microstructure of SRPC concrete (Surface)	74
Figure 4.15: Microstructure of SRPC concrete core	74
Figure 4.16: Microstructure of PC-PFA concrete (Surface)	75
Figure 4.17: Microstructure of PC-PFA concrete core	76
Figure 4.18: pH profile for different concretes at burial depth 2	78
Figure 4.19: Quantitative of thaumasite and calcite for different concretes at burial depth 2	79
Figure 4.20: Sulfate profiles for of different concretes at different burial depths	80
Figure 4.21: Correlation between exposure depth and sulfate concentration	81
Figure 4.22 Carbonate profile of different concretes exposed to clay burial depth 2	83
Figure 4.23: correlation between carbonate (CO <sub>3</sub> ) and pH	84
Figure 4.24: Correlation between pH values and burial depth of clay	87
Figure 4.25 water soluble sulfate of LLC for different concretes	88
Figure 4.26 Correlation between sulfate WWS and burial depth of clay	89
Figure 4.27: AAS of LLC adjacent to different concretes	92
Figure 4.28 Relation between total sulfur and deterioration depth for different concretes	94
Figure 4.29 Correlation between depth of clay and pyrite	95
Figure 4.30 Relation between consumed calcite and oxidised pyrite	97
Figure 5.1: CEMI concrete exposed to various conditions for 24 months at 5 and	105

20°C.

Figure 5.2: CEMI-LF concrete exposed to various conditions for 24 months at 5 and 20°C.	107
Figure 5.3: CEMI-PFA concrete exposed to various conditions for 24 months at 5 and 20°C	109
Figure 5.4: CEMI-GGBS concrete exposed to various conditions for 24 months at 5 and 20°C	110
Figure 5.5 pH variations of CEMI concrete at 5 and 20°C	113
Figure 5.6 pH variations of CEMI-LF concrete at 5 and 20°C	115
Figure 5.7 pH variations of CEMI-PFA concrete at 5 and 20°C	117
Figure 5.8 pH variations of CEMI- GGBS concrete at 5 and 20°C	118
Figure 5.9 XRD patterns of CEMI concrete exposed to different exposure conditions at 5°C	121
Figure 5.10 XRD patterns of CEMI concrete exposed to different exposure conditions in the presence of mobile ground water at 5°C	121
Figure 5.11 XRD patterns of CEMI concrete exposed to different exposure conditions at 20°C	122
Figure 5.12 XRD patterns of CEMI concrete exposed to simulated clay pore solutions at 5 and 20°C	123
Figure 5.13 XRD patterns of CEMI -LF concrete exposed to different exposure conditions at 5°C.	124
Figure 5.14 XRD patterns of CEMI-LF concrete exposed to different exposure conditions in the presence of mobile ground water at 5°C	125
Figure 5.15 XRD patterns of CEMI -LF concrete exposed to different exposure conditions at 20°C	126
Figure 5.16 XRD patterns for CEMI-LF concrete exposed to simulated clay pore solutions at 5 and 20°C	127
Figure 5.17 XRD patterns of CEMI -PFA concrete exposed to sulfate solutions and clays at 5°C	128
Figure 5.18 XRD patterns of CEMI-PFA concrete exposed to clays in the presence of mobile ground water.	129
Figure 5.19 XRD patterns of CEMI -PFA concrete exposed to sulfate solutions and clays at 20°C	129
Figure 5.20 XRD patterns of CEMI - GGBS concrete exposed to sulfate solutions and clays at 5°C	130
Figure 5.21 XRD patterns of CEMI-GGBS concrete exposed to clays in the presence of mobile ground water at 5°C	130
Figure 5.22 XRD patterns of CEMI 70 % GGBS concrete exposed to sulfate solutions and clays at 20°C	130
Figure 5.23 IR analysis of CEMI concrete exposed to different conditions at 5°C	133
Figure 5.24 IR analysis of CEMI concrete exposed to clays in the presence of mobile ground water	134
Figure 5.25 IR analysis of CEMI concrete exposed to different conditions at 20°C	134
Figure 5.26 shows IR analysis of CEM I concrete exposed to simulated clay pore solutions at 5 and 20°C	135
Figure 5.27 IR analysis of CEMI -LF concrete exposed to different conditions at 5°C	136

Figure 5.28 IR analysis of CEMI -LF concrete exposed to clays in the presence of mobile ground water at 5°C	137
Figure 5.29 IR analysis of CEMI -LF concrete exposed to different conditions at 20°C	137
Figure 5.30 IR analysis of CEMI -LF concrete exposed to simulated clay pore solutions at 5 and 20°C	138
Figure 5.31 IR analysis of CEMI-PFA concrete exposed to different conditions at 5°C	139
Figure 5.32 IR analysis of CEMI-PFA concrete exposed to clays in the presence of mobile ground water at 5°C	139
Figure 5.33 IR analysis of CEMI-PFA concrete exposed to different conditions at 20°C	140
Figure 5.34 IR analysis of CEMI-GGBS concrete exposed to different conditions at 5°C	141
Figure 5.35 IR analysis of CEMI-GGBS concrete exposed to clays in the presence of mobile ground water at 5°C	141
Figure 5.36 IR analysis of CEMI-GGBS concrete exposed to different conditions at 20°C	142
Figure 5.37 Microstructure analysis of CEMI concrete exposed to DS-4 sulfate solution at 5°C	144
Figure 5.38 Microstructure analysis of CEMI concrete exposed to DS-4 sulfate solution at 20°C	145
Figure 5.39 Microstructure analysis of CEMI concrete exposed to Lower Lias Clay at 5°C	146
Figure 5.40 Microstructure analysis of CEMI concrete exposed to Coal Measures Clay at 5°C	147
Figure 5.41 Microstructure analysis of CEMI-LF concrete exposed to DS-4 sulfate solution at 5°C	149
Figure 5.42 Microstructure analysis of CEMI-LF concrete exposed to DS-4 sulfate solution at 20°C	150
Figure 5.43 Microstructure analysis of CEMI-LF concrete exposed to Lower Lias Clay at 5°C	151
Figure 5.44 Microstructure analysis of CEMI-LF concrete exposed to Coal Measures at 5°C.	152
Figure 5.45 Microstructure analysis of CEMI-PFA concrete exposed to DS-4 sulfate solution at 5°C.	153
Figure 5.46 Microstructure analysis of CEMI-PFA concrete exposed to Lower Lias Clay at 5°C.	155
Figure 5.47 Microstructure analysis of CEMI-GGBS concrete exposed to DS-4 sulfate solution at 5°C.	157
Figure 5.48 Microstructure analysis of CEMIGGBS concrete exposed to Lower Lias Clay at 5°C.	159
Figure 5.49 Microstructure analysis of CEMIGGBS concrete exposed to Lower Lias Clay at 5°C.	160
Figure 5.50 Microstructure analysis of CEMI-GGBS concrete exposed to Lower Lias Clay at 5°C.	161
Figure 6.1 Water soluble sulfate of weathered Lower Lias Clay at different conditions	173

Figure 6.2 Water soluble sulfate of partially weathered Lower Lias Clay at different conditions	174
Figure 6.3 Water soluble sulfate of Coal Measures Clay at different conditions	175
Figure 6.4 Acid soluble sulfate of Weathered Lower Lias Clay at different conditions	177
Figure 6.5 Acid soluble sulfate of partially Weathered Lower Lias Clay at different conditions	178
Figure 6.6 Acid soluble sulfate of Coal Measures mudstone at different conditions	179
Figure 6.7 Total sulfur after 12 months of different clays at different conditions	181
Figure 6.8 SEM analysis of W-LLC before exposure	187
Figure 6.9 SEM analysis of W-LLC after exposure	188
Figure 6.10 SEM analysis of PW-LLC before exposure	189
Figure 6.11 SEM analysis of PW-LLC after exposure	190
Figure 6.12 SEM analysis of CM before exposure	191
Figure 6.13 SEM analysis of CM after exposure	191
Figure 6.14 sulfate concentration of simulated ground water at different clays	194
Figure 6.15 Calcium concentration of simulated ground water at different clays	196
Figure 6.16 Magnesium concentration of simulated ground water at different clays	196
Figure 6.17 Potassium concentration of simulated ground water at different clays	198
Figure 6.18 carbonate concentration of simulated ground water at different clays	198
Figure 6.19 Sodium concentration of simulated ground water at different clays	199
Figure 6.20 Chloride concentration of simulated ground water at different clays	199
Figure 7.1: The oxidation of pyrite in the presence of carbonate	209
Figure 7.2 Flowchart showing the pyrite oxidation process in different clay condition	210
Figure 7.3 Flowchart showing the amount of aggressive species generated in different clays	212
Figure 7.4 Flowchart showing aggressive species generated from the BRE, DS-2 sulfate solution	213
Figure 7.5: Schematic diagram of deterioration mechanism in sulfate solution	215
Figure 7.6: Schematic diagram of deterioration mechanism in Clay	216
Figure 7.7: Flowchart of deterioration summarising deterioration products and deterioration modes in different exposure conditions	217



## LIST OF TABLES

Table 2.1 processes of pyrite oxidation	17
Table 2.2: thaumasite formation for concrete contains limestone filler	26
Table 3.1: Parameters considered in the long-term investigation (9years)	35
Table 3.2: Experimental Programme for the influence of clay composition on TSA	37
Table 3.3: Initial characterisation of Lower Lias Clay used in this investigation	38
Table 3.4: Chemical composition of the Lower Lias Clay used in this investigation	38
Table 3.5: Chemical composition of CEMI, Limestone filler, PFA and GGBS	40
Table 3.6: Chemical composition of fine aggregate	41
Table 3.7: Chemical composition of clay used	43
Table 3.8: Major water soluble ions and cations	44
Table 3.9: Sulfur compound and Design Sulfate Class of Clay.	44
Table 3.10 BRE sulfate design class	44
Table 3.11 Test Solutions	45
Table 3.12: Chemical composition of water before interaction with clay	45
Table 3.13: Mix proportions of concrete	45
Table 4.1: Deterioration ranking of concrete	62
Table 4.2: Deterioration ranking of concrete after 9 years of exposure	62
Table 4.3: Quantitative XRD analyses for the degradation products for the four concretes	65
Table 4.4 Degradation phases detected in the four concretes	65
Table 4.5 pH values of concrete surface and stabilisation depth of pH at burial depth 2.	79
Table 4.6 Original sulfate contents of different binders	81
Table 4.7 pH of clay at 6 month.	85
Table 4.8 pH of clay after 9 years	86
Table 4.9 WWS of clay at 6 months	87
Table 4.10 Water Soluble species in clay	90
Table 4.11 Total sulfur values for clay	93
Table 4.12: Carbonate content of clay after 9 years of exposure	96
Table 6.1 pH changes in the presence of mobile ground water	169
Table 6.2 pH changes in the absence of mobile ground water	170
Table 6.3 pyrite oxidation in different clays at different exposure conditions	182
Table 6.4 reductions in carbonate content in different clays at different exposure conditions	185
Table 6.5 pH variation of simulated ground water up to 18 months	192
Table 7.1: Design sulfate classes in BRE SD :2001	218
Table 7.2: Design sulfate classes in BRE SD-1:2005	219
Table 7.3: Review UK guidance for the classification of aggressive ground	221
Table 7.4: Review the UK guidance for concrete in aggressive ground	222

## **LIST OF SYMBOLS AND ABBREVIATIONS**

C3A: Tricalcium Aluminate  
CH: Calcium Hydroxide (Portlandite)  
CSH: Calcium Silicate Hydrate  
PC: Portland cement  
MSH: Magnesium Silicate Hydrate  
SRPC: Sulfate Resisting Portland cement  
PLC: Portland Limestone Cement  
TSA: Thaumasite Sulfate Attack  
TF: Thaumasite Formation  
XRD: X-Ray Diffraction  
EDX: Energy Dispersive X-ray  
SEM: scanning Electron Microscopy  
FTIR: Fourier Transform Infrared Spectrometry  
GGBS: Ground granulated blast-furnace slag  
PFA: Pulverized - fuel ash  
LLC: Lower Lias Clay  
CM: Coal Measures mudstone  
W-LLC: Weathered Lower Lias Clay  
SW-LLC: Slightly Weathered Lower Lias Clay  
WSS: water Soluble Sulfate  
ASS: Acid Soluble Sulfate  
OS: oxidisable Sulfur  
TS: Total Sulfur  
DS: Design Sulfate Class  
ACEC: Aggressive Chemical Environment for Concrete  
DC: Design Chemical class.

# CHAPTER 1

## 1. Introduction

### 1.1 Background

In March 1998, serious deterioration due to the formation of thaumasite was discovered in the concrete foundations of a number of 30-year-old bridges in Gloucestershire. Deterioration due to thaumasite was found in other concrete foundations in the Cotswolds area. In both cases, carbonate coarse aggregates had been used and the affected concrete was in contact with Lower Lias Clay (LLC) (Crammond, 2003). Thaumasite Expert Group (TEG) established by the UK government in April 1998 determined that the deterioration was due to the thaumasite form of sulfate attack (TSA). About 85 new cases of TSA (Clark et al., 2000) have been identified since the publication of the first TEG Report. In addition, thaumasite has been identified in various other locations, including Canada, South Africa, Germany, Norway and Slovenia (Crammond, 2003; Tsvilis et al., 2007). The formation of thaumasite led to changes in the microstructure and the strength of the concrete, including extensive cracking, and loss of bond between the cement paste and the aggregate (Nobst and Stark, 2003). Nixon et al. (2003) reported that the formation of thaumasite requires a source of carbonate and sulfate ions which target the calcium silicate. In the case of the buried concrete structures constructed in Lower Lias Clay, weathering of pyrite ( $\text{FeS}_2$ ), which a constituent of the clay, was considered to have been the source of sulfate. Thaumasite growth depends on a number of factors, such as concrete type, backfill type, and chemistry and level of groundwater (Floyd and Wimpenny, 2003).

Many of the UK clay and mudrock formations containing pyrite (iron sulfide) are now recognised to be potentially detrimental to buried construction materials, including concrete. Pyrite may be found in most Carboniferous mudrocks, marine Mesozoic deposits and sedimentary clay deposits (Czerewko and Cripps, 2006). Czerewko and Cripps (2003) and many others have reported that weathering of pyrite in the presence of oxygen and water

leads to its oxidation. This process can be catalysed by presence of Thiobacillus bacteria. The acidic conditions produced by the oxidation processes and the increase in temperature provide favourable environmental conditions for the growth of sulfate-reducing bacteria which increase the rate of pyrite oxidation. Moreover, engineering work such as excavation and change in groundwater may result in rapid oxidation. The oxidation of pyrite process generates sulfate and sulfuric acid as the main products, in which sulfuric acid is considered to be corrosive to both metals and concrete. The acidic condition can be buffered by the presence of certain minerals such as calcite. However, the concentration of sulfate and acidity might significantly increase in the groundwater as a result of absence of buffering mineral or incomplete of acid neutralisation due to high flow of ground water (Czerewko and Cripps, 2006).

Lower Lias Clay is known as a potential sulfate-bearing stratum and as it contains up to 5% pyrite by mass, Floyd and Wimpenny (2003) stated that, in the foundations of the M5 motorway, affected concrete was transformed into soft white mush as a result of the use of Lower Lias Clay around the buried concrete foundations. However, the occurrence of thaumasite was variable between structures. Slater and Wimpenny (2003) reported that there was more attack in the deep and wet sections where more oxidation of pyrite occurs. In addition, sulfate concentration levels showed good correlation with the amount of TSA. It was also indicated that the main ion species in the natural groundwater are  $\text{Na}^+$ ,  $\text{K}^+$ ,  $\text{Ca}^{2+}$ ,  $\text{Mg}^{2+}$ ,  $\text{Cl}^{2-}$ ,  $\text{CO}_3^{2-}$ ,  $\text{Ca}^{2+}$ , and  $\text{SO}_4$ , from which the sulfate and chloride ions diffuse into concrete.

An extensive search of the literature revealed very few studies into the interaction between buried concrete and pyrite-rich clays. This is in spite of the widespread occurrence of such clays, as noted by Czerewko and Cripps (2006), and the huge number of buried concrete structures. It would appear that only one field investigation has yet been carried out to assess the performance of buried concrete (Crammond et al., 2003). A study by Byars et al. (2003) has shown that the severity of thaumasite sulfate attack on concrete exposed to pyritic clay is greater than that in solution. Therefore, there is an urgent need to deepen understanding of the mechanism of TSA in buried concrete exposed to pyritic ground. The recommendations contained in BRE SD1 (2005) and similar standards are based upon laboratory studies involving the immersion of concrete specimens in test sulfate solutions, which might be magnesium sulfate or sodium sulfate or a combination of both. However, there is no laboratory study that has investigated TSA in simulated field conditions, considering the influence of the chemical composition of clay on thaumasite formation and the extent of TSA. In addition, Hobbs and Wimpenny (2003) indicated that the deterioration of buried

concrete in the M5 bridges was due to sulfuric acid, and thaumasite formation was a secondary deposition of mineral material. Another uncertain aspect of TSA in aggressive ground conditions which needs further investigation is whether sulfuric acid, produced from pyrite oxidation plays a role in thaumasite formation and the extent of TSA in buried concrete structures especially if the clay that contains calcite in its composition. In addition, it is not clear how the amount of pyrite in clay and its oxidation rate can affect thaumasite formation and the extent of TSA.

Since the late 1990s, there have been many attempts to investigate the performance of different cement binders, such as Portland cement, sulfate-resisting Portland cement, and blended cements including silica fume, pulverized- fuel ash and ground granulated blast-furnace slag (Nobst and Stark, 2003; Hartshorn et al., 1999; Torres et al., 2003; Higgins et al., 2003; Lee et al., 2008; Bellmann and Stark, 2007; Zhou et al., 2006; Crammond et al., 2003; Pouya, 2007). Several measures have been suggested to prevent the formation of ettringite and thaumasite. Cement with low  $C_3A$  is suggested to be used in order to avoid ettringite formation. Using cement blended with PFA and GGBS, which result in C-S-H with low Ca/Si ratio, is an additional method for avoiding TSA (Bellmann and Stark, 2007).

It appears that there is controversy about the performance of PFA-blended concrete in this respect, as some researchers (Nobst and Stark, 2003; Crammond et al., 2003; Pouya, 2007) have found it to be susceptible to TSA, while others (Thomas et al., 2001, 2003) reported good performance, which they attributed to such factors as a reduced Ca: Si ratio in concrete made with PFA. Crammond et al. (2006) reported that SRPC cast in situ concretes containing siliceous aggregates had performed satisfactorily against TSA. The same work reported on field trials at Shipston on Stour in Gloucestershire, UK, which showed that TSA was influenced by binder composition, with PC blended with ground granulated blast-furnace slag mixes showing higher resistance to TSA. Most reported investigations into the performance of different binders were conducted by exposing samples to sulfate solutions, rather than to pyritic ground conditions. In fact, despite an extensive literature review, no studies could be found which investigated the long-term performance of binders recommended in BRE SD-1(2005) for ground containing pyrite-bearing soils, such as SRPC, replacement with 25% and 50% PFA and replacement with 70% GGBS, which prompts the need for such investigation.

Bitumen has been suggested and an economical measure for coating buried concrete elements to increase their resistance to acid and water penetration. Pouya (2007) reported that PLC deterioration due to TSA could be prevented using bitumen surface coatings. However, it would appear that there is no technical information for the long-term durability

of bitumen coatings and there are no data in the literature with regard to the performance of bitumen as a surface coating to protect buried concrete in aggressive ground conditions such as pyritic clay.

Particular research questions arising from this review of literature that will be addressed in this work comprise the following:

- i. Why is the deterioration of concrete due to TSA more severe in concrete exposed to pyritic ground than in concrete in sulfate solution?
- ii. Is the sulfuric acid produced by pyrite oxidation mainly responsible for thaumasite formation and TSA in buried concrete?
- iii. Is the route to thaumasite formation in buried concrete similar to that in concrete exposed to sulfate solution?
- iv. Is there a relationship between the **amount of pyrite** present in the clay and the severity of TSA?
- v. Do concrete mixes such as SRPC, 25% PFA, 50% PFA and 70% GGBS, which are recommended by BRE guidance for aggressive ground, resistant to TSA after long-term (10s years) exposure to pyrite bearing clay?
- vi. Could the bitumen coating prevent TSA regardless of concrete type?
- vii. What are the most important factors influencing the rate of pyrite oxidation?
- viii. Does the current guidance for assessing ground aggressivity provide reliable assessment with regard to the likelihood of thaumasite form of sulfate attack?

## 1.2 Aims and objectives

The principal aim of this research is to investigate thaumasite formation and the severity of TSA in buried concrete. Several specific objectives are proposed to achieve the main aim, and are as follows:

1. to investigate the influence of clay composition on thaumasite formation and the extent of TSA
2. to clarify the role of sulfuric acid generated from pyrite oxidation and of clay pH on the extent of thaumasite sulfate attack in buried concrete

3. to determine the mechanisms of thaumasite formation in different exposure conditions
4. to study the long-term performance (nine years) of PC, SRPC, PLC and PC - 25% PFA concrete in exposure to aggressive ground conditions
5. to investigate the performance and relative resistance of 50% PFA and 70% GGBS concretes in exposure to aggressive pyritic clay
6. to assess the chemical alteration of concrete made with different binders due to long-term exposure to aggressive ground conditions
7. to investigate the effectiveness and long-term performance of bitumen coatings in protecting concrete in aggressive ground conditions
8. to investigate the chemical changes in pyritic clays and clay pore solutions during interaction with different concretes, and the influence of mobile groundwater on chemical changes in clay
9. to review and assess the current guidance regarding the influence of aggressive ground conditions with regard to TSA

### **1.3 Structure of the thesis**

This thesis consists of eight chapters. The first chapter introduces the background of the research problem and presents the main aim and objectives. An exhaustive literature review on the nature of the thaumasite form of thaumasite attack and its chemical and physical effects, the aggressivity of clay, factors influencing the occurrence of TSA, prevention of TSA, and guidance for concrete in aggressive ground is presented in Chapter 2. The experimental design and details, properties of materials and test methods are described in Chapter 3.

The results of a nine-year-long experiment in which different concretes were exposed to slightly weathered Lower Lias Clay at 5°C are addressed in Chapter 4. This chapter also includes evaluation of long-term performance, change in chemistry and microstructural alteration of PC, PLC, SRPC and PC-25% PFA concretes. Chapter 5 addresses the influence of the chemical composition of on the clay or mudstone adjacent to the concrete on thaumasite formation and the extent of TSA in CEMI, CEM-LF, CEMI - 50% PFA and

CEMI - 70% GGBS concretes. The results of changes in the clay and groundwater chemistry during interaction with concrete are discussed in Chapter 6.

An overall discussion on the influence of the chemical composition of clay on TSA, the aggressivity of clay, and guidance for assessing the aggressivity of ground in terms of TSA is presented in Chapter 7. Overall conclusions drawn from the study, the implications of the research for engineering and recommendations for future research work are summarised in Chapter 8.



## CHAPTER 2

### 2. Literature Review

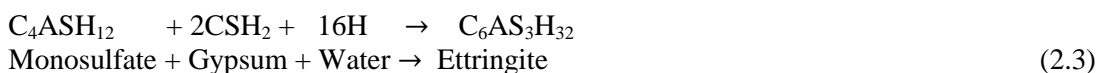
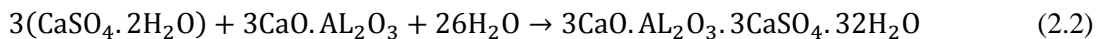
#### 2.1 Introduction

Concretes made with different binders perform well in normal environmental conditions; however, their durability can be reduced as a result of interaction with different chemical species derived from the surrounding ground (Glasser et al., 2008). The penetration of sulfate and carbonate into concrete may lead to deterioration of concrete. Therefore, designing for concrete durability and the mechanisms of attack have become an area of concern for research. Concrete deterioration due to physical attack, including salt crystallization attack and freeze-thaw damage is well studied. In addition, chemical attack, which includes acid attack, various forms of sulfate attack, alkali silica reaction and corrosion of reinforcement, has been extensively investigated, and extensive research findings have been reported in the literature. Salt crystallization is considered the most common type of physical attack, which solid sulfate sources is dissolved and recrystallized in concrete pores, causing cracks and spalling in concrete structures (Skalny et al., 2002). Sulfate attack is considered one of the most common chemical attacks that affect concrete durability and cause severe deterioration to concrete structures. Different investigations of sulfate attack on concrete made with different binders have revealed a series of possible physical and chemical processes, demonstrated through deterioration of the material, including expansion, cracking, and decomposition of cement hydration products. Gypsum, monosulphaluminate and ettringite as forms of sulfate attack have been well documented in the technical literature, which has focused on the deterioration of aluminum and calcium hydroxide phases in cement (Mather, 1966; Mather, 1968; Mather, 1969; Mather, 1980; Mather, 1984; Lea, 1971; Kalousek et al., 1972; Hanson, 1966; Cohen, 1983; Cohen, 1984; Skalny et al., 2002). Control and treatment of different causes of deterioration have been addressed in the guidance. Thaumasite sulfate attack is another kind of sulfate attack which has been reported during the last two decades. However, Clark (1999) reported that thaumasite sulfate attack received serious attention after the deterioration of bridge

foundations on the M5 motorway in the UK in 1998, which were suffering from an extreme case of TSA. On the other hand, the formation of thaumasite and the extent of thaumasite sulfate attack (TSA) on buried concrete have not been well studied yet.

## 2.2 Conventional form of sulfate attack

Sulfate attack is due to the exposure of concrete to sulfates and moisture, which causes a series of reactions of sulfate ions with cement hydration products. In conventional sulfate attack, the source of sulfate can be internal, derived from the sulfate incorporated in cement or aggregate, or external, derived from clay and groundwater and entering the concrete (Skalny et al., 2002). Gypsum and ettringite are the main reaction products in both cases. Newman and Choo (2003) pointed out that sulfate reacts with a source of calcium to form gypsum and with a source of aluminate to form ettringite, as shown in Equations 2.1 to 2.3. In addition, the formation of ettringite may occur directly, by reaction between gypsum and tricalcium aluminate in the presence of water, as described by Hime et al. (1999). On the other hand, it may be preceded by monosulfate, which is called the classic form of sulfate attack, as reported by Skalny et al. (2002), in Equation 2.3.



Skalny et al. (2002) reported that the formation of gypsum is accompanied by a limited increase in volume and might result in a significant problem if the sulfate concentration exceeds 3.0 g/l. The formation of ettringite is accompanied with an increase in volume, which results in significant expansion. Ettringite might form at a low sulfate concentration because of its low solubility and this might be the reason why expansion due to ettringite is more prevalent than that caused by gypsum. However, expansion resulting from the formation of ettringite from monosulfate in the case of external sulfate attack is greater than expansion from  $\text{C}_3\text{A}$ .

Concrete expansion can result in cracking, spalling and loss of mass and strength. Tian and Cohen (2000) pointed out that expansion occur due to formation of ettringite during sulfate

attack, while gypsum formation might cause softening and loss of strength in concrete. However, the extent of attack due to gypsum and ettringite is not necessarily severely expansive, and depends on the type and concentration of sulfate and surrounding environmental conditions (Skalny et al., 2002; Taylor, 1997).

### **2.3 Thaumasite form of sulfate attack**

Thaumasite is known as a complicated form of sulfate attack. It attacks the calcium silicate hydrates (C-S-H) and calcium hydroxide (Ca(OH)<sub>2</sub>). It is produced experimentally by subjecting starting material to conditions of thaumasite formation such as a source of silicate, carbonate, a source of sulfate and excess water (Bensted, 1999; Schmidt et al., 2008).

Thaumasite was found as a deterioration product in cement paste, mortar and concrete (Hill et al., 2003). Hobbs (2003) quoted Erlin and Stark (1965) who reported that as early as 1965 thaumasite formation was observed in sewer pipes and concrete pavements in the USA. Crammond (2003) suggested that the thaumasite form of sulfate attack had not been recognised previously in buried concrete because of a lack of improved analytical techniques that can differentiate between ettringite and thaumasite and because buried concrete was rarely inspected.

Because of the impact of sulfate attack on concrete durability and performance, TSA became a major concern in the UK. However, in the UK the thaumasite form of sulfate attack began receiving urgent attention in March 1998 when severe damage was discovered in concrete substructures of various 30-year-old M5 motorway bridges in Gloucestershire (Slater et al., 2003). Hobbs (2003) highlighted that, in the case of the M5, all of the affected concretes were in pyritic clay/mudstone which was used as fill around the cast-in-situ concrete foundations and which interacted with the concrete, as shown in Figure 2.1.

Clark (2002) reported that thaumasite was found in buried concrete structures elsewhere in southern England, including the M4 in Gloucestershire, Somerset and Wiltshire, and in County Durham in the north-east of England. In addition, thaumasite has been identified in various other locations, including Canada, South Africa, Germany, Norway and Slovenia (Crammond, 2003; Tsivilis et al., 2007).



Figure 2.1 Example of thaumasite sulfate attack in highway bridge sub-structure BRE, (2005)

According to Clark (2002), the Thaumasite Expert Group classified thaumasite into two categories. The first is the thaumasite form of sulfate attack (TSA) where all affected concrete is transformed to soft white mushy material. The second category is thaumasite formation (TF), which does not cause deterioration to concrete and is precipitated in voids and cracks. However, thaumasite formation can develop into the thaumasite form of sulfate attack with time (Clark 2002).

Clark (2002) in the Thaumasite Expert Group (TEG) report suggested that the following main factors should be present before the occurrence of severe TSA:

- sulfate or sulfide in the ground
- mobile groundwater
- a source of carbonate
- low temperature (below 15°C).

However, there are other factors that may contribute to the severity of TSA in buried concrete, such as:

- cement type, quantity of cement and concrete quality
- change to ground chemistry
- burial depth of concrete.

TSA has a significant influence on concrete durability, in which formation of thaumasite is usually associated with loss of strength and bond between the cement paste and the aggregate particles. The structural effect of TSA in buried concrete structures can be due to the reduction in the cross-sectional area of concrete, loss of concrete cover resulting in corrosion and reduction in skin friction at concrete-clay interface (Clark, 2002; Brueckner et al., 2012). A study by Gorst and Clark (2003) on the removal of columns that had suffered from TSA during the repair of the Tredington–Ashchurch overbridges in Gloucestershire showed that there was a marked impact on the bond strength between reinforcement and concrete, in which the bond coefficient decreased by 24%, associated with an increase in the thickness of soft materials.

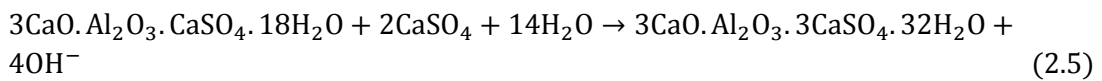
### 2.3.1 Formation of thaumasite

Thaumasite ( $\text{CaSiO}_3 \cdot \text{CaCO}_3 \cdot \text{CaSO}_4 \cdot 15\text{H}_2\text{O}$ ) incorporates carbonate ( $\text{CO}_3$ ), sulfate ( $\text{SO}_4$ ), silicate ( $\text{Si}(\text{OH})_6$ ) and calcium (Ca) in its structure. Bensted (1999) and Collete et al. (2004) reported that the sulfate might be derived from sulfate associated with different cations such as magnesium, calcium or sodium, dissolved in groundwater. The origin of the carbonate ions can be either an internal source, where carbonate aggregate or limestone is used, or an external source, either carbonate present in the clay or atmospheric carbon dioxide. In addition, the silicate becomes available as a result of the decomposition of calcium silicate hydrate (C-S-H), the main binder of Portland cement (Zhou et al., 2006). Generally, these chemical sources and water are needed to produce thaumasite.

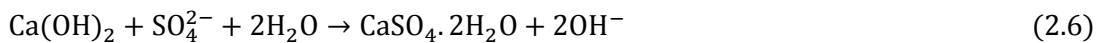
Bensted (1999, 2003) proposed two main routes for thaumasite formation, which are direct or indirect transformation of reactants into thaumasite. In the direct route, thaumasite can form by the reaction of sulfate with carbonate and silicate in presence of excess water and a source of calcium ions. The reaction is very slow and it can take up to several months to produce significant thaumasite. In the woodfordite route, **which is a name given for deterioration product contains both thaumasite and ettringite**, thaumasite might form by the reaction of ettringite with C-S-H and a carbonate source in the presence of water. However, this reaction is again very slow, but the reaction rate rises significantly after thaumasite initiate to form. Ma et al. (2008) investigated the chemical simulation of TSA on concrete, which proposed that the chemical process of TSA could be classified into four periods as follows:

**I. Ionic migration period:** in this stage, the  $\text{SO}_4^{-2}$  penetrates concrete and at the same time the  $\text{OH}^-$  and  $\text{Ca}^{+2}$  leach out.

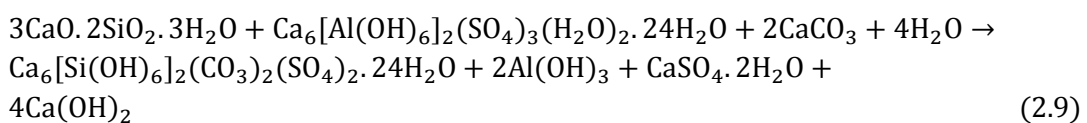
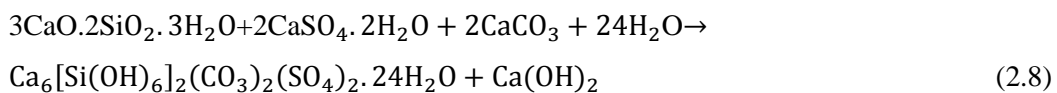
**II. Ettringite formation period:** in this stage, the following reactions occur, and the final product is ettringite:



**III. Gypsum formation period:** in this stage, the following reactions take place, and the final product is gypsum:



**IV. Thaumasite formation period:** the final product of this stage is thaumasite:



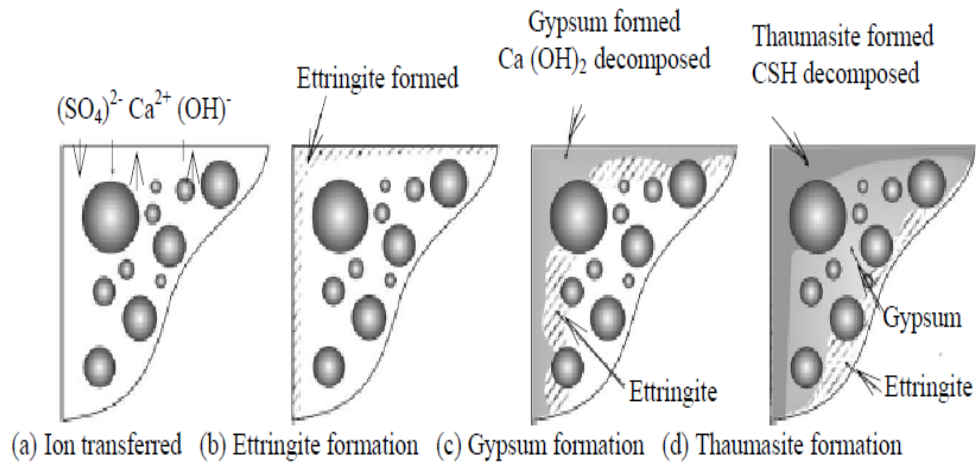


Figure 2.2: Stages in thaumasite formation. Ma et al. (2008)

Crammond (2003) proposed that thaumasite might also form via solution mechanism, in which conventional sulfate attack occurs first until ettringite ceases to form as a result of the consumption of alumina in the formation of ettringite. In addition, penetration of further sulfate will react with portlandite and in the presence of carbonate ions, thaumasite would form instead of gypsum.

A recent investigation into the role of ettringite in thaumasite formation by Kohler et al. (2006) pointed out that the rate of thaumasite formation might be controlled by ettringite and the reaction was linked to decomposition of C-S-H. According to Crammond and Nixon (1993), the breakdown of C-S-H phases is probably an important intermediate reaction product within the process of thaumasite formation. On the other hand, Brueckner (2007) claimed that thaumasite formation may be accompanied by one of three other main degradation processes: magnesium sulfate attack, sulfuric acid attack and decalcification.

Most reported investigations into the mechanism of thaumasite formation were conducted by exposing samples to sulfate solutions rather than to pyritic ground conditions. In addition, the mechanism of thaumasite formation by which concrete is more vulnerable to TSA when it is in contact with clay than when it is in contact with the equivalent solution is not clear. Therefore, further investigations are necessary to clarify the mechanism of thaumasite formation in concrete interacting with pyritic clay as well as whether deterioration products are similar to those in the case of exposure to sulfate solutions.



## 2.4 Thaumasite in buried concrete exposed to pyritic ground

Problems due to the thaumasite form of sulfate attack (TSA) in buried concretes have been extensively reported during the last fifteen years, with significant cases identified in the UK and worldwide (Slater et al., 2003; Hobbs, 2003; Clark, 2002; Crammond, 2003; Tsivilis et al., 2007). Oxidation of pyrite leads to the formation of sulfate and sulfuric acid, resulting in a rise in the groundwater sulfate level (Hobbs, 2003; Floyd et al., 2003).

Floyd and Wimpenny (2003) stated that, in the foundations of the M5 motorway, concrete was affected and the surface transformed into soft white mush as a result of the use of Lower Lias Clay around the buried concrete foundations. However, the occurrence of thaumasite was not constant with and between structures. Therefore, there are a number of factors which may contribute to the extent of TSA, such as concrete type, backfill type and the chemistry and level of groundwater. In addition, Loudon (2003) reported that the severity of TSA in concrete structures at the Tredington–Ashchurch road bridge was due to variations in a number of factors in combination rather than differences in concrete properties.

Slater et al. (2003) reported that the extent of TSA was linked to groundwater level. In addition, sulfate concentration level strongly correlate with the severity of TSA. It was also found that there was sufficient carbonate in the groundwater, which participates in the TSA. The Thaumasite Expert Group investigated the oxidation field trials on pyritic Lower Lias Clay around the M5 in Gloucestershire and Somerset. It was found that the rate of oxidation significantly increased in five months of tests on the two stockpiles of Lower Lias Clay. The rate of oxidation was greater in stockpiles exposed to wet conditions than those in dry warm conditions. Furthermore, there were no signs of development of sulfuric acid, which could be the result of the presence of a buffering mineral such as calcite in the location (Clark, 2002). An investigation into the contribution of construction activity to aggressive ground conditions performed by Longworth (2003) showed that sulfate concentration increased due to the disturbance of aggressive ground during construction. This was one of the main reasons for the deterioration of the concrete foundations of the bridge on the M5 where the concrete was classified to resist maximum sulfate of class DS-2. However, sulfates in classes 3 and 4 were generated as a result of pyrite oxidation in backfill, and therefore the concrete deteriorated as a result of thaumasite formation.

Crammond et al. (2003) investigated the resistance of buried concrete to TSA in a field trial at Shipston on Stour. Concrete made of different w/c ratios and different binders (PC, SRPC, PC-40%-70% GGBS, PC-15% limestone filler, PC-30% PFA, PC-10% microsilica and PC-25% metakaolin) were used. The three years' results showed that concretes generally performed similarly in both field and laboratory investigations, and the degradation of



concretes due to TSA varied from zero to moderate, depending on concrete quality and composition; concrete made of PC-GGBS showed a good resistance to TSA compared to other concretes.

An extensive search of the literature revealed very few studies into the interaction between buried concrete and pyrite-rich clays. This is in spite of the widespread occurrence of such clays, as noted by Czerewko and Cripps (2006), and the huge number of buried concrete structures. However, there are no technical studies on the effect of chemical compositions of clay on thaumasite formation and the development of TSA, because the reason behind the aggressiveness of clay towards concrete compared with exposure to sulfate solutions has not yet been investigated. Therefore, a laboratory investigation that describes deterioration in buried concrete due to TSA in simulated field conditions should be carried out.

#### **2.4.1 Sulfate and sulfide in aggressive ground**

Sulfur can be found in a number of different forms: as a primary sulfate mineral, of which gypsum with 1.4 g/l soluble sulfate is the most commonly encountered in the UK, and as a sulfide mineral such as pyrite, which is commonly present in clays, mudstone and mineral veins. In addition, secondary sulfate can be formed as a result of weathering of sulfide minerals (Czerewko and Cripps, 2006). In addition, Czerewko and Cripps (2006) reported that sulfate minerals such as gypsum and epsomite may occur naturally. In the UK, it has often been leached out of natural rocks and soils in the near-surface zone where most civil engineering works are carried out.

With regard to pyrite, it has been found in most Carboniferous mudstone, marine Mesozoic deposits and sedimentary clay deposits, which account for up to 5% of the sample mass in Lower Lias Clay. It may also be present in recent sediments formed under anaerobic conditions (Czerewko and Cripps, 2006; Czerewko et al., 2003). Although aggressive ground conditions are associated with different physical, chemical and biological processes, Czerewko et al. (2003) suggested that the presence of sulfur minerals such as gypsum and pyrite is considered the major reason for the occurrence of the aggressive ground conditions due to an increase in the concentration of sulfate ions in groundwater. In addition, the sulfate concentration in solution is restricted because of the solubility of gypsum, but a much higher concentration is expected if a high-solubility sulfate mineral such as epsomite is present or the solubility of gypsum is increased due to lower pH resulted from sulfuric acid during oxidation of pyrite. However, not all forms of sulfur contribute to a rise in the sulfate concentration in the groundwater leading to problems in engineering sites, which barite and

organic sulfur for example are stable in weathering environment (Czerewko and Cripps, 2006).

#### 2.4.1.1 Weathering of pyrite

The oxidation of **pyrite** and the resulting sulfate formation is considered in the UK as a potential engineering hazard due to increase the level of sulfate in ground (Floyd et al., 2003). The chemical weathering of pyrite is an oxidation reaction mechanism which is metastable in damp environments. In addition, pyrite oxidation would only occur in the presence of both water and oxygen. The oxygen is necessary to oxidise the pyrite, whereas water acts as a catalyst in order to form sulfate and sulfuric acid, as shown in Table 2.1 (Czerewko and Cripps, 2006; Czerewko et al., 2003).

Research by Quispel et al. (1952) studied the contribution of the bacteria in pyrite oxidation in soil. It was found that pyrite can oxidise with and without the presence of bacteria but that the latter might catalyse the processes, through bacteriological catalysts such as Thiobacillus bacteria. Czerewko and Cripps (2006) stated that the oxidation rate can be increased through changes in ground conditions due to engineering works, **leading** to exposure to air. In addition, the rate of pyrite oxidation might be increased by ferric iron, **which was found** to be 3-100 times faster than by oxygen. Moreover, Quispel et al. (1952) reported that pH plays an important role in pyrite oxidation, in which acidic conditions are considered to be favourable for the growth of sulfate-reducing bacteria which increase the rate of oxidation by 5-6 orders of magnitude. Furthermore, in acidic conditions in which  $\text{pH} < 4$ , oxidation by  $\text{O}_2$  becomes extremely slow, and pyrite tends to be oxidised by ferric iron; the presence of Thiobacillus bacteria speed up the reaction (Czerewko and Cripps, 2006; Arkesteyn, 1980).

However, Schoonen et al. (2000) stated that the rate of oxidation of pyrite strongly depends on the temperature, since pyrite is thermodynamically unstable and oxidised. In addition, the oxidation reaction is also exothermic and the increase in temperature and acidity desirable for bacterial action promote further pyrite oxidation and increase the rate of oxidation (Czerewko and Cripps, 2006).

Sulfate and sulfuric acid are the main products of pyrite oxidation, and the latter can be neutralized in the presence of carbonate such as calcite. However, a much higher concentration of sulfate can occur in the absence of buffering minerals such as calcite or a high rate of mobile groundwater, which results in incomplete neutralisation of acid. In addition, sulfuric acid reacts with clay minerals such as illite and liberates exchangeable cations such as K, Na and  $\text{Mg}^+$  (Czerewko and Cripps, 2006).

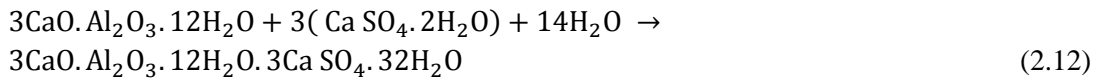
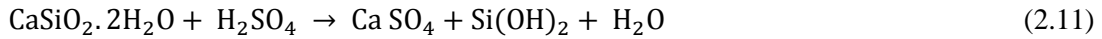
Table 2.1 Processes of pyrite oxidation (Floyd et al, 2003)

Saturated conditions		
1	$2\text{FeS}_{2(s)} + 2\text{H}_2\text{O} + 7\text{O}_2 \rightarrow 2\text{Fe}^{2+} + 4\text{SO}_4^{2-} + 4\text{H}^+_{(aq)}$ <p style="text-align: center;"><small>Pyrite</small>    <small>Ferrous iron</small></p> $4\text{Fe}^{2+} + 4\text{H}^+_{(aq)} + \text{O}_2 \rightarrow 4\text{Fe}^{3+} + 2\text{H}_2\text{O}$ <p style="text-align: center;"><small>Ferrous iron</small>                                      <small>Ferric iron</small></p> $\text{FeS}_2 + 14\text{Fe}^{3+} + 8\text{H}_2\text{O} \rightarrow 15\text{Fe}^{2+} + 2\text{SO}_4^{2-} + 16\text{H}^+_{(aq)}$ <p style="text-align: center;"><small>Pyrite</small>                                      <small>Ferric iron</small>                                      <small>Ferrous iron</small></p>	<p>Initial oxidation of pyrite proceeds by purely chemical means, producing ferrous iron</p> <p>Ferrous iron is oxidised to ferric iron by bacterial mediation</p> <p>Ferric iron is a strong oxidising agent, acts as an electron acceptor in further oxidation of pyrite</p> <p>If conditions of pH <math>\geq</math> 4, i.e. flushing of the system and atmospheric exposure, results in hydrolysis and precipitation of orange ochre</p>
1-b	$4\text{Fe}^{2+} + 10\text{H}_2\text{O} + \text{O}_2 \rightarrow 4\text{Fe}(\text{OH})_{3(s)} + 8\text{H}^+_{(aq)}$ <p style="text-align: center;"><small>Ochre</small></p>	
Humid conditions		
2	$2\text{FeS}_{2(s)} + 7\text{O}_2 + x \cdot \text{H}_2\text{O} \rightarrow 2\text{FeSO}_4 \cdot n\text{H}_2\text{O}_{(s)} + \text{H}_2\text{SO}_{4(l)}$ <p style="text-align: center;"><small>Pyrite</small>    <small>Ferrous sulfate salt</small>                                      <small>Sulfuric acid</small></p> <p>(<math>x \geq 2</math>, when <math>x = 2</math>, <math>n = 0</math>)</p>	<p>Ferrous sulfate salts seen as efflorescent deposits, such as yellow, blue green melantorite (<math>\text{FeSO}_4 \cdot 7\text{H}_2\text{O}</math>)</p>
3	$\text{H}_2\text{SO}_{4(l)} + \text{CaCO}_{3(s)} + \text{H}_2\text{O}_{(l)} \rightarrow \text{CO}_{2(g)} + \text{CaSO}_4 \cdot 2\text{H}_2\text{O}_{(s)}$ <p style="text-align: center;"><small>Sulfuric acid</small>                                      <small>Calcite</small>    <small>Gypsum</small></p>	<p>Calcite and limestones react with sulfuric acid forming gypsum</p>
4	$\text{Ca}(\text{OH})_2 + \text{SO}_4^{2-} + 2\text{H}_2\text{O} \leftrightarrow \text{CaSO}_4 \cdot 2\text{H}_2\text{O}_{(s)} + 2\text{OH}^-_{(aq)}$ <p style="text-align: center;"><small>Cement</small>                                      <small>Ground-water</small>                                      <small>Gypsum</small></p> $\text{Ca}_3\text{Al}_2\text{O}_6 + 3\text{CaSO}_4 \cdot 2\text{H}_2\text{O} + 30\text{H}_2\text{O} \rightarrow [\text{Ca}_3\text{Al}(\text{OH})_6]_2(\text{SO}_4)_3 \cdot 26\text{H}_2\text{O}$ <p style="text-align: center;"><small>Cement</small>                                      <small>Gypsum</small>                                      <small>Water</small>                                      <small>Ettringite</small></p>	<p>Ettringite formation requires a source of sulfate, mobile groundwater, calcium hydroxide and hydrated calcium aluminate from the cement matrix. The reaction initially produces gypsum due to calcium hydroxide and sulfate ion interaction. Ettringite is unstable in acidic conditions</p>
5	$\text{CaSiO}_3 \cdot 3\text{H}_2\text{O} + 2\text{Ca}(\text{OH})_2 + \text{SO}_4^{2-} + \text{HCO}_3^- + 8\text{H}_2\text{O} + 3\text{H}^+_{(aq)}$ <p style="text-align: center;"><small>Cement</small>                                      <small>Cement</small>                                      <small>Ground-water</small>                                      <small>Limestone</small></p> $\rightarrow \text{Ca}_3[\text{Si}(\text{OH})_6](\text{CO}_3)(\text{SO}_4) \cdot 12\text{H}_2\text{O}$ <p style="text-align: center;"><small>Thaumasite</small></p>	<p>Thaumasite formation requires a source of sulfate, ground-water, hydrated calcium silicate and carbonate phases present in concrete and a low temperature of <math>&lt;15</math> °C. Thaumasite is unstable in acidic conditions</p>
6	$12\text{FeSO}_4 + 4(\text{KAAlSi}_3\text{O}_8(\text{OH})_2) + 48\text{H}_2\text{O} + 4\text{O}_2$ <p style="text-align: center;"><small>Ferrous sulfate</small>                                      <small>Illite</small></p> $\rightarrow 4(\text{KF}_3(\text{SO}_4)_2(\text{OH})_6) + 8\text{Al}(\text{OH})_3 + 12\text{Si}(\text{OH})_4 + 4\text{H}_2\text{SO}_4$ <p style="text-align: center;"><small>Jarosite</small>                                      <small>Sulfuric acid</small></p>	<p>In clay-rich deposits under acidic conditions generated during pyrite weathering the oxidation products react with illite forming jarosite</p>

According to the literature, the relationship between the amount and rate of pyrite oxidation and the severity of TSA has not yet been investigated. Therefore, it is believed that the relationship between the rate of pyrite oxidation and the extent of TSA should be investigated.

## 2.4.2 The role of sulfuric acid produced as a result of pyrite oxidation in TSA

Quispel et al. (1952) stated that a significant amount of sulfide was formed in soils in the case of exposure to anaerobic conditions. The reactive forms of sulfide will oxidise rapidly when given access to oxygen and water, and will generate sulfuric acid, resulting in an increase in the acidity of soils in the absence of carbonates (Quispel et al., 1952). The deterioration of concrete that has interacted with an aggressive sulfuric acid environment is considered to be a key durability issue that affects structures; it can affect concrete **substructures** as well as concrete in industrial areas where it is susceptible to acid attack (Bassuoni and Nehdi, 2007). The sulfuric acid first reacts with calcium hydroxide in concrete to form gypsum. In addition gypsum will react with  $\text{C}_3\text{A}$  to form ettringite, which causes cracking. Both reactions result in expansion in volume and cracking. Moreover, sulfuric acid leads to the decomposition of calcium silicate hydrate C-S-H and the deterioration of the concrete matrix can accelerate the attack processes (Belie et al., 2004; Monteny et al., 2000; Bassuoni and Nehdi, 2007; Zivica and Bajza, 2001). The following equations illustrate the reactions with sulfuric acid to form ettringite:



Nijad et al. (1988) reported that sulfuric acid attack on concrete can occur in various ways; buried concrete structures can be attacked by sulfuric acid present in natural groundwater or resulting from the dumping of chemical waste from industry, causing localized deterioration of concrete. Kawai et al. (2005) stated that the extent of concrete deterioration is significantly influenced by sulfuric acid and sulfate attack. However, Bassuoni and Nehdi (2007) indicated that the effect of sulfuric acid on concrete is considered to be more severe than that of sulfate attack. In addition, the solubility of the calcium salts formed increased significantly as a result of acid attack. Moreover, Emmanuel et al. (1989) stated that concrete is susceptible to deterioration by sulfuric acid produced from sewage or pyrite oxidation, as a result of the high alkalinity of Portland cement concrete; it was found that the deterioration was increased by an increase in the cement content and sulfuric acid concentration, and sulfuric acid is particularly corrosive because of sulfate ions participating in sulfate attack.

With regard to the role of sulfuric acid in thaumasite formation and the extent of TSA, there are examples in which thaumasite was formed when sulfuric acid was present. Research by Li et al. (2009) on the effect of long-term exposure of cement to sulfuric acid found that cracks appeared in the surface, and crystals in the OPC mortar were observed. OPC mortar showed a low Ca/Si atomic ratio because of the reduction due to decalcification of C-S-H. In addition, the crystals were approximately 50 mm long, and EDX results indicated that the sample containing sulfur, carbon and aluminum, which might be a mixture of ettringite and thaumasite, as shown in Figure 2.3.

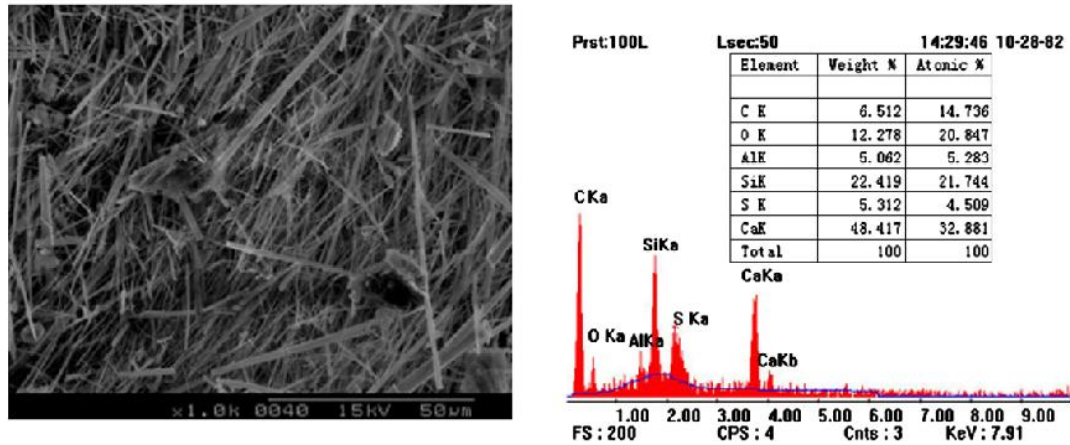


Figure 2.3: The formation of thaumasite in OPC mortar. Li et al. (2009)

Tulliani et al. (2002) reported a case history of concrete foundations in a 35-year-old building in northern Italy, which showed a significant amount of gypsum and in which ettringite and thaumasite were detected. The degradation effect was increased by a decrease in the distance of the concrete structure from an absorbing well located in the courtyard of the building. This well was recognised as the sulfate source because of the microorganisms of sulfur compounds present in sewage. It was observed that the slightly deteriorated sample showed high pH values (higher than 8). Under very low pH, when sulfuric attack is active, all hydration products can be easily decomposed, leading to severe disintegration, and the sulfate attack included attack by sulfuric acid.

Kim and Lee (2010) investigated the deterioration of concrete structures for sewage water treatment. XRD and SEM results showed the formation of gypsum, ettringite and thaumasite as a result of sulfuric acid attack. Hobbs and Taylor (2000) reported that sulfuric acid produced as a result of pyrite oxidation reduces the pH and increases the sulfate concentration in the groundwater, causing damage to the foundations. However, Hobbs and Taylor (2000) claimed that it was not clear whether the cause of TSA in the case of the foundations of M5 overbridges was sulfate attack or sulfuric acid attack or a combination of both. However, Fountain (2003) stated that sulfate attack occurred in low-quality concrete, and, according to the specification of concrete in the case of the M5 foundations at the time of construction, the strength was 60 Mpa, and therefore the concrete used in the column and base slab should have been resistant and fit for purpose. However, the process of generating sulfuric acid due to sewage can participate in concrete deterioration, and this happened in the sump around the M5 bridge. It was concluded that the sulfuric acid is always primary attack mechanisms which cause deterioration in the quality of structures where thaumasite and other sulfate-based minerals are found as deposits in deteriorated locations. Hill et al. (2003)

investigated the influence of combined acid and sulfate attack on concrete. The samples were exposed to a combination of sulfuric acid and sulfate solution for five years, and the w/c ratio was 0.35-0.5. The results showed the presence of thaumasite in SRPC and PLC samples stored in sulfate and weak acid. On the other hand, although thaumasite was detected in small quantities in PLC concrete exposed to sulfuric acid, they concluded that the presence of acid does not result in thaumasite formation.

The role of sulfuric acid in thaumasite formation and the extent of TSA in buried concrete exposed to pyritic ground have been extensively debated in the literature and is considered to be a highly controversial issue. Nevertheless, there is no published research on the role of sulfuric acid produced by pyrite oxidation in thaumasite formation and the development of TSA in buried concrete exposed to pyritic clay. Therefore, it is believed this aspect should be investigated.

#### **2.4.3 The presence of mobile groundwater**

The presence of mobile groundwater is considered an important factor that helps to bring sulfate ions into contact with concrete and participates in accelerating the reaction to form thaumasite and developing the extent of TSA. In clay soil, the flow of groundwater is greatest in the shallow depth. Therefore, shallow foundations and caps of piles might be considered to be subjected to more deterioration due to the flow of groundwater rich in sulfates. The topography of the ground and disturbance of the ground due to construction activity may lead to an increase in the groundwater flow near the foundations. The results of a site investigation at Cheltenham by BRE found that the concentration of sulfate in the groundwater was higher than the sulfate content in the clay. It was also found that the sulfate concentration depended on the flow in the permeable parts of the ground. However, the risk of severe TSA due to the presence of groundwater can be considered relatively small as groundwater conditions differ in individual locations and small parts of sites might have significant flows of groundwater rich in sulfates (Clark, 2002). Floyd et al. (2003) reported that concrete structures above the water table will not suffer from TSA as much as those below water level or in contact with the groundwater because of the replenishment of sulfate required for the reaction of the oxidation of pyrite. This was confirmed by Slater et al (2003) who reported that the extent of TSA was strongly related to groundwater level.

## 2.5 Factors controlling thaumasite formation and TSA

### 2.5.1 The role of pH on formation and stability of thaumasite

The reactivity and stability of thaumasite at various pH levels were studied by Jalled et al. (2003), who examined samples of natural thaumasite, placed in three solutions with different pH values. The research showed that the environmental pH levels play an important role in thaumasite formation. At low pH ( $< 11$ ) thaumasite reacted with ions present in the solutions, while at pH level  $> 11$  minor amounts of calcium carbonate were recorded. However, the reaction between ions and thaumasite does not seem to occur at pH ( $= 12$ ), and thaumasite was stable at pH level 13.

Zhou et al. (2006) investigated the role of pH in TSA by examining specimens made with OPC with 5% limestone, SRPC, and PLC with 20% limestone, stored in SD-3 sulfate solution with pH level  $> 12$ , whereas other samples were immersed in sulfuric acid solution. In alkaline solutions with pH = 12 or above, thaumasite formed and caused damage, especially in specimens made from PLC with 20% limestone. However, the presence of acid does not promote thaumasite formation; even less thaumasite formation was observed in samples immersed in sulfuric acid solution. On the other hand, Hobbs and Taylor (2000) stated that sulfuric acid produced as a result of pyrite oxidation reduces the pH and increases the sulfate concentration in the groundwater, causing damage to the foundations. Scrivener et al. (2007) reported that the thermodynamic stability of thaumasite depends on pH level, with thaumasite stable at low pH, even at high temperature (20°C). Gaze and Crammond (2000) reported that thaumasite will stop forming at pH below 10.5, whereas Hartshorn et al. (1999) and Tsvilis et al. (2003) proposed that, once thaumasite was formed, it might be stable at pH as low as 7. Crammond (2003) suggested that, when pH dropped to 7, hydroxyl ions are consumed, leading to maintenance of a high pH. However, as all hydroxyl ions are consumed, the pH decreases and thaumasite becomes less stable. Sahu et al. (2002) observed thaumasite and gypsum coexisting in a concrete slab at a pH of 10-11, whereas it was likely that thaumasite and ettringite would coexist at a pH range of 11-12, and the zone with a pH greater than 12 contained only ettringite. In terms of the role of pH in the stability of reaction products that might accompany TSA, ettringite becomes unstable at lower alkalinity and will eventually decompose to gypsum when the pH falls below about 10.5-10.7 (Gaze and Crammond, 2000; Lee et al., 2005; Taylor, 1997). Torres (2004), Jenni et al. (2013) and Kunther et al. (2013) reported that ettringite is also not a stable phase in the presence of a high concentration of bicarbonate, resulting in a reduction in pH in the pore solution of concrete. Collete et al. (2004) highlighted that the solubility of calcite and gypsum was high at pH of about 7-7.5, while more gypsum would precipitate at pH between

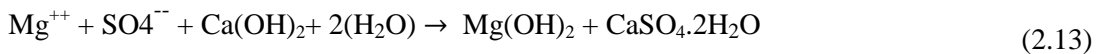


9-10 and 5-6. According to the literature, there has been no technical investigation of the effect of pH of pyritic clay containing calcite in its composition on thaumasite formation and the extent of TSA. Therefore, investigation into this aspect is required.

### 2.5.2 The role of magnesium

Magnesium-bearing components are known as the most harmful chemicals in respect of concrete durability. The work carried out by the University of Sheffield (Hartshorn et al., 1999; Hartshorn et al., 2002) indicates that **small amounts** of thaumasite, accompanied by ettringite and gypsum were found in cement past containing 5% and 15% limestone filler placed in 1.8 % magnesium sulfate solution, while thaumasite, brucite and calcite were identified in the deteriorated material from specimens containing 35% limestone. They concluded that magnesium plays an important **role in** deterioration of cement paste. Hobbs, (2003) reported that the presence of magnesium ions along with carbonate aggregate found to reduce the performance of SRPC concrete. In addition, in the absence of magnesium ions, the performance of SRPC concretes and OPC-70% slag concretes at 5°C was independent of aggregate type.

The primary step in the interaction between cement hydration products and magnesium sulfate solution is the reaction with calcium hydroxide to form brucite  $Mg(OH)_2$  and calcium sulfate in the form of gypsum, as shown below:



The C–S–H phase is significantly degraded in the presence of magnesium compared to other sulfate compounds. The pH of the concrete pore solution decreases after the consumption of all calcium hydroxide, leading to a complete degradation of the C-S-H phase and transforming to the non-cementitious M-S-H (Skalny, 2002).

The reaction mechanism of  $C_3A$  and magnesium sulfate interactions, as reported by Clark and Brown (2000), resulted in ettringite and gypsum formation, and the reaction rate increased with temperature, as shown below:



### 2.5.3 The effect of sulfate solution concentration

Concentration of sulfate solution may accelerate thaumasite formation and cause severe damage. Kim et al. (2005) investigated the effect of solution concentration on thaumasite formation with mortar samples made with Portland cement and metakaolin as replacement



material with different percentages of replacement (0%, 5%, 10% and 15%). Specimens were stored in magnesium sulfate solution with different concentrations 0.42%, 1.27% and 4.24%. It was found that no signs of TSA were observed in low concentrations of solution (0.42%) for up to 360 days. However, mortar samples containing 10% and 15% metakaolin which were exposed to 1.27% magnesium sulfate solution were more susceptible to thaumasite sulfate attack than those with 0% metakaolin, deterioration detected was recorded after 81 days. Moreover, specimens exposed to high concentrations (4.2%) showed significant deterioration, including spalling and wide cracking throughout specimens. It was also found that formation of ettringite was observed at low concentrations (<4000 ppm of  $\text{SO}_4$ ), while ettringite and gypsum formed at medium concentrations (> 4000 and <7500 ppm of  $\text{SO}_4$ ), and thaumasite formed at high concentrations (>7500 ppm  $\text{SO}_4$ ). Pouya, (2007) investigated the performance of OPC and SRPC concrete exposed to DS-3 (3000 mg/l  $\text{SO}_4$ ) and DS-4 (6000 mg/l  $\text{SO}_4$ ) at 5, 10 and 15 °C. It is found that OPC concrete samples suffered from extensive thaumasite attack at 5, 10 and 15 °C with greater damage on samples in DS-4 compared to DS-3 conditions after 12 months. In addition, the effect of sulfate concentration on extent of attack became more evident as temperature decreased probably due to enhanced TSA at temperatures below 20 °C.

#### 2.5.4 The effect of temperature

Temperature is an important factor that may affect the formation of thaumasite. As many investigators have reported, the optimum temperature for the formation of thaumasite is about 5°C (Thaumasite Expert Group, 1999; Bensted, 1988; Halliwell et al., 1996; Crammond and Halliwell, 1995; Halliwell and Crammond, 2000; Van et al., 1975). However, there is an argument regarding the temperature for thaumasite formation, since Diamond et al. (1999) reported that TSA was identified in warm regions of California. Moreover, Hartshorn et al. (2002) showed that the extent of thaumasite sulfate attack would be greater at 5°C than at 20°C.

Scrivener et al. (2007) investigated the influence of temperature on thaumasite formation at 8°C and 20°C. Thaumasite formation was observed at both temperatures, although less thaumasite was recorded at 20°C than at 8°C. They concluded that thaumasite might form at temperatures up to 45°C under the same experimental conditions. Furthermore, an investigation of the decay of pavement mortar caused by thaumasite formation carried out by Rojas et al. (2008) revealed that thaumasite was formed at temperatures between 18°C and 40°C with a high degree of humidity. Pipilikaki et al. (2008) investigated the effect of temperature on thaumasite formation in mortar samples made of CEM I and CEM II

containing 15% limestone filler. The samples were exposed to 5% sodium sulfate solution for a year at 5°, 10° and 20° C. It was found that there was some damage in samples stored at 5° C and 10° C, showing the formation of thaumasite. However, specimens stored at 20° C remained intact and thaumasite could not be identified. Collet et al. (2004) reported that at low temperature the amount of dissolved carbonate in solution at 0°C was twice the amount at 25°C. In addition,  $(\text{Si}(\text{OH})_6)^{2-}$  groups is stable at lower temperatures, as reported by Bensted (2003).

### 2.5.5 The role of chloride in the thaumasite form of sulfate attack

Thaumasite formation has been reported in many field investigations in the presence of chloride ions. Eden (2003) investigated core samples which were taken from bridges and other motorway structures throughout the UK. The results showed that there is a high level of  $\text{Cl}^-$  in the cement paste damaged concretes due to TSA, for which the source of chloride is de-icing salt from motorway, suggests that chloride might contribute in the development of TSA, as solubility of gypsum increases in the presence of chloride ions at low temperatures.

Hagelia et al. (2003) examined thaumasite formation in some Norwegian concrete, including sprayed concrete on alum shale in Oslo, the Akebegvier road cutting and the Ekberg highway tunnel. It was noticed that thaumasite was detected in all the concrete, and the relative severity rank ranged from 1 to 4, which gave an indication that  $\text{Cl}^-$  may play a role in the development of TSA. Romer et al. (2003) investigated the concrete damage in Swiss tunnel structures due to thaumasite formation. It was found that neutral groundwater conditions led to thaumasite sulfate attack rather than the formation of ettringite. It was noticed that thaumasite was formed also in the corrosion zone and the analysis of groundwater indicated that it contains chloride with a concentration of 1700 g/l. Wimpenny and Slater (2003) investigated the evidence from the highway agency in Gloucestershire that support the mechanism of thaumasite formation. It was noticed that there was a reduction in chloride concentration in the area of sulfate attack. Moreover, the microstructural analysis also indicated the presence of chloride ion in deteriorated material due to TSA. Sibbick et al. (2003) reported that thaumasite formed in areas in contact with seawater containing 13,496 mg/l of  $\text{Cl}^-$ . This was evidence for considering that  $\text{Cl}^-$  has an important effect on TSA.

Brown and Doerr (2003) studied the chemical change in concrete due to ingress of aggressive species. It was found that sulfate attack has occurred in homes built on soil contained significant amounts of soluble salts  $\text{NaCl}$ ,  $\text{NaSO}_4$  and  $\text{MgSO}_4$ . The microstructural

examination indicated that Na, Mg, SO<sub>4</sub> and Cl<sup>-</sup> have participated in the formation of various phases in concrete such as brucite, Friedel's salt and thaumasite. Ma et al. (2006) investigated the formation of thaumasite in a tunnel at Bapanixa Dam in western China. A significant amount of sulfate, chloride and carbonate was found in the groundwater. It was found that Friedel's salt was not observed, which suggests that instability of Friedel's salt in the presence of carbonate ions in a system likely to develop thaumasite. However, Knight and Wimpenny (2003) reported that there was no correlation between the depth of thaumasite and the maximum depth of SO<sub>3</sub>, and the Cl diffusion coefficient suggested that Cl does not influence the severity of thaumasite attack. In addition, the Cl<sup>-</sup> diffusion coefficient was found to be approximately five times the magnitude of the sulfate diffusion coefficient. This indicates that concrete is more vulnerable to Cl<sup>-</sup> ingress than sulfate ingress. Moreover, the exposure to Cl<sup>-</sup> is relatively low for buried concrete compared to other elements of highway structures. There was evidence, from comparing the depth Cl<sup>-</sup> levels with the sulfate profile, that Cl<sup>-</sup> ingress has been increased by the damage caused by thaumasite formation.

In the laboratory study, Torres (2004) investigated thaumasite form of sulfate attack in mortar containing calcium carbonate in the presence of chloride. The mortar samples were cast using Portland cement replaced by 10% or 15% of limestone filler. In addition, samples were stored in combined sulfate and sodium chloride at 5° and 20°C. The results indicated that the effect of chloride on sulfate attack is temperature-dependent. Moreover, sulfate attack was mitigated at samples stored at 20°C. However, thaumasite was formed in all samples stored at 5°C. It was reported from the microstructure results that chloride does not seem to enter the thaumasite crystal structure. Therefore, the role of chloride in the thaumasite form of sulfate attack appears to be primarily catalytic. The attack appeared to be mitigated at the chloride concentration of 0.5% and the critical concentration was found to be between 1% Cl<sup>-</sup> and 2% Cl<sup>-</sup>.

However, Sotiriadis et al. (2010), who investigated the effect of chloride on TSA in limestone cement concrete, found that chloride played an inhibitory role. Concrete samples made from OPC with two limestone fillers, 15% and 35%, were exposed to six solutions of sulfate and chloride, and stored at 5 °C . The sulfate and chloride solutions contained 10 g/l or 20 g/l of SO<sub>4</sub> and 21.14 g/l of Cl<sup>-</sup>. The results indicated that chloride delayed the deterioration of concrete specimens and improved the behaviour of concrete in a corrosive environment, as shown in Figure 2.4.

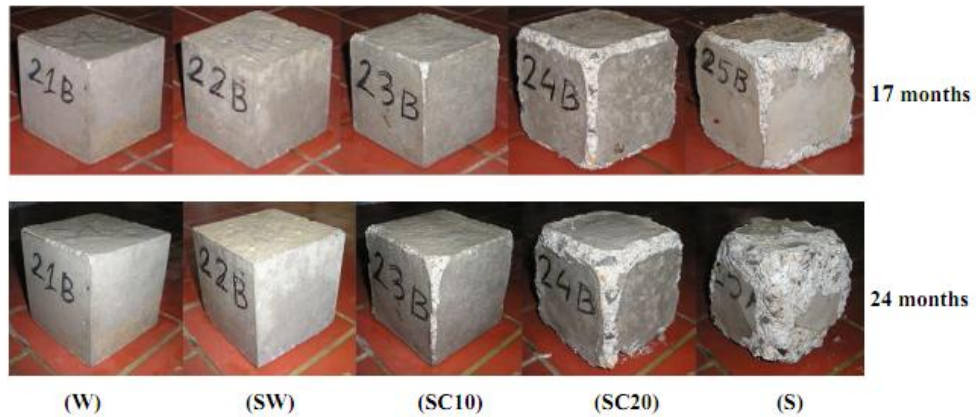


Figure 2.4: The mitigation effect of chloride on TSA. Sotiriadis et al. (2010)

## 2.5.6 Relative resistance of cement and cement binder

### I. Limestone filler

Hartshorn et al. (2002, 1999) studied the formation of thaumasite in Portland limestone cement, using mortar prism specimens made from OPC and OPC with limestone filler; the replacement levels were 5%, 15%, and 35%, and samples were stored in 1.8% magnesium sulfate solution at 5°C and 20°C. They concluded that the amount of thaumasite was greater at 5°C than 20°C. In addition, the mortar prisms containing 35% limestone filler were significantly damaged after 126 days of exposure, and up to 7% of mass was lost after 280 days. However, a small amount of thaumasite was formed in the case of 5% limestone filler.

Table 2.2 summarises the results of the research.

Table 2.2: Thaumasite formation in concrete containing limestone filler (Hartshorn et al. 1999)

Limestone replacement (%)	Onset of thaumasite formation (Days)
0	Not detected
5	252
15	196
35	126

Choi et al. (2008) investigated the effect of limestone filler on mortar specimens. The specimens were made with OPC with and without limestone filler (10%, 20% and 30%) and saturated in sodium and magnesium sulfate solution contain 33,880 ppm as  $\text{SO}_4$ . It was found that the test results emphasised the poor performance of concrete containing 10% to 30% limestone filler when subjected to sodium and magnesium sulfate attack, which was reported from the visual observation, in contrast with specimens without limestone filler.

Furthermore, Tsivilis et al. (2007) reported that thaumasite was detected after one month of exposure to magnesium sulfate solution at 5°C and that samples made from 30% replacement limestone filler severely suffered compared to those with 15% limestone replacement. The research showed that, while samples made with PC showed very slight attack. The results of research concluded that paste containing limestone filler is susceptible to TSA at low temperature, and the deterioration becomes significant as the amount of limestone filler increases. Irassar et al. (2003) emphasised the poor performance of limestone filler in research which investigated mortar samples containing 20% limestone filler saturated in sodium sulfate solution at 20°C and compared the samples to those containing OPC and SRPC. Justnes (2003) examined concrete specimens containing 20% limestone filler made according to the Norwegian cement standard and exposed to 5% sodium sulfate solution at 5°C. It was found that thaumasite formed within ten months and caused mass loss and expansion.

European standard EN 197-1 (2011) classified Portland limestone cement into two types: II/A-L, which contains 6-20% limestone filler, and II/B-L, which contains 21-35% limestone filler. However, Portland cement with limestone filler has been found less durable and more susceptible to TSA.

## **II. Pulverized - fuel ash (PFA)**

An investigation carried out by Nobst and Stark (2003) examined the performance of OPC with 20% PFA replacement concluded that the addition of PFA in cement has a positive effect on the sulfate resistance. However, the results show that replacement with small quantities of fly ash does not resist thaumasite formation. Zhou et al. (2006) investigated the influence of OPC with 25% PFA replacement. They found that 25% PFA replacement provided a little protection, which deterioration due to TSA was observed. Pouya (2007) investigated the performance of concrete made with 36% PFA, with a cement content of 300 and 380 Kg/m<sup>3</sup>, exposed to DS-3 and DS-4 sulfate solutions and Lower Lias Clay, at 5°, 10°, 15° and 20°C. It was found that PFA concrete containing 300 kg/m<sup>3</sup> placed in DS-4 and clay showed no apparent sign of TSA at all temperatures. However, concretes containing 380 kg/m<sup>3</sup> showed signs of deterioration due to TSA at 5°, 10° and 15°C. It is concluded that PFA might be able to delay TSA in normal ground conditions but that PFA concrete seems to be vulnerable to TSA at normal ground temperature as well as at 5°C in the long term.

On the other hand, an examination of ten-year-old concrete sample blended 30% and 50% and exposed to marine environment by Thomas et al. (2003, 2001) showed no sign of thaumasite formation in spite of the presence of sulfate and carbonate. Hill et al. (2002), in

part of an investigation of the long-term durability of PFA concrete in sulfate solutions, observed that PFA concrete was attacked due to ettringite rather than thaumasite. However, the retarding effect of fly ash against sulfate attack has been reported by Tsivilis et al. (2003). Mulenga et al. (2003) stated that limitation or increasing thaumasite formation by blending cement with fly ash is depending on the type of cement used. They found that SRPC mortars did not show thaumasite formation whereas those containing 50% fly ash were accompanied by thaumasite deterioration. Furthermore, PLC mortars made with 40% fly ash showed limited thaumasite formation, while in mixes with 50% fly ash no thaumasite was formed. Crammond et al. (2003) investigated TSA on concrete made with 30% PFA and different types of aggregate. Concrete cubes were buried in clay in the field trial at Shipston on Stour for three years. It was concluded that concrete made with 30% PFA performed well irrespective of aggregate type. However, concrete with 30% PFA replacement did not perform well in a parallel laboratory study in the case of exposure to DS-3 sulfate solution. Bellman and Stark (2007, 2008) investigated the prevention of thaumasite sulfate attack by studying the effect of using PFA cement as replacement material. Specimens were made with CEM I and PFA with a replacement percentage of 20% and 40%, CEM II with 5% silica fume, and CEM III/B. The results showed that PFA 20% and 40% replacements performed well in resisting the thaumasite form of sulfate attack at low temperature, compared to other types of cement used in this study. They suggest that a low calcium/silica ratio in C-S-H resulted from consuming of calcium hydroxide by PFA might be the reason for the high resistance to TSA.

### **III. Ground granulated blastfurnace slag (GGBS)**

Higgins and Crammond (2003) investigated the effect of OPC with 70% GGBS replacement in controlling TSA in a laboratory study. The study revealed that concrete blended with 70% GGBS showed good performance, and no signs of TSA were observed with either normal or high-aluminate GGBS. Zhou et al. (2006) confirmed the good performance of GGBS by testing specimens with 65% GGBS replacement. Although the specimens were in an aggressive solution for a period of two years, the GGBS performed well, with no evidence of TSA; this was attributed to:

- the lower permeability of concrete made of GGBS, which prevents sulfate species from penetrating concrete and causing TSA.
- the lack of portlandite as reactant in thaumasite formation as well as the low pH of concrete pore solution due to high replacement with GGBS as thaumasite will not form at low pH.



Tsivilis et al. (2003) investigated the effect of mineral admixtures in concrete in preventing TSA by examining samples made with OPC containing 15% limestone filler, PFA and GGBS. The specimens were placed in magnesium sulfate solution and cured at 5° and 25°C. It was found that the GGBS had a higher resistance to thaumasite sulfate than other concretes. Barnett et al. (2002) carried out an investigation of thaumasite formation in specimens containing OPC, OPC - 70% GGBS and 100% GGBS which were exposed to magnesium sulfate solution. It is found that OPC specimens produced much thaumasite, but the OPC - 70% GGBS specimens produced only trace amounts of thaumasite. Moreover, the 100% GGBS specimens did not show any thaumasite. Crammond et al. (2003), in the three years of the field trial at Shipston on Stour, found that concrete made with 40% and 70% GGBS performed well irrespective of aggregate type. However, 40% GGBS did not perform well in a parallel laboratory study in the case of exposure to DS-3 sulfate solution. Pouya (2007) investigated the performance of concrete made with 66% GGBS, exposed to DS-3 and DS-4 sulfate solutions and Lower Lias Clay at 5°, 10°, 15° and 20°C for twelve months. The superior performance of GGBS concrete in sulfate-enriched clay was in line with the performance of concrete cubes immersed in DS-3 and DS-4. However, minor quantities of thaumasite were identified in the case of sulfate solutions. Pouya (2007) also investigated the performance of 66% GGBS replacement, exposed to DS-4 for five years at 5°C. It was found that large cracks formed along edges, indicating that GGBS does not provide absolute resistance against sulfate attack. Gypsum formation was the predominant form of deterioration in GGBS concrete; however, ettringite and thaumasite were found in minor quantities.

#### **IV. Sulfate resistant Portland cement (SRPC)**

SRPC which contains low amounts of  $C_3A$  is extremely resistant to conventional sulfate attack. Bensted (1999) also revealed that SRPC, which provides protection against normal sulfate attack by maximizing the ferrite phase at the expense of the aluminates phase, can be subjected to thaumasite formation if the conditions are right. A study carried out by Higgins and Crammond (2003) found that TSA was present in all specimens made from SRPC and stored in sulfate solution. In addition, TSA increased with time, and there was no difference between the performance of SRPC and that of concrete made with OPC. The results of an investigation of the effect of  $C_3A$  by Varela et al. (2006) revealed that thaumasite can form whether the cement has a high or a low  $C_3A$  content. Moreover, low- $C_3A$  cement can produce a higher amount of thaumasite than high- $C_3A$  cement, which emphasises the poor resistance of SRPC as low  $C_3A$  cement. Crammond (2003) also reported that a low  $C_3A$  content does not improve the cement resistance to thaumasite attack. Further investigations carried out by Blanco et al. (2006) showed that thaumasite detected in mortars with low- $C_3A$

cement, whereas thaumasite- ettringite solid solution identified in mortars made with high- $C_3A$  cement. Mulenga et al. (2003) investigated TSA in SRPC and SRPC blended with 50% fly ash. It was found that thaumasite was formed in both concretes; however, no significant signs of deterioration were identified in SRPC, in contrast with 50% replacement fly ash, where extensive damage occurred. Pouya (2007) investigated the performance of concrete made with SRPC and exposed to DS-3 and DS-4 sulfate solutions and sulfate-enriched clay at 5°, 10°, 15° and 20°C for 12 months. It was found that SRPC concrete suffered from TSA in the case of exposure to DS-4 sulfate solution and sulfate-enriched clay at 5° and 10°C, while no signs of deterioration were observed at 15° and 20°C. On the other hand, Crammond et al. (2003), in the field trial at Shipston on Stour, concluded that cast-in-situ SRPC concretes made with siliceous aggregates performed satisfactorily, while SRPC concrete containing carbonate aggregates showed severe signs of attack. In addition, SRPC cement with 1%  $C_3A$  and made with siliceous aggregate performed well, and no signs of attack were observed. Hobbs (2003) highlighted that SRPC performance was reduced by the presence of magnesium ions and carbonate aggregate, but performed well in the absence of magnesium. Irassar et al. (2004) carried out work on thaumasite formation in limestone filler cements exposed to sodium sulfate solution at 20°C. They found that thaumasite was not identified in either SRPC or cement with 0%  $C_3A$ , containing limestone filler. It would appear that the formation of ettringite, which is prevented by SRPC, might be important for the later formation of thaumasite at 20°C.

It seems that there are very few published investigations concerned with the interaction between pyritic ground and concrete (Crammond et al., 2003; Floyd et al., 2003). Most reported investigations into the performance of different binders were conducted by exposing samples to sulfate solutions rather than to pyritic ground conditions. In fact no studies into the long-term performance of SRPC and 25% PFA binders exposed to pyrite-bearing soils were found, despite an extensive literature review. In addition, the performance of concrete made with 50% PFA and 70% GGBS in actual ground conditions containing pyrite and carbonate has not yet been investigated. Therefore, the long-term performance in terms of resistance to TSA of SRPC and 25% PFA replacement, which are still recommended in BRE SD-1 (2005) and BS 8500 (2006), should be investigated. In addition, the performance of concrete with 50% PFA and 70% GGBS should also be examined with regard to protection against TSA in pyritic clay.

### **2.5.7 Surface Coatings**

Controlling concrete durability becomes a concern as the long-term durability of concrete might not be achieved. Swamy et al. (1998) and Aguiar et al. (2008) pointed out that



concrete is a porous material, in which ingress of harmful species cannot be prevented even if concrete quality is improved. Therefore the low porosity and permeability of concrete might not stop concrete degradation. Thus, a surface coating is required in aggressive environments in order to act as a barrier between the aggressive environment and the concrete. Ariyaratne (2008) reported that concrete coatings are mentioned in many references but not as many as for steel. In addition, the selection of a coating for concrete is a complex process and is affected by several factors:

- the type of surface to be coated and its conditions
- construction methods
- the environment and the level of aggressiveness
- temperature at the time when the coating is being cured
- system life required.

Delucchi et al. (1997) carried out work on the physico-chemical properties of organic coatings for degradation control. They concluded that coatings should have a capability to resist gases and liquids, low permeability, good adhesion and alkali resistance in order to protect concrete. Guidance on the use of concrete in aggressive clay (BRE SD-1, 2005) recommended the use of a coating in the case of sulfate class SD-5 in order to provide additional protection for concrete.

There is a wide range of surface coatings on the market, including chlorinated rubber, epoxy and bitumen. It becomes difficult to choose the appropriate type of coating. Almusallam et al. (2002) reported that many manufacturers ignored the engineering requirements of such coatings, with the result that concrete coatings have either failed to fulfill their intended functions or have lacked reasonable durability. The performance of different coatings under various conditions has been extensively investigated (Swamy et al., 1998; Swamy and Tanikawa, 1993; Aguiar et al., 2008; Almusallam et al., 2002; Saraswathy and Rangaswamy, 1998). Other coatings that normally react with the hydration products of cement and penetrate and block the capillary pores of cement have shown adequate improvement in concrete durability in aggressive conditions (Fattuhi and Hughe, 1983; Marusin, 1987). There is also a need to develop guidance for the selection of appropriate coatings in different conditions. Aguiar et al. (2008) investigated the performance of coated and uncoated CEM I concrete under different exposure conditions, namely chloride, sulfate and acid attack; acrylic and epoxy resin coatings were applied on concrete. They concluded that coated concretes perform well against chloride penetration and sulfate attack compared to uncoated concrete, and epoxy coatings result in lower chloride penetration than acrylic coatings.

However, degradation was observed in both coated and uncoated concrete exposed to sulfuric acid. On the other hand, the investigation by Vera et al. (2013), who studied the effect of surface coatings of reinforced concrete placed in an acid environment for 589 days, revealed that better performance of concrete against acid attack was achieved by using an epoxy coating. Moradillo et al. (2012) claimed that most surface coatings appeared to be effective in their early stages, whereas their performance declined in the long term. Almusallam et al. (2003) investigated the effectiveness of surface coatings in improving concrete durability. They recommended using epoxy, polyurethane, or acrylic coatings, in the order given, for protecting concrete in the case of exposure to chemical attack.

Ariyaratne (2008) stated that bitumen provides an economical alternative for coating buried concrete; with good resistance to acid, aggressive species and water penetration as well as adhering well to the concrete surface. Bitumen-protected PLC concrete samples that were subjected to DS-4 sulfate solution for five years were studied by Pouya (2007). He suggested that the coating acted to prevent ingress of sulfate and carbonate ions by reducing permeability at the surface, and thus provided a simple and effective barrier safeguarding the concrete against chemical degradation. However, it would appear that there is no technical information on the long-term durability of bitumen coatings, and there are no data in the literature with regards to the performance of bitumen as a surface coating to protect buried concrete in aggressive ground conditions such as pyritic clay. Therefore, there is a need to investigate the long-term durability of bitumen coatings for buried concrete subject to pyritic clay in order to prevent deterioration caused by the thaumasite form of sulfate attack, where the conditions favorable for thaumasite formation are available.

## **2.6 UK guidance on the assessment of aggressive ground conditions**

Guidance and standards for concrete design to prevent sulfate attack were developed, especially in the UK, after the discovery of the severe deterioration due to thaumasite sulfate attack. For example, the report issued by the Thaumasite Expert Group (TEG) recommended the appropriate specification to minimize the risk of TSA (Clark 2002). In addition, there is guidance issued by the Building Research Establishment (BRE, 2005) which is recommended in the UK. Moreover, Pouya, (2007) reported that the British institution and the UK Highways Agency (HA) have established standards related to sulfate attack. According to Nixon et al. (2000), new guidance was developed after the publication of the TEG report in 1999, including BRE Special Digest 1 (SD1), an amendment to the British Standard BS 5328 published in 2001, amendments to BS 882, BS 8500, and the Manual of Concrete Documents for Highways Agency. All these guides and standards summarise the important points in minimising sulfate attack in aggressive ground conditions.

With regard to the assessment of ground aggressivity, BRE SD1:2005 part C deals with the assessment of aggressive ground conditions. It outlines procedures for determination of sulfate class (DS) and aggressive chemical and environment for concrete (ACEC) from the soluble sulfate and magnesium and potential total sulfur present in the ground. However, the effect of other species such as Ca, Na, Cl and K and the presence of carbonate in the ground have not been included in the assessment of the aggressiveness of ground. The chemical testing protocol to determine sulfur compounds has been addressed by TRL 447. For total sulfur, microwave digestion of samples to liberate all sulfur into solution and sulfur is analysed using ICP-AES. Another technique to determine the total sulfur is the LECO technique.

The recommendations suggested in BRE SD1 (2005) and similar standards are based upon laboratory studies involving the immersion of concrete specimens in test sulfate solutions which might be magnesium sulfate or sodium sulfate or a combination of both. Therefore, the influence of field conditions such as the presence of a carbonate source in clay, the chemical composition of clay, the effect of burial depth on the extent of TSA and the assessment of aggressive ground with regard to TSA should be investigated, and guidance should be developed accordingly.

# CHAPTER 3

## 3. Methodology

### 3.1 Introduction

This chapter details the experimental design for the investigation of the thaumasite form of sulfate attack in buried concrete made with different binders. It also presents the materials that were used to study both the nine-year-long interaction of pyritic clay and concrete and the influence of chemical compositions of different clays on the severity of the thaumasite form of sulfate attack. Environmental exposure conditions, including sulfate solution, clays, and simulated clay pore solutions, are also described. The proposed tests to examine chemical, physical, mineralogical and microstructural changes of concrete and clay which were carried out to investigate thaumasite in buried concrete are also presented.

Some of the limitations of this study are associated with the limited time available for a PhD Programme, especially when durability issues are examined. Deterioration in structures, subjected to real environmental conditions, occurs over a long period of time. Hence, for the purpose of this work, the deterioration processes need to be accelerated. In addition, there was a limited access to XRD and SEM test. Therefore, samples were selected for XRD and SEM test on basis of deteriorated concrete specimens. Furthermore, as several different factors were considered in this investigation, for practical reasons the the number of samples exposed to clay had to be limited. The repeat monitoring of the progress of deterioration and testing these samples was carried out every 3 months as done for samples in solutions. Under these circumstances it would be difficult to make exact assessments of the repeatability of the data presented in the thesis, but subjective assessments of the accuracy of the data have been considered in coming to the conclusions derived from the findings.

### 3.2 Experimental design and programme

The experimental programme was designed after reviewing the literature and identifying important factors that have not been previously documented with regard to thaumasite in buried concrete made with different binders. The experimental programme was divided into two series: **series I** relates to the laboratory study of long-term interaction of buried concrete

with Lower Lias Clay, while **series II** relates to the influence of chemical composition of clay on the extent of TSA, as described below.

### 3.2.1 Long-term study (nine years) of interaction between concrete and Lower Lias Clay

The aim of series I was to investigate the long-term durability and chemical changes of different concrete binders exposed to Lower Lias Clay for nine years. Series I also studied the effect of bitumen coating in preventing the disintegration of concrete due to TSA; the influence of exposure depth on the extent of TSA; the long-term chemical changes in Lower Lias Clay, including level of sulfate concentration, rate of pyrite oxidation, and reduction in carbonate content; and the relationship between the reduction in total and oxidisable sulfur and the severity of TSA. The concrete binders and experimental parameters are illustrated in Table 3.1.

Table 3.1: Parameters considered in the long-term investigation (nine years)

Experimental series	Parameters			
	Mixes	Temperature	Sample size	Exposure conditions
I	PC	5 °C	Columns 100x100mm and 1.2m high	Slightly weathered Lower Lias Clay
	PLC			
	SRPC			
	PC- 25%PFA (PC-PFA)			
<ul style="list-style-type: none"> <li>• Mobile groundwater was simulated.</li> <li>• Exposure period for series I is 9 years</li> </ul>				

### 3.2.2 The influence of the composition of clay on the severity of TSA

In order to evaluate the formation of thaumasite in buried concrete and the severity of TSA, series II studied factors such as exposure to sulfate solution, pyritic clay, and sulfuric acid generated from pyrite oxidation, and the composition of different clays, which included sulfate, calcium, carbonate and pyrite. The ultimate aim of the project was to investigate the influence of the chemical composition of clay on the severity of TSA. To achieve this, a number of key criteria had to be met. These are listed below:

- In order to develop thaumasite **formation** in a short time frame during the investigation period and to observe differences that could occur with changes in experimental variables, thaumasite formation needed to be accelerated. On the other

hand, ground conditions in the field must be simulated accurately. Therefore, a relatively high water /binder ratio (0.6) was used for the concrete, to accelerate any thaumasite formation and at the same time to control ground exposure conditions. The high W/C ratio is acceptable method to accelerate the reaction as reported by Brueckner (2007), which would increase permeability and porosity of concrete, allowing chemical species to penetrate concrete more rapidly and initiate reactions. In addition, Portland cement (CEM I), replaced with 10% of limestone filler was used, in order to accelerate thaumasite.

- In order to simulate the underground conditions, the degree of compaction and presence and absence of mobile groundwater were also considered.
- To discover how thaumasite formation and the rate of pyrite oxidation are influenced by temperature, two temperatures were considered: 20°C and 5°C.
- The influence of changes in clay chemistry during exposure that might lead to an increase in the aggressivity level of the ground was also considered as an important factor in this study. Therefore, different compositions of clay, with regard to the amount of sulfate, pyrite and carbonate available which lead to the generation and buffering of acid conditions, and the extent of the absence of these factors in sulfate solutions, were also addressed.
- To assess the severity of TSA that might be caused by clay, it is important to compare thaumasite formation and TSA in similar concretes placed in sulfate solutions with different concentrations and in simulated solutions equivalent to clay pore solution compositions without considering the acid conditions produced in the clay.
- Using different binders in order to control TSA, as recommended by BRE SD-1 (2005), was also considered.

The concrete binders and experimental parameters are summarised in Table 3.2.

Table 3.2: Experimental programme for the influence of clay composition on TSA

experimental Series		Parameters			
		Mixes	Temperature	Sample size	Exposure Conditions
II	A	CEMI	5	70 mm cubes	- DS-4 (6 g/l SO <sub>4</sub> ) magnesium sulfate solution. - DS-2 (2 g/l SO <sub>4</sub> ) magnesium sulfate solution
		CEMI-10%LF (CEMI-LF)			
		CEMI-50%PFA (CEMI-PFA)	20		
		CEMI-70%GGBS (CEMI-GGBS)			
	B*	CEMI	5	Columns 70 mm and 1.2m high	-Weathered Lower Lias Clay (W-LLC)  - Slightly weathered Lower Lias Clay (SW-LLC)
		CEMI-10%LF (CEMI-LF)			
		CEMI-50%PFA (CEMI-PFA)			
		CEMI-70%GGBS (CEMI-GGBS)			
	C	CEMI	5	70 mm cubes	- Coal Measures mudstone (CM)
		CEMI-10%LF (CEMI-LF)			
		CEMI-50%PFA (CEMI-PFA)	20		
		CEMI-70%GGBS (CEMI-GGBS)			
	D	CEMI	5	70 mm cubes	-Solution equivalent to weathered LLC pore solution
		CEMI-10%LF (CEMI-LF)			20
Remarks		* Ground water mobility is simulated in series II (B), while its absence in series II (C) * Exposure period for series II is 24 months.			

### 3.3 Experimental details

In this section, the materials used, environmental exposure conditions and the proposed tests to examine chemical, physical, mineralogical and microstructural changes of samples (soil and concrete) are presented for both series I and series II of the experiment.

#### 3.3.1 Long-term study (nine years) of interaction between concrete and Lower Lias Clay

##### 3.3.1.1 Cementitious binders and concrete mixes

Concrete mixes were prepared using Portland cement (PC), Portland limestone cement containing 20% limestone filler (PLC), sulfate-resisting Portland cement (SRPC) and PC blended with 25% PFA (PC-PFA). A water/binder ratio of 0.45 was used in all mixes and siliceous aggregates were used for both the coarse and fine fractions.

### 3.3.1.2 Lower Lias Clay

Partly weathered Lower Lias Clay obtained in May 2002 from Moreton Valence, Gloucestershire, UK was used to simulate the ground conditions. The clay contained 1.00% sulfur and its sulfate class conformed to DS-4 according to the current BRE SD1 (2005) classification. The amounts of water- and acid-soluble sulfate and total sulfur prior to interaction with concretes are listed in Table 3.3, together with the BRE specification for the sulfate design class. The water-soluble cations and anions together with the carbonate content and pH are shown in Table 3.4.

Table 3.3: Initial characterisation of Lower Lias Clay used in this investigation: sulfates and pyrite (DS: design sulfate class; ACEC: aggressive chemical environment class for concrete; DC: design chemical class)

Water Soluble Sulfate (mg/l)	Acid Soluble Sulfate %( $\text{SO}_4$ )	Total Sulfur %( $\text{S}$ )	TPS %( $\text{SO}_4$ )	Oxidisable Sulfur %( $\text{S}$ )	BRE Classification (BRE 2005)		
					DS	ACEC	DC
1260	0.4	1.00	3.1	0.9	DS-4	AC-4	DC-4

Table 3.4: Chemical composition of the Lower Lias Clay used in this investigation

Average Water Soluble Compositions (mg/l)						Avg. Carbonate (% $\text{CaCO}_3$ )	Average pH
$\text{SO}_4^{2-}$	$\text{Na}^+$	$\text{K}^-$	$\text{Cl}^-$	$\text{Ca}^+$	$\text{Mg}^{2+}$		
1260	42.3	66.4	12.7	497.1	98.7	21.3	7.8

### 3.3.1.3 Specimen preparation and exposure

Four separate prisms 100 mm square by 1.2 m long were cast using the four mixes mentioned above in Section 3.3.1.1. These were removed from the casting moulds after 18 hours, and then placed in a mist room at 95% RH and 20°C for 28 days to cure. After curing, one face of each prism was coated with one layer of bitumen as shown in Figure 3.1 (a) and (b). The prisms were assembled to form a column that was then buried in the slightly weathered Lower Lias Clay. Thus each concrete specimen exposed two faces to the clay, one of which was bitumen-coated. To simulate damage that might occur during construction, in some places the bitumen coating was scratched with a blade to expose the underlying concrete. The initial moisture content of the clay was between 20% and 35% and it was compacted in layers to a density of approximately 1960 kg/m<sup>3</sup>. Open-ended 2-mm-diameter piezometer tubes were placed at various depths in the clay, as illustrated in Figure 3.1(c). These were later used to extract samples of the pore water from within the body of the clay sample.



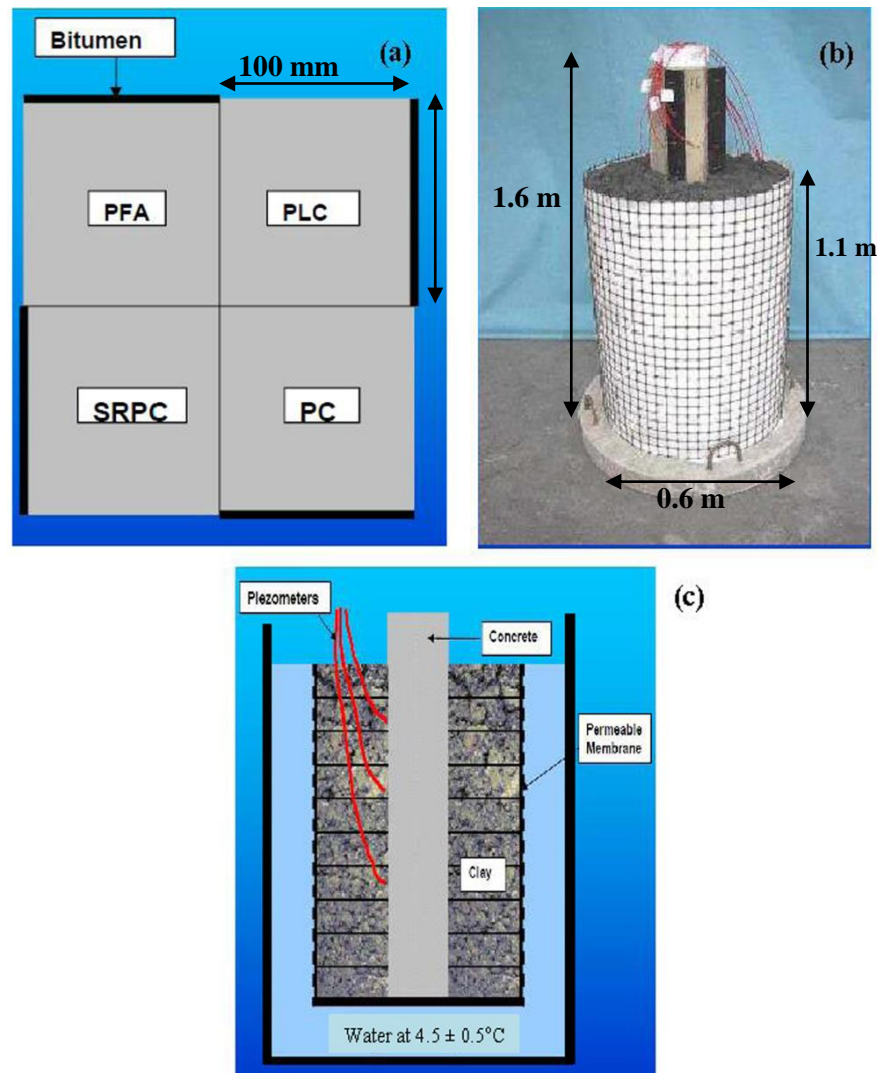


Figure 3.1 Concrete columns in disturbed Lower Lias Clay

The clay surrounding the concrete columns, was confined in a permeable cylindrical jacket as shown in Figure 1(c), and the whole assembly was placed in a tank containing water to the same height as the clay and maintained at a temperature of  $4.5 \pm 0.5^\circ\text{C}$ . This temperature was chosen to create optimum conditions for the formation of thaumasite to accelerate the deterioration processes. It should be mentioned that the clay was probably not fully saturated as some pores in the clay would have contained air.

During the initial twelve months of the experiment, the top 200 mm of the specimens were examined and photographed after removal of a 100-mm layer of clay at six months and a further 100 mm at twelve months. The experiment was run for a further eight years, after which it was entirely dismantled and the observations and testing described below were carried out. The results of visual assessment and chemical changes in the clay at twelve months were reported earlier by Byars et al. (2003).

### 3.3.2 The influence of clay compositions on severity of TSA (series II).

#### 3.3.2.1 Materials

##### I. Cementitious binders

- **Cement**

CEM I (52.5 N), manufactured by Paragon, conforming to the requirement of BS EN 197-1:2011 was used. The chemical composition of the cement was analysed using XRF techniques and the results are given in Table 3.5.

- **Ground granulated blastfurnace slag (GGBS)**

The ground granulated blastfurnace slag (GGBS) was obtained from Hanson Heidelberg Cement Group. The chemical composition was determined using XRF to ensure that it conformed to the requirement of BS EN 15167-1:2006, as shown in Table 3.5.

- **Pulverized -fuel ash (PFA)**

The pulverized -fuel ash (PFA) (Class N, category B) was obtained from Ash Solutions Ltd, and conformed to BS EN 450-1:2005+A1:2007. The chemical composition of the cement is presented in Table 3.5.

- **Limestone filler**

The limestone filler was obtained from the Hanson group, and conformed to BS EN 197-1:2011 Section 5.2.6. The composition was analysed by XRF, and the chemical properties are given in Tables 3.5.

Table 3.5: Chemical composition cementitious binders

Oxide/Phase Mass (%)	Material			
	CEMI	Limestone filler	PFA	GGBS
SiO <sub>2</sub>	22.19	0.63	51	35.96
CaO	62.74	55.2	2.60	40.31
Al <sub>2</sub> O <sub>3</sub>	4.08	0.28	24.8	13.00
Fe <sub>2</sub> O <sub>3</sub>	3.16	0.15	10.7	0.67
Na <sub>2</sub> O	0.20	<0.003	1.04	0.50
K <sub>2</sub> O	0.5	0.054	3.4	0.3
MgO	1.09	0.47	1.60	7.80
SO <sub>3</sub>	3.1	<0.002	0.52	0.05
TiO <sub>2</sub>	0.24	0.02	1.00	0.68
MnO	0.049	0.02	0.07	0.51
P <sub>2</sub> O <sub>5</sub>	0.220	<0.001	0.261	<0.001
LOI	2.52	42.89	3.04	0.22

## II. Aggregate

Medium-graded natural sand and siliceous aggregate (size 10 mm) complying with BS EN 12620:2002+A1:2008 were used in the mixes. The chemical composition of aggregate was determined by XRF and the results are given in Table 3.6.

Table 3.6: Chemical composition of aggregate

Oxide/Phase Mass (%)	Aggregate	
	Coarse	Fine
<b>SiO<sub>2</sub></b>	93.67	93.77
<b>CaO</b>	0.26	0.15
<b>Al<sub>2</sub>O<sub>3</sub></b>	2.52	2.21
<b>Fe<sub>2</sub>O<sub>3</sub></b>	1.39	1.72
<b>Na<sub>2</sub>O</b>	0.18	0.23
<b>K<sub>2</sub>O</b>	0.74	0.7
<b>MgO</b>	0.21	0.25
<b>SO<sub>3</sub></b>	0.04	0.03
<b>TiO<sub>2</sub></b>	0.19	0.14
<b>MnO</b>	0.01	0.02
<b>P<sub>2</sub>O<sub>5</sub></b>	0.04	0.05
<b>LOI</b>	0.58	0.62

## III. Clay

Weathered Lower Lias Clay (W-LLC) and slightly weathered Lower Lias Clay (SW-LLC) obtained from the A46 Newark to Widmerpool highway improvement scheme from a site near Cotgrave in Nottinghamshire, as well as Coal Measures mudstone (CM) excavated from Hatfield Colliery near Doncaster, as shown in Figure 3.2, were used to simulate the ground conditions.

According to the visual assessment of the clay, the clay used has three different colours, as shown in Figure 3.4. The Lower Lias Clay that has a dark grey colour, indicating that the material is slightly weathered and was located at depth 5 m. In addition, the dark colour may be attributed to the presence of iron sulphide (pyrite). On the other hand, Lower Lias Clay that has light grey colour, indicating that the material is completely or moderately weathered and that it was located at shallow depth, between 0 and 2.4 m, as shown in Figure 3.4. Moreover, the light colour indicates that it contains less pyrite and more calcite. Coal Measures Clay has a dark colour, as shown in Figure 3.3. The dark colour is considered to belong to material containing a high amount of pyrite and low calcite. The chemical compositions of clays are shown in Table 3.7.

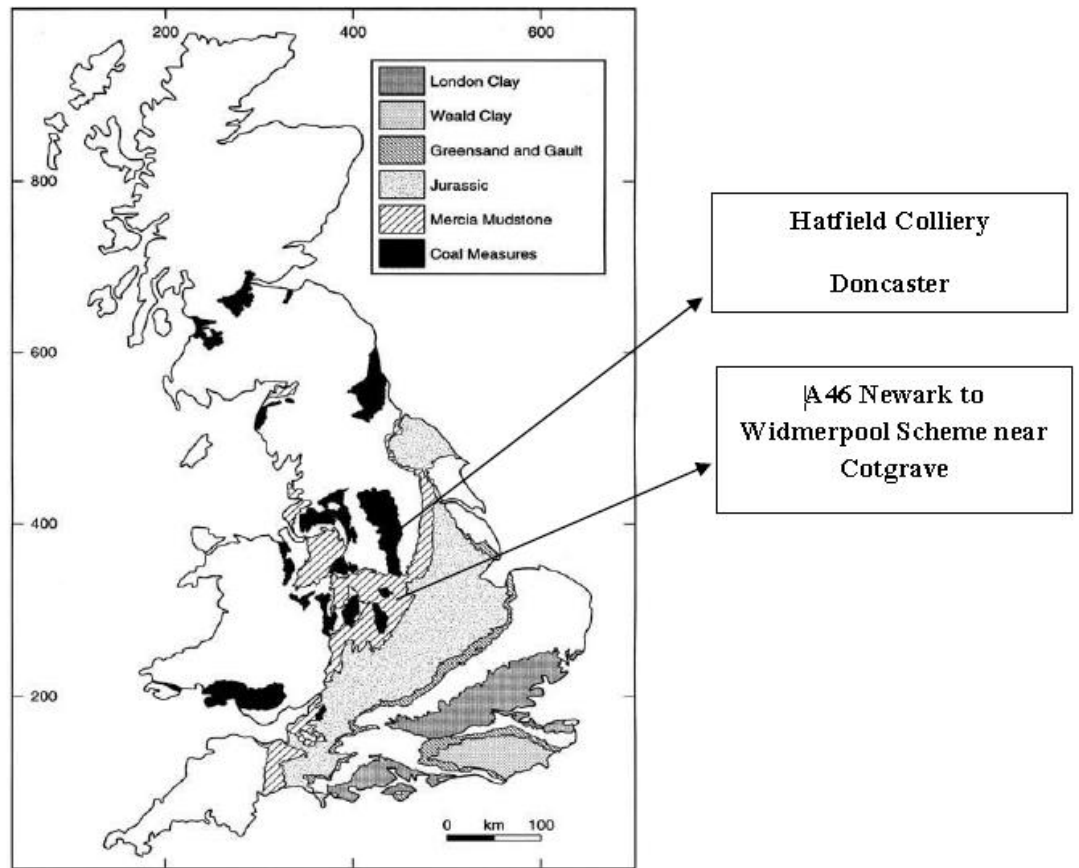


Figure 3.2: Locations of clay used in this investigation

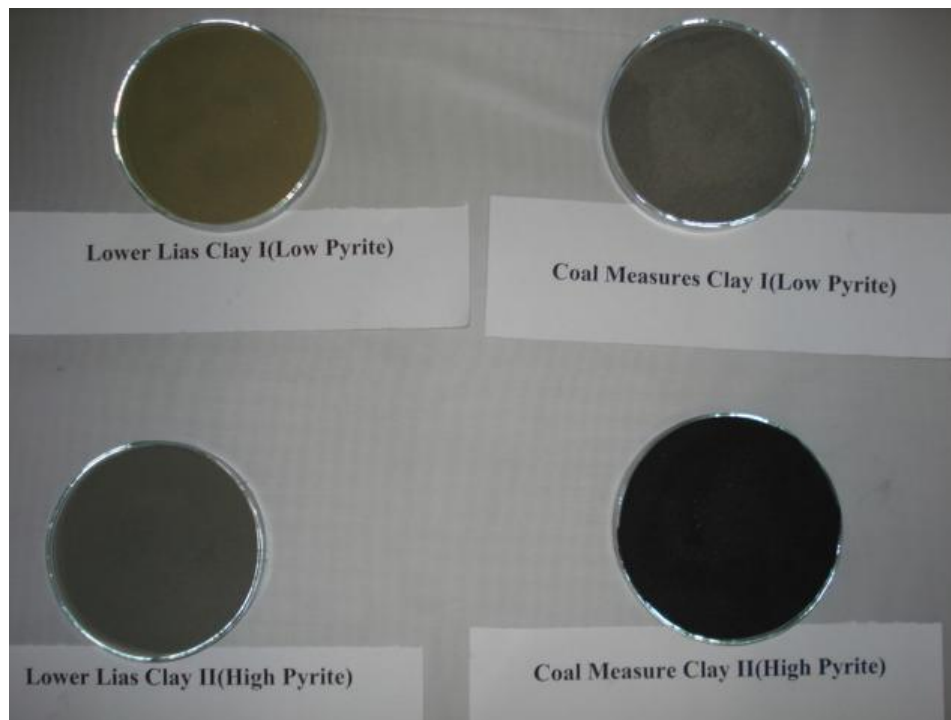


Figure 3.3: Visual appearance of clay used in this investigation



Figure 3.4 Elevation which explains the depth of weathered Lower Lias Clay

Table 3.7: Chemical composition of clay used

Clay Type	Oxide (Mass,%)											
	SiO <sub>2</sub>	CaO	Al <sub>2</sub> O <sub>3</sub>	Fe <sub>2</sub> O <sub>3</sub>	Na <sub>2</sub> O	K <sub>2</sub> O	MgO	SO <sub>3</sub>	TiO <sub>2</sub>	MnO	P <sub>2</sub> O <sub>5</sub>	LOI
<b>Weathered Lower Lias Clay</b>	55.7	8.46	21.35	3.64	0.69	3.79	1.28	2.38	0.95	0.03	0.05	11.94
<b>Slightly weathered Lower Lias Clay</b>	43.75	12.91	15.36	5.69	0.3	3.118	2.52	0.398	0.74	0.116	0.079	15.73
<b>Coal Measures mudstone</b>	41.9	0.6	19.37	4.83	0.66	3.34	1.03	0.281	0.71	0.018	0.064	27.13

The amounts of water, acid soluble sulfate and major ions and cations are shown in Table 3.8 together with the specified BRE SD-1 (2005) sulfate classification. Table 3.9 shows the results of water and acid soluble sulfates together with total sulfur in terms of percentage of sulfur. The amount of pyrite, calculated as the difference between total and acid-soluble sulfate, is also presented in Table 3.9. It should be mentioned that the amounts of pyrite and calcite were varied between clays in order to simulate different exposure environments.

It should be noted that in clay the total amounts of SiO<sub>2</sub> and Al<sub>2</sub>O<sub>3</sub> represent quartz and clay minerals, while CaO might be in the form of calcite and gypsum. However, with regard to sulfur, XRF would not give reliable values for SO<sub>3</sub>, and therefore other methods, such as those described in BS 1377-3:1990, should be used to determine the sulfate content in clay. On the basis of the water-soluble sulfate results shown in Table 3.9, the weathered LLC and slightly weathered LLC are classified as BRE DS-3 and DS-2 respectively, while the Coal

Measures clay was classified as DS-1. It should be noted that weathered Lower Lias Clay is classified as DS-4, while slightly weathered Lower Lias Clay and Coal Measures Clay is classified as DS-5, on the basis of the total potential sulfate shown in Table 3.10.

Table 3.8: Major water soluble ions and cations

Clay	Average Water Soluble Compositions (mg/l)						Avg. Carbonate (% CaCO <sub>3</sub> )	Average pH
	SO <sub>4</sub> <sup>2-</sup>	Na <sup>+</sup>	K <sup>-</sup>	Cl <sup>-</sup>	Ca <sup>+</sup>	Mg <sup>2+</sup>		
W-LLC	2450	42.13	25.48	16.27	559.45	57.30	30	7.80
SW-LLC	1366	31.68	26.26	18.27	510.63	101.60	21.30	8.10
CM	160.9	1234	34.46	1419.7	93.11	11.46	7.40	7.24

Table 3.9: Sulfur compounds and design sulfate class of clay according to BRE, (2005)

Clay	Water Soluble Sulfate (mg/l)	Acid Soluble Sulfate %(SO <sub>4</sub> )	Total Sulfur %(S)	TPS %(SO <sub>4</sub> )	Pyrite %(FeS <sub>2</sub> )	DS- BRE Classification according to	
						WWS	TPS
W-LLC	2450	0.82	0.6	1.8	0.6	DS-3	DS-4
SW-LLC	1366	0.25	1.04	3.12	1.8	DS-2	DS-5
CM	160.9	0.05	0.8	2.4	1.4	DS-1	DS-5

Table 3.10 BRE design sulfate class (BRE, SD-1, 2005)

Design Sulfate Class for site	2:1 water/soil extraction		Ground water		Total Potential Sulfate
	SO <sub>4</sub> Mg/l	Mg Mg/l	SO <sub>4</sub> Mg/l	Mg Mg/l	SO <sub>4</sub> %
DS-1	<500	-	<400	-	<0.24
DS-2	500-1500	-	400-1400	-	0.24-0.6
DS-3	1600-3000	-	1500-3000	-	0.7-1.2
DS-4	3100-6000	≤ 1200	3100-6000	≤ 1000	1.3-2.4
DS-4m	3100-6000	>1200	3100-6000	> 1000	1.3-2.4
DS-5	>6000	≤ 1200	>6000	≤ 1000	>2.4
DS-5m	>6000	>1200	>6000	> 1000	>2.4

### 3.3.2.2 Water and Solutions

Laboratory-grade magnesium sulfate (MgSO<sub>4</sub>.7H<sub>2</sub>O) was used to prepare test solutions for DS-2 and DS-4 sulfate solutions, while combinations of magnesium sulfate (MgSO<sub>4</sub>.7H<sub>2</sub>O), calcium sulfate (CaSO<sub>4</sub>.2H<sub>2</sub>O), sodium chloride (NaCl), sodium sulfate (Na<sub>2</sub>SO<sub>4</sub>) and sodium bicarbonate (NaHCO<sub>3</sub>) were used to prepare solutions equivalent to the Lower Lias Clay and Coal Measures Clay. It should be mentioned that it was difficult to obtain the same concentrations as those in the clay pore solutions. However, the concentrations were similar



and within the BRE sulfate classifications. De-ionised water was used to make solutions. Table 3.11 shows details of the solutions and concentrations used.

Table 3.11 Test solutions

Test Solution	Solution Compositions (mg/l)					
	SO <sub>4</sub> <sup>2-</sup>	Mg <sup>2+</sup>	Ca	Na	Cl	CO <sub>3</sub>
BRE DS-2: 3.85 g/l (MgSO <sub>4</sub> .7H <sub>2</sub> O)	1500	500	-	-	-	-
BRE DS-4: 15.4 g/l (MgSO <sub>4</sub> .7H <sub>2</sub> O)	6000	1520	-	-	-	-
W-LLC: (2.4g/l CaSO <sub>4</sub> .2H <sub>2</sub> O) + 0.6MgSO <sub>4</sub> .7H <sub>2</sub> O + (0.03g/l NaCl) + 0.4 NaHCO <sub>3</sub> )+(0.16 NaSO <sub>4</sub> )	1700	57	560	42	16	300
SW-LLC: (1.8 g/l CaSO <sub>4</sub> .2H <sub>2</sub> O) + (1g/l MgSO <sub>4</sub> .7H <sub>2</sub> O) + (0.03g/l NaCl) + 0.4 g/l NaHCO <sub>3</sub> )+(0.1g/l NaSO <sub>4</sub> )	1350	105	380	32	18.5	300
CM: (0.09g/l CaSO <sub>4</sub> .2H <sub>2</sub> O) + (0.12 g/lMgSO <sub>4</sub> .7H <sub>2</sub> O) + (3 g/l NaCl) + 0.4g/l NaHCO <sub>3</sub> )+(0.3g/l NaSO <sub>4</sub> )	500	12	90	1200	1350	300

Tap water was used in this investigation in order to simulate groundwater and the composition of water before being subjected to different clays was analysed as shown in Table 3.12.

Table 3.12: Chemical composition of water before interaction with clay

Average Water Soluble Compositions (mg/l)							Average PH
SO <sub>4</sub> <sup>2-</sup>	Na <sup>+</sup>	K <sup>-</sup>	Cl <sup>-</sup>	Ca <sup>+</sup>	Mg <sup>2+</sup>	CO <sub>3</sub>	
41.3	15.7	9.4	26.6	23.2	3.2	6	8.27

### 3.3.2.3 Concrete mixes and casting

A series of 70-mm cubes and large prisms (70 x 70 x 1000 mm) were cast using plastic and wood moulds, respectively. The large prisms were used in large-scale samples of clay (series II, B) whereas 70-mm cubes were cast to be placed in containers containing either clay or solution. The mixes were designed using **380 kg/m<sup>3</sup>** binder and the water/binder ratio was a constant 0.6. The maximum nominal aggregate size of 10 mm was used. The blended **cements variously contained** 70% GGBS, 10% limestone filler and 50% PFA. The amount of cement replaced with PFA and GGBS was chosen in order to evaluate the performance of high levels of replacement of 50% PFA and 70% GGBS in **clay that contains** pyrite, for which the replacement of 50% PFA has not yet been reported in the literature. The mix proportions for concretes are summarised in Table 3.13.

Table 3.13: Mix proportions of concrete

MIX	Mix Properties <b>kg/m<sup>3</sup></b>							
	CEMI	Limestone Filler	PFA	GGBS	Water	W/B	Sand	Aggregate (10 mm)
<b>CEMI</b>	380	0	0	0	228	0.6	750	1020
<b>CEMI/10%LST</b>	342	38	0	0	228	0.6	750	1020
<b>CEMI/50%PFA</b>	190	0	190	0	228	0.6	750	1020
<b>CEMI/70%GGBS</b>	114	0	0	266	228	0.6	750	1020

In mixes incorporating limestone, PFA and GGBS, the materials were dry-mixed to achieve an even mixture before the water was added. The concretes were mixed in a 50-litre horizontal pan mixer as follows:

- i. Part of the water was mixed with coarse and fine aggregate for 30 seconds to allow the absorption to take place.
- ii. Half of the remaining water, PFA and GGBS were added to the mixed cement and mixing was continued for a further 60 seconds.
- iii. The mixer was then stopped, and the mixture was scraped off the sides of the pan and hand-mixed before the next step.
- iv. The remaining water was added, and mixing continued for a further two minutes; care was taken to ensure all the mixes had the same consistency.

The concrete specimens were cast in pre-oiled moulds and fully compacted in three layers using **vibration**. Wet hessian and plastic sheets were used in order to cover moulds were for the first 24 hours at room temperature.

#### 3.3.2.4 Curing

##### I. Initial curing

**Cubes (70mm)** and prisms (70 x 70 x 1000 mm) were demoulded after 24 hours. **These were** removed from the casting moulds after 18 hours, and then placed in a mist room at 95% RH and 20°C for 28 days to cure before being exposed to sulfate solutions or clay environments.

##### II. Long-term exposure to solutions and pyritic clay

After the initial curing, the 70-mm cubes were buried in the centre of containers 35 by 55 by 15 cm deep, filled with weathered Lower Lias Clay, slightly weathered Lower Lias Clay or Coal Measures mudstone clay, compacted to a density of about 1960 kg/m<sup>3</sup>, similar to the density of the backfill on the M5 motorway bridges (Floyd and Wimpenny, 2003; Byars et al., 2003). Each cube face was exposed to a similar volume of clay and the volume ratio of concrete to clay was 1:20. Specimens of the same concretes were also placed in sulfate solutions equivalent to design solutions (sulfate class DS-2 and DS-4, simulated clay pore solutions) as listed in Table 3.11, and here the ratio of concrete volume to solution was 1:3. Each individual container of buried concrete or concrete in solution was placed in a water tank maintained at either 5° or 20°C ( $\pm 0.5^\circ\text{C}$ ) as shown in Figure 3.5. The solutions were renewed every three months for the first nine months of the tests in order to simulate replenishment due to mobile groundwater, as recommended by Higgins and Crammond (2003).





Figure 3.5 the long –term curing in tanks



Figure 3.6 Temperature controlled tanks and exposure of concrete to clay

Large prisms 70 x 70 x 1000 mm were exposed to weathered and slightly weathered Lower Lias Clay and Coal Measures Clay after the prisms were assembled to form a column as shown in Figure 3.6. The dimensions of the clay samples were (0.8m (diameter) and 0.8m (height)) for large-scale simulation. The clay was compacted to simulate the target

compaction, which is  $1960 \text{ kg/m}^3$ . Open-ended 2-mm-diameter plastic tubes were placed at various depths in the clay at different distances from the column. These piezometer tubes were later used to extract samples of the pore water from within the body of the sample. The clay, together with the column, was contained in a permeable cylindrical jacket as shown in Figure.3.6, and the whole assembly was placed in a tank containing water that was maintained at a temperature of  $5 \pm 0.5^\circ\text{C}$ , using a cold water circulation system in order to simulate mobile groundwater.

### 3.4 Test methods

#### 3.4.1 Sampling

Clay was removed in series I after nine years' long-term exposure to LLC. The clay samples were removed in 300-mm layers, and samples were taken from different levels of exposure and different positions, including adjacent to concrete columns and far away from concrete columns. The concrete columns were then visually observed, and the deterioration depth of each concrete column at different levels of exposure was measured, as explained in Section 3.4.2. In addition to the visual assessment, a sample of deteriorated materials for XRD and SEM analysis was collected from the concrete surface. In addition, cores from different levels of exposure for each concrete column were taken in order to carry out the chemical analysis of the concrete profile which was discussed in Section 3.4.2.

For Series II, concrete specimens were removed from test solution containers on a six-monthly basis and samples were tested. The method of sampling clay and concrete for X-ray and SEM analysis is discussed in Sections 3.4.2 and 3.4.3.

In the case of exposure to clays, clay samples were taken from each container every three months; the samples were taken from different positions including adjacent to the concrete cubes. However, the concrete cubes were totally removed after 24 months in order to be examined and photographed. With regard to large-scale simulation, a 50-mm layer of clay was removed from each clay specimen every three months, and clay samples were taken from different positions and radially at distances of 0-90 mm, 90-180 mm and 180-270 mm. The concrete columns are examined and photographed after layer of clay was removed completely.

In addition to photography, a sample of any deteriorated materials for XRD analysis was collected by scratching the surface of the concrete. Pore solutions of clay were taken every three months from the attached piezometer at different depths and examined as described in Section 3.5.3.

### 3.4.2 Concrete cores

Concrete columns were cored using a 70-mm-diameter cutting tube in the long-term experiment (series I). The concrete cores were taken from the uncoated face of columns at different burial depths, with three cores being selected in each column. As the material of the surface was mushy soft material, cores were taken after columns had dried to avoid loss of material from the surface. However, where the material was soft and could be easily removed, the scraping technique with a spatula was used to ascertain depth, and materials were collected at every 10 mm of depth. It should be mentioned that it was difficult to take cores in PLC concrete at burial depth 1 because of the significant attack, in which deterioration thickness reached about 47 mm and most of the material was spalled during the removal of the clay. Concrete cores were cut into a series of 10-mm-thick slices up to a depth of 50 mm. Sliced cores were then ground and sieved samples passed 450 micron in order to prepare them for wet chemistry tests. Cores from burial depth 2 were tested in order to determine pH and carbonate content. Cores from each level were examined to determine total sulfate content and the effect of depth of exposure to clay on penetration of sulfate.

### 3.4.3 Concrete testing

#### 3.4.3.1 Visual observation

Specimens were visually assessed for signs of deterioration, such as blistering, cracking, softening, spalling, loss of corners or edges, loss of aggregate and the presence of any precipitated minerals. In the long-term experiment (series I), the visual assessment was made after nine years in order to identify evidence of damage; discolouration or loosened or weakened concrete was photographed at different burial depths, namely burial depth 1 (200-300 mm), burial depth 2 (300-600 mm) and burial depth 3 (600-900 mm). Visual observation was carried out in order to evaluate and monitor the deterioration and physical changes such as spalling and loss of edges and corners. In the case of the series II specimens, the visual observation and photography of concrete were done at 6, 12 and 24 months for concrete cubes immersed in solutions, while in concrete buried in clay the visual observation was done at 12 and 24 months.

#### 3.4.3.2 Deterioration thickness

The thickness of deteriorated material was measured for concrete samples (series I) using a modified hand-held penetrometer, which, as shown in Figure 3.7, was equipped with a thick rigid steel needle attached to the plunger. Measurements were taken immediately after the concrete specimens had been removed from the clay, before any loss of moisture. A force equivalent to a pressure reading of 3 kPa on the penetrometer scale was found to be

sufficient to enable penetration of the probe through the full thickness of softened and deteriorated material without piercing the underlying sound concrete. The average of a minimum of five measurements in each 100-mm length of column at different burial depths for all columns was taken. The deterioration thickness reported here refers to the thickness of deterioration into the concrete from the original specimen surface. The un-attacked edge of the prism was used as a reference.



Figure 3.7: Modified penetrometer fitted with a thick needle attached to plunger

### 3.4.3.3 Chemical analysis

A chemical analysis of the concrete profile was carried out in concrete cores that were taken after nine years of long-term concrete–LLC interaction (**Series I**). The following tests were adopted:

#### I. Determination of sulfate content

Five sub-samples (from 0-10 mm to a depth of 50 mm) from three different levels of concrete columns exposed to LLC were tested in order to determine the profile's total sulfate content and to investigate the effect of exposure depth on the diffusion process. The method in BS 4551:2005+A2:2013 was adopted in order to determine the concentration of sulfate ions in pore solutions. Averages of 5 measurements were determined and the differences between results should not be more than  $\pm 0.02\%$ .

#### II. Determination of pH

Concrete powder was extracted using a 1:10 ratio of solid to water, and the sample was shaken for 24 hours according to BS 1881-124:1988; then the pH of each sample was measured using a glass calibrated pH electrode. Averages of 5 measurements were recorded and the differences between results should not be more than  $\pm 0.05$ .

### III. Carbonate content profile

Selected samples from the concrete powder taken from cores at level 2 of exposure were prepared to determine the total carbonate content according to the acid neutralizing capacity method. The carbonate ion exchange for different concrete types that had interacted with clay for nine years was measured using titration of carbonate against diluted hydrochloric acid (HCl) and using phenolphthalein as an indicator. Averages of 5 measurements were determined and the differences between results should not be more than  $\pm 0.1\%$ .

#### 3.4.3.4 Mineralogy and microstructure of concrete

Deteriorated concrete was taken from the surface and material was taken from the intact core of each specimen at different burial depths in order to identify the minerals that formed due to TSA in the case of samples exposed to LLC for nine years. Deteriorated material was sampled after 24 months and analysed in order to identify the phases present in the case of concrete samples (series II) exposed to different clays, sulfate solutions and simulated clay pore solutions. Where deterioration products were absent, a part of the outer layer of the specimen was removed and analysed. The following techniques were used in order to investigate the concrete microstructure and to detect thaumasite and other minerals.

##### I. X-Ray Diffraction (XRD)

Specimens for XRD were taken from the surface and core of the concrete. Samples for XRD were dried in a desiccator at room temperature in order to prevent change in the crystallization of deteriorated materials and then gently crushed using a porcelain mortar and pestle to pass a 150- $\mu\text{m}$  sieve, in order to reduce the amount of sand particles in the powder. Material smaller than 150  $\mu\text{m}$  was further reduced to 63  $\mu\text{m}$  by the same method, and this was then packed carefully into an aluminium holder. In order to avoid contamination, acetone was used to wash all the used tools (sieves, brush, mortar and pestle) between each sample preparation. Finally, the powders obtained were kept in air-tight containers before testing. Philips PW 1830 X-ray generator machine with a copper electrode operating at 40 kV and 30 mA was used for XRD analysis with a scanning speed of  $2\theta/\text{min}$  and step size  $0.02^\circ$  over a  $2\theta$  range of  $5-60^\circ$ . In addition, the database of the Joint Committee for Powder Diffraction Files (JCPDF) built into WinXPow software was used to identify the different phases in the XRD patterns. Moreover, ICDD-PDF-4<sup>+</sup> software was utilised for the quantitative XRD determinations.

##### II. Fourier Transform Infrared Spectrometry (FTIR)

FTIR is a powerful technique in the detection and differentiation between thaumasite and ettringite- thaumasite solid solution. It can also determine the compositions of materials. The



resulting infrared spectrum represents a unique molecular structure like fingerprint of the sample, which make IR a useful to differentiate between minerals. Moreover, the time required for measurement is a few seconds. The preparation of samples is similar to that of XRD samples, as detailed above (I). Pellets of 12mm(diameter) were made prepared using 2 mg of <math> < 63 \mu\text{m}</math> ground samples mixed with 200 mg of potassium bromide, which were ground together until a fine powder was produced. The powdered sample was then placed in a 12-mm-diameter press mould in order to press it at 10 Pa for two minutes. The IR spectrum was determined using a Perkin–Elmer FTIR 2000 spectrometer with a resolution of  $\pm 1\text{cm}^{-1}$ .

### III. Scanning Electron Microscopy (SEM)

Scanning electron microscopy is an established method that can provide useful information about the structure of materials. In SEM a high-energy beam of electrons at 60KeV is directed at samples. The secondary electrons have low energy which 50eV are emitted from the samples surface (Rendell et al., 2002). The samples were dried in desiccators for three days at room temperature. The samples were cast in epoxy resin and left under vacuum for about ten minutes. They were then left for hardening for 24 hours at room temperature. After hardening, the samples were manually ground using four grades of silicon carbide paper (nos.120, 400, 800 and 1200). The samples were polished with four grades of diamond discs, from 6  $\mu\text{m}$  to 1/4  $\mu\text{m}$ . After polishing, the samples were submitted to an ultrasonic bath in acetone for fifteen minutes, in order to ensure a clean surface. They were then carbon-coated and placed in plastic containers until required for testing. Inspect-F microscope machine was used to identify the microstructural features of both surface and concrete core samples in both secondary imaging (SEI) and backscatter imaging modes (BSI) using SEM. In order to provide data regarding the chemical composition of the phases present in the samples, the SEM was equipped with an EDX analysis facility.

#### 3.4.4 Changes in pH of exposure solutions

The pH of solutions in the individual containers was measured using a Hanna HI 931000 pH meter with an HII 217D electrode. It should be noted that the electrode was damaged and replaced on several occasions. The electrode was rinsed with distilled water before each measurement in order to avoid any contamination. The initial pH of solutions was measured and presented as the value at age zero. The pH was measured at 1, 7, 30, 90, 180 and 270 days for the first nine months after the placing of concrete samples in test solutions and prior to solution replenishment every three months. After the first nine months the pH was monitored at three-monthly intervals up to 720 days. The pH at age zero of solutions was

measured before the specimens were immersed. . Averages of 3 measurements were determined and the differences between results should not be more than  $\pm 0.05$ .

### 3.4.5 Clay samples

In the case of the **long-term** investigation, chemical changes in the clay over the duration of the experiment were also determined. These were based on analyses of clay samples taken from radial distances of 9, 18 and 27 cm from the surface of each concrete core at different burial depths after nine years. Furthermore, clay samples from boxes and large experimental were taken as described in Section 3.4.1.

#### 3.4.5.1 Sample preparation

Clay samples were prepared according to BS 1377-3 (1990) and Reid et al (2005) as follows:

- Clay samples were oven-dried at temperatures between 60° - 75°C. The weight was measured at intervals of four hours until the difference became no longer exceeded 1%, and then the clay was cooled at room temperature in a desiccator.
- Clay was sieved to pass a 2-mm sieve and then ground to pass a 425-micron sieve.
- The powdered samples were oven-dried for 24 hours and cooled at room temperature in desiccators.
- Powdered samples were stored in air-tight containers and kept at a temperature of 0°-4°C before testing.

#### 3.4.5.2 Chemical analysis of clay

The clay samples were subjected to analysis for water-soluble sulfate, acid-soluble sulfate, pH and total sulfur, and decreases in oxidisable sulfur. The amounts of water-soluble calcium, magnesium, chloride, sodium and potassium were also determined, using dionex analytical equipment for analysing 2:1 water-clay extractions prepared according to BS 1377-3 (1990). In addition, the clay pore solutions were extracted using 2:1 water-clay extraction according to BS 1377-3 (1990), and the pH of the clay was determined using a Hanna HI 931000 pH meter with an HII 217D electrode, using the same solutions. The acid-soluble sulfate was determined by acid extraction followed by the BS 1377-3 (1990) gravimetric method, while total sulfur present was found by oxidising all sulfur to sulfate using potassium chlorate followed by the BS 1377-3 (1990) gravimetric method. The carbonate content of the clay was determined by the titration method given in Section 6.3: BS 1377-3 (1990). Duplicate samples were examined for all the above mentioned tests. An Average of 5 measurements was calculated for pH, WSS, ASS and TS. However, the

difference between measurements should no longer exceed 0.05 in case of pH, while it should not be exceeded 0.02% in case of ASS and TS. In addition, 0.1% is the allowed difference between measurements in determination of carbonate content. In addition, water and acid soluble sulfate and total sulfur were measured every three months up to 12 months, while pH of clay was measured every three months up to 24 months.

#### **3.4.5.3 Clay mineralogy**

SEM technique was used in order to investigate the soil mineralogy and the features of and changes in the microstructure of clay due to exposure to concrete. The preparation of the samples was similar to that for concrete samples for SEM tests.

#### **3.4.6 Clay pore solutions analysis**

Pore solutions of Lower Lias Clays and Coal Measures mudstone clay were extracted from the attached piezometer. The extracted pore solutions were analysed using dionex analytical equipment in order to determine water-soluble sulfate, calcium, magnesium, chloride, sodium and potassium. In addition, the concentration of carbonate ions ( $\text{CO}_3$ ) was determined using the method described in Laboratory methods guidelines, (2004), which is based on titration of 20 ml of pore solution using a methyl orange indicator, titrated against HCl till the colour of the solution changes to colourless. Clay pore solution was analysed every three months up to 18 months.



## CHAPTER 4

### **4. The Influence of Long Term Interaction of Concrete with Lower Lias Clay.**

This chapter describes the results of a nine-year-long experiment in which different concretes were exposed to slightly weathered Lower Lias Clay (LLC) (Series I) at 5°C. In this experiment the performance and deterioration depths for different concrete samples made with Portland Cement (PC), Portland Limestone Cement (PLC), Sulfate-Resistant Portland Cement (SRPC) and PC-25% Pulverized - Fuel Ash (PFA) were evaluated in terms of severity of thaumasite sulfate attack (TSA). The effects of burial depth on the progress of TSA and the role of bitumen coating in reducing or preventing deterioration were also investigated. The materials and methodology used are described in Chapter 3. The results presented include the assessment of chemical changes in concrete and clay due to their interaction. The evaluations were made by means of visual observations and by measurement of thickness of deterioration and chemical changes in both the concrete and the LLC. Also, to identify phases formed on the surface and concrete core of samples, XRD and FTIR analysis was carried out on dry powders of materials, along with SEM for microstructural analysis.

#### **4.1 Long-Term Durability of Buried Concrete Exposed to Lower Lias Clay**

##### **4.1.1 Visual observation**

This section presents the observations of the performance and mode of deterioration of the concretes. It should be mentioned that the surface of the clay had been lowered by 200 mm twelve months after the start of the experiment when clay samples were taken. However, the remainder of the columns remained buried for a total of eight years. The results of visual assessment after 12 months were reported by Byars et al. (2003). The visual inspection was recorded at different burial depths: (1) 0-300 mm, (2) 300-600 mm, and (3) 600-900 mm.

### **I. Portland cement concrete column**

Figure 4.1 illustrates the appearance of a PC concrete column at different burial depths of exposure; from which it can be seen that there is no sign of attack on concrete that is not in contact with clay. Concrete not exposed to clay was coated with a white precipitation after the nine years. In addition, there was evidence of attack, with the formation of white and yellowish mushy material and spalling and flakiness of the concrete, which resulted in exposed aggregate at a burial depth of 0-200 mm.

Concrete exposed to burial depth 1 (200-300 mm) in clay was substantially attacked, with the loss of the sharp corners on both coated and uncoated faces of the column. The white and yellowish crumbly reaction product had spalled and the aggregate was totally exposed. In concrete exposed to burial depths 2 and 3, significant attack was observed, and the concrete surface was transformed into a white mushy material. In addition, there was loss of the column edge in concrete exposed at burial depth 2.

In the coated concrete column, a white mushy material was observed at the shared corners of uncoated concrete faces at all burial depths of exposure. However, there were no signs of deterioration such as white mushy material or expansion and spalling of the concrete surface affecting the bitumen-coated face. Overall observation revealed that damage decreased with increasing burial depth.

### **II. Portland limestone cement concrete column**

As Figure 4.2 shows, the PLC concrete column levels in contact with clay suffered significantly. Severe loss of corners and spalling of reaction products were recorded. This was most serious in the lower part of the upper 200 mm of the column and at burial depths 1 (200-300 mm) and 2 where the column was exposed to clay for nine years. In the upper 100 mm, layers of flaky yellowish material and white mushy material had spalled, while at burial depth 1 (200-300 mm) and burial depth 2, intensive deterioration occurred in which aggregate was exposed in uncoated face of the column. However, the deterioration was severe at burial depth 1, compared to other parts of the column, with the loss of approximately 50% of cementitious material. Significant deterioration was observed in the bottom part of the uncoated column at burial depth 2 and 3, with white mushy reaction product, as shown in Figure 4.2. On the other hand, no signs of deterioration appeared on the coated face, and signs of deterioration were observed in the corner shared with the uncoated face of the PLC concrete column at burial depth 1 and 2. The overall assessment of the visual inspection of the PLC concrete column showed that intensive damage was present at burial depth 1 and 2, with less damage occurring at burial depth 3.

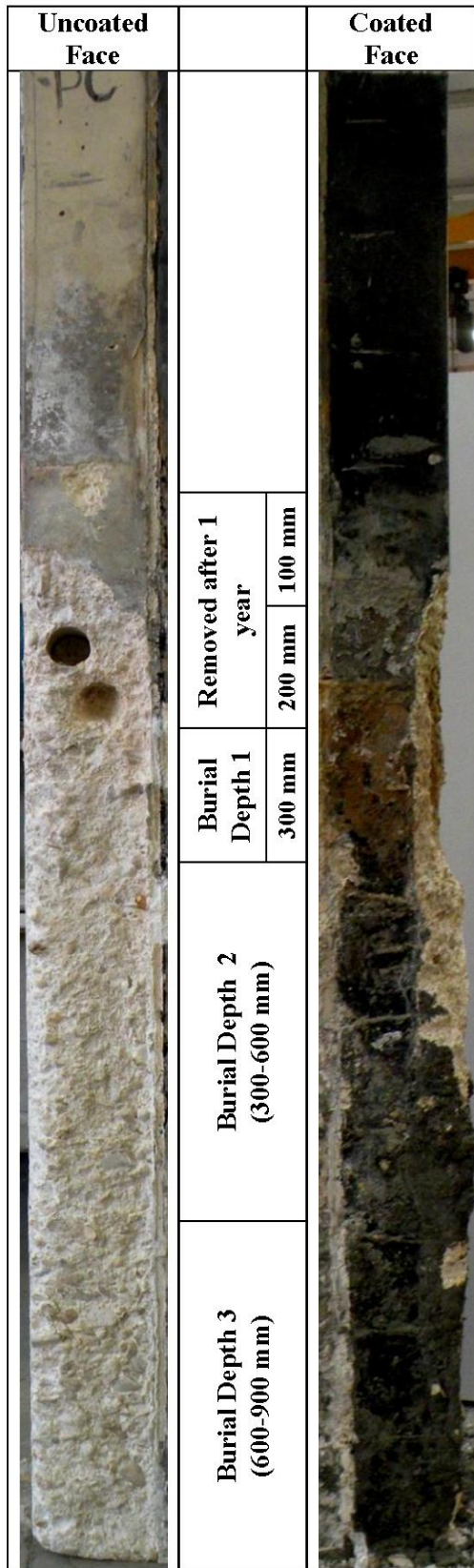


Figure4.1: Appearance of PC concrete

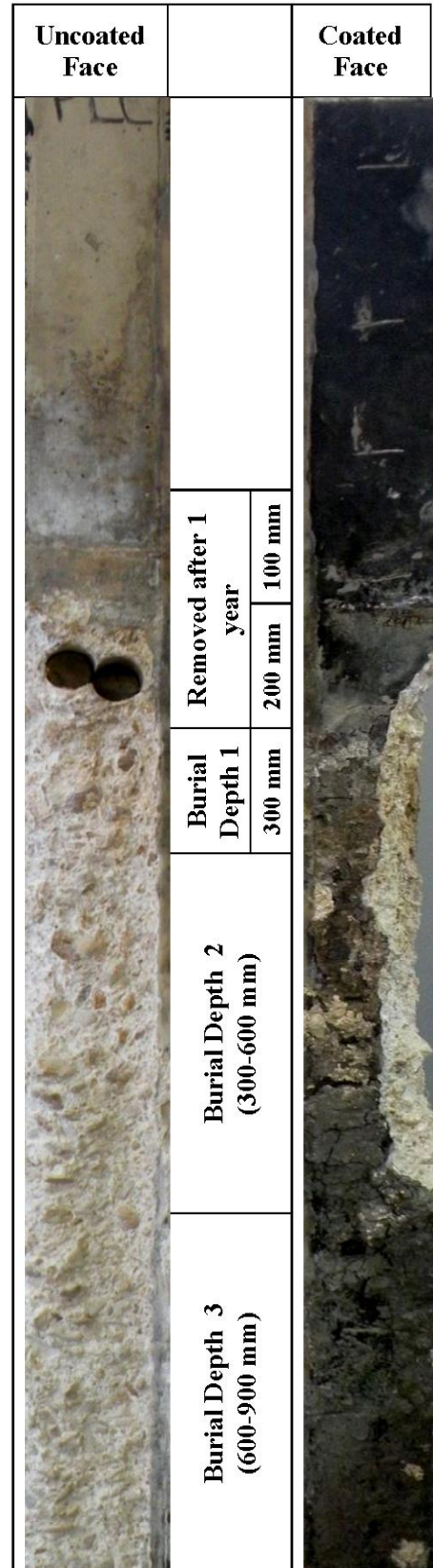


Figure 4.2: Appearance of PLC concrete

### **III. SRPC concrete column**

The extent of deterioration of SRPC concrete is shown in Figure 4.3. It can be seen that the upper concrete part exposed to clay for twelve months remained intact, although there was some efflorescence or precipitation covering the coated and uncoated faces. In addition, there were blisters, particularly on the coated face of the concrete. However, spalling of deteriorated material was the dominant type of attack in a column buried for nine years, in which aggregate was exposed and there was a loss of column edge at burial depth 1 and 2 in uncoated concrete.

White and yellowish crumbly reaction product appeared in concrete exposed at burial depth 1, while white crumbly reaction product was observed in concrete at burial depth 2. The uncoated concrete face also disintegrated at burial depth 3, and white mushy reaction product was formed in concrete face and in the edge of and uncoated face of the column. Again the deterioration of the coated face occurred at the shared corner. The general appearance revealed that concrete exposed at burial depth 1 deteriorated more than concrete at other burial depths, suggesting that the depth of exposure plays an important role in the extent and progress of deterioration.

### **IV. PC-PFA concrete column**

The visual appearance of the PC-PFA concrete column is illustrated in Figure 4.4. No clear signs of deterioration were observed in the upper part of the column exposed to clay for twelve months. However, a white precipitated efflorescence was present. The surface of the uncoated concrete face at burial depth 1 was covered with blisters, and white reaction product was formed underneath the surface layer. This was a slightly significant attack, in which signs of deterioration such as spalling of mushy material at the edge of the column and blistering were obvious at burial depth 1 and in the lower part at burial depth 2.

However, the deterioration was not severe at burial depth 3, and the deterioration of this column was found to be at the edges of the column. The bitumen-coated face at burial depths 1, 2 and 3 showed no signs of deterioration except on part of the corner at burial depth 1. Overall, the PC-PFA concrete column suffered less damage, with the deterioration reaction products apparently formed at the surface of the concrete. In addition, the corners of the concrete column retained their original shape and the concrete was sound although there was some slightly soft mushy material.





Uncoated Face		Coated Face	
	Burial Depth 1 300 mm		Removed after 1 year
			200 mm
	Burial Depth 2 (300-600mm)	100 mm	
Burial Depth 3 (600-900 mm)			

Figure4.3: Appearance of SRPC concrete



Uncoated Face		Coated Face	
	Burial Depth 1 300 mm		Removed after 1 year
			200 mm
	Burial Depth 2 (300-600 mm)	100 mm	
Burial Depth 3 (600-900 mm)			

Figure4.4: Appearance of PC- PFA concrete

## **V. Overall comparison**

The overall comparison of the extent of deterioration showed that deterioration was greatest in the PLC concrete, followed by PC concrete, although both were heavily attacked, as shown in Figures 4.1 and 4.4. Intense damage was also seen to the SRPC concrete, which suffered spalling and expansion accompanied by the formation of mushy material. Although the use of 25% PFA replacement retarded the deterioration, as shown in Figure 4.6, it was not entirely prevented, with the more obvious damage occurring at column edges rather than other parts at **burial depths** 1 and 2. Deterioration seems to be progressive and to worsen with time in comparison to the twelve-month visual assessment reported by Byars et al. (2003). In all concrete types, deterioration was more severe in parts exposed at burial depth 1 and 2. The style of deterioration was similar in all concretes and comprised the formation of white mushy material, spalling, loss of edge, exposure of aggregate and loss of cementitious matrix. While still damp, the deteriorated concrete could be removed easily by hand.

**It should** be mentioned that the attack was prevented in the bitumen-coated faces. Even where the coating had been deliberately scratched at the start of the experiment, to simulate damage to the coating during construction, for example, there was little sign of damage, as shown in Figures 4.1-4.4. The results of long-term exposure showed the effectiveness of bitumen coating in controlling the concrete deterioration. The visual observations of coated concrete agree with the investigation by Pouya (2007), who found that no signs of attack were identified in PLC concrete coated with bitumen and exposed to DS-4 sulfate solution for five years. It is suggested that coating makes the concrete less permeable to aggressive substances and reduces its moisture content. Moradillo et al. (2012) and Almusallam et al. (2002) reported that coating protects concrete against aggressive substances and improves the physical and chemical resistance of concrete. Therefore, it enhances the service life of concrete structures.

The severity of deterioration of different concrete types exposed to Lower Lias Clay was as follows: PLC > PC > SRPC > PC-PFA; the degree of severity became less as burial depth and exposure increased.

### **4.1.2 Deterioration thickness and rate of attack**

The main focus in this section is to investigate the effect of binder type and burial depth on the extent of attack. Deterioration thickness was measured using a modified hand-held penetrometer, as shown in Figure 3.10. The methodology used to measure deterioration is described in Chapter 3, Section 3.4.2.

Figure 4.5 revealed that the results are in line with the visual observations, where the PLC concrete had the greatest deterioration thickness over the nine-year exposure period, reaching 47 mm, followed by PC concrete, in which the deterioration thickness was 33 mm. The PC-PFA concrete proved to be the most resistant to deterioration, with the greatest thickness of damage about 10 mm at a depth of 300 mm and about 2 mm at a burial depth of 900 mm. The thickness of deterioration in concrete made with SRPC cement had a maximum of 22 mm. Therefore, it is clear that cement type is a controlling factor for the deterioration which occurred in these experiments on types of concrete.

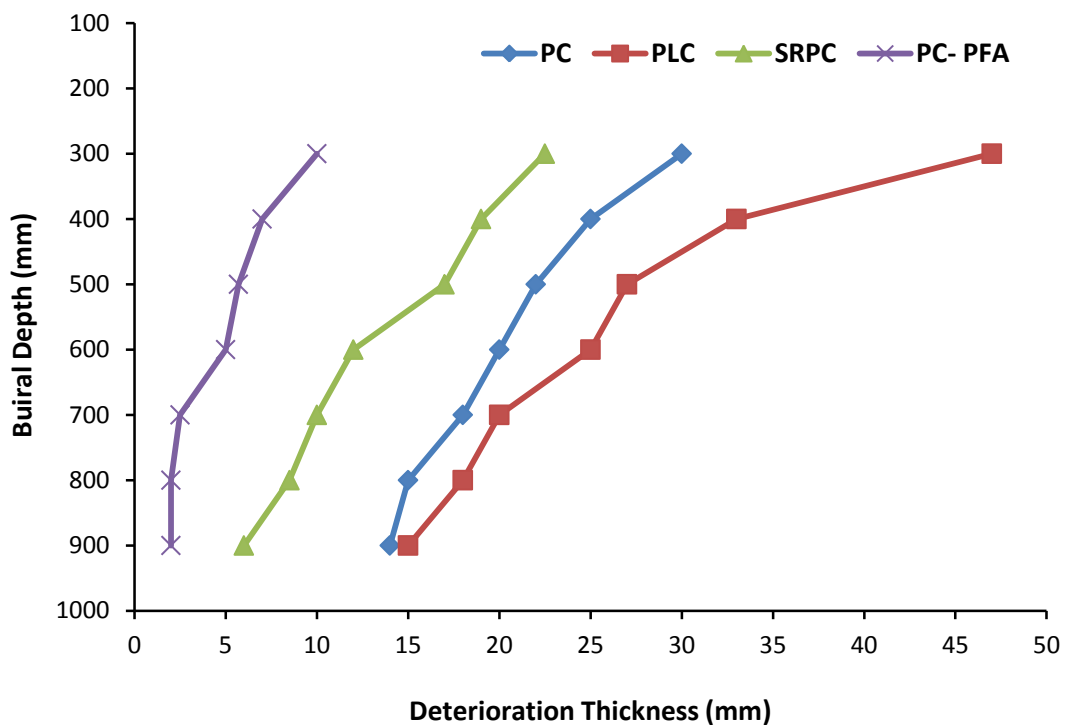


Figure 4.5: Deterioration thickness of different concretes due to TSA after nine years

As seen in Figure 4.5, there was a remarkable reduction in deterioration thickness as burial depth increased. The greatest thickness of damage occurred at the shallow burial depth of 200-300 mm in all concretes and the reduction was about 55% at a depth of 600 mm. Therefore, the thickness of deterioration in the concrete depends not only on the type of binder but also on the buried depth of the concrete–clay interaction where interface pressure increases. The level of attack has been compared to the field assessment of Halcrow Group. Their scheme is classified into four different attack ratings as shown in Table 4.1, which is based on the maximum depth of attack as reported by Slater et al (2001).

The rating of the severity of attack is shown in Table 4.2. The results confirm that the level of degradation decreases as burial depth increases. In addition, they confirm that binder type controls the extent of deterioration.

Table 4.1: Deterioration rating of concrete (Slater et al 2003)

Rating	Degree of deterioration	Description of concrete condition
1	No attack	No softening and damage observed in concrete.
2	Slight attack	Maximum depth of attack does not exceed 15 mm
3	Moderate attack	Maximum depth of attack exceeds 15 mm
4	Severe attack	Maximum depth of attack exceeds 25 mm

Table 4.2: Deterioration ranking of concrete after nine years of exposure

Concrete-clay burial level (mm)		Deterioration Rating			
Depth	(mm)	PC	PLC	SRPC	PC/25%PFA
Burial depth 1	200-300	4	4	3	2
Burial depth 2	300-400	3	4	3	2
	400-500	3	4	3	2
	500-600	3	3	2	2
Burial depth 3	600-700	3	3	2	2
	700-800	2	3	2	2
	800-900	2	2	2	1

It is believed that the deeper buried sections of concrete were least severely attacked because of the lower availability of oxygen and carbon dioxide in the clay pore solutions at greater burial depth. Thus there would be a tendency for more of the pyrite to oxidise in the near surface clay which would increase the supply of acidity and sulfate at the concrete interface. Moreover, the availability of dissolved CO<sub>2</sub> would be greater, leading to an increase in CaCO<sub>3</sub> solubility and a consequential greater concentration of bicarbonate and CO<sub>3</sub> ions. All these effects would accelerate the deterioration. On the other hand, it is likely that the clay had become more compacted at greater depths, which would reduce its permeability and influence the transport of reaction species and thereby reduce the potential for deterioration.

These findings are in agreement with the results of Brueckner et al. (2012 a & b) and Brueckner (2007) on thaumasite formation in Portland cement concrete involving shear box tests under various confining pressures, in which deterioration thickness was reduced by about 50% by an increase of pressure from 10 kPa and 70 kPa leading to the conclusion that an increase in confining pressure at the clay-concrete interface may indeed reduce the deterioration thickness into the concrete. However, it is unclear whether this effect was due



to reduction of the permeability of the clay, as clay become more compacted at greater depth or a more direct effect on the penetration of species into concrete and precipitation of deteriorated product. In the present work the maximum burial depth is limited to just over 1.1 m, so the increase in confining pressure with depth is not likely to have a significant influence on deterioration thickness.

Results of the effect of burial depth and thickness of deterioration on the ingress of sulfate and carbonate into concrete and chemical changes in concretes are presented in Section 4.2.

### 4.1.3 Mineralogy of deteriorated products: X-Ray Diffraction (XRD)

In this section the results of XRD are presented for materials from the deteriorated surface and the interior of the columns at burial depth 1. The methodology for preparing XRD samples is described in Chapter 3.

Figures 4.6 and 4.7 show the XRD patterns for surface and interior samples respectively from the different concretes. The traces for the deteriorated materials from the surface are all similar to each other, which suggests that a similar mechanism of deterioration has operated. It can be seen that thaumasite was identified as the main deterioration product in all concretes, as shown in Figure 4.6. Furthermore, two forms of carbonate minerals, namely calcite and aragonite, were present as moderate peaks in all XRD patterns for all concretes. However, relatively less calcite was present in the PC-PFA concrete than in PLC (20% LF) and PC (5% LF), respectively, as shown in the quantitative analysis in Table 4.3. This corresponds to the involvement of more carbonate in the reaction of thaumasite formation in these concretes. Small amounts of brucite  $Mg(OH)_2$  were also identified in PC and SRPC concretes, which presumably are due to the availability of low concentrations of magnesium from the clay. Gypsum and ettringite were only detected in some of the concretes. Minor quartz was also detected in all patterns, which would be due to the presence of aggregate particles.

With regard to XRD analysis of the interior samples of the different concretes, thaumasite was identified in the PC and PLC concretes, as shown in Figure 4.7. However, in the SRPC and PFA concretes only small traces of ettringite were observed. Only a small peak of gypsum was detected in PLC. In addition, portlandite was identified in all concrete types, except PFA concrete because of the pozzolanic reaction. Calcium Carbonate silicate hydrate (C-C-S-H) and calcite were observed as major products together with moderate peaks of aragonite in all concretes. More carbonate was formed in PLC and PC concretes, but relatively less in SRPC and PC-PFA concretes, as shown in Table 4.3, with the possibility of

continued thaumasite formation in these latter concretes as more sulfate diffuses into the core concrete.

Tables 4.3 and 4.4 summarise the quantities of minerals detected in samples at burial depth 1 as well as degradation phases identified in all the samples.

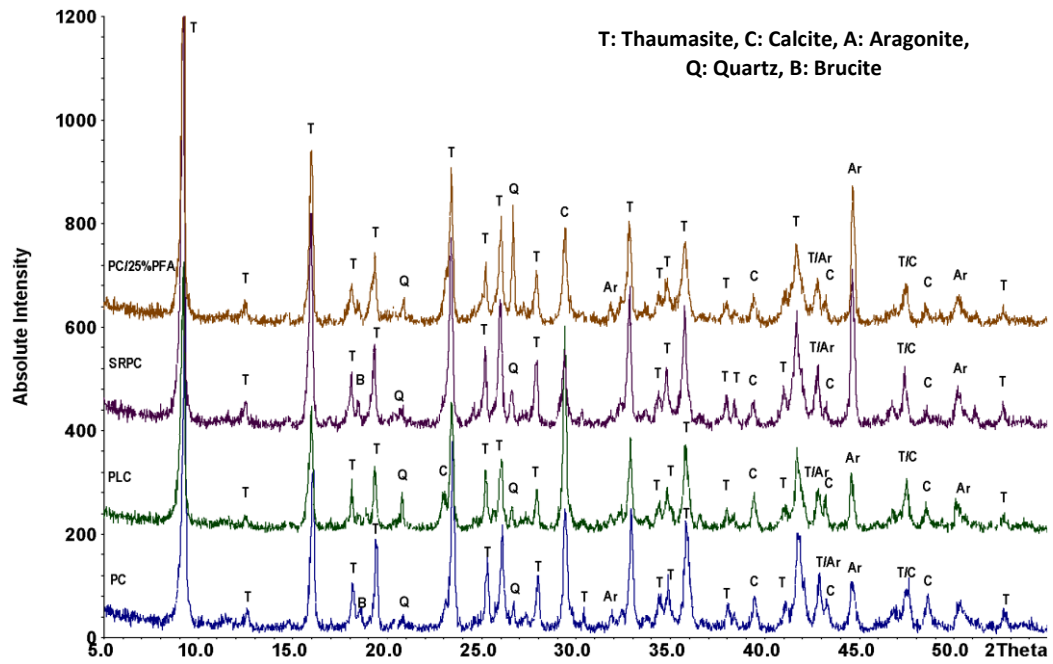


Figure 4.6 XRD results for the surface samples of the four concrete types at burial depth 1

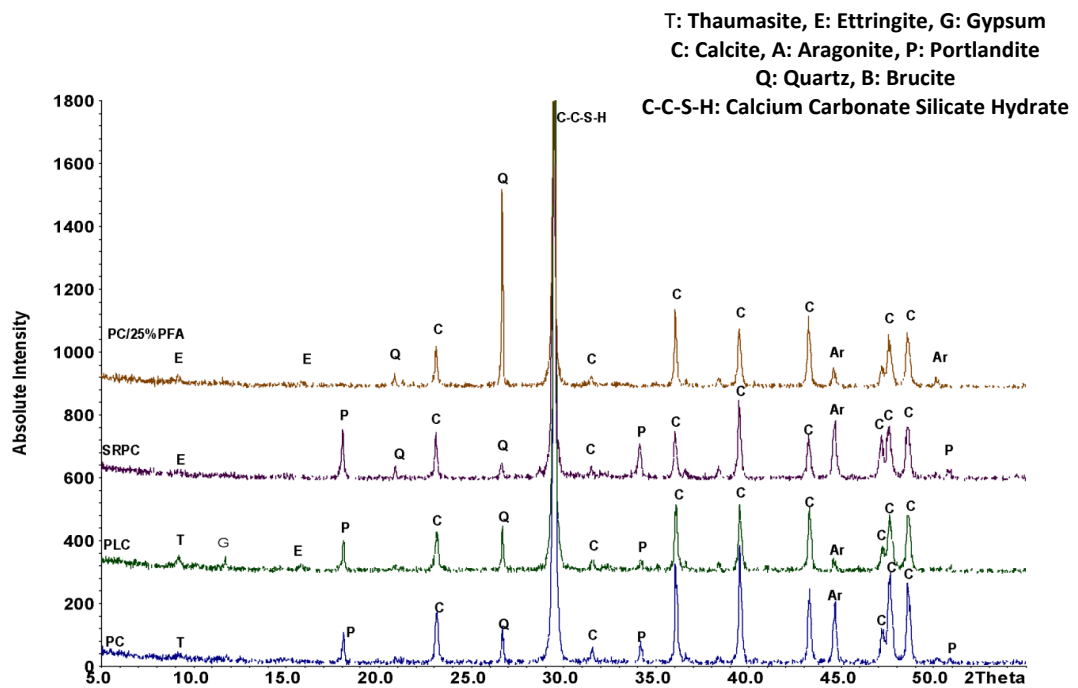


Figure 4.7 XRD results for the interior samples of the four concrete types at burial depth 1

Table 4.3: Quantitative XRD analyses for the degradation products for the four concretes

Concrete Type	Depth	Quantitative (% sample weight)							
		T	C	Ar	E	G	P	B	C-C-S-H
PC	Surface	37.7	30	15.40	0	0	0	1.2	0
PLC		43	41	7.90	0	0	0	1.0	0
SRPC		45.7	22	6.50	0	0	0	4.7	0
PC-PFA		50	17	8.20	0	0	0	2.8	0
PC	Interior (50mm)	1.6	16.2	8.4	2.1	0	7.3	0	56.1
PLC		2.4	25.6	6.3	2.9	2.3	4.5	0	46.8
SRPC		0	15.6	11.9	1.7	0	11.1	0	56.8
PC-PFA		0	18.7	7.3	1.2	0	0	0	49.1

Table 4.4 Degradation phases detected in the four concretes.

Binder	Sample location	E	T	G	Q	C	B	Ar	P	C-C-S-H
PC	Surface	-	xxx	-	x	xx	x	x	-	-
	Interior (50mm)	x	x	-	xx	xx	-	x	x	xxx
PLC	Surface	-	xxx	-	x	xxx	x	x	-	-
	Interior (50mm)	x	x	x	x	xx	-	x	x	xxx
SRPC	Surface	-	xxx	-	x	xx	x	x	-	-
	Interior (50mm)	x	-	-	xx	xx	-	x	xx	xxx
PFA	Surface	-	xxx	-	x	x	x	x	-	-
	Interior (50mm)	x	-	-	xx	xx	-	x	-	xxx

Relative importance in sample: x=low, xx=medium, xxx=high

The XRD analyses revealed that the degradation due to TSA occurred in all concrete types, with a severe attack in PLC and a minor attack in PFA concretes. The overall comparison of XRD patterns showed a higher content of carbonate in PLC concrete in which thaumasite production was greatest, which agrees with the visually observed deterioration. Taylor (1997) reported that the composition of CSH gel in SRPC cement is similar to that in OPC. The delayed TSA attack on SRPC samples might be due to the low aluminate phases that assist the nucleation of thaumasite within the matrix, as reported by Taylor (1997) and Pouya (2007).

Formation of thaumasite on PC-25%PFA concrete was investigated by Bellmann (2004, 2007), who suggests that the ability of thaumasite to form from CSH, calcium carbonate and

gypsum, even in the absence of portlandite, which is required for this reaction. Therefore, the consumption of portlandite by a pozzolanic reaction prior to the contact with gypsum might not be able to prevent the thaumasite formation in concrete blended with PFA. Therefore, as all parameters necessary for TSA were available at the PFA concrete-clay interface, the PFA concrete was vulnerable to the thaumasite form of sulfate attack. Overall, although SRPC cement and PFA can delay the formation of thaumasite, thaumasite may form over time, so these binders might not prevent severe damage to concrete which is subjected to long-term exposure to aggressive ground at low temperatures.

The absence of gypsum and ettringite might be due to the consumption of portlandite and sulfate to form thaumasite. Bellmann (2004) agrees that thaumasite might form directly from CH and C-S-H in the presence of sulfate and carbonate ions, which would limit gypsum production or restrict it to a late stage in the process associated with thaumasite decomposition, as postulated by Hagelia et al. (2003). Additionally, the absence of ettringite and gypsum could also be due to the presence of a high concentration of bicarbonate ions due to the dissolution of calcite and the dissolving of CO<sub>2</sub> in water would affect the stability of ettringite and gypsum in such a way that they would be absent, as discussed by Kunther et al. (2013). The low concentration of Mg in the clay may explain the absence and limited formation of brucite, which would otherwise be derived from portlandite. The large amount of calcite apparently present in all concretes implies that more carbonate ions were supplied from the clay which then participated in reactions with the concrete. On the other hand, it is thought that the presence of high quantities of calcite associated with thaumasite resulted from the ingress of bicarbonate and carbonate ions from clay into concrete by reaction with a source of calcium.

With reference to the interior samples, it is suggested that the ingress of high concentrations of CO<sub>3</sub> and HCO<sub>3</sub> supplied from clay into the concrete pore solution would be the main process responsible for forming calcium carbonate calcium silicate hydrate and forming more calcite in the non-PLC concretes. Calcium carbonate silicate hydrate might form as a result of the reaction of CO<sub>3</sub> and HCO<sub>3</sub> ions from clay with calcium silicate hydrate. It is suggested that HCO<sub>3</sub> ions lead to a reduction in the pH of the concrete pore solution. This results in metastability of CSH and might modify CSH to become a solid solution. Part of the calcium would be replaced by carbonate ions, and calcium carbonate silicate hydrate would form. In addition, the released calcium reacts with CO<sub>3</sub> ions, and calcium carbonate minerals in the form of calcite and aragonite would precipitate. With increases in the concentrations of CO<sub>3</sub> and HCO<sub>3</sub>, more calcite would form and silica gel would be available, as stated by Suzuki et al. (1985, 1994). Borges et al. (2010) highlighted that decalcification

of CSH takes place before to the formation of silica gel, which silica gel formed at a later stage of carbonation. Moreover, the formation of aragonite is a good indicator of CSH carbonation.

Although Portlandite reacts with carbonate ions to form calcite, portlandite was available in the interior concrete after nine years. It is suggested that part of the portlandite might be covered by a calcium carbonate layer which would prevent the consumption of  $\text{Ca}(\text{OH})_2$ . Borges et al. (2010) suggest that carbonation of CH might be rapid than that of the CSH. However, surface of the CH might be covered by a layer of  $\text{CaCO}_3$  micro-crystals, results in preventing further carbonation of CH.

Once the surface of the sample has deteriorated, sulfate ingress becomes easier and more rapid. A reduction in concrete quality and therefore the possibility of the degradation of interior concrete due to TSA would be time-dependent as sufficient carbonate and sulfate ions are required to initiate thaumasite formation. Further explanation for the pH values measured for the concrete at different depths and the profile of diffusion of sulfate and carbonate and its influence on the formation of thaumasite are presented in Section 4.3. The results of XRD provide further confirmation of the vulnerability of buried concrete to TSA. Thus all concretes, even the PFA mix, were damaged.

#### **4.1.4 FTIR results**

FTIR analysis is considered a powerful technique for distinguishing between mineral phases by the unique wavelength which each phase emits when subjected to infra-red scanning. Here the method is particularly helpful. In other analysis techniques, such as XRD, there is a difficulty in differentiating between ettringite and thaumasite at peak around 9.2, in which ettringite detected at 9.21 and thaumasite 9.24, which have a similar XRD signature structure, especially at  $2\theta = 9.60$ . However, in the FTIR, thaumasite has unique wave length of thaumasite is 496-500, 660 and 756 which is attributed to  $\text{SiO}_6$ , whereas ettringite has a wave length of  $852 \text{ cm}^{-1}$  due to the presence of  $\text{AlO}_6$ . (Zhou et al., 2006, Ma et al., 2008; Torres et al., 2003). The results of the IR spectrum for different concretes are discussed in this section.

Figure 4.8 presents the comparison of the IR analysis of deteriorated material from the surface. These IR spectra are similar to each other in all concrete types, suggesting that similar deterioration mechanisms were operating in the different concretes. As noted from XRD data, thaumasite and carbonate minerals were the dominate deterioration product and no ettringite and gypsum were detected. The presence of  $499.6$ ,  $672.7$  and  $755.1 \text{ cm}^{-1}$  peaks,

which attributed to  $\text{SiO}_6$ , emphasised that the deterioration observed in all concretes was due to thaumasite whereas the IR analysis confirms the absence of ettringite and gypsum from the XRD results of all samples. Moreover, the strong peak associated with  $\text{SO}_4$  was detected at  $1103.8 \text{ cm}^{-1}$ , which refers to sulfate in the form of thaumasite. A carbonate phase was also detected at peaks  $712$ ,  $875.6$  and  $1397 \text{ cm}^{-1}$  which are typically assigned to C-O. These are attributed to the presence of  $\text{CO}_3$  groups that belong to calcite and thaumasite. In addition a relatively weak stretching peak at  $1485$  of  $\text{CO}_3$  which was related to aragonite was also observed.

Figure 4.9 illustrates the IR analyses for different interior concrete samples in which the presence of thaumasite was confirmed in PC and PLC concretes by the identification of an Si octahedral peak at a waveband of  $675 \text{ cm}^{-1}$  and a small peak at  $500 \text{ cm}^{-1}$ , whereas in SRPC and PC-PFA concretes the key evidence for thaumasite formation was not observed. In addition, the peak at  $855 \text{ cm}^{-1}$  associated with  $\text{AlO}_6$  confirms the presence of ettringite. Peaks corresponding with carbonate minerals identified as calcite and aragonite were observed in all concretes. However, the carbonate phases observed in all interior concrete samples would in this case be indicative of C-S-H carbonation as well as calcium hydroxide, which would result in calcite formation and participate in the decomposition of C-S-H. The carbonation of C-S-H is confirmed by the presence of  $\text{SiO}_4$  peak at  $940 \text{ cm}^{-1}$  which has resulted from the reaction of C-S-H with carbonate ions. The detected sulfate probably relates to the formation of ettringite, which was identified in all concrete types.

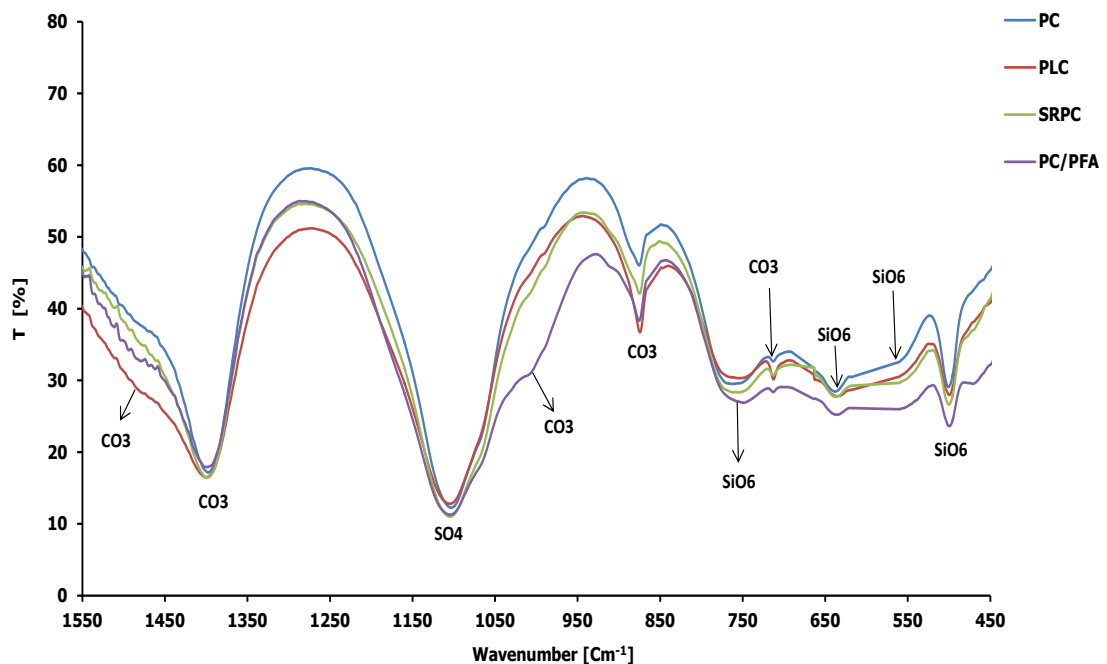


Figure 4.8 FTIR results for deteriorated (surface) materials for the different concretes at burial depth 1

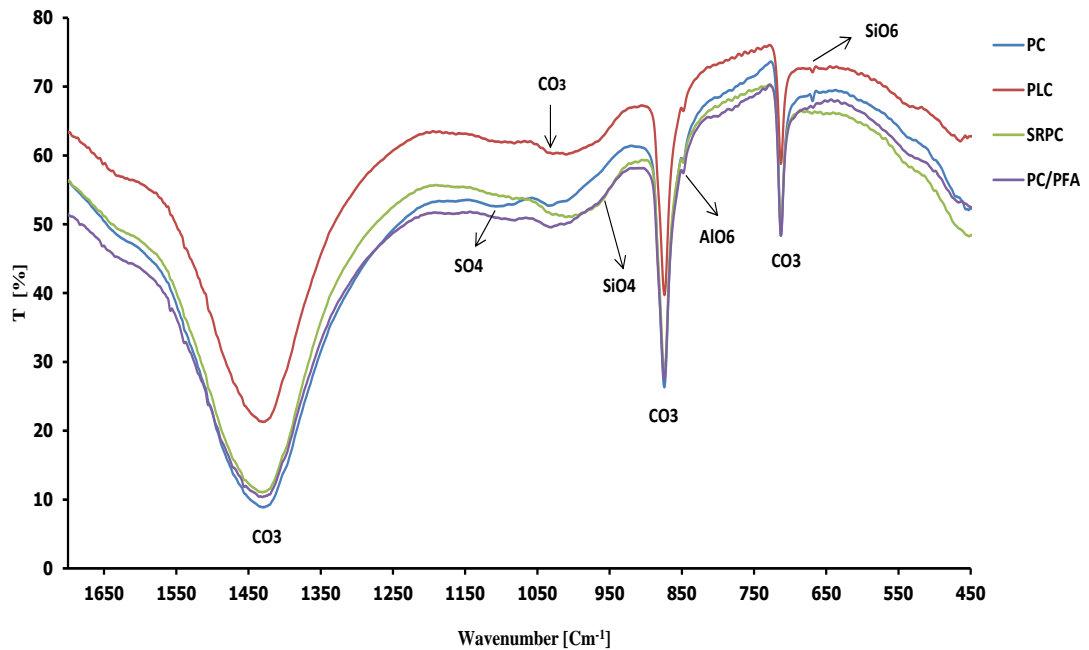


Figure 4.9 FTIR results for core samples for different concretes at burial depth 1

#### 4.1.5 Microstructural analysis of concrete: SEM observations

Scanning electron microscopy (SEM) was used to determine the phases and microstructural features of a range of deteriorated samples. The identification of phases was assisted by means of Energy Dispersive X-Ray analysis (EDX) linked to the SEM. Backscatter images from polished sections were used, since they provide more accurate and reliable EDX analyses than from fractured and irregular surfaces. One of the limitations of electron microscopy is that only a small portion of the surface is imaged, so selecting the areas to be documented generally involves some interpretation of what is present, which introduces an element of subjectivity into the observations. An effort was made in this research to incorporate findings of other researchers in order to provide a clear assessment of the internal structure of the samples analysed.

##### I. Portland cement concrete

Figure 4.10 shows the backscattered image for spalled white mushy material from the uncoated face of the PC concrete. The reaction zone at the surface of the specimen takes the form of a dark grey layer, which was identified as consisting entirely of thaumasite. The magnified details show that the morphology of this thaumasite is dense needles, as shown in Figure 4.10(b), confirming the results of XRD analysis in Section 4.1.3 in which thaumasite was identified. The EDX analysis of the dark grey layer shown in Figure 4.10(c) confirms the occurrence of TSA by the presence of Ca, S and Si. Thaumasite solid solution was also confirmed as indicated by the relevant EDX micrograph in Figure 4.10(d).



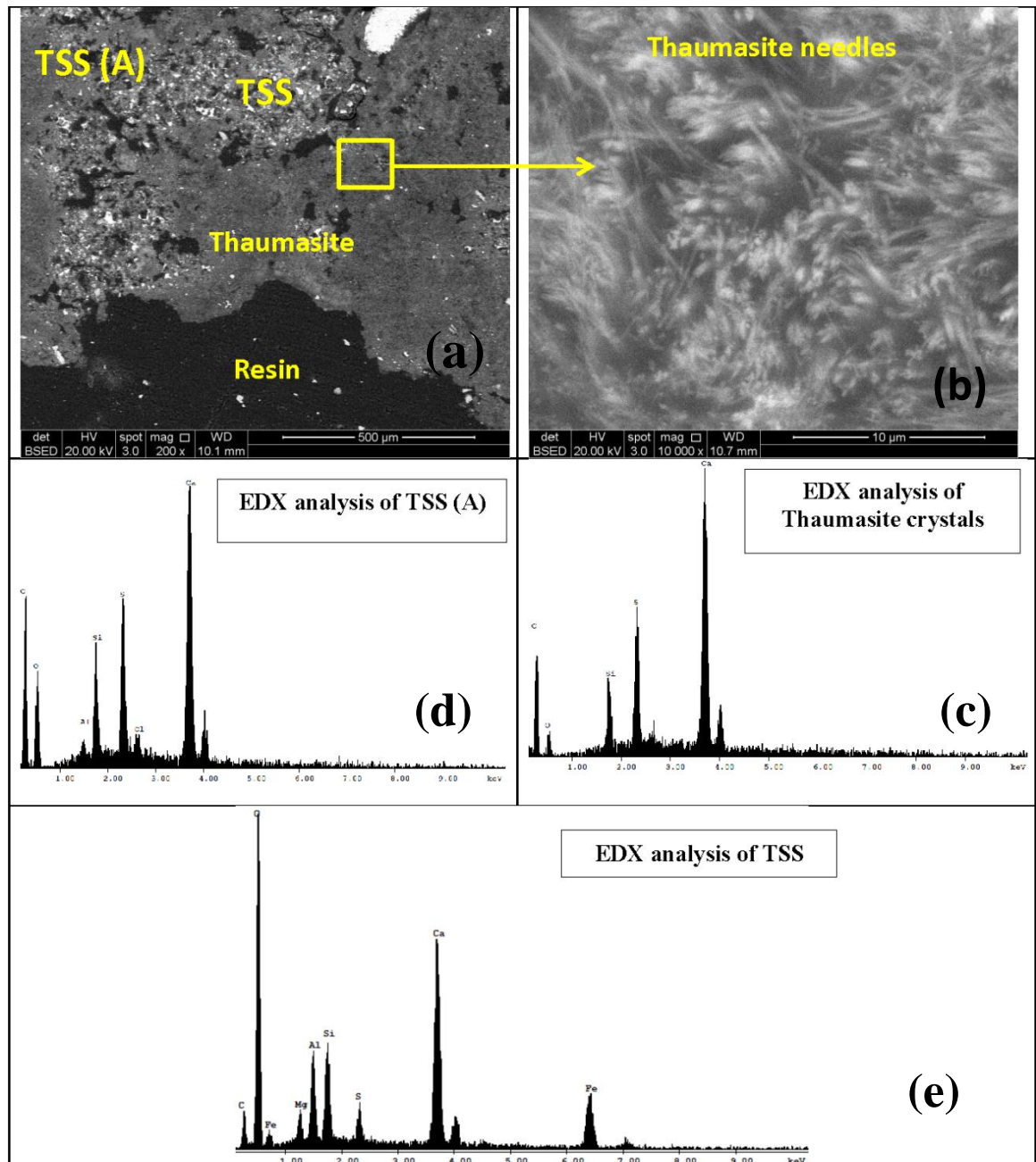


Figure 4.10: Microstructure of PC concrete

According to Grijalvo et al. (2000) and Torres et al. (2006), thaumasite can be formed from ettringite by replacing the Al with Si. Therefore, the ratios of Al, Si and S vary from one solid solution to another. Figure 4.10(e) also shows the presence of magnesium and the incorporation of Fe in the complex structure of these solid solutions. This is in line with Crammond et al. (1995) and Torres et al. (2006), who reported that the ferrite phase can be attacked during the formation of thaumasite. Microstructural analysis of this type of concrete showed that the TSA could proceed through direct transformation of CSH and also at a faster



rate by transformation of ettringite to thaumasite. Thus ettringite acts as a catalyst in the reactions, as reported by Bensted (2003).

The microstructural analysis of PC concrete from the interior of the column reveals that C-S-H was modified to a Ca-C-Mg-S-H phase in which EDX analysis indicated the presence of carbon, magnesium and sulfur, as shown in Figure 4.11. This implies the diffusion of magnesium and sulfate into the concrete core. The presence of a moderate carbon peak in the EDX analysis might indicate the ingress of  $\text{CO}_3$  ions into concrete, which agrees with the XRD finding in Section 4.1.3, in which calcium carbonate silicate hydrate was the dominant phase.

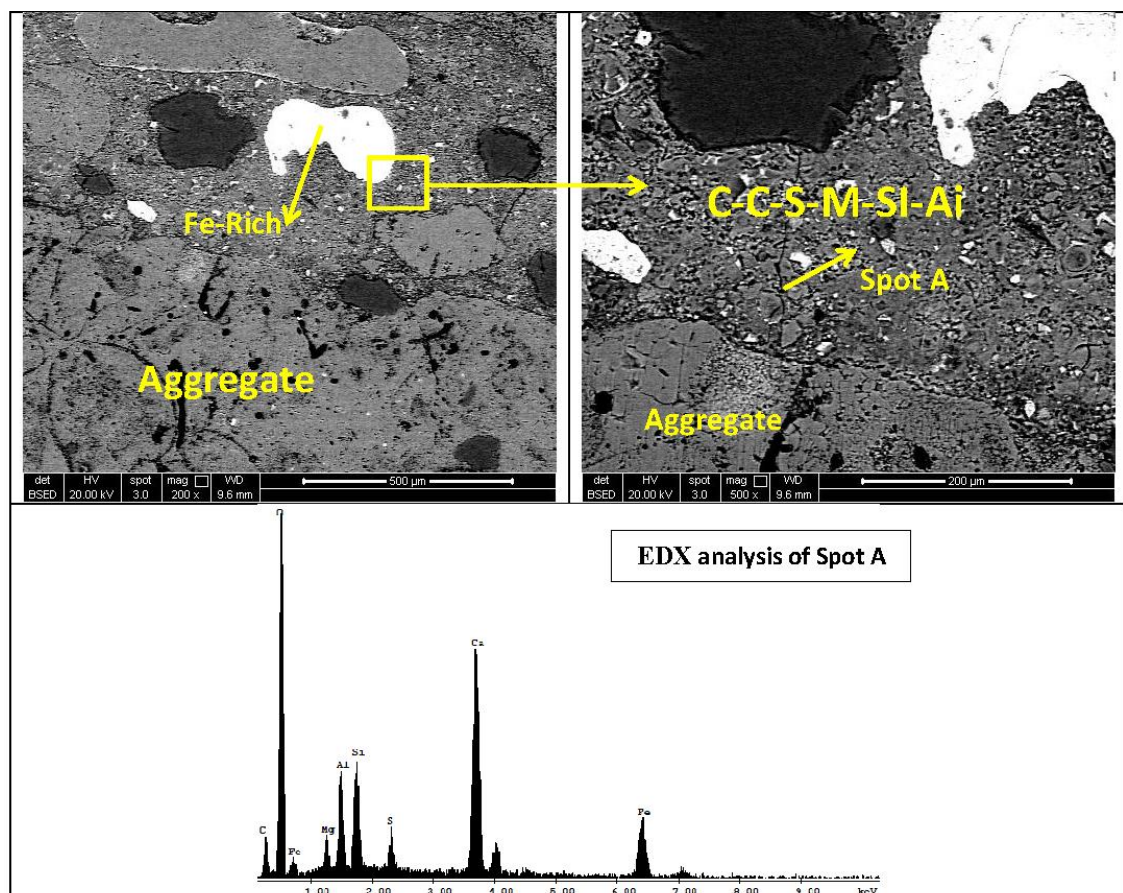


Figure 4.11: Microstructural analysis of PC core concrete

## II. Portland limestone cement concrete

The microstructure of disintegrated PLC concrete is shown in Figure 4.12. The layout of the phases formed within the matrix was similar to that observed for PC concrete, in which thaumasite was the main phase in the reaction zone. Micro-cracking developed around aggregate particles, particularly in areas close to the reaction zone, which might be due to the formation of non-cementitious material and loss of binding with aggregate.

Thaumasite in the form of clumps of dense needles form the dark grey zone shown in Figure 4.12(b). The chemical analysis for the magnified backscattering image in Figure 4.12(c) revealed S, Si and Ca, which is indicative of thaumasite. The presence of ettringite-thaumasite solid solution was confirmed in the grey zone by the EDX analyses, as seen in Figure 4.12(e). Generally, the micrographs shown in Figure 4.12 indicate that concrete made with PLC suffered considerably greater damage than PC concrete, and the EDX analysis implies that thaumasite became all-pervasive in the concrete matrix.

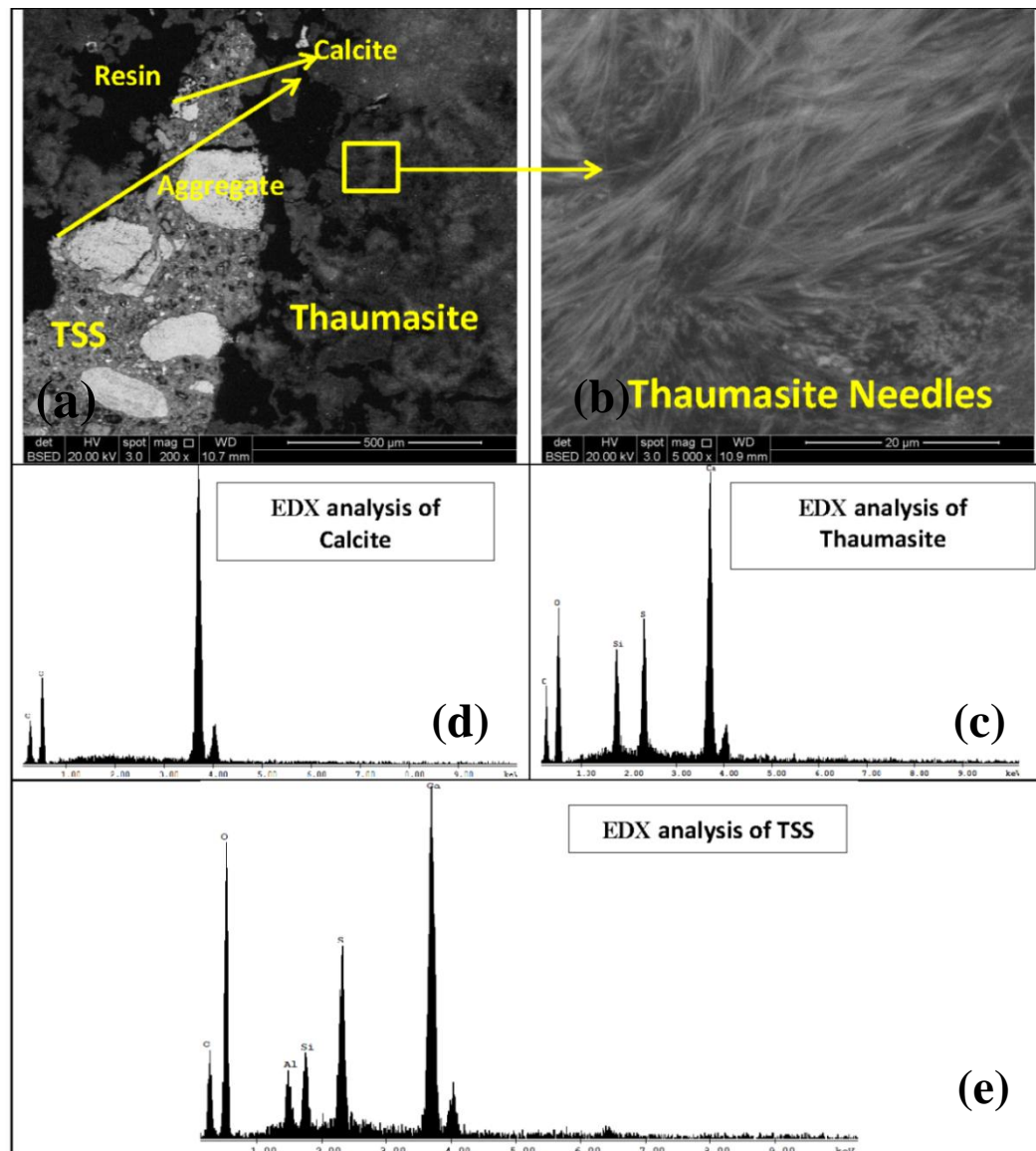


Figure 4.12: Microstructure of PLC concrete (Surface)

Figure 4.13 presents the microstructural features of PLC concrete from the core. Modification to the cement matrix due to attack involves the formation of carbonate in the C-S-H. This indicates that a carbonation reaction of C-S-H has occurred, with carbonate ions derived from clay becoming diffused into the concrete. C-S-H gel with intrusions of

sulfate and magnesium and C-S-H with thaumasite-ettringite solid solution are identified in the EDX results in Figure 4.13. Overall, the findings revealed an absence of ettringite, and the presence of thaumasite solid solution confirms the instability of ettringite in the presence of carbonate, as reported by Kunther et al. (2013).

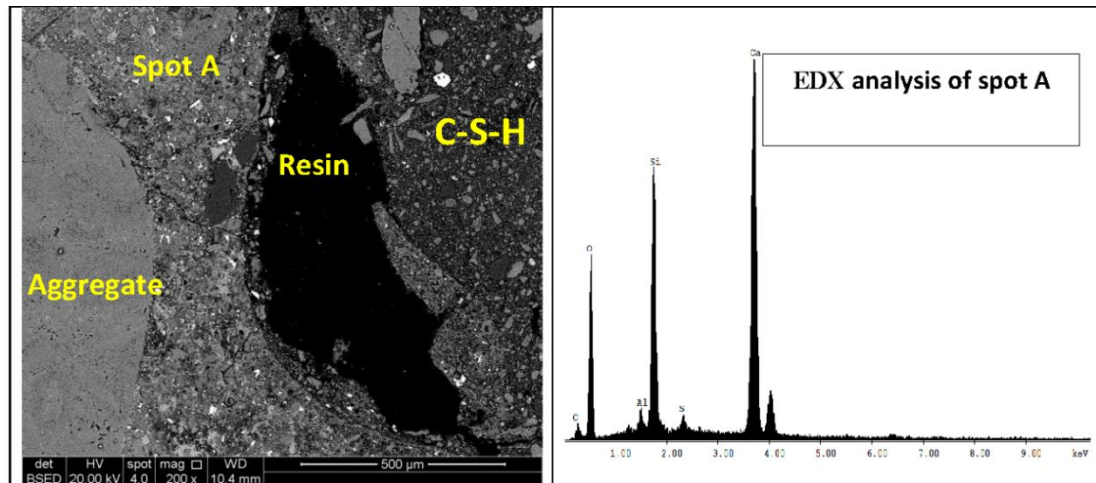


Figure 4.13: Microstructure of PLC concrete core

### III. SRPC concrete

The microstructure of the white surface material of the SRPC concrete is shown in Figure 4.14. It can be seen that the cement matrix appearance is a mixture of grey and dark grey, as seen in Figure 4.14(a). The EDX analysis of the dark grey area confirmed the presence of thaumasite, as shown in Figure 4.14(b). In addition, thaumasite-ettringite solid solution was observed in the grey region, along with calcite. Small traces of Mg and Cl and carbon were also present within the thaumasite, as shown in Figure 4.14(d), which would be indicative of the penetration of these ions from clay into the inner cementitious matrix. As the thaumasite found to be present in this concrete occurred as a solid solution, it may be possible for thaumasite to tolerate some ions, as reported by Bensted (2003). Fe also occurred in the complex structure of these solid solutions; as discussed previously, this can arise as a result of an attack on the ferrite phase during the formation of thaumasite.

Microcracks were found in the cement matrix of the core concrete, as shown in Figure 4.15. These would facilitate the ingress of sulfate and magnesium ions and assist the decomposition of the cementitious matrix. Crack propagation was also observed along the cement matrix but no microcracks passed through aggregate particles, thus indicating the cause was reactions within the cementitious matrix. The EDX analysis of the cement matrix confirmed a carbonation reaction of C-S-H due to carbonate ions becoming diffused into the concrete. In addition, magnesium, S and Al were observed in the composition of the cement

matrix, as shown in Figure 4.15. The presence of a complex compound containing Mg-Ca-Si-S and Al in the inner part of the specimen confirmed the transportation of magnesium and sulfate ions towards the unaltered concrete.

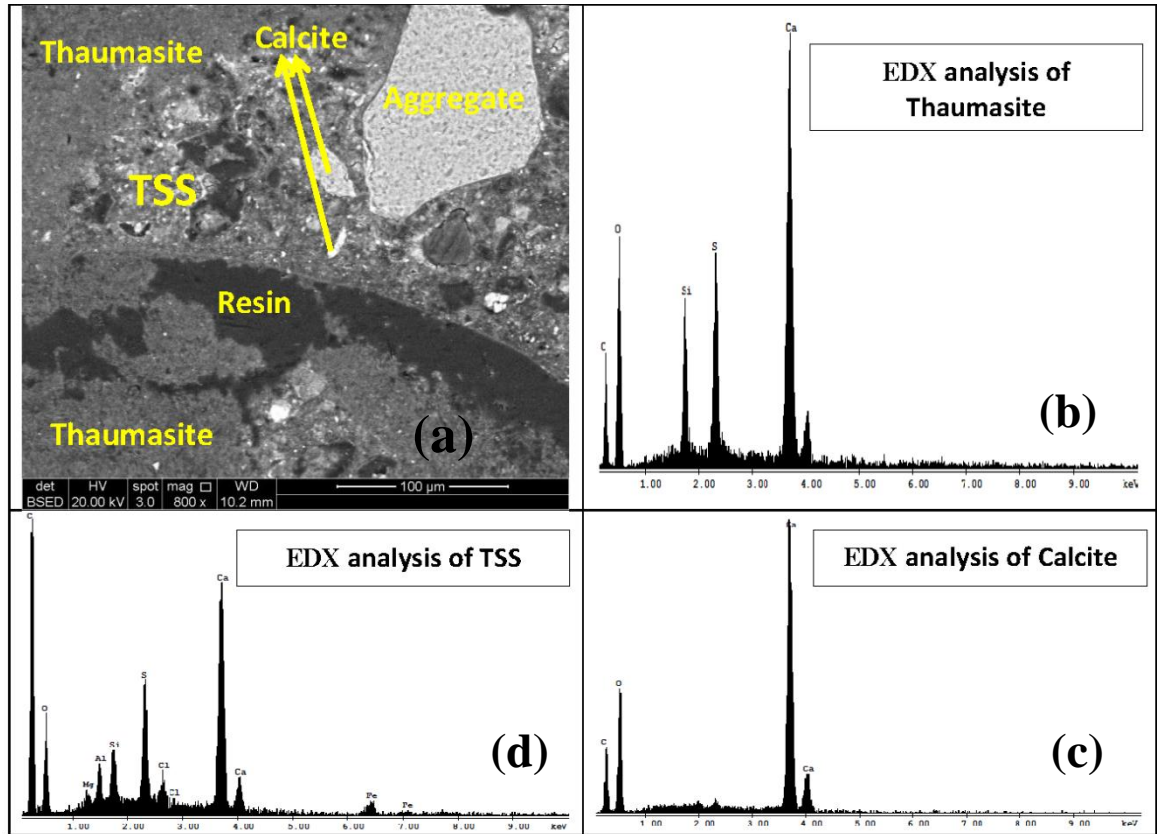


Figure 4.14: Microstructure of SRPC concrete (Surface)

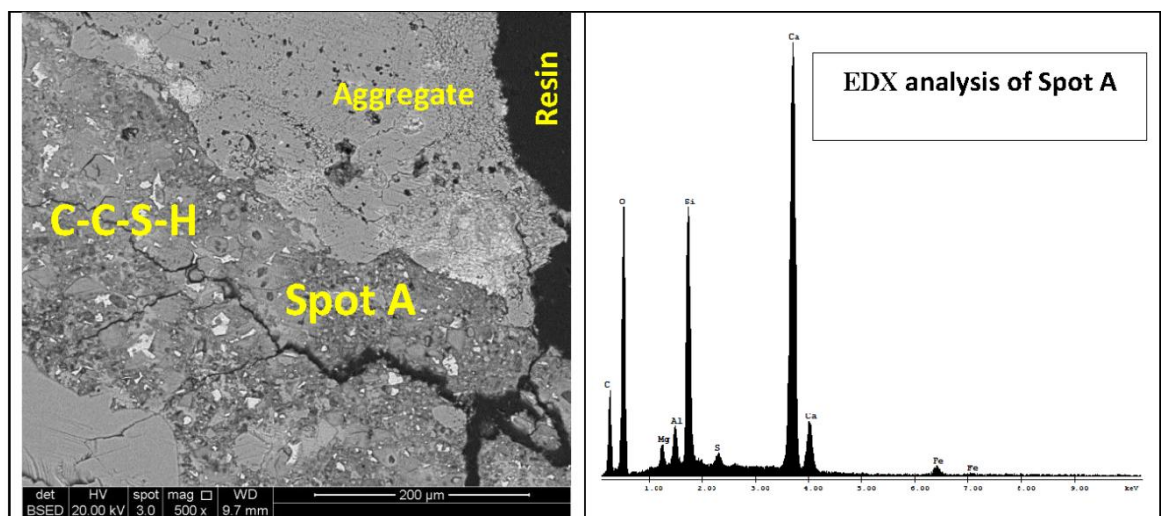


Figure 4.15: Microstructure of SRPC concrete core



#### IV. PC-PFA concrete

Figure 4.16 shows the microstructural features of the deteriorated white surface material from the PC-PFA concrete in which aggregate particles and the dark grey of the cement matrix appear alongside grey regions within the concrete matrix. Microcracks within the matrix indicate an expansive alteration of the binder and this would assist the ingress of ions for the conversion of C-S-H to extensive zones of dense thaumasite needles.

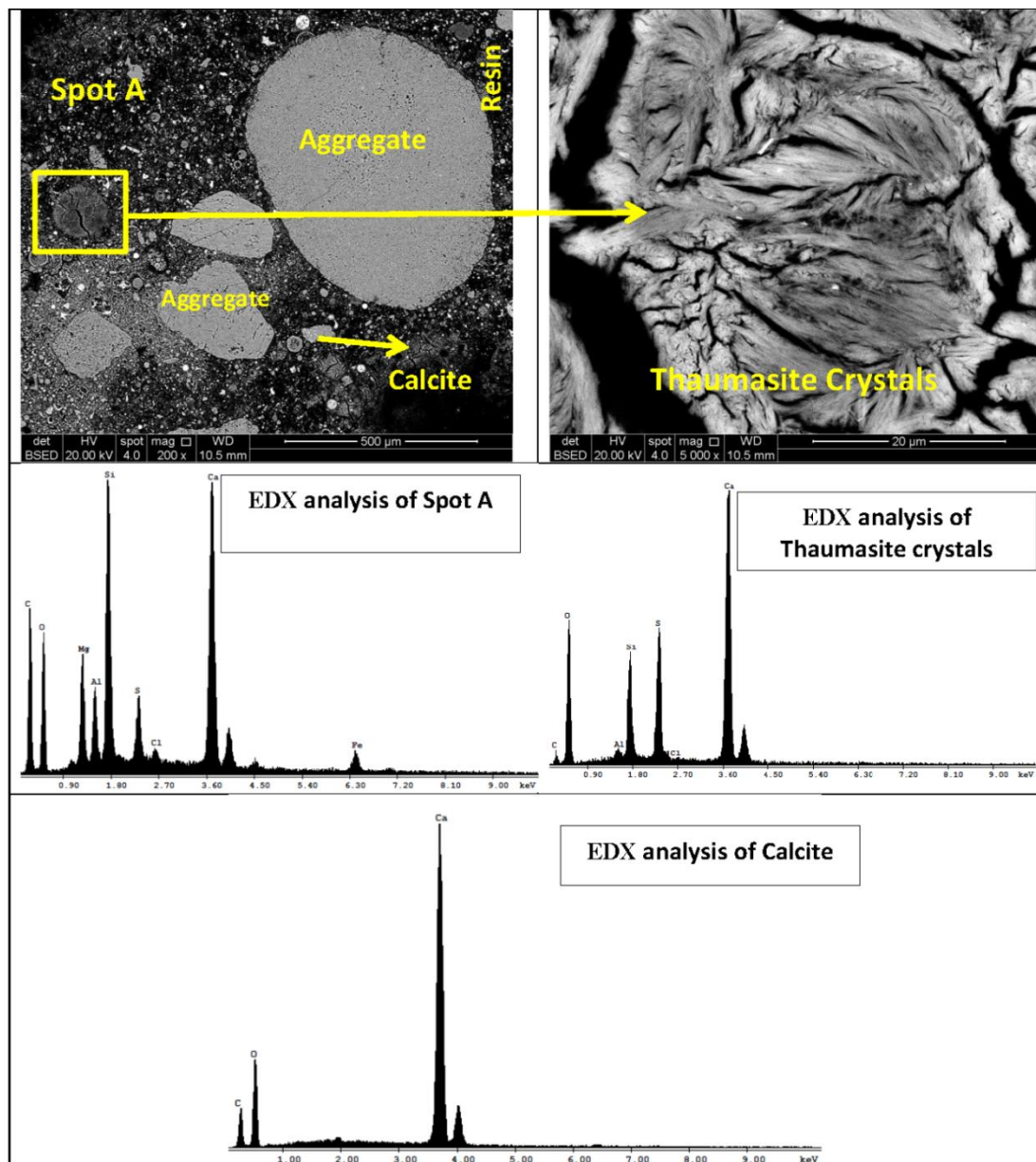


Figure 4.16: Microstructure of PC-PFA concrete (Surface)

Close investigation of the dark grey area shows evidence for thaumasite and an embedded thaumasite solid solution in the matrix. The EDX micrograph in Figure 4.16 of the reaction

products in the grey region shows that this region was mainly Mg-CSH solid solution with the incorporation of sulfate, and Cl ions along with carbonate and Al within the structure. This may be due to the diffusion of magnesium and other ions into the cementitious matrix. As it was possible to detect the presence of carbonate within the Mg-C-Si-S-H-Al layer, it is suggested that there could be a similarity between thaumasite and this phase which might accelerate thaumasite formation. Calcium and silica were also available from CSH with amorphous silica from PFA to form thaumasite. Although the absence of portlandite from the system and the incorporation of aluminates within the pozzolanic CSH might reduce the amount of ettringite formed, it seems that the formation of thaumasite proceeded through a direct route from CSH or amorphous silica, as reported by Pouya (2007). The direct route for thaumasite formation from CSH according to the thermodynamic calculation was also studied by Bellman (2004), who suggested that this can occur without calcium hydroxide as a reactant. Figure 4.17 shows the microstructure of the PC-PFA core concrete where slight colour differences are the main features of the microstructure. Medium to dark grey areas are present around aggregate particles with grey elsewhere.

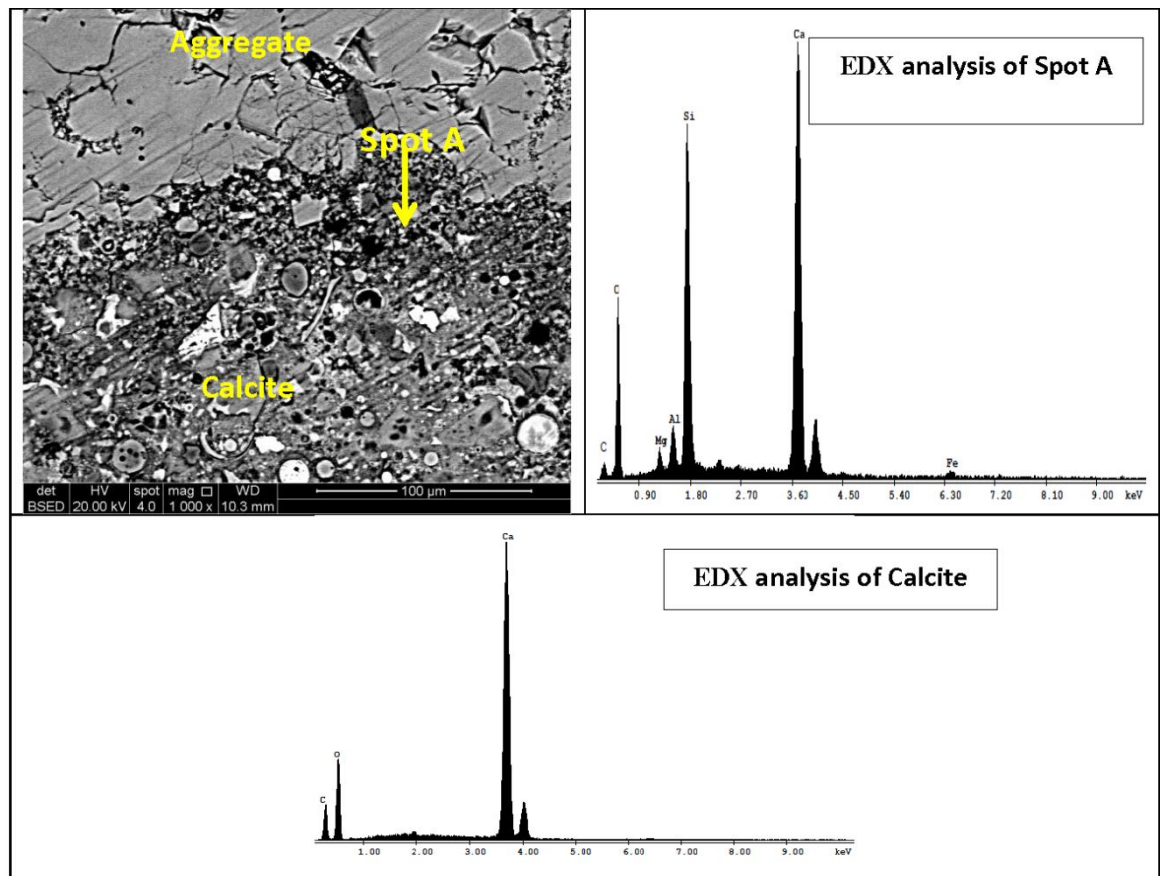


Figure 4.17: Microstructure of PC-PFA concrete core

EDX analysis confirmed moderate carbonation of the C-S-H. In addition, magnesium, S and Al were also components of the cement matrix in contact with aggregate particles, as seen in Figure 4.17. The presence of complex compounds containing Mg-Ca-Si-S and Al in the inner part of the specimen confirmed the diffusion of magnesium and sulfate ions into sound concrete. EDX analysis also revealed the formation of a carbonate phase (probably calcite and aragonite) in the grey regions in Figure 4.17, which would imply that carbonate minerals have been formed as a result of the reaction of CSH with carbonate ions diffused into the concrete core, it being expected that all calcium hydroxide was previously consumed in the pozzolanic reaction. Although sulfate attack was probably delayed by ettringite being less readily formed within the matrix and by the improvement of porosity, this binder is vulnerable to TSA in the longer term, in this case after nine years' exposure to suitable conditions.

An overall comparison of the microstructures for the concretes made with different binders confirmed that thaumasite formation was the main product responsible for concrete attack. In addition, microcracks that were detected in the concrete matrix would assist the transfer of species into the interior of the columns. Such a process might lead to decomposition of CSH and facilitate thaumasite formation in sound concrete. These results agree well with the XRD data, and there was also confirmation by EDX analyses that gypsum and ettringite were absent from the deterioration products.

## **4.2 Changes in concrete chemistry due to long-term exposure to Lower Lias Clay**

This section presents the findings of the assessment of changes in total sulfate, carbonate and pH values in different concrete at different depths within the concretes that resulted from long-term exposure to LLC resulting in TSA. The methodology for sample preparation and chemical assessment is described in Chapter 3.

### **4.2.1 pH profile**

The results for changes in pH of different concrete and the effect of different cement blends on extracted pore fluid pH are presented in this section. As explained in Chapter 3, the samples were cut into five slices each 10 mm thick, cut from a 70-mm-diameter core drilled to a depth of 50 mm into the uncoated faces of the different columns. The methodology for sample preparation and test is detailed in Chapter 3.

The pH profile for all four concretes is shown in Figure 4.18, which indicates that all concretes had a surface pH which was lower than that measured further into the concrete core and reaches a reasonably constant value at a depth at which any signs of deterioration cease. In addition, the profiles also reveal that there is a correlation between the measured deterioration thickness and stabilisation of pH as shown in Table 4.5. The pH values for the sound PC, PLC and SRPC concretes were very similar, in which a constant values of 12.47, 12.48, 12.43 and 12.08 were recorded where no signs of deterioration in PC, PLC, SRPC and PC-PFA concretes respectively. These values are slightly lower than a typical value for natural concrete as reported by Collins et al. (1987), He et al. (2011), Rasanen et al. (2003) and McPolin et al., (2009) who stated that pH for OPC concrete would normally be between 12.8 and 13.0, whereas in PC-30%PFA the value would be about 12.7. This indicates that there was a further episode of reaction between clay and concrete leading to a pH reduction in the concrete surface and the core in which carbonate and sulfate ions from the clay have reacted with available  $\text{Ca}^+$  and CSH, and the reaction product has relatively low pH than the original pH of concrete matrix before exposure to clay. It is also clear that the chemical environment extends about 30 mm from the face of the concrete. However, the variation in the pH of the concrete surface correlates directly with the ability of each concrete type to resist deterioration as shown in Figures 4.18 and Table 4.5, as exemplified by the PC-PFA concrete. The high pH in the concrete surface compared to other concretes is an indicative for the delay of deterioration due to replacement with 25%, whereas the deterioration in PLC occurred after six months of exposure to Lower Lias Clay (Byars 2003). Therefore, pH and the depth of constant pH can be considered as a method of assessing the performance of the concrete and the progress of reaction of aggressive species with cement matrix in which a low pH of 9 was recorded where concrete had deteriorated.

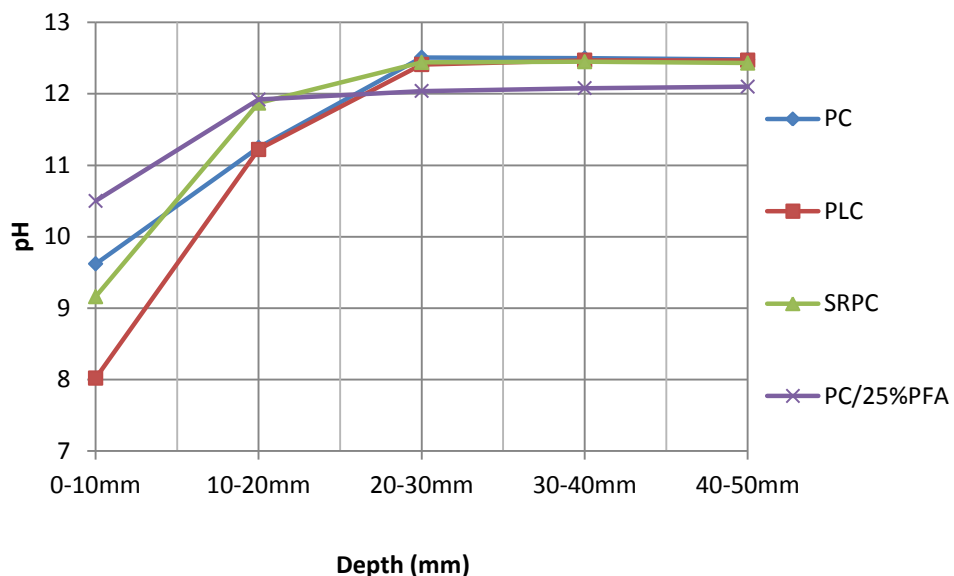


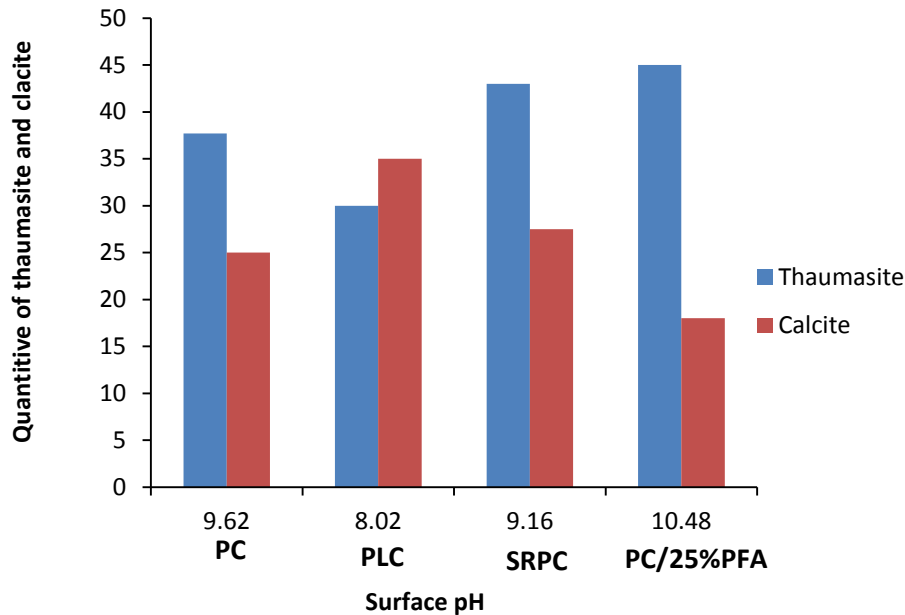
Figure 4.18: pH profile for different concretes at burial depth 2



**Table 4.5** pH values of concrete surface and stabilisation depth of pH at burial depth 2.

Mix	Stabilisation depth of pH (mm)	Maximum depth of deterioration (mm)
PC	30	25
PLC	40	33
SRPC	30	19
PC/25%PFA	20	7

The relation of surface concrete pH and quantities of deteriorated materials are shown in Figure 4.19. It reveals that as pH dropped the quantities of thaumasite decreased, confirmed that the decomposition of thaumasite as reported by Hageli et al (2003) in which thaumasite reacts with carbonate and bicarbonate ions derived from clay and secondary calcite would form as shown in case of PLC concrete.

**Figure 4.19:** Quantitative of thaumasite and calcite for different concretes at burial depth 2

The high pH in intact concrete is achieved by the presence of hydroxyl ions and other alkaline ions. However, where PC is replaced with PFA, more portlandite is consumed in the pozzolanic reaction, resulting in a reduction in hydroxyl ion production, and therefore a lower pH, as stated by Anstice et al. (2005). Although pH of less than 9 was expected to result from reactions of carbonate ions with the concrete matrix, more calcium hydroxide was present due to the use a high volume of cement in this study ( $390 \text{ kg/m}^3$ ), together with other high-pH-maintaining compounds, such as potassium and sodium oxides, which limited the reduction in pH. Overall, the change in pore fluid pH is associated with changes in the chemistry of concrete due to thaumasite sulfate attack, carbonation or a combination of both as a result of the ingress of certain anions or cations.

### 4.2.2 Sulfate profile

The transfer of sulfate ions between the Lower Lias Clay and the concretes is considered in this section. The amount of sulfate in the clay increased during the experiment from 0.5 g/l after six months to 1.68 g/l after nine years. The amount of water soluble sulfate present in the concretes is assumed to be in the form of thaumasite, ettringite and gypsum. The methodology for sample preparation and test is described in Chapter 3. It should be mentioned that only sulfate concentration at surface and core for PC and PLC was measured at burial depth 1 due to greater deterioration thickness and spalled material.

Figure 4.20 shows the cumulative amounts of sulfate in the four concretes at various burial depths. It can be seen that the concentration of sulfate is highest at the clay–concrete interface, where the concrete was converted into white mushy material consisting of up to 35% by weight of  $\text{SO}_3$  in case of PLC concrete, bound in the form of sulfate-bearing phases such thaumasite. Clearly, the concentration in the core concrete was much less than at the interface.

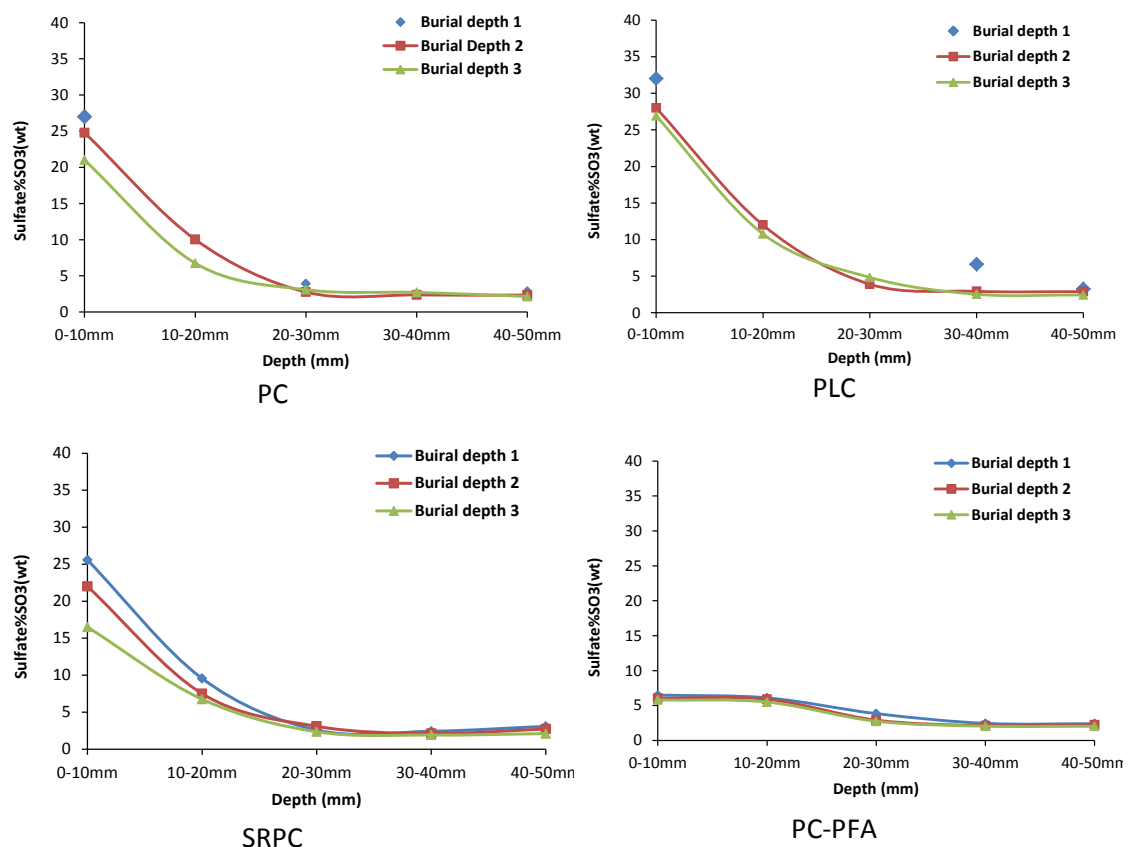


Figure 4.20: Sulfate profiles for different concretes at different burial depths

With reference to concrete type, in the cases of the PC, PLC and SRPC concretes there is a higher concentration of sulfate in the outer 20 mm of the concrete, which drops to the normal level at a depth of 30 mm. Low sulfate was diffused into PC-PFA at a depth of 0-10 mm, which was about 6.3% wt of cement. This can be due to the influence of adding PFA to refine and improve the permeability of concrete. It was also found that the concentration in the sound concrete was slightly higher than the original value shown in Table 4.6, confirmed the transfer of sulfate ions into core concrete especially at burial depth 1.

Table 4.6 Original sulfate contents of different binders

Concrete Type	PC	PLC	SRPC	PC/25%PFA
<b>SO<sub>3</sub>% wt</b>	2.48-3.28	2.04-2.68	2.1	2.11-2.71

With regard to burial depth, Figure 4.21 demonstrates that there is a **correlation** between the burial depth of clay and sulfate concentration at the concrete–clay interface. It was observed that the amount of sulfate concentration at a burial depth of 900 mm was lower than that at shallower burial depths as more deterioration was identified at this level in all concretes. In the sound concrete, the concentration of sulfate was slightly higher at burial depth 1 than at deeper burial depths, as seen in Figure 4.21. This might be due to the migration of more sulfates into sound concrete, as the thickness of deterioration in the concrete at burial depth 1 is greater than at deeper burial depths.

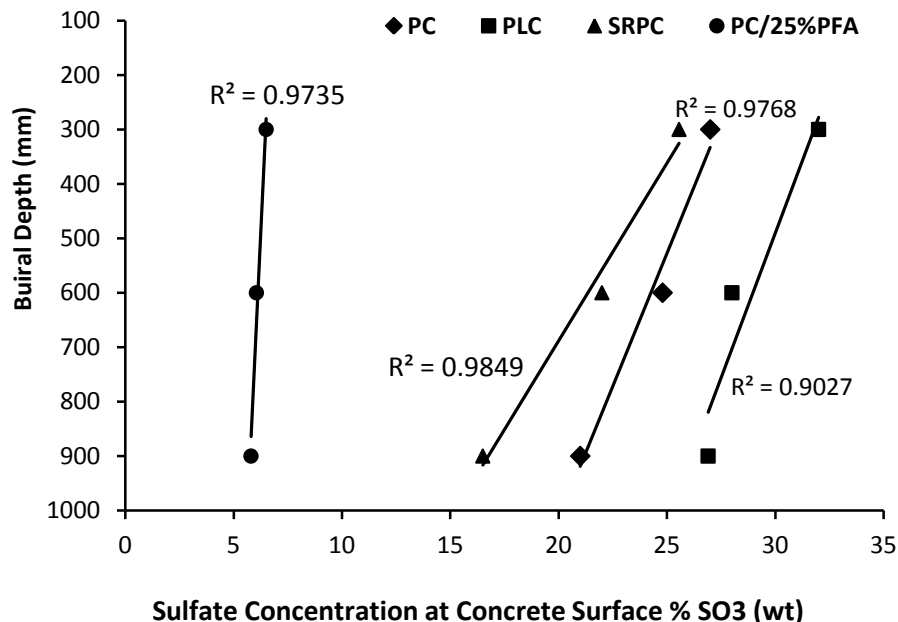


Figure 4.21: **Correlation** between exposure depth and sulfate concentration

Brueckner et al. (2012 a & b) suggested that sulfate penetration was affected by the pressure applied in the interface, where high sulfate penetration was observed at low interface pressure; this may explain why concrete at a low-pressure interface had a greater thickness of deterioration product. This was visible in the present study, in which the concentration of sulfate was lower at a deeper clay–concrete interaction, where the pressure of the concrete–clay interface is high, than in shallow clay–concrete interaction.

In this study, higher sulfate concentrations were found at the front reaction region in each concrete type, and the normal trend of diffusion could be measured behind the front reaction. It is assumed that, at the initiation of deterioration, cracking and spalling facilitated access for sulfates from the clay. This means that the rate of ingress of sulfates into the concrete is not known as it would not have occurred at a constant rate. This agrees with results by Brueckner (2007) who described the transfer of sulfate into TSA-affected concrete prior to visible signs of deterioration in terms of three phases, and it was assumed that, behind the front reaction the diffusion is subjected to common diffusion law. Therefore, the diffusion rate can be determined for the depth at which the concrete remained intact.

It was not possible in this study to measure the amount of sulfate required to initiate thaumasite formation; however, these results imply that the high concentration of sulfate is not the only controlling factor that can be relied on in order to diagnose the occurrence of the thaumasite form of sulfate attack on concrete in the field. Clear evidence for that was found in concrete with 25% PFA which had deteriorated as a result of TSA; the sulfate concentration at the deteriorated surface was about 6.3% wt cement, in comparison with PLC concrete, in which the concentration of sulfate was about 35% wt cement. Therefore, the high concentrations of sulfate might be only used as an indication for the severity and progress of thaumasite sulfate attack, which other parameters such as availability of carbonate and temperature which are required to initiate thaumasite formation should be present. However,

### **4.2.3 Carbonate profile**

This section details the carbonate ion exchange for different concrete types, which was determined using the methodology described in Chapter 3. The clay used in this experiment contained about 24% carbonate as  $\text{CaCO}_3$ , which is there the external source of carbonate. In addition, siliceous aggregates were used in the mixes, but the PLC concrete contained about 20% limestone filler.

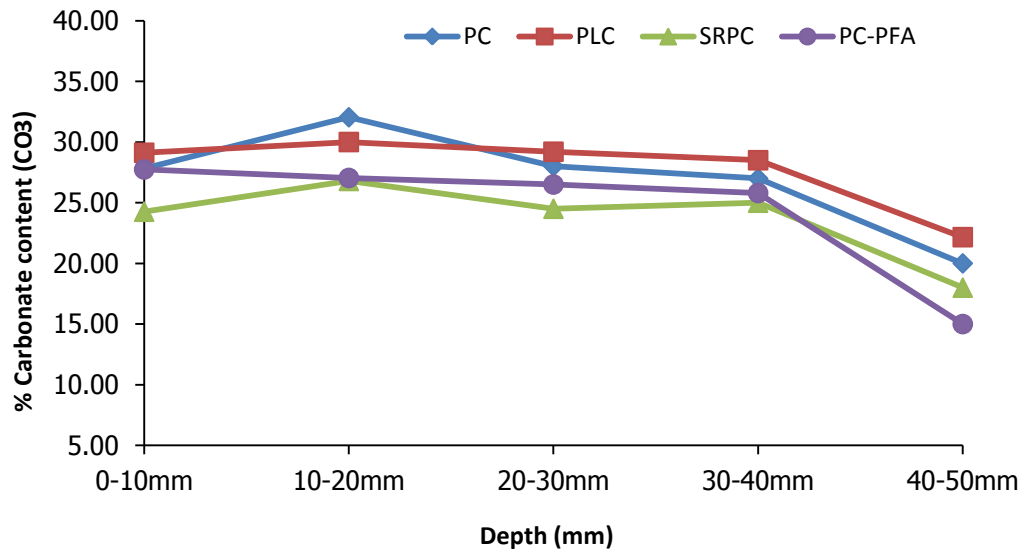


Figure 4.22 Carbonate profile of different concretes exposed to clay at burial depth 2

As shown in Figure 4.22, it can be clearly seen that carbonate content in PLC and PC concretes is **slightly higher** than in SRPC and PC-PFA concretes. This is due to the presence of calcium carbonate in the composition of both PC, in which it was about 5%, and PLC, in which it was 20% limestone filler. The carbonate content was higher in concrete with PC-PFA than in SRPC concrete although the deterioration was less. This implies that concrete containing PFA is more susceptible to carbonation, which confirms reports by Collins et al. (1987) and He et al. (2011). On the other hand, it was surprising that the amount of carbonate in the bulk concrete at depth 50 mm was as high as 22%  $\text{CO}_3$  in PLC concrete and about 15%  $\text{CO}_3$  in PFA concrete (%wt of hydrated product). It would appear that the penetrated carbonate ions derived from clay into concrete would react with calcium hydroxide and CSH might be the main reason for the higher measurements of carbonate in concrete, in which calcium hydroxide and CSH accounts for around 18% and 54 of the total hydration products as reported by Newman and Choo (2003). However, in PC-PFA concrete a large amount of C-S-H has reacted with carbonate ions, as the amount of portlandite is consumed in the pozzolanic reaction of cement hydration. The carbonation of CSH has been reported in the literature by Suzuki et al. (1985), Kobayashi et al. (1994) and Black et al. (2008). On the other hand, the high values of total carbonate occurring in the deteriorated materials might be a result of decomposition of thaumasite, which would raise the carbonate measurement. The results of carbonate measurements agree with XRD analysis for concrete samples from surface and core, in which calcite, aragonite and thaumasite were the dominant deterioration products in concrete surface, while calcite, aragonite and calcium carbonate silicate hydrate was the main minerals form in concrete cores. Furthermore, as the amount of

concrete deterioration increases, there is an increase in carbonate, and it would appear that more carbonate ions are able to migrate into the concrete.

As shown in Figure 4.23, no correlation was found between carbonate content and pH; the pH value was higher than 10 at depths of 20 - 50 mm. Crammond (2003) suggested that a reduction in concrete pH pore solution to 8.4 was expected when concrete reacted with atmospheric CO<sub>2</sub>. However, the presence of other alkaline ions might mitigate the reduction of pH. In addition, it is suggested that more calcite formed as a result of the reaction of carbonate ions derived from clay with Ca-bearing hydration phases than the reaction of CO<sub>2</sub> with portlandite and C-S-H, which would lead to a drop in pH, as reported by Torres (2004), in which calcite was found to precipitate at a pH above 10.3 (Crammond, 2003).

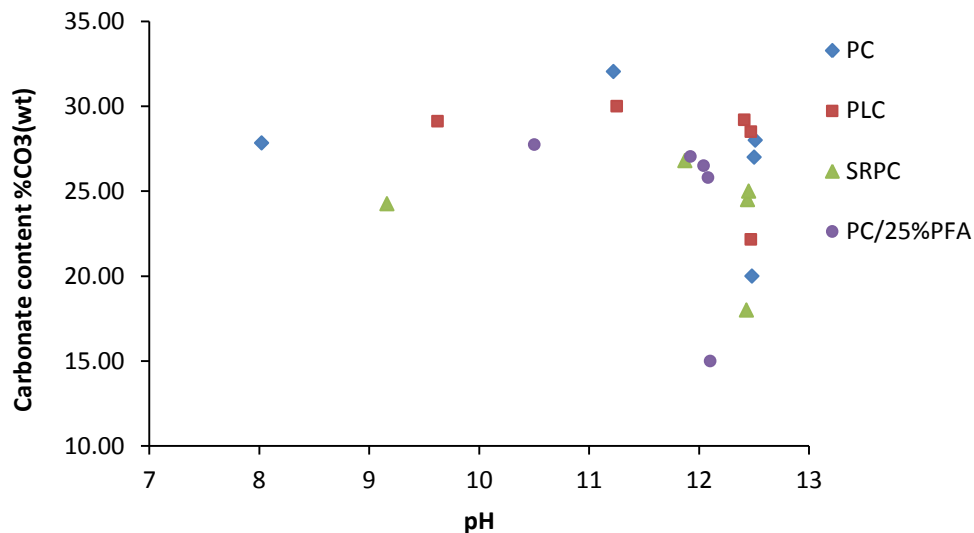


Figure 4.23: Correlation between carbonate (CO<sub>3</sub>) and pH

### 4.3 Chemistry of the clay:

Chemical changes over the duration of the experiment are based upon analyses of clay samples taken from the radial distances of 0-9 cm, 9-18 cm and 18-27 cm from the interface of each concrete. Besides water-soluble sulfate, acid-soluble sulfate, pH, total sulfur and reduction in oxidisable sulfur, the water-soluble calcium, magnesium, chloride, sodium and potassium were also determined. The preparation of the samples and the tests adopted are explained in Chapter 3.

#### 4.3.1 Change in pH

Tables 4.7 and 4.8 respectively summarise the pH results at six months and nine years. As shown, after six months the pH remained approximately neutral, with values in the range

between 7.3 and 8, but with a slight increase at the concrete-clay interface, which may be attributed to leaching of alkalis such as  $\text{Na}^+$ ,  $\text{K}^+$  and  $(\text{OH})^-$  from concrete.

Table 4.7 pH of clay at six month

Clay depth (mm)	Concrete type	Distance from column(mm)	pH value 6 months
Burial depth 1 (0-100 mm)	PC	0-90	7.63
		90-180	7.52
		180-270	7.6
	PLC	0-90	8
		90-180	7.58
		180-270	7.62
	SRPC	0-90	7.7
		90-180	7.25
		180-270	7.02
	PC/25%PFA	0-90	7.68
		90-180	7.3
		180-270	7.5

At nine years the pH values remained neutral, between 7.2 and 8.9, except for a few samples in which the pH was slightly lower than 7.0, which may be the result of pyrite oxidation in regions in which calcite was absent or inaccessible. The neutral pH implies buffering of acid by reaction with calcite in the clay or calcium hydroxide from concrete in the interface region where this would give rise to gypsum production. In addition, the pH values at the PC, PLC and SRPC interfaces were slightly higher than for PC-PFA concrete at all depths.

As the PC, PLC, SRPC concretes were more deteriorated, it is postulated that more calcium hydroxide and other alkaline species such as K and Na would have leached from the concrete. Moreover, pH increased with increased burial depth, as shown in Figure 4.24. This may be due to a lower availability of oxygen, which might lower the rate of pyrite oxidation with increases in the burial depth, as shown in Section 4.3.5. All four concretes suffered from TSA at the concrete–clay interface. This is in spite of the neutral pH of the interfacial clay, whereas, as discussed in Section 4.2.1 (see Gaze et al., 2000), thaumasite is unstable at a pH of less than 10.5. There are two possible explanations for the presence of thaumasite in near-neutral pH conditions, as follows: (1) the pH of clay at the interface was above the threshold for thaumasite formation, reported to be 10.5 (Gaze et al., 2000); (2) natural pH resulting from the buffering reaction of acid produced by pyrite oxidation as well as carbonic acid from the dissolving of  $\text{CO}_2$  in the pore solution of clay might lead to decalcification of CSH. In the presence of  $\text{SO}_4$ ,  $\text{HCO}_3$  and  $\text{CO}_3$  from clay, extensive thaumasite might form with essential of neutral pH or mild acid condition. According to Karim et al. (2003), once

thaumasite forms, it can be stable at a pH as low as 7.0. In this study pH values were between 7.36 and 8.86 after nine years, which is in line with the findings of researchers in terms of stability of thaumasite at lower pH. It should also be mentioned that, although thaumasite is stable at pH lower than 10.5, it tends to react with carbonate ions to form popcorn calcite as the end product of the deterioration reaction.

Table 4.8 pH of clay after nine years

Clay depth (mm)	Concrete type	Distance from column(mm)	pH 9 years
L-1	PC	0-90	7.94
		90-180	7.62
		180-270	7.36
	PLC	0-90	7.84
		90-180	7.64
		180-270	7.23
	SRPC	0-90	7.63
		90-180	6.91
		180-270	6.38
	PC/25%PFA	0-90	7.68
		90-180	7.23
		180-270	6.94
L-2	PC	0-90	7.67
		90-180	7.5
		180-270	7.47
	PLC	0-90	7.87
		90-180	7.67
		180-270	7.44
	SRPC	0-90	7.87
		90-180	7.39
		180-270	7.16
	PC/25%PFA	0-90	7.61
		90-180	7.56
		180-270	7.57
L-3	PC	0-90	8.86
		90-180	7.79
		180-270	7.58
	PLC	0-90	7.8
		90-180	7.73
		180-270	7.41
	SRPC	0-90	7.71
		90-180	7.68
		180-270	7.56
	PC/25%PFA	0-90	7.76
		90-180	7.73
		180-270	7.53



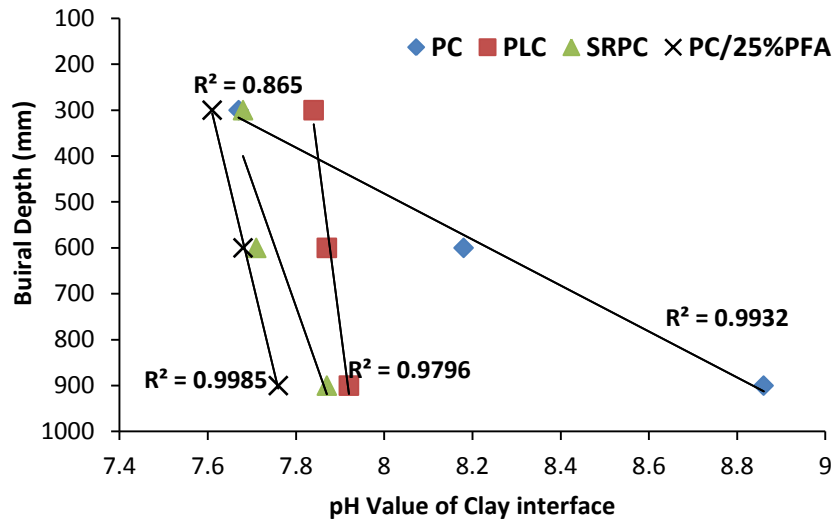


Figure 4.24: Correlation between pH values and burial depth of clay

### 4.3.2 Water-soluble sulfate

The results of chemical analyses of water extracts of clay samples from the concrete–clay interface as well as concrete samples from various distances after six months of exposure are presented in Table 4.9. The sulfate concentration was higher at the PC-PFA concrete–clay interface, followed by the PC, PLC and SRPC concretes. The lower concentrations were observed at the PLC, PC and SRPC interfaces, such that more sulfate would diffuse into the concrete and contribute in thaumasite formation, as observed by visual observation in Section 4.1.1. In addition, it was noticed that the sulfate concentration decreased with increase distance from the concrete. This may be due to the migration of sulfate towards the concrete.

Table 4.9 WWS of clay at six months

Clay depth (mm)	Concrete type	Distance from column(mm)	WWS(ppm SO <sub>4</sub> ) 6 months	WWS(%S) 6 months
Burial Depth 1 (0-100 mm)	PC	0-90	1575	0.105
		90-180	1500	0.1
		180-270	300	0.02
	PLC	0-90	1260	0.084
		90-180	1800	0.12
		180-270	630	0.042
	SRPC	0-90	1125	0.075
		90-180	1650	0.11
		180-270	750	0.05
	PC/25%PFA	0-90	975	0.065
		90-180	1590	0.106
		180-270	1500	0.1

The variation in the concentration of water-soluble sulfate after nine years is illustrated in Figure 4.25 for the different concretes. A high sulfate concentration was observed close to the concrete column compared to that at distance 270 mm. These data confirm the migration of sulfate ions towards the concrete column due to the groundwater. On the other hand, a higher concentration of sulfate was found at deeper burial depths, as shown in Figures 4.25 and 4.26. This would seem to imply that burial depth affected the migration of sulfate ions to concrete, in which sulfate is removed from the clay and more sulfate enters the concrete at shallower burial depth, where deterioration is greatest. On the other hand, It is not clear whether the high concentration of sulfate in at deeper burial depth is due to less deterioration that occurred as a result of low sulfate ingress into concrete due to differences in pressure applied at the interface, as suggested by Brueckner et al. (2012 a & b), or due to the lower permeability of clay at deeper burial depths, which results in less leaching of sulfate from the clay, as suggested by Irshaid and Renken (2002), who stated that the absolute permeability of the clay will decrease with increasing confining pressure due to increasing depth and that therefore the transportation of ions decreases. However, it might be due to a combination of both suggestions.

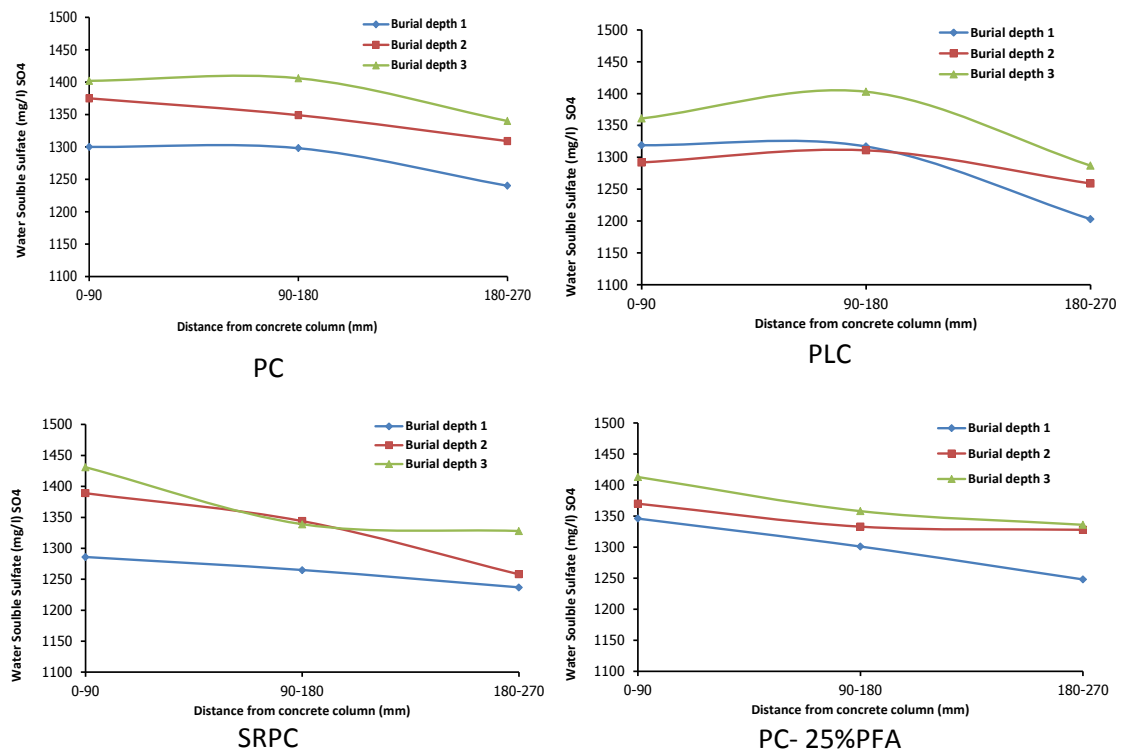


Figure 4.25 Water soluble sulfate of LLC exposed to different concretes

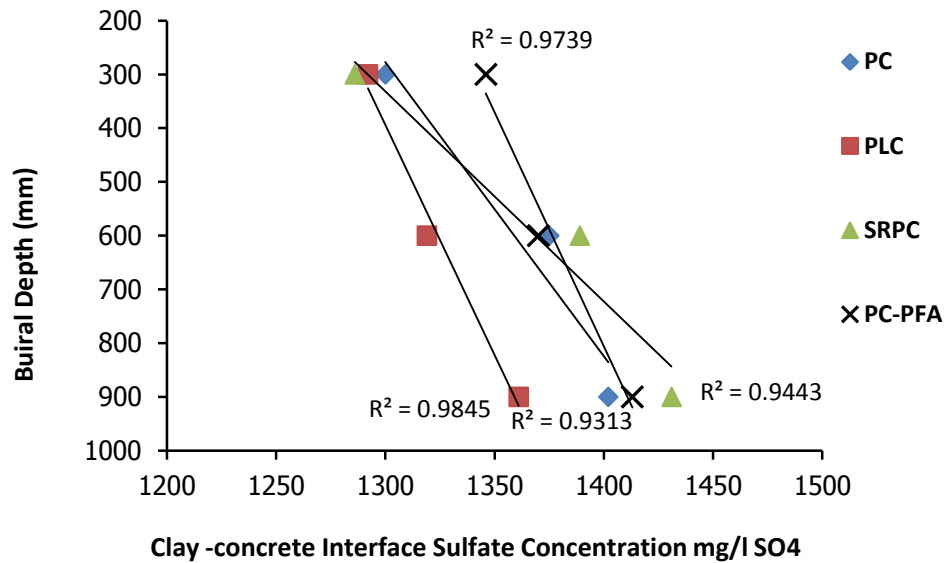


Figure 4.26 Correlation between sulfate WWS and burial depth of clay (0-90mm)

With regard to the interaction with different concretes, the concentration of sulfate in the interface zones of PC and PLC concretes was lower than in those in SRPC and PC-PFA. This might be attributed to the resistance of each concrete to attack. In PC and PLC concretes more sulfate was consumed in TSA, and these suffered from greater deterioration than was observed in PC-PFA concrete, in which the amount of water-soluble sulfate was higher, but less sulfate entered the concrete, as shown in Section 4.2.2. It is suggested that the clay pore solution was saturated with sulfate in PFA concrete. Therefore, there was less variation in sulfate concentrations with burial depth and distances from the concrete column in the case of PC-PFA.

### 4.3.3 Water-soluble species

The variation in the water-soluble composition of Lower Lias Clay after nine years is illustrated in Table 4.10. In particular, a higher concentration of water soluble species was identified at the clay-concrete interface in all concretes at all burial depths.

The concentration increased with increasing burial depth, suggesting that at shallow depths, where the chemical attack was greatest, soluble species were depleted by the movement of ions into the concrete. The responses for the different ions were variable; calcium has the greatest concentration at all clay burial depths and distances from the columns. The concentration of water-soluble calcium was lower in the clay adjacent to PC-PFA and SRPC concrete, which also suffered less deterioration than PC and PLC concrete.

Table 4.10 Water soluble species in clay

Clay depth (mm)	Concrete type	Distance from column(mm)	Ca ppm	Mg ppm	Na ppm	K ppm	Cl ppm
<b>Burial depth 1 (200-300mm)</b>	PC	0-90	741.87	49.41	46.82	50.93	14.33
		90-180	610.329	58.4	46.7	39.43	10.02
		180-270	612.01	77.57	68.77	56.37	36.37
	PLC	0-90	732.813	33.1	43.41	62.6	25.78
		90-180	600.89	54.06	39.91	41.18	4.1
		180-270	659.437	102.04	113.5	161.94	144.23
	SRPC	0-90	679.931	66.3	80.16	64.22	26.43
		90-180	618.817	50.79	43.54	39.52	10.62
		180-270	625.931	117.35	153.12	155.12	154.59
	PC-PFA	0-90	618.776	107.1	147.65	68.34	77.74
		90-180	652.404	83.04	65.27	42.01	13.58
		180-270	662.74	96.53	63.43	67.06	25.28
<b>Burial depth 2 (300-600 mm)</b>	PC	0-90	765.75	46.56	41.43	67.53	9.19
		90-180	707.54	64.64	34.55	37.11	13.16
		180-270	761.502	55.68	44.01	66.16	16.06
	PLC	0-90	730.574	43.74	41.91	69.92	9.44
		90-180	687.63	60.18	34.97	38.15	6.52
		180-270	671.75	52.93	36.63	48.43	9.8
	SRPC	0-90	795.5	39.49	39.04	86.26	28.69
		90-180	777.37	57.83	32.13	39.32	170.62
		180-270	635.545	59.97	39.83	153.61	103.25
	PC-PFA	0-90	707.83	63	39.77	64.25	10.07
		90-180	661.39	69.83	34.73	42.68	6.47
		180-270	629.76	57.51	38.42	60.38	24.66
<b>Burial depth 3 (600-900 mm)</b>	PC	0-90	772.265	19.67	45.74	81.04	8.49
		90-180	700.08	66.75	32.62	48.88	5.13
		180-270	678.934	63.11	41.41	49.99	11.88
	PLC	0-90	681.349	47.55	41.63	63.14	10.6
		90-180	682.02	68.54	36.32	47.08	5.7
		180-270	653.92	55.63	38.16	52.31	16.5
	SRPC	0-90	717.85	50.5	39.24	79.54	26.24
		90-180	703.61	56.84	36.36	41.99	6.57
		180-270	765.06	63.53	39.61	49.25	7.23
	PC-PFA	0-90	672.08	70.32	39.92	57.89	8.32
		90-180	682.02	68.54	36.32	47.08	5.7
		180-270	717.32	69.61	41.75	50.67	9.44

It is postulated that the increase in the concentration of water-soluble calcium at the interface with PC and PLC concrete was due to the leaching out of calcium from portlandite. In the PC-PFA concrete, which contains portlandite, the latter would be consumed in the hydration of pozzolans, which would reduce the amount of portlandite available to be leached out. In addition, the saturation of clay pore solution might affect the rate of pyrite oxidation, and

therefore less gypsum would be available because of the acid buffering reaction. Moreover, the extent of deterioration was much less; no calcium was released back to the clay in the interfacial zone.

The water-soluble concentrations of magnesium, sodium and potassium were much lower than that of calcium; the values varied over relatively narrow ranges but increased with burial depth. The concentration of water-soluble chloride was lower than that of other species at all burial depths of clay and distances from the concrete in addition, there was a slight difference in the concentration of chloride at different clay depths. However, it rose to a maximum of 170 mg/l at burial depth 2 of clay adjacent to the SRPC concrete, followed by the PLC interface zone with clay, where the concentration of chloride was the highest, at a value of 144 mg/l. This could imply that the concentration of chloride in the original clay was variable and was highest adjacent to the SRPC and PLC

#### **4.3.4 Acid-soluble sulfate in the clay**

The results of total acid-soluble sulfate tests (ASS) for clay are presented in Figure 4.27. As described in Chapter 3, the acid-soluble sulfate extraction was carried out according to BS 1377-3:1990. The minerals involved are gypsum, epsomite, **marcasite** and other sulfate components that dissolve in weak acid.

Low ASS was observed in the clay interfaces for PC, PLC, and SRPC concretes compared with the clay from the periphery of the clay. It is suggested that less gypsum would be available in the zone near the concrete column where sulfate migrated into the concrete and engaged in the deterioration process, where severe deterioration was observed. On the other hand, in the case of PC-PFA concrete, the ASS value was higher both close to and far from the column. Thus it appears that the ASS is highest in the vicinity of the least deteriorated concretes, which, it is postulated, is because less sulfate ingressed into the adjacent concrete, with the result that gypsum and other acid-soluble sulfate compounds were precipitated in the clay. With respect to the burial depth of clay, it can be clearly seen that ASS decreased with increasing burial depth of clay at different distances from the concrete. The reduction is about 40% at burial depth 3 in interface zone with concrete, which might be as a result of that less pyrite oxidised and thus less gypsum would form as burial depth increased.

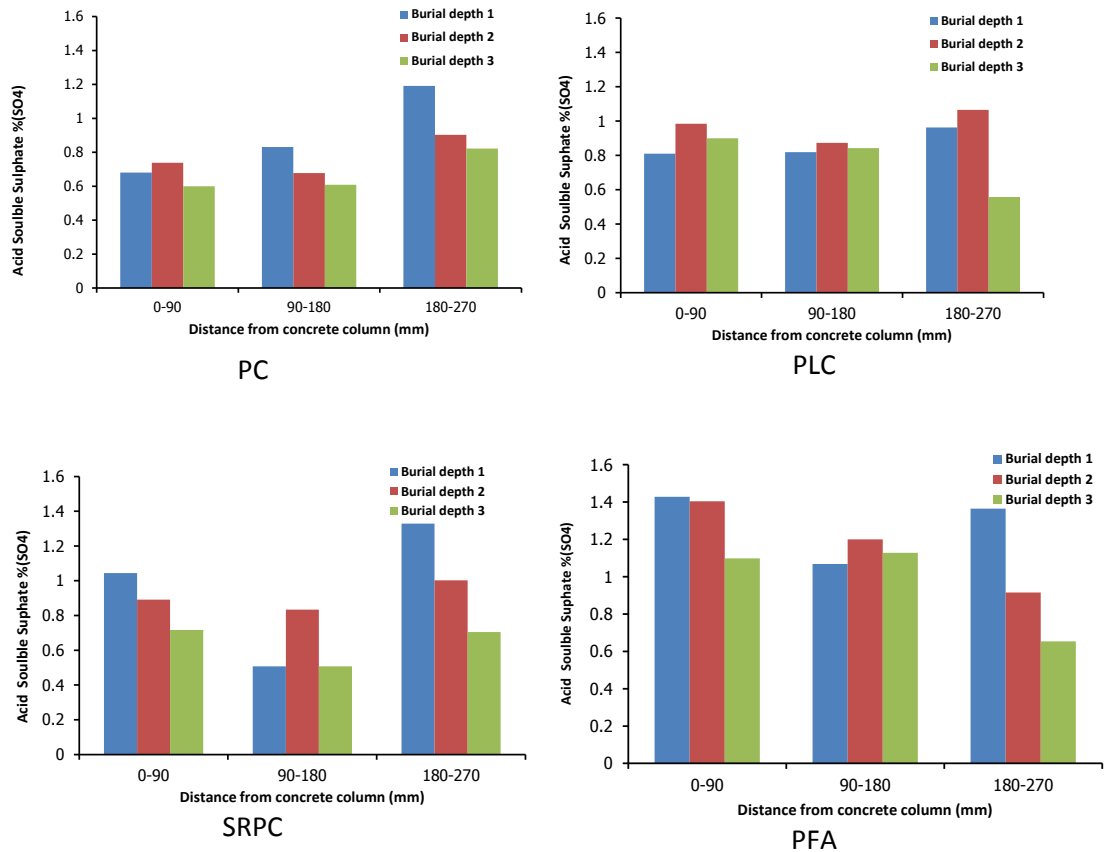


Figure 4.27: AAS of LLC adjacent to different concretes

The high ASS at a distance of 27 cm from the concrete implies that more pyrite oxidation had occurred, which would increase the amount of gypsum formed. In addition, the distribution of pyrite in the clay might be another factor that controls the amount of gypsum formed. However, Czerewko and Cripps (2006) pointed out that neutralisation of sulfuric acid produced from pyrite oxidation may not remove all the calcium carbonate and acidity, as the calcium carbonate may occur in relatively impermeable fragments of rock. Therefore, less gypsum might be measured, and this explains the low ASS in cases of contact with SRPC at a distance of 18 cm, as shown in Figure 4.27.

### 4.3.5 Total sulfur and pyrite oxidation

Table 4.11 contains the total sulfur (TS, %S) measurements, together with water- (WSS) and acid-soluble (ASS) sulfur values, presented as percentages of S (%S) in order to enable comparisons between them. The total sulfur includes all forms of sulfur in the clay, such as epsomite, which is soluble in water, gypsum, which is partially soluble in water and soluble in acid, and pyrite, which is not soluble in either HCl acid or water. Sample preparation and test method are described in Chapter 3. The amount of pyrite is calculated from the

difference between the TS and ASS according to the recommendations of TRL 447 (2005) and BRE SD1 (2005). This calculation assumes that any sulfur not accounted for by acid mobilisation is pyrite.

Table 4.11 Total sulfur values for clay

Clay depth (mm)	Concrete type	Distance from column (mm)	WWS % S	ASS % S	TS % (S)	OS %SO <sub>4</sub>	Pyrite % FeS <sub>2</sub> After 9 years	%FeS <sub>2</sub> At 1 year	Rate of Oxidation % wt/year
Level 1 200-300 mm	PC	0-90	0.092	0.23	0.67	1.33	0.83	1.68	0.09
		90-180	0.083	0.20	0.70	1.26	0.79	1.68	0.10
		180-270	0.087	0.4	0.84	1.32	0.82	1.68	0.10
	PLC	0-90	0.088	0.27	0.55	0.84	0.52	1.68	0.13
		90-180	0.080	0.17	0.62	1.05	0.65	1.68	0.11
		180-270	0.094	0.32	0.82	1.49	0.93	1.68	0.08
	SRPC	0-90	0.086	0.35	0.71	1.08	0.673	1.68	0.11
		90-180	0.082	0.17	0.74	1.7	1.06	1.68	0.07
		180-270	0.090	0.44	0.82	1.13	0.71	1.68	0.11
	PC-PFA	0-90	0.094	0.47	0.92	1.3	0.82	1.68	0.10
		90-180	0.091	0.36	0.87	1.55	0.97	1.68	0.08
		180-270	0.089	0.46	0.85	1.18	0.73	1.68	0.11
Level 2 300-600 mm	PC	0-90	0.093	0.25	0.69	1.32	0.83	1.68	0.09
		90-180	0.089	0.23	0.77	1.64	1.03	1.68	0.07
		180-270	0.094	0.27	0.98	1.57	0.98	1.68	0.08
	PLC	0-90	0.091	0.30	0.65	0.8	0.61	1.68	0.12
		90-180	0.087	0.28	0.68	1.17	0.73	1.68	0.11
		180-270	0.084	0.36	0.86	1.50	0.94	1.68	0.08
	SRPC	0-90	0.095	0.24	0.77	1.4	0.89	1.68	0.09
		90-180	0.084	0.26	0.82	1.62	1.01	1.68	0.07
		180-270	0.084	0.33	0.84	1.52	0.95	1.68	0.08
	PC-PFA	0-90	0.090	0.37	0.98	1.53	0.96	1.68	0.08
		90-180	0.087	0.38	0.93	1.58	0.98	1.68	0.08
		180-270	0.083	0.22	0.89	1.74	1.09	1.68	0.07
Level 3 600-900 mm	PC	0-90	0.092	0.20	0.82	1.85	1.2	1.68	0.05
		90-180	0.090	0.28	0.83	1.87	1.17	1.68	0.06
		180-270	0.087	0.30	0.92	1.93	1.2	1.68	0.05
	PLC	0-90	0.086	0.33	0.78	1.44	0.9	1.68	0.09
		90-180	0.088	0.29	0.79	1.52	0.95	1.68	0.08
		180-270	0.085	0.27	0.87	2.05	1.28	1.68	0.04
	SRPC	0-90	0.089	0.30	0.83	1.77	1.11	1.68	0.06
		90-180	0.089	0.28	0.86	2.1	1.29	1.68	0.04
		180-270	0.093	0.24	0.85	1.87	1.17	1.68	0.06
	PC-PFA	0-90	0.089	0.48	0.98	1.85	1.15	1.68	0.06
		90-180	0.089	0.40	0.91	1.61	1.0	1.68	0.08
		180-270	0.091	0.31	0.94	2.17	1.35	1.68	0.04

According to Table 4.11, lower values of TS were identified in the zone close to the concrete column, where more sulfate had migrated into the concrete and engaged in the TSA. In

contrast, TS increased towards the periphery of the clay cylinder. There is a clear correlation between the type of concrete, the extent of damage and the total sulfur values, as shown in Figure 4.28. This was obvious with respect to the PC and PLC concretes, which suffered severely from attack, so that less total sulfur was observed. However, in the clay adjacent to the PC-PFA concrete, total sulfur was high as small amount of sulfate was diffused into the concrete.

With regard to the amount of pyrite, it can be noticed that lower quantities are present near to the column, suggesting that more pyrite was oxidised in the zone close to the concrete. Furthermore, the amounts were low for the PC, PLC and SRPC concretes, whereas the values of pyrite recorded in the region close to the PC-PFA concrete column were slightly higher. It is postulated that the involvement of more sulfate in the TSA reactions in PC, PLC and SRPC concretes would increase the rate of pyrite oxidation owing to the replenishment of sulfate, while the clay pore solution was saturated with sulfate in PFA concrete, resulting in a decrease in the rate of pyrite oxidation. The ASS was about 3-5 times more than WSS, indicating the presence of a large amount of gypsum in the clay. This can be an indication for the progress of pyrite oxidation in which gypsum was formed as a result of acid neutralising produced from pyrite oxidation.

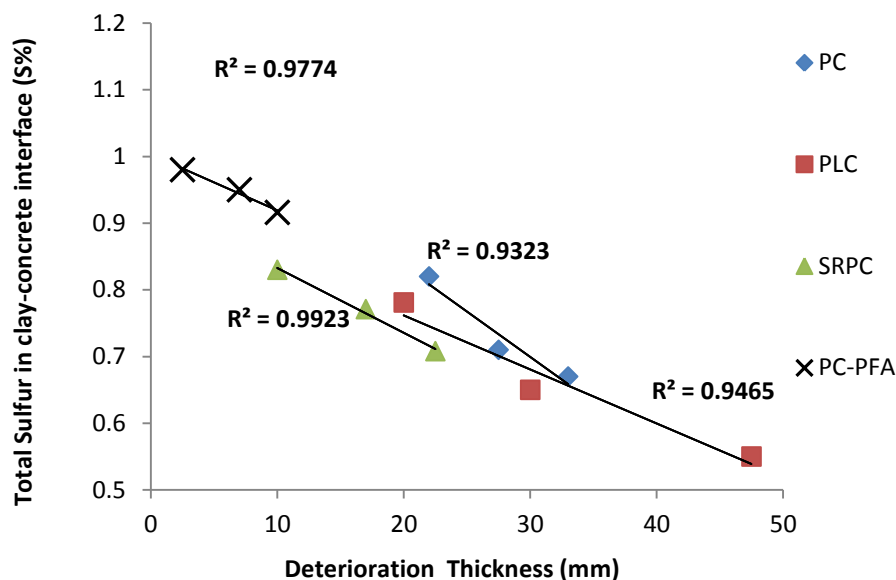


Figure 4.28 Relationship between total sulfur and deterioration thickness for different concretes at different clay burial depths

Figure 4.29 shows that less pyrite was oxidised with increasing burial depth. This implies that the burial depth influenced the oxidation process and the rate of oxidation, as shown in



Table 4.11. This may be attributed to the greater availability of oxygen at shallow depths, which is probably the most important factor controlling the process and the rate of oxidation. In addition, the mobility of pore water was probably found to be higher at shallow depth. This could lead to an increase in the supply of oxygen and the removal of reaction products, thus tending to increase the rate of oxidation of pyrite.

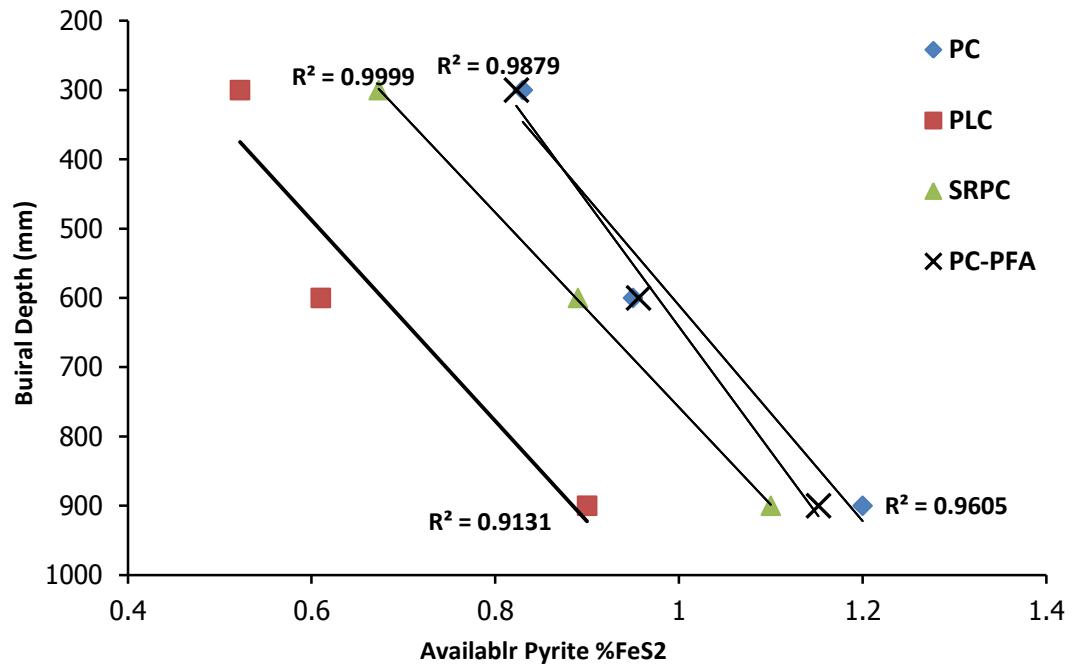


Figure 4.29 Correlation between depth of clay and pyrite

#### 4.3.6 Carbonate content

The carbonate content of the clay is presented in Table 4.12, where the original calcite content of the clay was 24% wt as  $\text{CaCO}_3$ . The consumption of calcite varied in the range between 3.5% and 12.79% of the original calcite. According to Table 4.12, the reduction of carbonate was greatest at shallow depths for all concrete types and all distances from the concrete. It was also observed that the carbonate content decreased more in clay adjacent to the PC and PLC concretes than SRPC and PC-PFA concretes. The higher reduction in calcite from clay adjacent to the PC, PLC and SRPC concretes might be due to the ingress of carbonate ions into the concrete as the deterioration depth exceeded an average of 20 mm, which would result in an increase in the permeability and porosity of these concretes. This was obvious in the carbonate profile in which high carbonate was observed in all concretes, as discussed in Section 4.2.3.

Table 4.12: Carbonate content of clay after nine years of exposure

Clay depth(mm)	Concrete type	Distance from column(mm)	Carbonate content %CaCO <sub>3</sub> 9 years	Consumed Carbonate %CaCO <sub>3</sub>	Rate of consuming % CaCO <sub>3</sub> wt/year
Burial depth 1 (200-300mm)	PC	0-90	13.69	10.31	1.15
		90-180	14.83	9.17	1.02
		180-270	13.92	10.08	1.12
	PLC	0-90	11.44	12.56	1.40
		90-180	12.57	11.43	1.27
		180-270	12.57	11.43	1.27
	SRPC	0-90	15.05	8.95	0.99
		90-180	13.47	10.53	1.17
		180-270	14.83	9.17	1.02
	PC-PFA	0-90	13.7	10.3	1.14
		90-180	11.21	12.79	1.42
		180-270	15.05	8.95	0.99
Burial depth 2 (300-600 mm)	PC	0-90	14.83	9.17	1.02
		90-180	14.83	9.17	1.02
		180-270	15.95	8.05	0.89
	PLC	0-90	12.57	11.43	1.27
		90-180	13.7	10.3	1.14
		180-270	14.83	9.17	1.02
	SRPC	0-90	15.23	8.77	0.97
		90-180	15.95	8.05	0.89
		180-270	14.83	9.17	1.02
	PC-PFA	0-90	15.6	8.4	0.93
		90-180	13.7	10.3	1.14
		180-270	15.95	8.05	0.89
Burial depth 3 (600-900 mm)	PC	0-90	15.95	8.05	0.89
		90-180	14.37	9.63	1.07
		180-270	14.83	9.17	1.02
	PLC	0-90	14.83	9.17	1.02
		90-180	12.57	11.43	1.27
		180-270	13.47	10.53	1.17
	SRPC	0-90	19.12	4.88	0.54
		90-180	16.86	7.14	0.79
		180-270	17.31	6.69	0.74
	PC/PFA	0-90	20.47	3.53	0.39
		90-180	14.83	9.17	1.02
		180-270	15.67	8.33	0.93

Figure 4.30 shows a weak correlation relationship between the calcite consumed and the oxidised pyrite in the clay at the interface with concrete. It is suggesting that more calcite was dissolved in the groundwater in case of more calcite was consumed and less pyrite was oxidised. However, the buffering reaction might not be completed where more pyrite was oxidised and less calcite was consumed, the greater mobility of groundwater at shallow

depth may lead to incomplete neutralisation of acid, as reported by Czerewko and Cripps (2006).

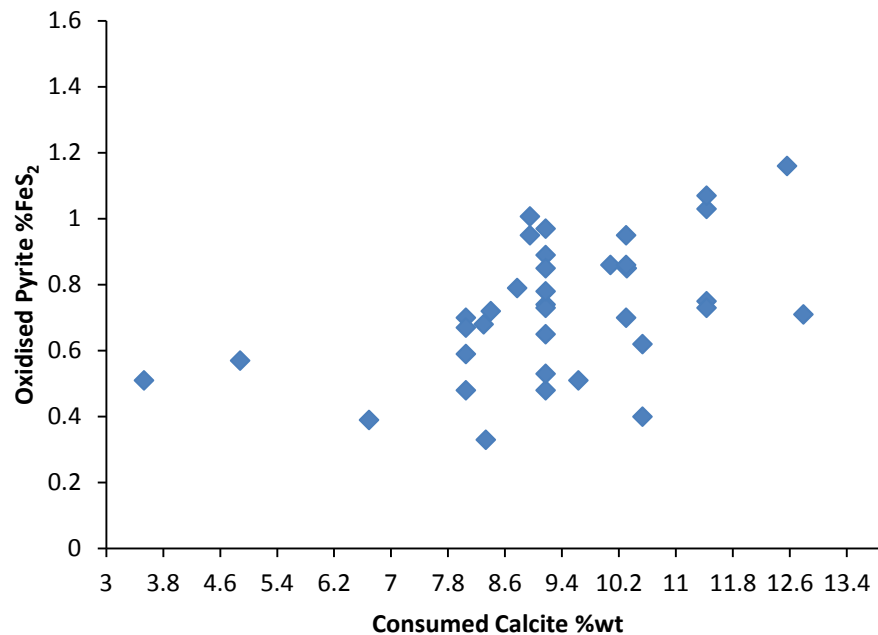


Figure 4.30 Relationship between consumed calcite and oxidised pyrite

Generally, the differences in the measurements of calcite after nine years of interaction with concrete imply the migration of carbonate in different amounts into the different concretes as well as consumption calcite in buffering the acid produced from the oxidation of pyrite. The reduction in calcite might be due to the buffering reaction of acid produced as a result of pyrite oxidation. An additional factor leading to the reduction in calcite might be dissolution. Although calcite solubility is low, it is increased by the presence of CO<sub>2</sub> especially. This would also be assisted at shallow burial depth by more dissolved CO<sub>2</sub> being present. Crammond (2003) and Torres (2004) reported that calcite does not decompose at pH less than 10.33, whereas the pH of the clay pore solution was in the range between 7 and 8. This might be responsible for dissolution of more calcite. Although the increase in pressure with depth would increase the solubility of calcite, this would have a very minor effect on the amount removed.

#### 4.4 Summary

The key findings of the investigation of the long-term durability of PC, PLC, SRPC and PC-PFA concretes in contact for nine years with pyritic Lower Lias Clay at 5°C are presented in

this section. This is thought to be the first systematic study of the long-term performance of concrete made with different binders and exposed to pyritic ground in simulated field conditions. The performance of the concretes was evaluated in terms of visual observation, deterioration depth, mineralogy of deteriorated materials, and changes in concrete and clay chemistry, and the following conclusions can be drawn from the results:

- Severe cases of TSA were observed in the PC concrete column, with the formation of white and yellowish mushy material, spalling and the exposure of aggregate. The deterioration was greatest at shallow depth, with the loss of the column edge, and successively less deterioration at burial depths 2 and 3.
- The damage to the PLC concrete was more severe at **burial depths** 1 and 2, with the loss of corners, spalling, and the loss of up to approximately 50% of cementitious material. White mushy material was identified as a reaction product of the interaction of the PLC concrete column with clay. Moreover, there was less damage in concrete parts exposed to a deeper burial depth of clay (burial depth 3).
- The SRPC concrete column showed signs of attack at burial depths 1 and 2, with spalling of deteriorated material, exposure of aggregate and loss of edge. In addition, white and yellowish crumbly reaction products appeared in the concrete at burial depth 1, while white crumbly reaction products were observed at burial depth 2. At burial depth 3 the extent of deterioration was less than in the upper part of the column.
- PC-PFA concrete suffered less deterioration at all burial depths, with surface blistering and white material reaction products at burial depth 1. Slight but significant attack, with signs of deterioration such as spalling of mushy material at the edge of the column and blistering, occurred at burial depth 1 and the lower part of burial depth 2. The corners of the column retained their original shape and the concrete was sound although there was slight soft mushy material formed.
- In all concrete types, the mode of degradation deterioration was similar, and comprised the formation of white mushy material, spalling, loss of edge, exposure of aggregate and loss of cementitious matrix. While still damp, the deteriorated concrete could be removed easily by hand, and this indicates that all concrete suffered a similar form of TSA.

- The bitumen coating, even when scratched, proved effective in protecting the concretes, including PLC concrete, from attack in aggressive ground conditions created in this investigation.
- The severity of deterioration decreased as follows: PLC > PC > SRPC > PC-PFA; the degree of severity became less as the depth below the surface increased. The observations provide confirmation of the vulnerability of buried concrete to TSA. Thus all concretes, even the PFA mix, were damaged.
- Limestone filler in cement increased vulnerability to TSA; however, its absence does not guarantee immunity to TSA, as the carbonate required can come from other sources, including atmospheric CO<sub>2</sub> and carbonate from the clay.
- The most serious attack occurred at around a burial depth of 300 mm, and PLC concrete had the highest deterioration depths, reaching 47 mm, followed by PC concrete. Less deterioration, with a maximum thickness of 22 mm, was measured in concrete made with SRPC cement. However, concrete made with PC-PFA showed less deterioration, with a maximum of about 10 mm. The maximum thickness of deterioration in the concretes over the nine years of exposure was as follows: PC = 30; PLC = 47; SRPC = 22; and PFA = 10 mm.
- Irrespective of the type of binder, a clear reduction in deterioration thickness occurred as burial depth increased. The maximum thickness of deterioration was recorded at a burial depth of 300 mm in all concretes and the reduction was about 55% at a burial depth of 600 mm. This implies that the burial depth plays an important role in the extent of attack.
- XRD, FTIR and SEM analysis revealed that the minerals present are similar for all surface samples, indicating a similar mechanism of deterioration. Thaumasite was the dominant deterioration product in all concretes, so although SRPC and PC-PFA showed delay in the TSA, with time they are vulnerable to thaumasite formation. Low levels of calcite and aragonite were identified as deterioration products. Gypsum and ettringite were absent.
- Thaumasite was identified in the core of PC and PLC concretes and there was overlapping between thaumasite and ettringite in SRPC concrete. However, in PFA concrete only low amounts of ettringite were present. Gypsum was detected only in PLC. In addition, portlandite was identified in all concrete types but was limited in

PC/PFA concrete because of the pozzolanic reaction. Calcium carbonate silicate hydrate (C-C-S-H) and calcite were observed as major products in the core concretes. This implies that thaumasite sulfate attack may cause deterioration in all concretes in the longer term as further sulfate migrates into the core concrete.

- With regard to the pH profile of different concretes, all concretes had a surface pH which was lower than that measured further into the concrete core. There was a constant value of 12.4 where no signs of deterioration were observed. This value was slightly lower than that in natural concrete. The pH of concrete pore solution PC-PFA was lower than for other concrete types at a depth further into the concrete core. The pH at the concrete surface varied directly with resistance to TSA. The depth of relatively constant pH can be considered as a method of assessing the performance of the concrete in which a low pH of 9 was recorded where concrete had deteriorated.
- The profile of sulfate concentration in the different concretes revealed that the cement binder strongly influenced the diffusion of sulfate ions into concrete. It was lowest for PC-PFA concrete, and highest for PLC concrete, followed by PC and SRPC. In all concretes, a high sulfate concentration was found in the surface and deteriorated concrete. In all cases the concentration of sulfate was slightly higher than normal, indicating that sulfates had migrated from the ground into the core concrete.
- The effect of burial depth and therefore the interface pressure on the diffusion process of sulfate ions into concrete was significant: it was observed that the amount of sulfate concentration at deep clay-concrete interaction was lower than in shallow clay.
- The carbonate content was higher in PLC and PC concretes than in SRPC and PC-PFA concretes, and higher in PC-PFA than in SRPC. Although the amount of carbonate decreased slightly with distance from the interface, the amount of carbonate was higher than expected in cement composition, which suggests that more carbonate ions diffused into sound concrete.
- The chemistry of the clay changed during the experiment, but the pH of the clay remained neutral with values between 7.16 and 8.86, except for a few samples in which the pH was slightly lower than 7.0. Higher pH values were measured close to the concrete interface with the clay. The pH values of clay adjacent to the PC, PLC and SRPC concretes were slightly higher than those for PC-PFA concrete, in

which less deterioration was observed. It should be mentioned that the pH values increased with an increase in depth of concrete–clay exposure, where less deterioration was observed as the depth below the surface increased.

- Water-soluble species concentration decreased in the clay adjacent to the concrete as a result of the ingress of sulfate and other species. However, the amount of sulfate and other species was higher at deep burial depths where deterioration was less. In addition, the concentration of sulfate in the surface PC and PLC concretes was lower than in PC-PFA, which implies the high concentration of sulfate in this concrete's profile as well as the high deterioration depth.
- The amount of acid-soluble sulfate was reduced in the clay adjacent to concrete. The value was highest at shallow burial depths, and it was higher for PC-PFA than for PC and PLC concretes at all depths below the surface. This, it is postulated, is because the amount of acid-soluble sulfate increased where there was less deterioration. This implies that less sulfate ingressed into the concrete, so the clay pore solution became saturated with sulfate, so that gypsum and other forms of acid-soluble sulfate precipitated in the clay.
- The amount of total sulfur in the clay was lowest in the zone close to the concrete column and highest at the periphery of the clay cylinder. In addition, the amount of total sulfur in the clay increased with depth below the surface. There was a good correlation between the type of concrete, the extent of damage and the total sulfur present. Thus, in clay adjacent to PC and PLC concretes, the concrete suffered severe TSA where lower total sulfur was observed. However, in the clay next to the PC-PFA, the total sulfur was high and less sulfate was diffused into concrete.
- It was apparent that more pyrite was oxidised in the zone close to concrete columns and the oxidised pyrite was greatest for PC, PLC and SRPC concretes. However, the values of available pyrite were slightly higher in the clay near PC-PFA concrete. In addition, the values of available pyrite very clearly increased with increasing burial depth. It is suggested that concrete type plays an important role in the control of pyrite oxidation as it affects pH and dissolved sulfate concentration.
- After nine years it can be seen that the amount of calcite decreased from 24% to between 11.4% and 20.5%wt CaCO<sub>3</sub>, and it decreased for shallow burial depth. The carbonate content of the clay adjacent to PC and PLC concretes decreased more than that of the clay adjacent to SRPC and PC-PFA concretes. A relatively weak



correlation was observed between the reduction in pyrite and calcite removal, which reveals that the buffering reaction is probably incomplete and more calcite is dissolved in groundwater.

- Movement of groundwater and transportation of ions and cations into concrete are influenced by burial, and permeability of clay is reduced by increasing burial depth.

## CHAPTER 5

### 5. The Influence of Chemical Composition of Clay on The Extent of TSA

#### 5.1 Introduction

This chapter discusses the results of the investigation into the influence of different clay compositions on thaumasite formation and the severity of thaumasite sulfate attack (TSA), as explained in the experimental design (Series II) in Chapter 3. Concrete cubes made with different binders, namely CEMI, CEMI- 10%LF(CEM I-LF), CEMI-50%PFA(CEMI-PFA), and CEMI-70%GGBS(CEM I-GGBS), were exposed to different conditions at 5° and 20°C. The cubes were buried for 24 months in weathered Lower Lias Clay, slightly weathered Lower Lias Clay and Coal Measures mudstone, for which water-soluble sulfate corresponded to BRE sulfate classes DS-3, DS-2 and DS-1 respectively. A parallel investigation was also carried out in which specimens of the same concretes were placed in BRE DS-2 and DS-4 sulfate solutions and solutions that mimicked the pore solutions of the clays, but without considering the acid produced by pyrite oxidation. Finally, columns of the same concretes 70 mm square and 1000 mm long were exposed to the same clays at 5°C in conditions which simulated the field ground conditions, including the presence of mobile groundwater, so that the effects of mobile groundwater on the extent of TSA could be evaluated. The performance of CEMI, CEMI-LF, CEMI-PFA and CEMI-GGBS in different exposure conditions was also investigated. The materials and methodology used are described in Chapter 3. The performance of the specimens was evaluated by means of visual observation, pH of the clay, and compositional changes revealed by XRD, IR and SEM techniques, as described in Chapter 3. An extensive search of the literature revealed very few studies into the interaction between buried concrete and pyrite-rich clays. This is in spite of the widespread occurrence of such clays, as noted by Czerewko and Cripps (2006), and the huge number of buried concrete structures. The recommendations

contained in BRE SD1 (2005) and similar standards are based upon laboratory studies involving the immersion of concrete specimens in test sulfate solutions, which might be magnesium sulfate or sodium sulfate or a combination of both. It would appear that Crammond et al. (2003) report the only field investigation that has assessed the performance of buried concrete, and it is believed that this investigation is the first published account of TSA deterioration observed in buried concrete in simulated field conditions.

## **5.2 Visual assessment**

This section presents the observations of the performance and mode of deterioration of different concretes after 24 months. It was possible to monitor the changes in visual appearance of samples due to the different exposure conditions.

### **5.2.1 CEM I concrete in sulfate solutions, clays and simulated clay pore solutions at 5 and 20°C.**

Figure 5.1 shows CEMI concrete samples after 24 months of immersion in sulfate solutions, clays and simulated clay pore solutions at 5° and 20°C. The specimens exposed to DS-2 solution at 5°C suffered corner cracking. However, white soft mushy material along with a white precipitated layer on the concrete surface was observed in specimens exposed to DS-4 at 5°C. The only apparent effect at 20°C in both DS-2 and DS-4 solutions was the formation of a white surface deposit, which was in greater quantity for samples immersed in DS-4 solution. In the case of pyritic clays at 5°C, a thickness of about 2 mm of the surface of the concrete immersed in weathered and slightly weathered Lower Lias Clay had deteriorated. White mushy material was the main deterioration product and was easily removed by scratching the surface. Immersion in CM mudstone at 5° and 20°C resulted in deterioration to the corners and edges of the samples, which was less severe than in LLC. Surprisingly, contact with SW-LLC and W-LLC at 20°C resulted in severe damage accompanied by white soft deterioration product at the top edges of specimens. However, less damage was found at 20°C than at 5°C.

The visual assessment of CEMI concrete prisms buried in different clays at 5°C in the presence of mobile groundwater revealed that weathered LLC caused the development of friable white mushy material, as shown in Figure 5.1. No signs of attack were observed in concretes exposed to slightly weathered LLC and Coal Measures mudstone, although a white deposit formed on the surfaces, which was of greater extent for SW-LLC.

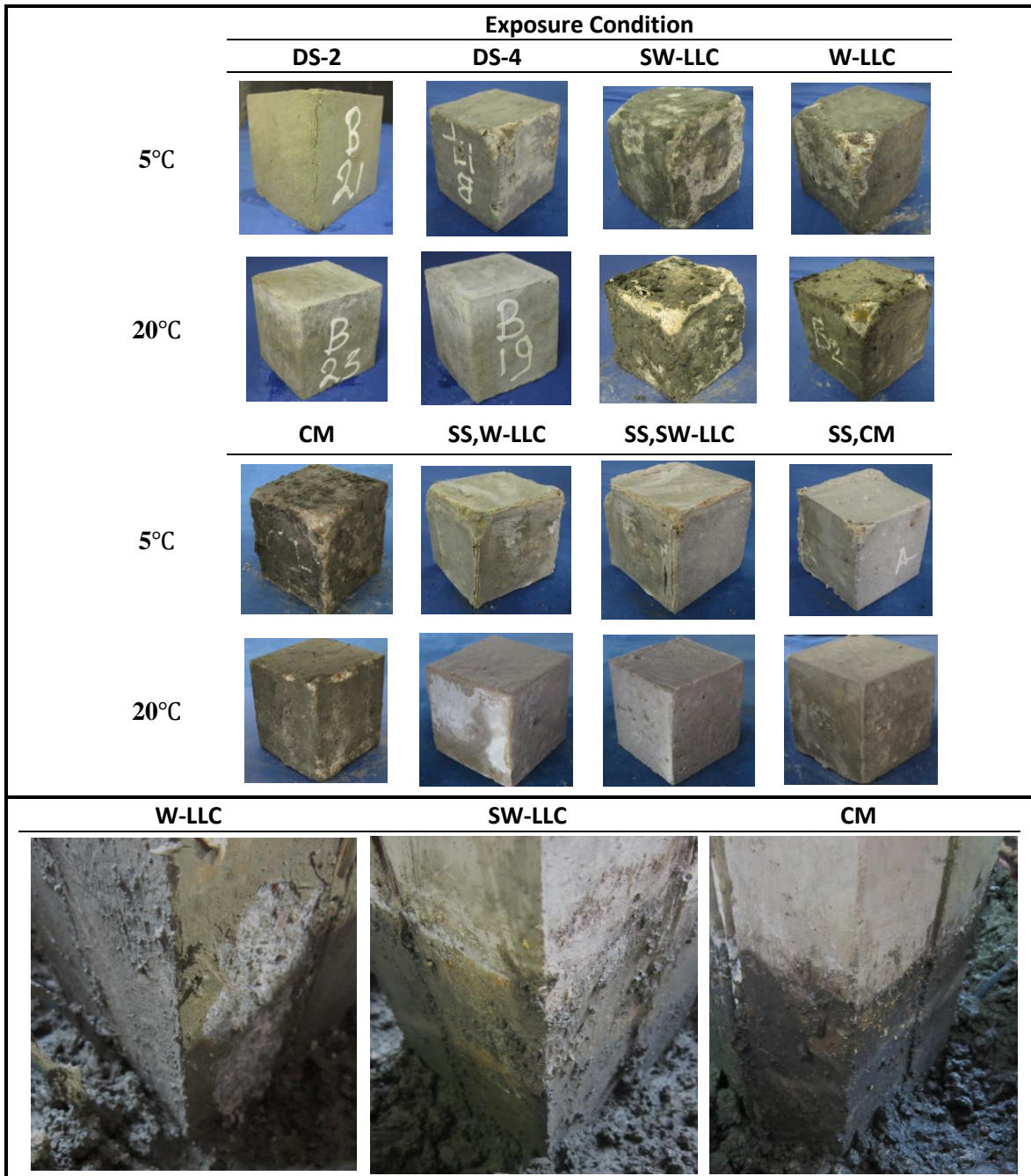


Figure 5.1: CEMI concrete exposed to various conditions for 24 months at 5 and 20°C.

The results of tests with simulated clay pore solutions at 5°C showed that damage was caused at the corners and edges of the cubes, with the formation of white mushy material and a white surface coating, as seen in Figure 5.1. The deterioration was less severe in concretes exposed to solutions equivalent to Coal Measures mudstone than that in weathered and slightly weathered

pore solution. At 20°C the formation of a hard white coating was the only observation in all simulated pore solutions and there was no visible sign of attack.

The order of the degree of deterioration of concrete exposed to various conditions was as follows: SW-LLC > W-LLC > DS-4 > CM mudstone >> DS-2. The simulated clay pore solutions caused damage that was intermediate in severity between the DS-2 and DS-4 sulfate solutions and the clays. In all cases there was less damage at 20°C than at 5°C. In addition, the deterioration was less severe in samples in contact with clay in the presence of mobile groundwater.

### **5.2.2 CEM I –LF concrete in sulfate solutions, clays and simulated pore solutions at 5 and 20°C.**

Figure 5.2 illustrates the appearance of CEMI-LF concrete. It can be clearly seen that there is significant deterioration in the top edges and corner of the concrete specimens placed in DS-4 sulfate solution at 5°C. The aggregate was exposed in the deteriorated area and white soft mushy material was the attack product. However, no sign of deterioration was observed in concrete cubes interacting with DS-2 sulfate solution at 5°C. At 20°C, cracks and spalling in the top edges and in the bottom corner were observed in cubes exposed to DS-4, but the disintegration was less at 20°C than at 5°C. On the other hand, the only effect of exposure to DS-2 solution at 20°C was a white surface deposit, and this was in greater quantity for samples placed in DS-4. In the case of pyritic clays, concrete cubes interacting with weathered and slightly weathered Lower Lias Clay at 5°C showed severe deterioration, as shown in Figure 5.2. The attack was extensive in the skin surface, edges and corners of concrete samples exposed to slightly weathered LLC, while concrete surfaces was only damaged weathered LLC.

In both W-LLC and SW-LLC, the aggregate was exposed and white soft mushy material was identified as a deterioration product. However, remarkable deterioration was identified in specimens exposed to Lower Lias Clays at 20°C. The deterioration was observed in the edges and commenced to the concrete surface in SW-LLC while the deterioration was in the top edge and right side of concrete cube in case of W-LLC. In addition, the degree of severity at 20°C was less than that observed at 5°C. Concrete cubes immersed in Coal Measures mudstone at both temperatures showed less attack than those in contact with Lower Lias Clay, where the attack was on the edges, and greater at 5°C.



The visual observation of CEMI-LF columns immersed in different clays in the presence of mobile water at 5°C showed that deterioration in the case of exposure to LLC was more severe in W-LLC than in SW-LLC, as shown in Figure 5.2.

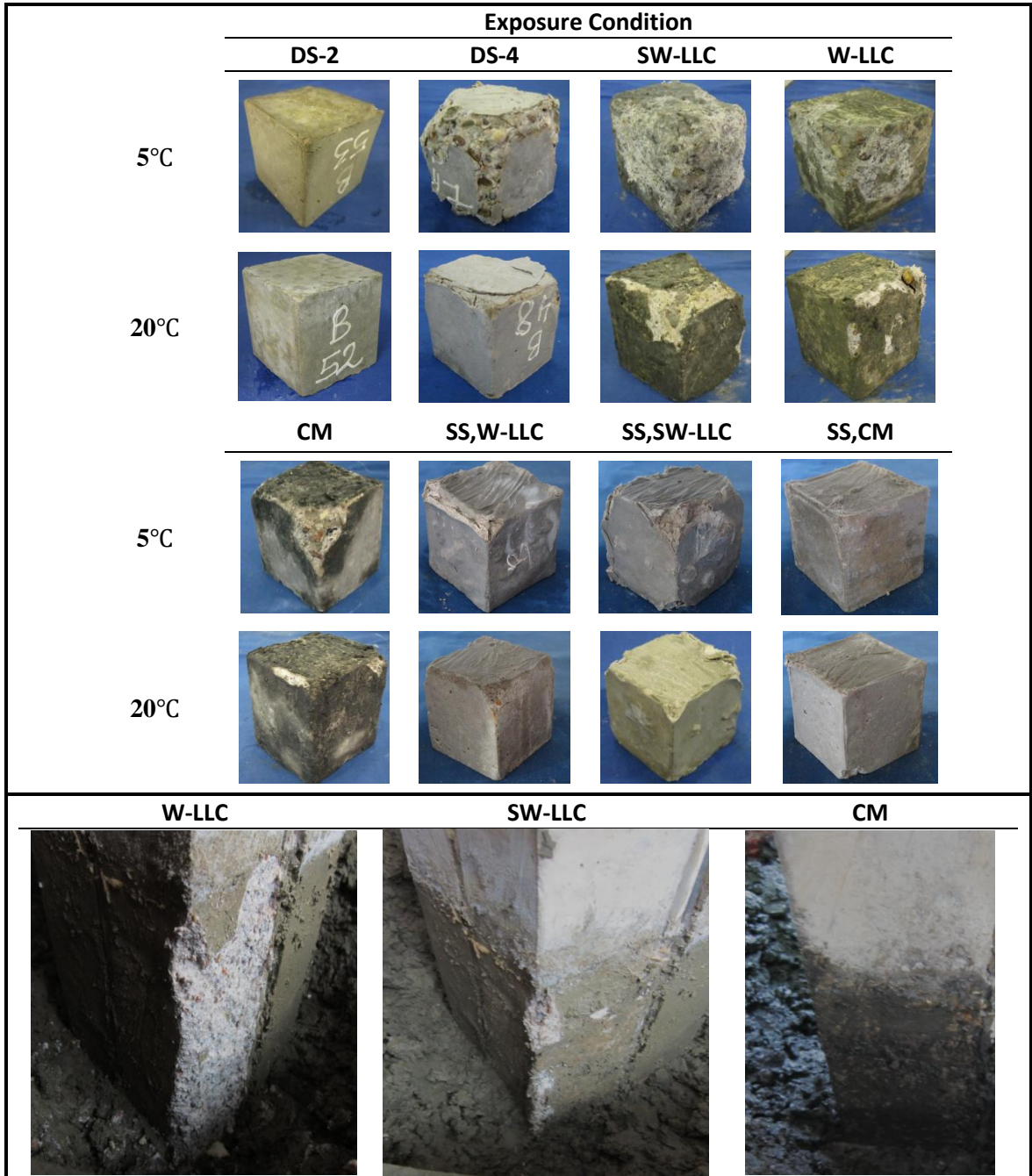


Figure 5.2: CEMI-LF concrete exposed to various conditions for 24 months at 5 and 20°C.

However, no damage was observed on the concrete column exposed to Coal Measures mudstone, and only a white deposit was observed clearly in the un-buried part of the column.

The visual inspection of specimens placed in simulated clay pore solutions of clays showed that attack was significant at 5°C in concrete samples exposed to the SW-LLC pore solution. In addition, blistering accompanied by a white deposit occurred on the top surface of cubes, and the aggregate was exposed in all deteriorated areas. Damage which occurred at the edges of cubes in specimens immersed in W-LLC solution was less than in samples immersed in SW-LLC solution. However, less deterioration was recorded on concrete specimens interacting with the CM solution than other simulated clay pore solutions, along with a white precipitated layer which was the dominant feature. Less deterioration was observed at 20°C than at 5°C in all pore solutions. Generally the degree of deterioration can be ranked as follows: SW-LLC = W-LLC = DS-4, equivalent LLC solutions > Coal Measure mudstone > equivalent CM mudstone solution >> DS-2 sulfate solution.

### **5.2.3 CEMI–PFA concrete in sulfate solutions, clays and simulated pore solutions at 5 and 20°C.**

The extent of deterioration of PFA concrete is shown in Figure 4.3. It can be seen that up to 24 months no signs of deterioration progress was observed in concrete exposed to sulfate solutions, pyritic clays at 5° and 20°C. All comers and edges remained intact and only a white layer of deposit was observed on concrete surfaces immersed in DS-4 sulfate solution at both temperatures. Similar observations were made in the case of PFA concrete columns exposed to different pyritic clays in the presence of mobile groundwater at 5°C. However, a white deposit layer was found on concrete that was not buried, as shown in Figure 5.3. The deposit was found in greater amounts on concrete which had interacted with SW-LLC and Coal Measures mudstone. The visual appearance might be an indication of the better performance of concrete with 50% PFA replacement in controlling and preventing deterioration.



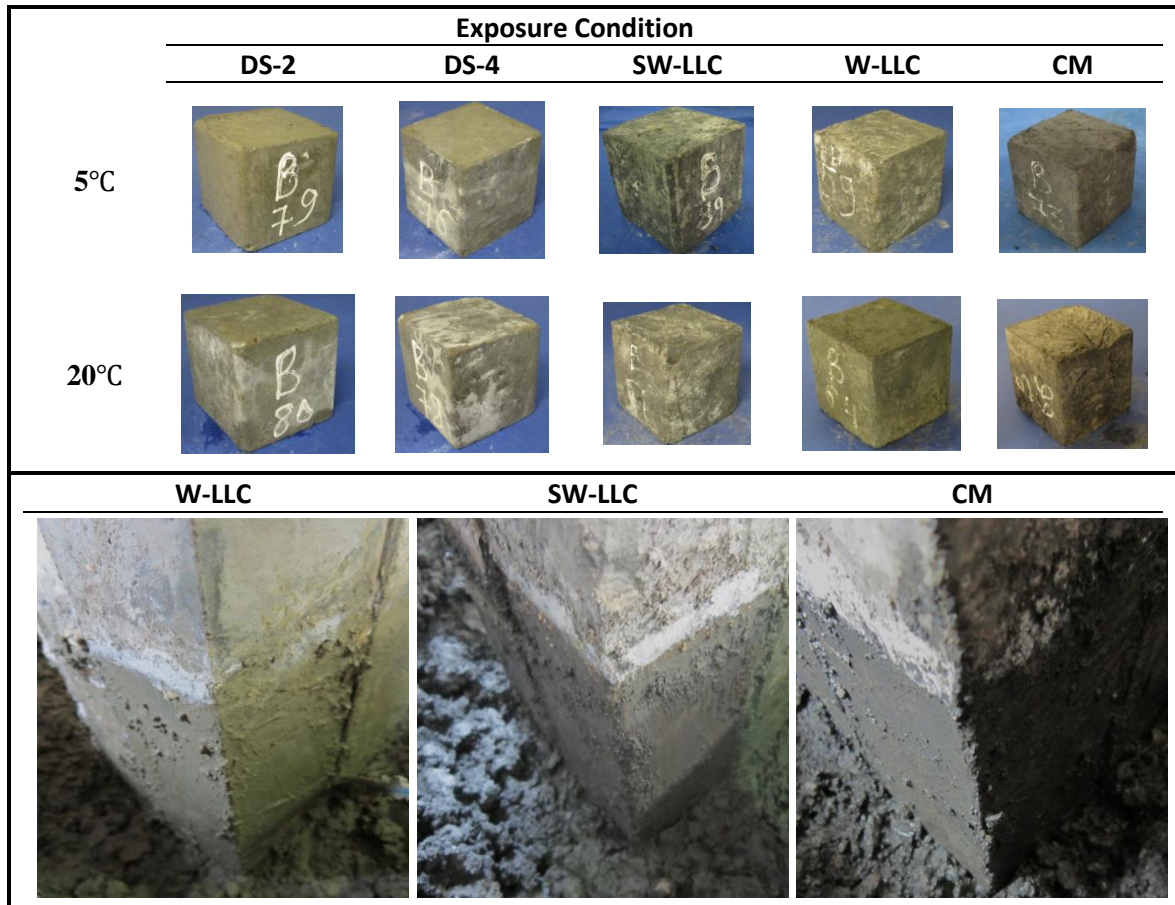


Figure 5.3: CEMI-PFA concrete exposed to various conditions for 24 months at 5 and 20°C.

#### 5.2.4 CEMI-GGBS concrete in sulfate solutions, clays and simulated pore solutions at 5 and 20°C.

The visual appearance of PC- GGBS concrete is illustrated in Figure 5.4. It can be seen that GGBS concrete exposed to sulfate solutions, clay and clays pore solutions at 5 and 20°C did not suffer from spalling and white mushy reaction products and all corners and edges remain intact. Only a white deposit was precipitated on concrete surface in specimens exposed to sulfate solution and SW-LLC. The visual assessment of GGBS concrete column exposed to different clays in the presence of mobile ground water at 5°C showed that no deterioration was detected as shown in Figure 5.4. On the other hand, white layer of salt deposit was found in the non-buried part of column.

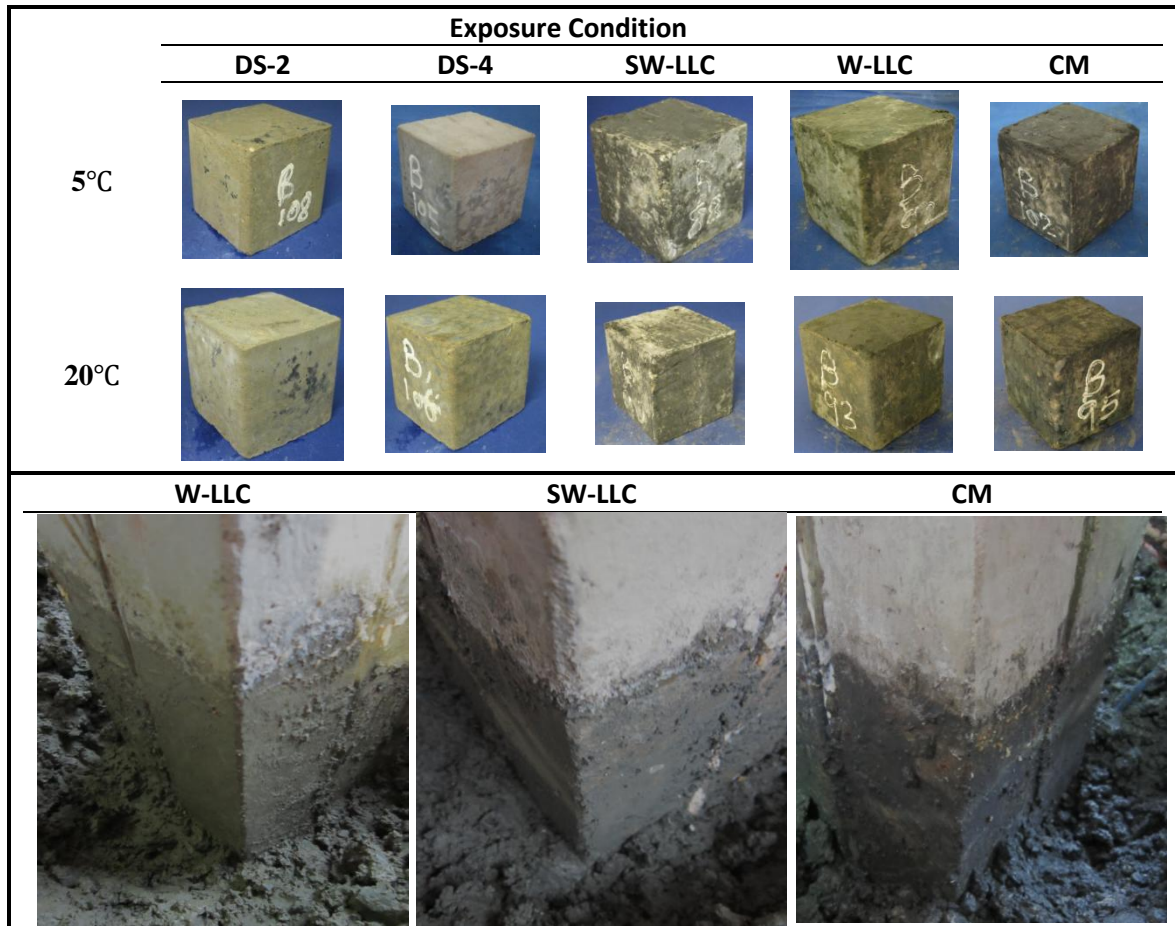


Figure 5.4: CEMI-GGBS concrete exposed to various conditions for 24 months at 5 and 20°C.

### 5.2.5 Overall comparison of performance of different concretes in different exposure conditions.

The severity of deterioration of different concrete types exposed to sulfate solutions, clays and clay pore solutions was as follows: CEMI-LF > CEMI > PFA > GGBS. The superior performance when using 50% PFA and 70% GGBS replacement was remarkable, with no sign of attack observed at either temperature. The superior mitigating effect of GGBS in relation to deterioration at different exposure condition might be due to the replacement of a high percentage of cement with GGBS in comparison to other concrete types used in this research. Zhou et al. (2006) suggested that using GGBS resulted in low permeability which prevented ions and cations from penetrating the concrete.

In the case of CEMI and CEMI-LF concretes, cubes buried in Lower Lias Clay suffered from severe deterioration at 20°C at rate less than that suffered at 5°C and at a similar rate to or more

than that in a DS-4 solution. It is suggested that temperature can be considered to be a secondary factor for thaumasite formation in concrete exposed to pyritic clays. The extent of attack was less in the presence of the effect of mobile groundwater. In addition, the severity of deterioration was more severe in weathered Lower Lias Clay. This might be due to the availability of a high concentration of water-soluble sulfate before exposure in comparison to SW-LLC and CM mudstone. Moreover, the precipitation of white deposit materials in the atmospheric zone might be attributed to the rise of sulfate solution by capillary action into the dry portion of the concrete column, where the water evaporates easily, as reported by Irassar et al. (1996); they found that salt crystallization occurs when the pore solution of concrete becomes supersaturated and this produces internal stresses in concrete pores, causing concrete cracking. This would be noticeable in concrete with a high replacement level of fly ash and slag, as capillary suction increases with an increase in replacement level.

Concrete exposed to Lower Lias Clays with water-soluble sulfate design class DS-2 deteriorated at a faster rate than corresponding specimens in a DS-2 sulfate solution and at a similar rate to or faster than those exposed to the DS-4 sulfate solution at 5°C. This suggests that the aggressivity of clay and resulting concrete deterioration could exceed what might be observed in concrete exposed to equivalent standard test solutions. Furthermore, the simulated clay pore solutions are intermediate between standard test solutions in aggressivity towards concrete cubes, and the mode of deterioration was different at the two temperatures. It would appear that clay composition plays an important role in the extent of concrete degradation. The attack may be enhanced by chemical reactions that occur during pyrite oxidation processes, which are absent in standard test solutions.

### **5.3 pH values**

The majority of chemical reactions take place **through solution** and clay pore solution with numerous dissolution and precipitation processes involved. In addition, pH is known as a suitable indicator for changes that occur during reactions between ions and cations, including test solution and clays with concrete matrix. This section presents the changes in pH of test solutions and clay pore solutions of different clays in the absence of mobile groundwater at 5 and 20°C as a function of time over 24 months for different concretes. The methodology, including solutions replenishment, is described in Chapter 3.

### **5.3.1 CEMI in different exposure conditions at 5° and 20°C**

Figure 5.5 illustrates the variation with time of pH of test solutions and clay in interaction with CEMI concrete at 5° and 20°C. It can be seen that there is a significant difference between the pH measurements of sulfate solutions, simulated clay pore solutions and clays, in which higher pH was recorded at 5°C. The pH values of the sulfate solutions increased at 30 days when they reached a maximum of 10.68 and 10.42 in DS-2 and DS-4 respectively at 5°C. The highest values were 10.08 and 9.64, in DS-2 and DS-4 respectively, at 20°C. The pH of DS-2 and DS-4 solutions decreased after this to values of 9.47 and 9.8 at 5°C and 9.05 and 9.25 at 20°C respectively before the solutions were renewed at 90 days. The distinctive difference between DS-2 and DS-4 sulfate solutions is the slightly higher pH for the DS-2 sulfate solution in the first month of interaction with CEMI concrete at both temperatures. After renewal of the sulfate solutions at 90 days, the pH values increased, and these were higher at 360 days in the DS-4 solution at both temperatures. The pH measurements for the DS-4 solution started to decrease after 360 days, while pH continued to slightly increase in the DS-2 up to 720 days, which suggests that the initiation of attack occurred after 360 days.

The reduction in pH for the DS-4 solution after 360 days might be due to the precipitation of a thin layer of magnesium hydroxide, which is relatively insoluble in water, as reported by Kalousek and Benton (1970) and Liu et al. (2013), and which might inhibit the leaching out of hydroxyl and alkaline species into solutions to raise pH. However, the regular renewal of sulfate solution provided a supply of magnesium sulfate that resulted in the disintegration of calcium hydroxide and CSH in the sound concrete, thus releasing more hydroxyl ions. This corresponds with a slight rise in pH with severe deterioration in the older samples. In addition, the higher concentration of magnesium sulfate in DS-4 caused a faster depletion of calcium hydroxide and therefore more decalcification of CSH. This would result in more deterioration of the cementitious matrix of the concrete, which aligns with the findings by Liu et al. (2013), Torres et al. (2003) and Hartshorn et al. (2002), and this would release hydroxide ions into the solution. As the structure of the concrete deteriorates, the attack continues, because magnesium and sulfate ions are able to penetrate further into the concrete. At a later stage the concentration of magnesium sulfate would decrease as a result of the formation of insoluble magnesium hydroxide, but the rate of pH increase would fall, or the pH might drop slightly.

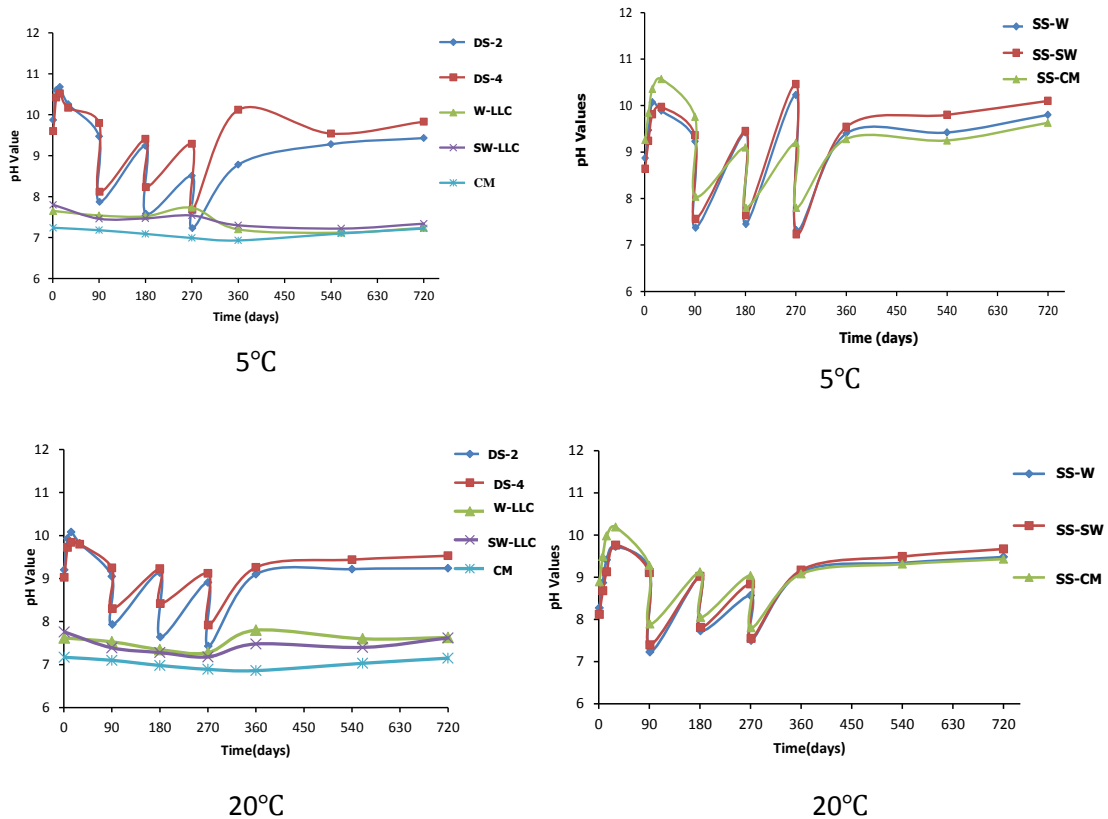


Figure 5.5 pH variations of CEMI concrete at 5 and 20°C

In the simulated clay pore solutions, pH initially increased, and was highest for CM, probably because it contains relatively high concentration of sodium. The values of pH increased to a maximum of 10.07, 9.81 and 10.57 for W-LLC, SW-LLC and CM respectively at 30 days at 5°C, and then gradually decreased. There was a rapid rise in pH at 180 and 270 days at both temperatures when the solutions were renewed; it declined slightly from 360 to 540 days and then increased slightly at 5°C. However, pH values were higher at 270 days in W-LLC and SW-LLC solutions at the lower temperature, indicating that deterioration had commenced at this age. At 20°C the pH increased gradually after 360 days, suggesting that some attack occurred after 12 months of exposure to solutions. The increase in pH values may be due to the release of hydroxyl ions and alkaline species into solutions. However, the reduction of pH after 360 days may be the result of the depletion of alkaline species in the outer layer of the concrete. Further deterioration of the concrete would allow the release of hydroxyl ions and alkaline species, which would result in increased pH of solutions.



The pH values of W-LLC and SW-LLC at both temperatures decreased gradually during the first 90 days, increased slightly to 7.73 at 270 days for W-LLC and 7.54 after 180 days for SW-LLC at 5°C, then continued to fall slightly, while pH reached maximum pH values at 360 days at 20°C in the case of interaction with LLC. However, the pH values in CM mudstone at 5°C continued to decrease up to 540 days, and then increased slightly at 720 days. Generally the pH of clays was almost neutral. This implies that the hydrogen ions produced during pyrite oxidation are being buffered by reaction with calcite and clay minerals. Bicarbonate and weak carbonic acid might also result in reduction of clay pH with age. The distinctive difference between pyritic clays and sulfate and simulated clay pore solutions is that in pyritic clays the pH values were between 7 and 7.65, while they were above 9.0 in simulated solutions.

Overall comparison of pH values in different conditions in the experiment revealed that the higher the temperature was, the lower the pH was in all cases. Moreover, pH values in simulated clay pore solutions were quite similar to those in the DS-4 solution at 5°C and slightly lower at 20°C. It was also found that the pH increased after 12 months in the DS-4 solution and after 9 months in both pyritic clay and simulated clay pore solutions, although the high concentration of sulfate in the DS-4 solution implies that the initial signs of attack appeared at a minimum of 360 days of exposure. This is evidence that clay of a particular class of aggressivity is more aggressive than the standard sulfate solution equivalent to that class.

### **5.3.2 CEMI - LF in different exposure conditions at 5 and 20°C**

Figure 5.6 shows significant differences in the pH of test solutions and clay in interaction with CEMI-LF concrete at 5° and 20°C. In the case of sulfate solutions, pH values for DS-2 were slightly higher than in DS-4 at 14 days at both temperatures. However, after this, both DS-2 and DS-4 solutions gradually decrease at 90 days before the solutions were replenished. The pH values increased rapidly for both DS-2 and DS-4 solutions after the solutions were renewed at 90, 180 and 270 days, becoming higher for DS-4 solution. There was a difference in behavior between DS-4 and DS-2 solutions after 360 days, with the former undergoing a gradual decrease up to 540 days followed by a small increase, while in DS-2 the pH increased slowly up to 720 days at both temperatures. The increase in the pH values for the DS-4 solutions implied that the concrete was undergoing deterioration involving the release of hydroxyl ions and alkaline species, which agrees with the visual observation, as severe deterioration was observed after 180 days of exposure to DS-4 at 5°C.

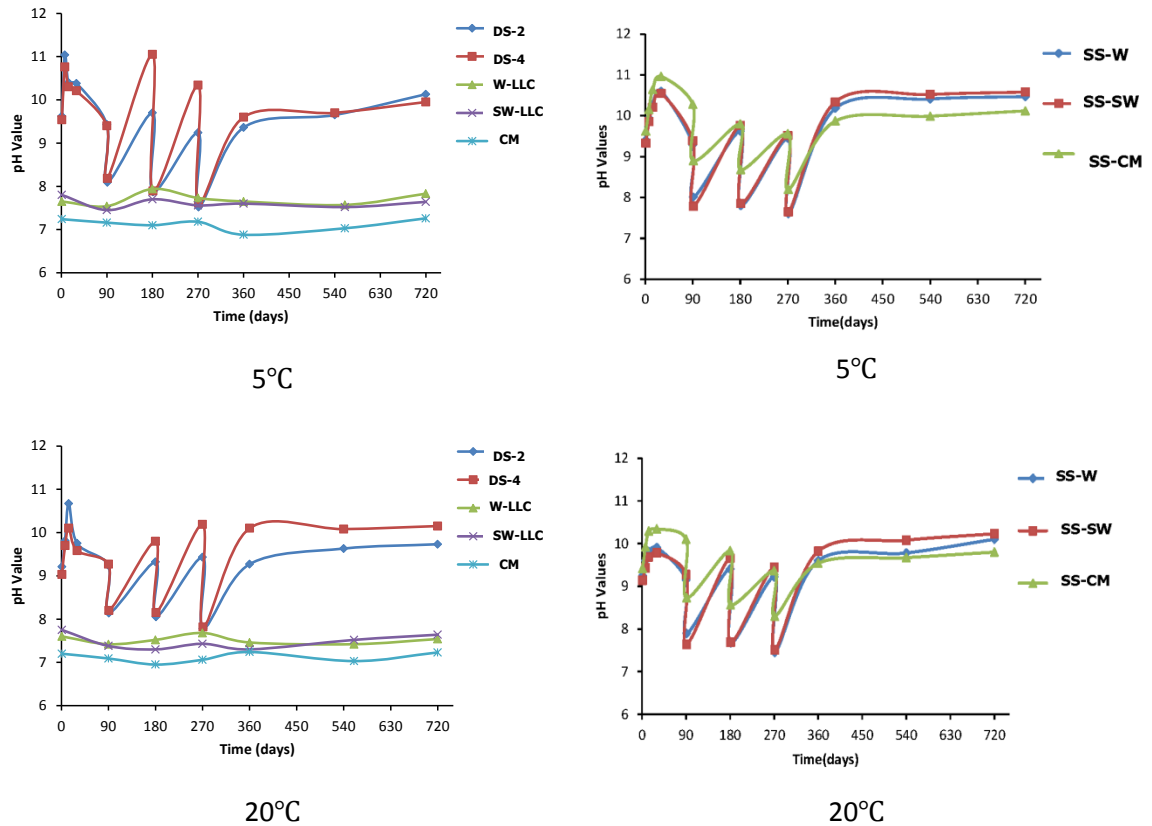


Figure 5.6 pH variations of CEMI-LF concrete at 5 and 20°C

It should be mentioned that a slightly higher pH occurred after the solution renewal at 180 days in DS-4 at 5°C, which might be due to the detachment of the flake-like layer on the top surface of the samples. This would expose the unreacted cementitious matrix directly to the sulfate solution. The continuation in the reduction of pH in the DS-4 solution between 360 and 540 days might be due to the formation of an insoluble brucite layer on the surface of the concrete, which might prevent the release of more alkaline species into the solution, as discussed in Section 5.3.1. In addition, the precipitation of calcite in the concrete could fill in cracks and reduce the permeability and porosity, so fewer alkaline species and hydroxyl ions would leach out into the solution. The reduction of pH values after the first change of the sulfate solution might have resulted from fewer hydroxyl ions being available to be leached out into the solution as well as restriction of the movement of ions into the concrete. The higher concentration of magnesium sulfate would have caused a faster depletion of calcium hydroxide and therefore more decalcification of CSH, which would release hydroxide ions and maintain the pH of the solution,



as discussed in Section 5.3.1. This may have resulted in the enhanced deterioration seen in concrete exposed to DS-4 sulfate solution.

According to Figure 5.6, in all simulated clay pore solutions at both temperatures, the pH increased at 30 days and then decreased at 90 days, before solutions were renewed. In addition, pH increased significantly after solutions were renewed at 90, 180 and 270 days, with slightly lower pH being recorded at 270 days than at 180 days. It is postulated that depletion of all available alkaline species in the outer layer of the concrete had occurred, as no deterioration was apparent, whereas there were fewer hydroxyl ions available to be leached out of the concrete. On the other hand, the pH increased after 270 days, when signs of deterioration were identified, pH reached a maximum after 360 days at 5°C and 720 days at 20°C. The pH of the CM simulated pore solution at 5° and 20°C was higher than that for LLC, especially at ages up to 270 days. This may be because the CM contained a relatively high sodium concentration, leading to increased pH. However, the pH of simulated LLC pore solutions was higher after 270 days than that of the CM solution, in which more deterioration of concrete was observed, probably due to the release of more hydroxyl ions and alkaline species from the intact concrete. This would account for the increased pH of solutions. The pH values appear to be lower for just the magnesium sulfate solution. This is because of the presence of bicarbonate ions in the solutions which reduced the pH.

The clay pH varied in a different manner to that seen for the sulfate solutions, where the maximum pH of clay was 7.94 in weathered LLC at 5°C. The pH values for LLC clays decreased slightly at 90 days and then increased to maxima at 180 and 270 days at 5° and 20°C respectively before decreasing. In addition, they continued to increase after 540 days in weathered and slightly weathered LLC at 5°C, while they rose again after 630 days at 20°C, which suggests the progress of deterioration and the exposure of intact concrete to clay. On the other hand, the CM mudstone pH decreased at 180 days and then increased to maxima at 270 and 360 days at 5° and 20°C respectively; corresponding signs of deterioration were obvious, as recorded in Section 5.2.2. After that the pH rose for both temperatures. Overall the pH of the clays was slightly higher at 5°C than at 20°C. This might be the result of the progress of pyrite oxidation, which results in production of sulfuric acid, which would have been buffered by calcium carbonate and clay minerals in the clay, and would have kept clay pH at about neutral, as reported by Czerewko and Cripps (2006) and Floyd et al. (2003). In addition, the presence of bicarbonate and weak carbonic acid would also result in the reduction of clay pH with age as more would be produced over time.

The overall comparison of pH values in different conditions in CEMI-LF concrete revealed that the higher the temperature, the lower the pH of all sulfate solutions, clays and simulated pore solutions. It was also found that pH increased after 6 months for both DS-4 and LLC clays, while it rose after 9 months for simulated LLC pore solutions. This implies that attack first appeared at an age of 6 months in sulfate solutions and LLC clays, even though the concentration of sulfate in DS-4 was higher. This is further evidence that clay is more aggressive than sulfate solution of the same nominal aggressivity.

### 5.3.3 CEMI - PFA in different exposure conditions at 5 and 20°C

Variations in the pH for the different exposure conditions in contact with CEMI-PFA at 5° and 20°C are shown in Figure 5.7. In the case of DS-2 sulfate solutions at both temperatures, the pH increased for the first 7 days, then decreased at 30 days, after which there was a gradual increase at 90 days when the solutions were replenished. Maximum pH values of 9.70 for DS-4 and 9.24 for DS-2 at 5°C were recorded, while at 20°C the maximum values were 9.32 and 9.47 for DS-4 and DS-2 respectively. After the solutions were replenished at 90, 180 and 270 days, the pH increased up to 360 days; it then remained almost constant up to 720 days, with a slight drop to 8.83 and 8.89 for DS-2 and DS-4 respectively at 5°C and 8.54 and 8.68 for SD-2 and SD-4 respectively at 20°C.

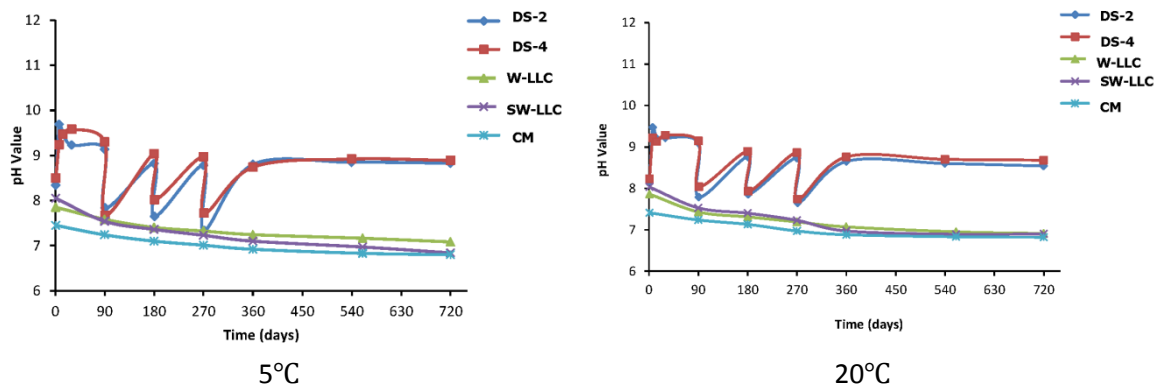


Figure 5.7 pH variations of CEMI-PFA concrete at 5 and 20°C

It is suggested that, as CEMI is replaced with PFA, more portlandite would be involved in the hydration of PFA and therefore fewer hydroxyl ions and alkaline species would be leached into the solution. The rate of increase of pH is slow and no signs of deterioration were detected

during the test. This is a reflection of the superior performance of PC-PFA as a binder. The inner parts of the samples would not be exposed to the solution, which would not result in the release of hydroxyl ions and a progressive reduction in pH.

The pH values for the clays were lower than those in sulfate solutions. The pH values continued to decrease slightly to 7.08, 6.84 and 6.80 for W-LLC, SW-LLC and CM respectively at 5°C after 720 days of exposure, unlike the situation for CEMI and CEMI-LF, in which pH increased as deterioration started.

Overall, the pH of solutions in which PFA concrete was exposed was lower at 20°C than at 5°C. In addition, there was a remarkable difference between pH measurements for test sulfate solutions and the different clays, in which lower pH values were found. In the case of clay, pH continued to fall with age, and the rate of reduction was lower compared to other concretes.

### 5.3.4 CEMI - GGBS in different exposure conditions at 5 and 20°C

Figure 5.8 shows changes in the pH for CEMI-GGBS in interaction with different exposure conditions at 5° and 20°C. In the case of DS-2 and DS-4 sulfate solutions, pH values increased at 7 days to a maximum of 9.38 and 9.24 for DS-2 and DS-4 respectively at 5°C, and 9.22 and 9.18 for DS-2 and DS-4 respectively at 20°C.

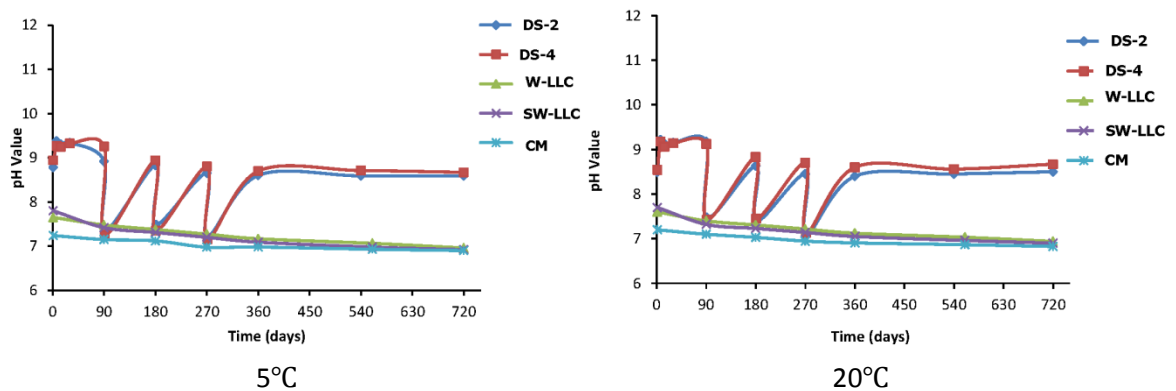


Figure 5.8 pH variations of CEMI- GGBS concrete at 5 and 20°C

In addition, a reduction in pH with time was observed after renewal of the solutions at 90, 180 and 270 days. This implies that calcium hydroxide was consumed in the pozzolanic reaction and the rest was leached into the solution. However, pH continued to decrease slightly after 360

days for the remaining period of investigation, to 8.59 and 8.67 for DS-2 and DS-4 respectively at 5°C and 8.50 and 8.62 for SD-2 and SD-4 at 20°C. It was also found that the pH values in DS-2 were lower than those in the DS-4 sulfate solution at both temperatures. This might be because fewer hydroxyl ions and alkaline species were released back into the solution in the case of DS-2, which contained less magnesium sulfate that would attack calcium hydroxide and CSH, leading to the decomposition of both, and facilitate the release of hydroxyl ions into the solution. This is probably the situation in DS-4 as it contains much magnesium. As the percentage of replacement is high, the concrete pore solution has lower pH than in other concretes because of less alkaline was available in the cement matrix. This is implied by the lower pH measurements during this stage of the test. In addition, the permeability of concrete is enhanced by using a high percentage of replacement of GGBS, and therefore fewer alkaline species would be released into the solution. On the other hand, as all alkaline species in the outer surface of the concrete would be leached into the solution and no signs of deterioration were found, the pH decreased gradually with time.

The pH values for the different pyritic clays show low values of pH in comparison with those for different concretes and exposure conditions. The values were as low as 7.69, 6.92 and 6.90 for W-LLC, SW-LLC and CM, respectively, at 5°C after 720 days of interaction. This might be due to the acid produced by pyrite oxidation coupled with buffering by carbonate sources in the clay. In turn this would lead the pH to be neutral, and this was obvious at high temperature. In addition, the presence of bicarbonate ions and weak carbonic acid might reduce the clay pH below 8, as was observed in the investigation. However, the pH of the clay remained almost constant, with a slight reduction in the case of exposure to GGBS concrete. This implies that less pyrite might be oxidised and therefore less acid would be produced. Overall the pH measurements fell as temperature increased.

### **5.3.5 Overall comparison**

The changes in pH were found to vary among different conditions and in contact with different concretes. Temperature plays an important role in controlling the pH, which was found to become lower as temperature increased. This may be relevant to the difference in the degree of solubility of calcium hydroxide and other alkaline species, especially in the case of pyritic clays, in which more pyrite would be oxidised at a higher temperature and therefore more acid would be produced. In addition, as concrete was cured in air for 21 days it is expected that more CO<sub>2</sub> would react with portlandite and CSH in the outer layer of concrete to produce calcium

carbonate. This would result in fewer hydroxyl ions being leached out to the solution and a rapid pH increase would occur with time as signs of deterioration appeared. This is thought to be the underlying reason why the pH of the solutions was less than the expected value of 12 at early age. With reference to cement type, it was found that pH values in the case of interaction of different concretes increased in the following order: CEMI-LF > CEMI > CEMI-PFA > CEMI-GGB. This would reflect the resistance of these concretes to deterioration.

#### **5.4 Mineralogy of the deterioration products: X-ray Diffraction (XRD)**

This section presents the XRD mineralogical analyses for different concretes that were stored at 5° and 20°C in different exposure conditions for 24 months. Deteriorated materials from the surface of severely attacked concrete were analysed, but where concrete remained intact samples were taken from the surface and analysed after crushing the sample. Sample preparation and test methods are described in Chapter 3.

##### **5.4.1 XRD analysis of CEMI concrete exposed to different conditions at 5 and 20 °C**

XRD patterns for CEMI concrete cubes after 24 months of exposure are shown in Figures 5.9 to 5.12. In case of exposure at 5°C, thaumasite and small traces of ettringite were identified in concrete specimens placed in the SD-4 solution, as shown in Figure 5.9, while in DS-2 ettringite and small traces of thaumasite-ettringite solid solution were identified. Gypsum was stronger in DS-4 solution than in DS-2, and calcite and aragonite were also identified in these solutions. Small traces of brucite were also identified in DS-4 specimens, whereas this material was absent in the DS-2 solution. Quartz appears because of the presence of aggregate in the sample. Portlandite was only detected in samples exposed to the DS-2 sulfate solution, which implies that less portlandite was engaged to form gypsum and contribute to thaumasite formation.

In CEMI concrete in contact with Lower Lias Clays at 5°C, thaumasite was the dominant mineral, followed by calcite and aragonite. Gypsum, portlandite and ettringite were not identified, as shown in Figures 5.9 and 5.10. This emphasises that more sulfate was engaged in the formation of thaumasite than gypsum and ettringite. In addition, portlandite was not identified, suggested that all the Ca(OH)<sub>2</sub> contributed to thaumasite formation as well as reacting with dissolved carbonate diffused into concrete from the clay pore solution to form carbonate phases such as calcite and aragonite.

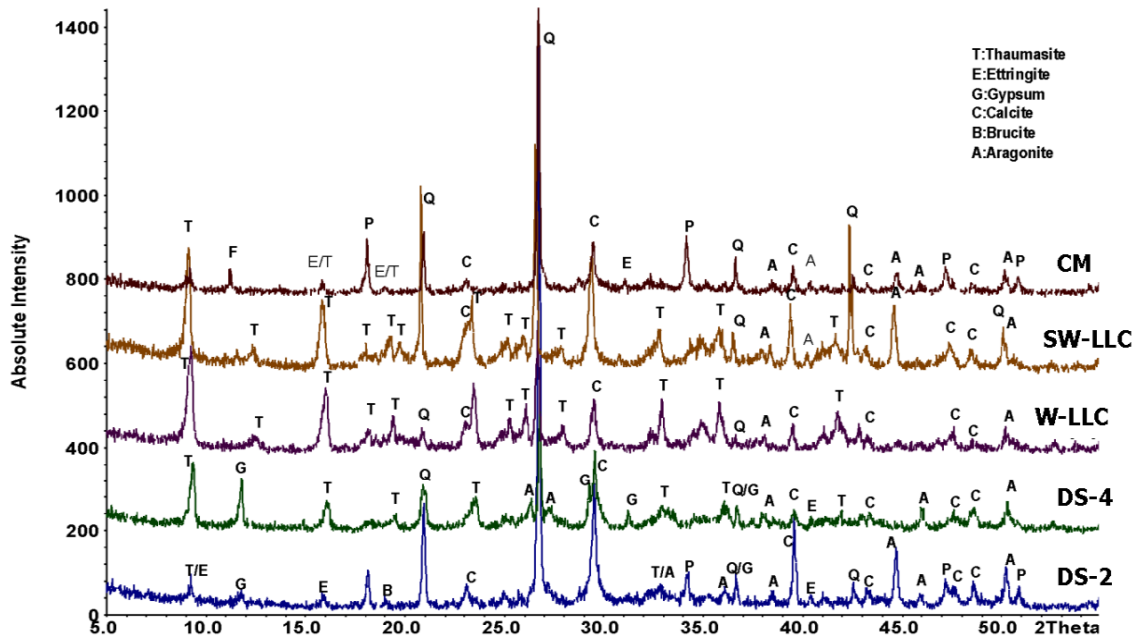


Figure 5.9 XRD patterns of CEMI concrete exposed to different exposure conditions at 5°C

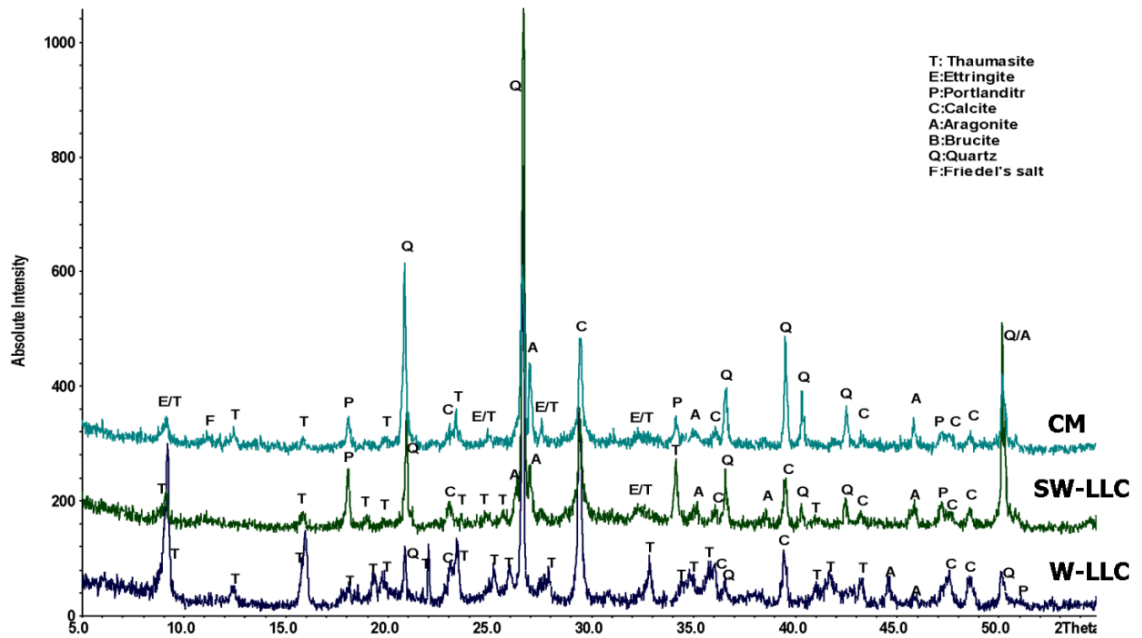


Figure 5.10 XRD patterns of CEMI concrete exposed to different exposure conditions in the presence of mobile ground water at 5°C

Thaumasite was present in concrete samples buried in Coal Measures Mudstone Clay, although calcite and aragonite were the dominant minerals, followed by portlandite, along with an ettringite-thaumasite solid solution. The presence of ettringite in these samples may be due to the presence of sodium from NaCl present in the clay, which may have diffused into concrete and stabilized the pH of the pore solution, so that the ettringite became stable. Furthermore, it should be highlighted that Friedel's salt was detected, which would be due to a reaction between chloride and  $C_3A$ .

In the case of exposure at 20°C, concrete placed in sulfate solution showed only ettringite in the DS-2 sulfate solution, as shown in Figure 5.11, whereas thaumasite and thaumasite-ettringite solid solution were found in the DS-4 sulfate solution. Moreover, portlandite was only observed in concrete exposed to DS-2 sulfate solutions, confirming that not all portlandite was engaged in the formation of gypsum as a result of reaction with sulfate. Gypsum was present but in much smaller quantity in DS-2. Carbonate phases such as calcite and aragonite were also detected in slightly higher quantity at 20°C, probably because calcite has low solubility at higher temperature.

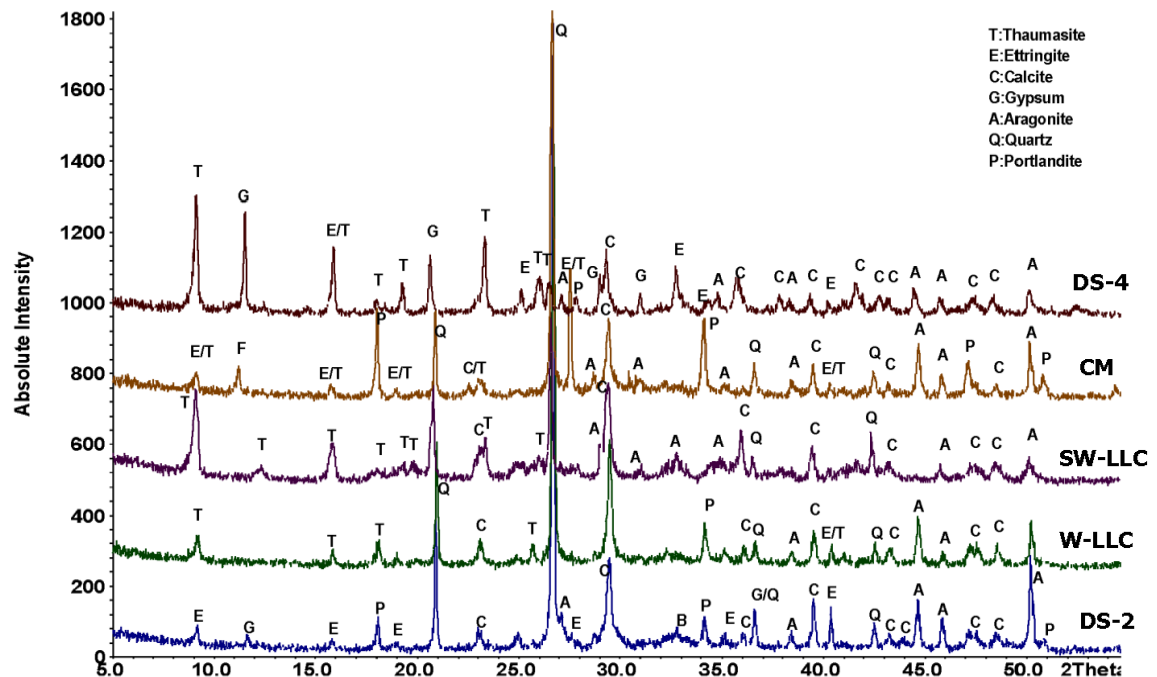


Figure 5.11 XRD patterns of CEMI concrete exposed to different exposure conditions at 20°C



Exposure to clays at 20°C caused thaumasite to be formed in W-LLC and SW-LLC as shown in Figure 5.11; the amount was greater for SW-LLC. However, ettringite-thaumasite solid solution was formed as deterioration product in the case of exposure to CM. Ettringite, gypsum and portlandite were absent and much calcite and aragonite was observed. The absence of portlandite may be the result of reacting with dissolved carbonate ions derived from clays, in which calcite is present. Friedel's salt was identified in specimens immersed in CM as a result of the presence of chloride in the composition of CM clay.

Figure 5.12 illustrates the XRD pattern for CEMI concrete exposed to simulated clay pore solutions at 5° and 20°C. At 5°C, gypsum is the dominant mineral in W-LLC, along with thaumasite-ettringite solid solution, followed by calcite, aragonite, ettringite and brucite. Samples exposed to SW-LLC contained thaumasite, together with ettringite and thaumasite-ettringite solid solution, gypsum, calcite and aragonite. In the CM solution, ettringite and thaumasite-ettringite solid solution were the dominant deterioration products, along with calcite, aragonite and Friedel's salt. However, at 20°C, only ettringite-thaumasite solid solution was present in W-LLC and SW-LLC, along with ettringite and gypsum, followed by carbonate minerals and thaumasite. Samples in the CM simulated solution produced ettringite as the main deterioration product at 20°C, with calcite, aragonite and portlandite also present.

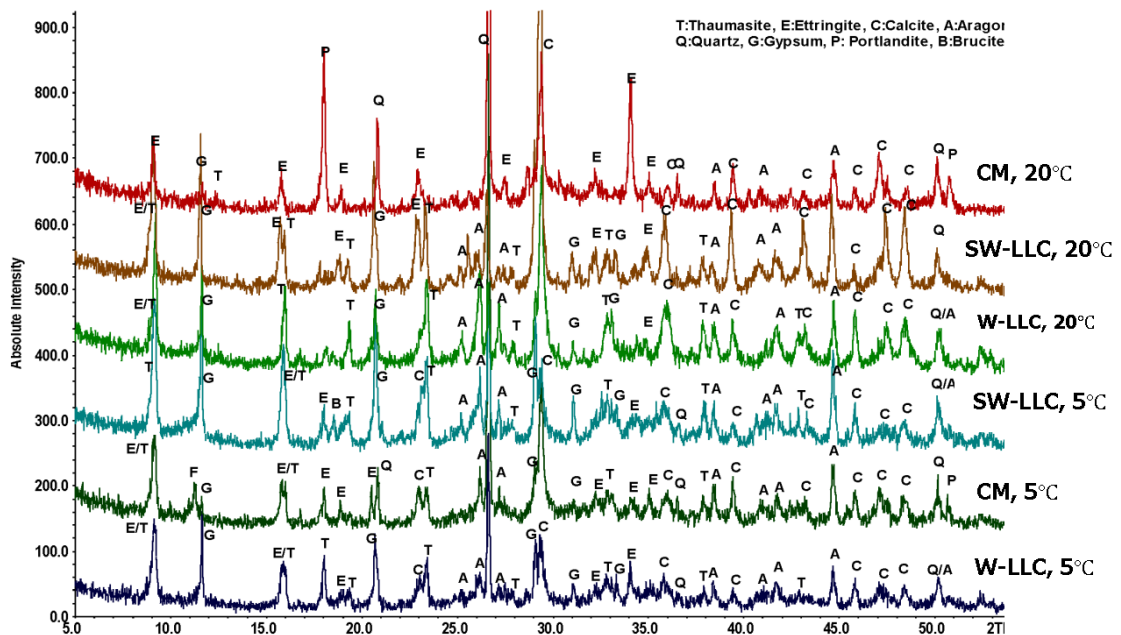


Figure 5.12 XRD patterns of CEMI concrete exposed to simulated clay pore solutions at 5 and 20°C

### 5.4.2 XRD analysis of CEMI-LF exposed to different conditions at 5°C and 20°C

Figures 5.13 to 5.16 illustrate the XRD patterns for CEMI-LF concrete at 5° and 20°C. Exposure to DS-2 solution at 5°C resulted in the formation of ettringite-thaumasite solid solution as the main deterioration product, together with small traces of gypsum and portlandite. Calcite and aragonite were also detected in strong peaks, as shown in Figure 5.13. On the other hand, concrete placed in DS-4 sulfate solution contained much thaumasite, with gypsum and ettringite. Calcite and aragonite were also identified in low intensity compared to DS-2 solution. Brucite was also detected in small traces. It should be also mentioned that portlandite was not detected, indicating that most of it was consumed in the gypsum or calcite formation. The formation of thaumasite and gypsum means that more sulfates were engaged in the formation of both minerals. In addition, the slightly lower carbonate compared to concrete exposed to DS-2 solution suggests that part of the carbonate formed was involved in thaumasite formation.

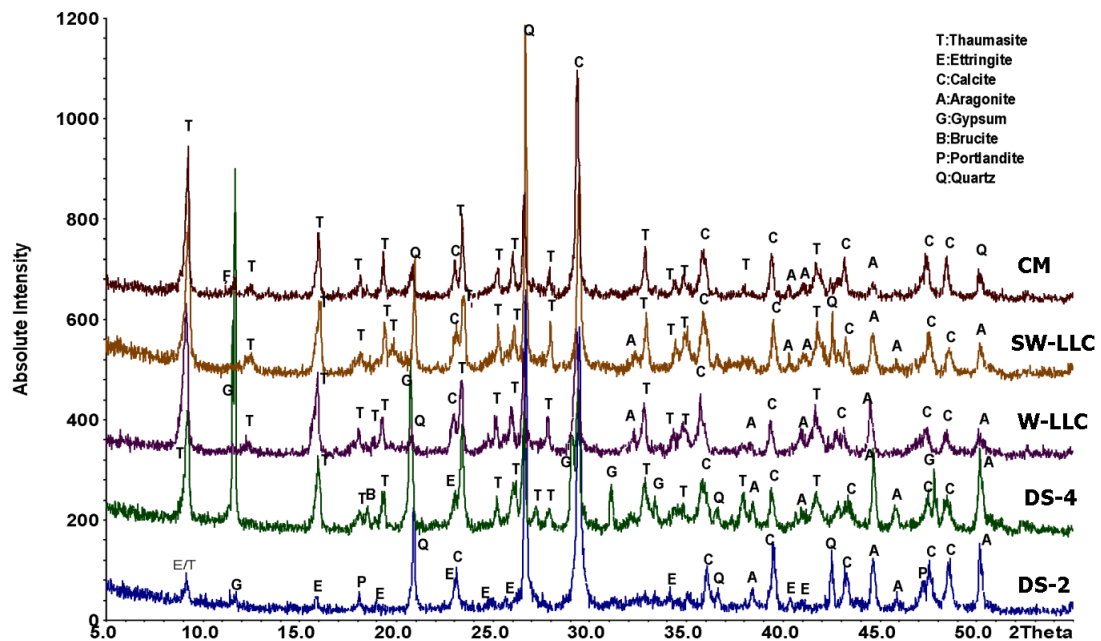


Figure 5.13 XRD patterns of CEMI -LF concrete exposed to different conditions at 5°C.

At 5°C the clays caused the formation of thaumasite, which was the dominant sulfate attack mineral, followed by calcite and aragonite, as shown in Figures 5.13 and 5.14. However, gypsum and ettringite were not observed. Exposure to CM resulted in ettringite-thaumasite solid solution as the dominant phase in presence of simulated ground water, while thaumasite was the

dominant phase in cubes in which mobile groundwater was restricted. Portlandite was only observed in the case of exposure to CM in the presence of mobile groundwater, where no signs of attack were observed, as shown in Figure 5.14. Friedel's salt was also detected in concretes buried in Coal Measures Clay, in which a moderate concentration of chloride would react with  $C_3A$  and form Friedel's salt. The presence of much calcite is probably the result of limestone filler. Furthermore, calcite would precipitate where less thaumasite was formed, which means no calcite was consumed in this reaction.

It was surprising that thaumasite was formed in samples placed in Coal Measures Clay, although it contained a low concentration of sulfate, equivalent to water-soluble sulfate class DS-1, and 7% calcite, at time of exposure. In addition, the lower degree of deterioration might be due to the fact that chloride plays an important role in delaying thaumasite formation, as found by Torres (2004), Sotiriadis et al. (2013, 2012) and Ma et al. (2006). Chloride may delay thaumasite formation, especially at low sulfate concentrations.

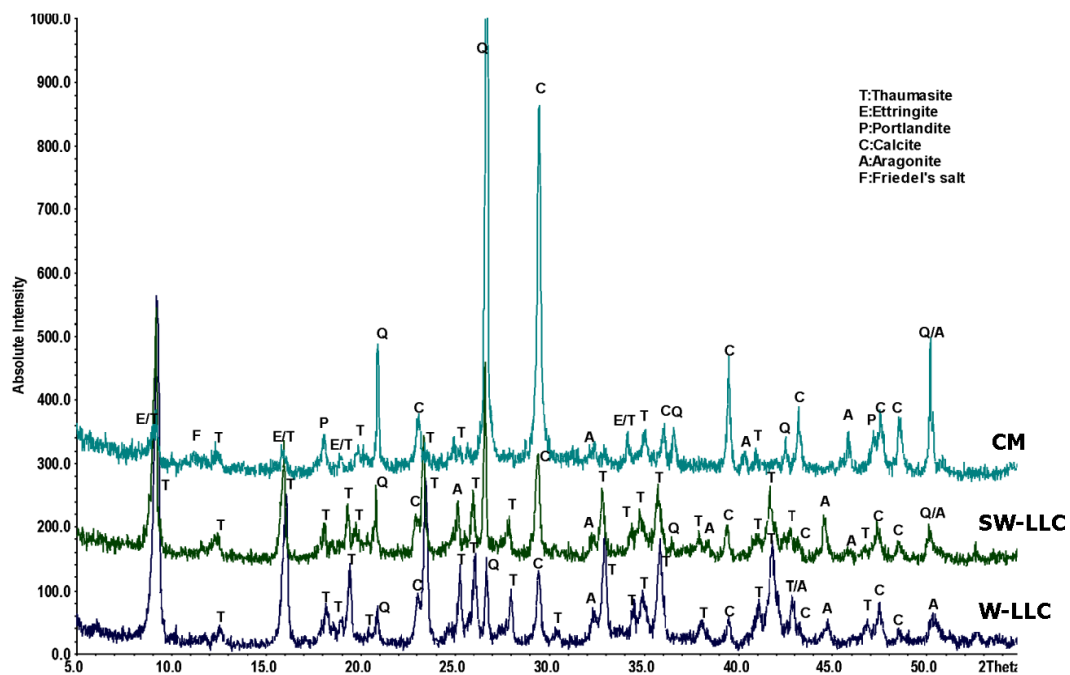


Figure 5.14 XRD patterns of CEMI-LF concrete exposed to different conditions in the presence of mobile ground water at 5°C

The results for CEMI-LF concrete at 20°C are illustrated in Figure 5.15, which shows that in DS-2 ettringite is the main sulfate attack product, following by calcite and aragonite. In addition,

moderate portlandite and small traces of gypsum were also identified. The **slightly high** amount of carbonate minerals indicates that, as thaumasite was not formed, calcite was precipitated, in addition to the internal source of calcite in the filler. However, with DS-4 solution, gypsum and moderate amounts of thaumasite and calcite were formed, and small traces of ettringite and possibly brucite were detected. The absence of portlandite was recorded in concrete exposed to DS-4 sulfate solution, which may be a result of more sulfate being involved in the reaction with  $\text{Ca}(\text{OH})_2$  to form gypsum. The exposure to clays resulted in thaumasite as the dominant TSA mineral formed, whereas gypsum, ettringite and portlandite were not observed. However, **a trace** of ettringite was observed for the Coal Measures mudstone. Friedel's salt was only identified in the sample exposed to Coal Measures mudstone.

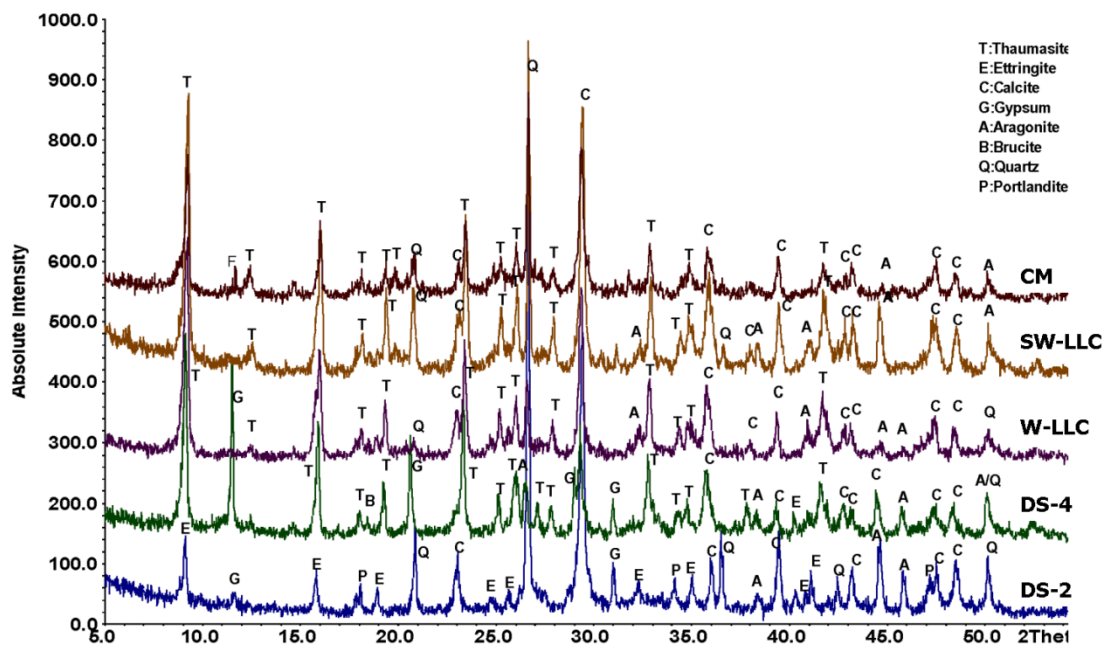


Figure 5.15 XRD patterns of CEMI-LF concrete exposed to different conditions at 20°C

Figure 5.16 shows the XRD patterns for CEMI-LF concrete exposed to various simulated clay pore solutions. Thaumasite was identified along with gypsum in the samples exposed to the simulated clay pore solutions at 5°C, while thaumasite-ettringite solid solution as well as gypsum was identified at 20°C along with thaumasite in simulated LLC pore solutions. On the other hand, **portlandite** only was observed in cubes exposed to CM solution at 20°C, and no gypsum was detected. Ettringite was also detected samples exposed to CM solution at 20°C.

Carbonate minerals such as calcite and aragonite were also present in all cases of exposure and it was less at 20°C than at 5°C, as seen in Figure 5.16.

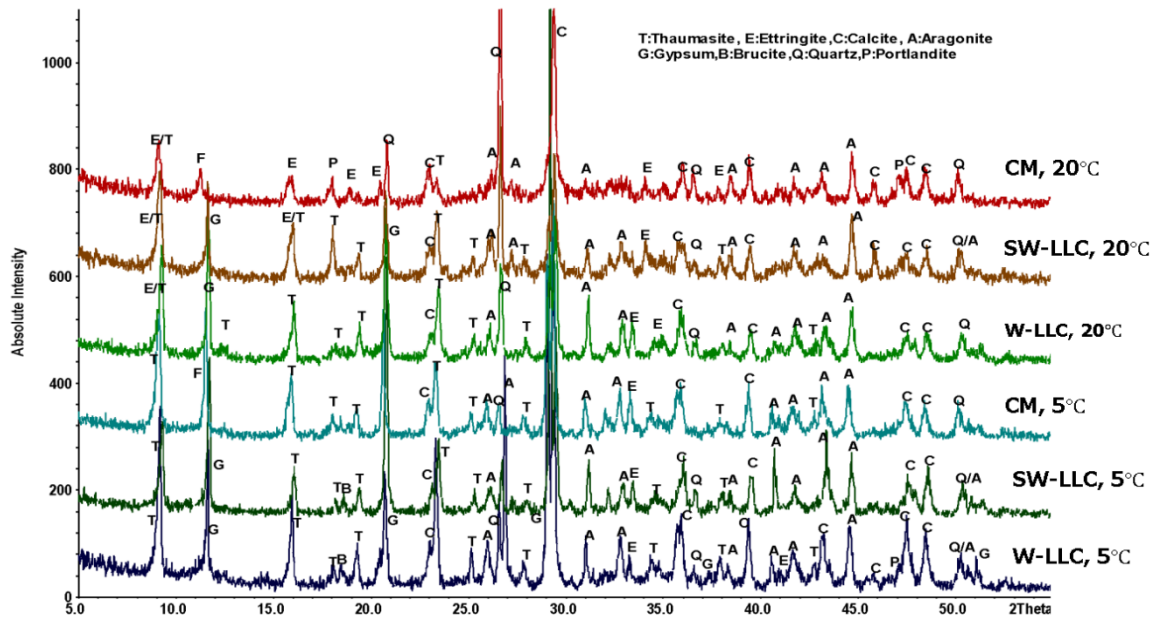


Figure 5.16 XRD patterns for CEMI-LF concrete exposed to simulated clay pore solutions at 5 and 20°C

#### 5.4.3 XRD analysis of CEMI-PFA concrete exposed to different conditions at 5 and 20°C

Figures 5.17 to 5.19 show the XRD patterns for CEMI-PFA concrete. Exposure to DS-2 showed smaller traces of ettringite at 5°C than at 20°C. Calcite and aragonite were dominant minerals and moderate gypsum was also identified at both temperatures. On the other hand, concrete exposed to DS-4 showed slightly higher ettringite at both temperatures, with carbonate minerals such as calcite and aragonite as the dominant minerals. However, relatively low peaks of gypsum were detected, which would imply that all available sulfates were involved in the formation of ettringite in DS-4 solution.

According to Figures 5.17 and 5.18, thaumasite-ettringite solid solution was found in concrete in contact with Lower Lias Clays and Coal Measures mudstone at 5°C. In addition, calcite and aragonite were also present, but ettringite was only observed in Coal Measures mudstone. Small traces of thaumasite were also observed in concrete that interacted with Lower Lias Clay and Coal Measures mudstone in case of presence of mobile ground water as shown in Figure 5.18.

This implies that, in the long term, thaumasite might form in high quantities, and signs of deterioration would appear.

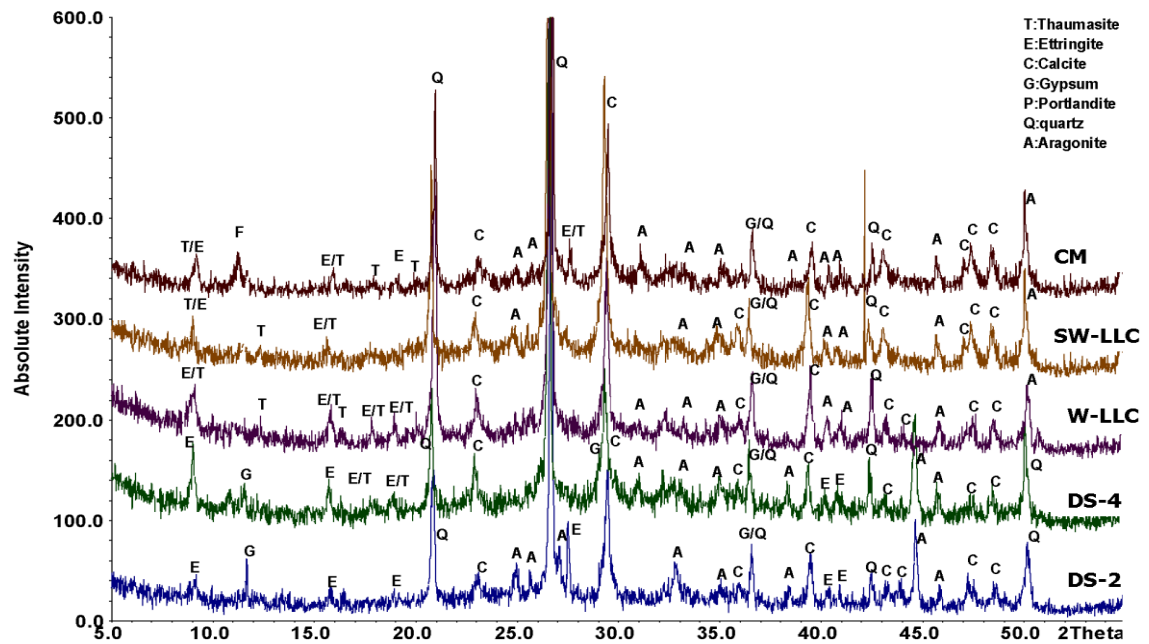


Figure 5.17 XRD patterns of CEMI -PFA concrete exposed to sulfate solutions and clays at 5°C

At 20°C ambient temperature, only ettringite along with carbonate minerals was detected, with no thaumasite or thaumasite-ettringite solid solution phases, as shown in Figure 5.19. In addition, gypsum was not observed in the case of interaction with clays at 5° and 20°C. The quartz was due to the presence of aggregate in the sample. A small trace of Friedel's salt was also detected in the concrete sample exposed to Coal Measures mudstone. The formation of more calcite suggested that some of the decalcification of CSH was due to reaction with carbonate ions. The absence of portlandite would be a result of the consumption of calcium hydroxide in the hydration of PFA replacement cement, indicating that all portlandite was consumed in the hydration of PFA.

In addition, the absence of brucite may be related to the absence of portlandite due to pozzolanic reactions between PFA and calcium hydroxide. Therefore, it can be postulated that the surfaces of samples were covered with a layer of aragonite-calcite or gypsum or both. Furthermore, ettringite was less evident in the case of exposure to CM clay than in specimens exposed to sulfate solutions and Lower Lias Clay. This would be because of the lower concentration of sulfate that should contribute in the reaction. In addition, chloride, present in CM clay, reacted



with  $C_3A$  to form Friedel's salt, and therefore less aluminate contributed to the formation of ettringite.

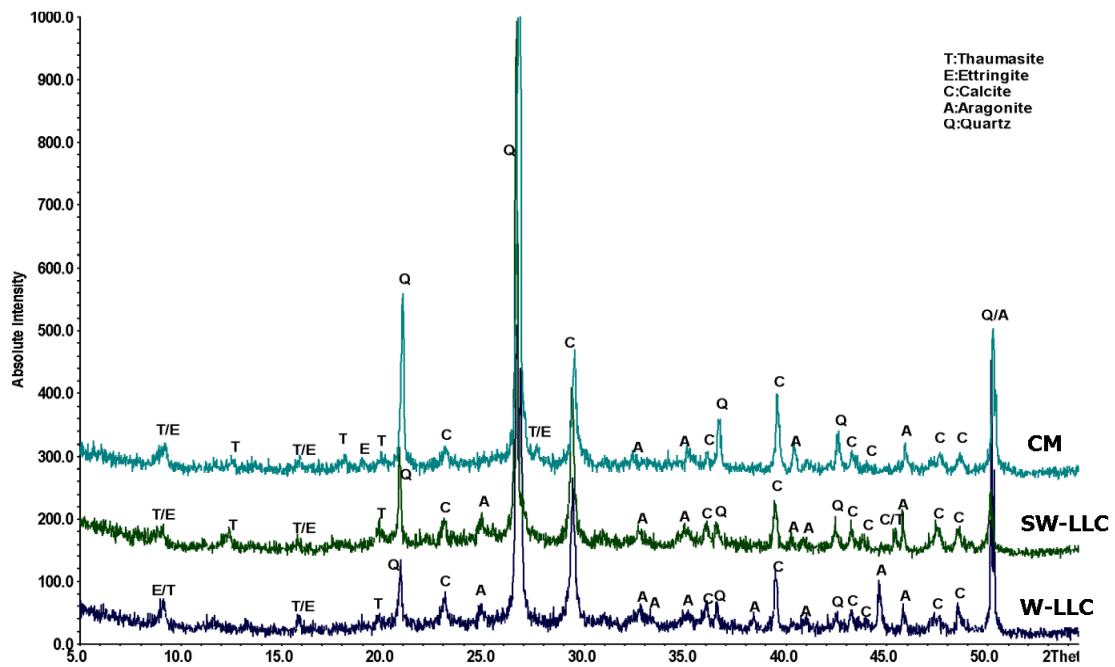


Figure 5.18 XRD patterns of CEMI-PFA concrete exposed to clays in the presence of mobile ground water at 5°C

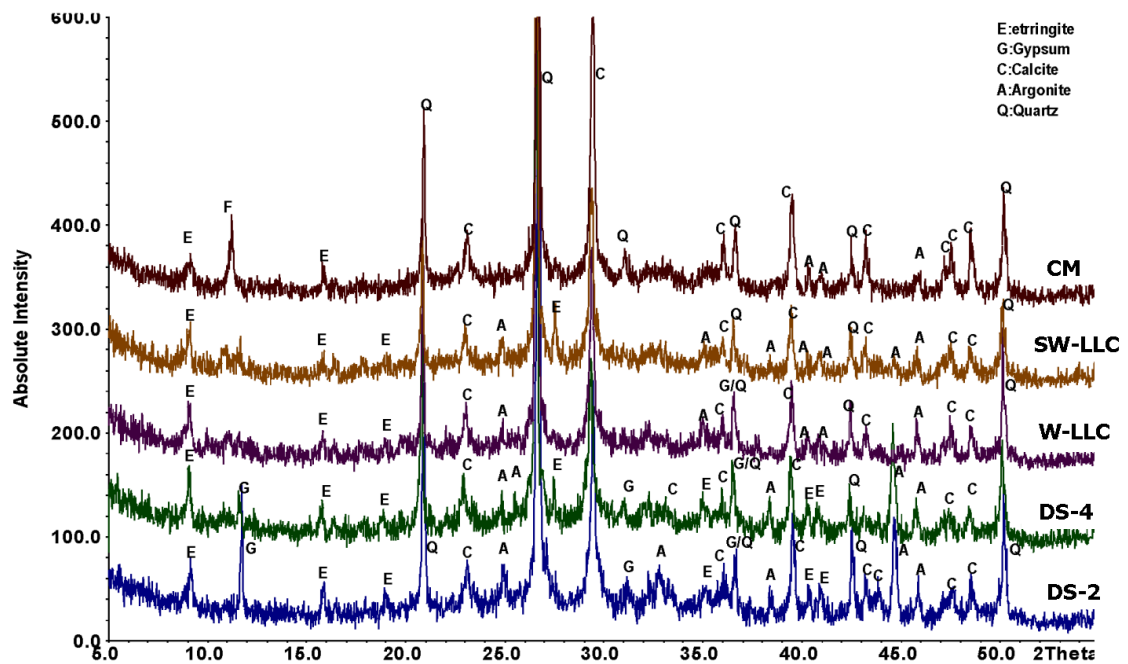


Figure 5.19 XRD patterns of CEMI-PFA concrete exposed to sulfate solutions and clays at 20°C



#### 5.4.4 XRD analysis of CEMI-GGBS concrete exposed to different conditions at 5 and 20°C

XRD patterns of GGBS concrete after 24 months of exposure to different conditions are shown in Figures 5.20 to 5.22. It can be seen that ettringite was detected in all samples placed in DS-2 and DS-4 sulfate solutions and Coal Measures mudstone at 5° and 20°C, while it was identified in the XRD pattern of Lower Lias Clays only at 20°C. Thaumasite-ettringite solid solution was observed in the case of exposure to DS-4, Lower Lias Clays and Coal Measures mudstone at 5°C, as shown in Figures 5.20 and 5.21. However, small peak for thaumasite were found in XRD patterns for concretes exposed to Lower Lias Clays at 5°C. Gypsum was only observed in moderate peaks in DS-2 and DS-4 sulfate solutions at both temperatures, the peaks being slightly higher in DS-4 than in DS-2 sulfate solution. However, peaks of gypsum were identified in concrete exposed to Coal Measures Clay. This might be attributed to the reaction of C<sub>3</sub>A with chloride to form Friedel's salt, with less aluminate therefore becoming available to contribute to ettringite formation, with the result that more sulfate would be engaged in the formation of gypsum.

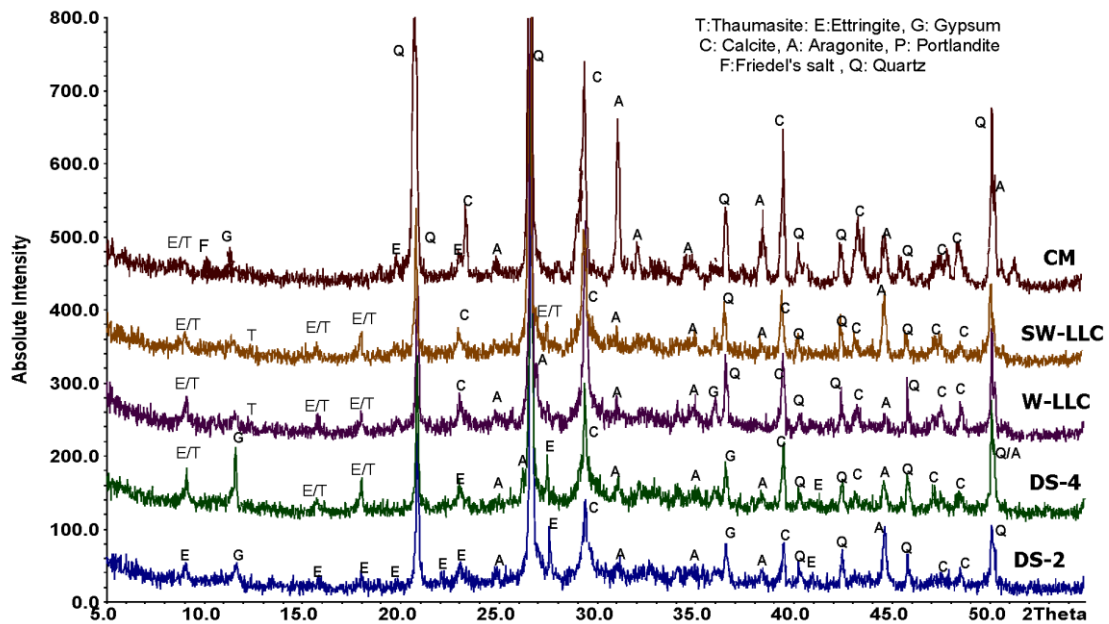


Figure 5.20 XRD patterns of CEMI - GGBS concrete exposed to sulfate solutions and clays at 5°C

Calcite and aragonite were the dominant minerals in all exposure conditions, and peaks were higher in LLC and CM clays than in sulfate solutions at 5 and 20°C. This might be a result of the presence of a carbonate source in clay which would provide carbonate and bicarbonate ions to

react with pozzolanic CSH and form calcite. A small peak for Friedel's salt was identified in the case of exposure to Coal Measures mudstone, while portlandite was not observed in any XRD patterns in any exposure conditions.

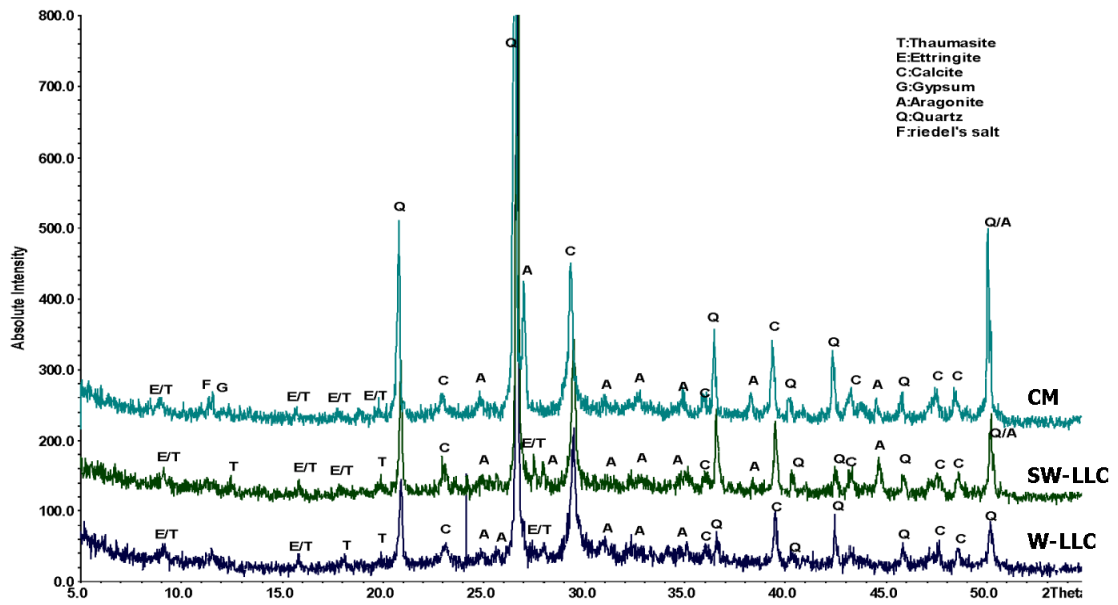


Figure 5.21 XRD patterns of CEMI-GGBS concrete exposed to clays in the presence of mobile ground water at 5°C

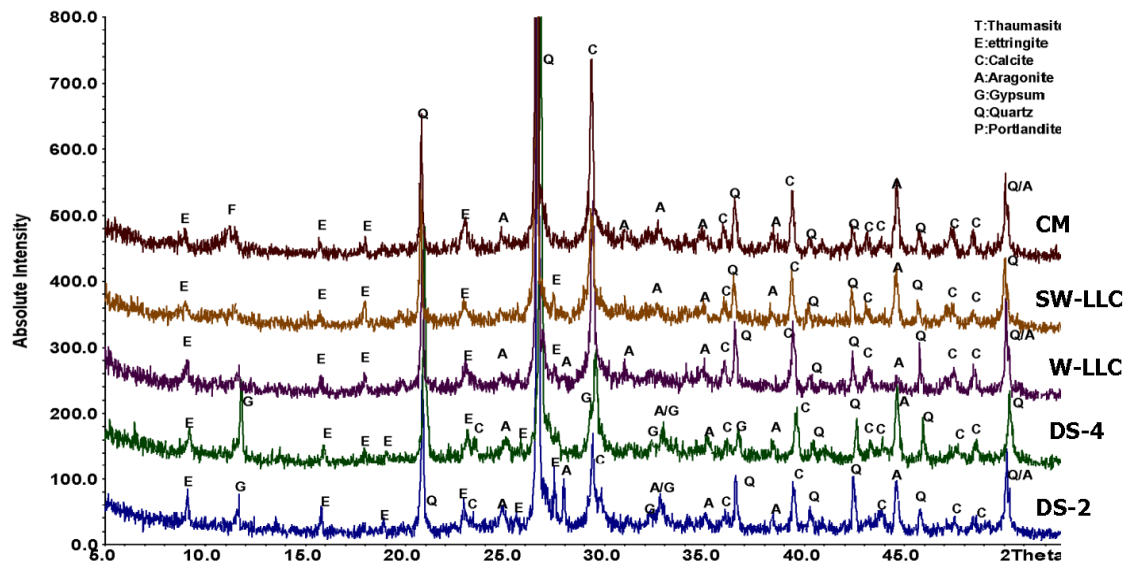


Figure 5.22 XRD patterns of CEMI 70 % GGBS concrete exposed to sulfate solutions and clays at 20°C

#### **5.4.5 Overall comparison**

Although water-soluble design sulfate class in clays was between DS-1 and DS-3, the deterioration was severe compared to BRE standard sulfate solutions and was noticeable at 20°C, **exceeding the expectation**. In addition, the deterioration products were different: thaumasite was solely responsible for attacks which occurred in concrete exposed to pyritic clays in CEMI and CEMI-LF concretes, and thaumasite-ettringite solid solution appeared in XRD results of PFA and GGBS concretes, which are known for their superior performance against sulfate attack. On the other hand, thaumasite, along with gypsum and ettringite, was the main deterioration product for samples exposed to different sulfate solutions in simulated clay pore solutions. It seems that simulated clay pore solutions do not represent the actual conditions for clay, as demonstrated by XRD results analysis. This implies that the mechanism of deterioration in concrete exposed to clay is different from that in sulfate solutions and simulated clay pore solutions. Thus the composition of the clay plays an important role in the production of deteriorated material as well as accelerating the attack in comparison with sulfate and equivalent solutions.

### **5.5 FTIR results analysis**

This section describes the 24 months' results of the FTIR analysis of concrete made with different cements and placed in different exposure conditions as described in Chapter 3. Sample preparation and test methods are described in Section 3.4.2.

#### **5.5.1 IR analysis of CEMI concrete exposed to different conditions at 5 and 20°C**

Figures 5.23 to 5.26 show FTIR analysis of CEMI concrete. IR spectra showed the formation of thaumasite which peaks at 499, 660 and 756  $\text{cm}^{-1}$  that belongs to  $\text{SiO}_6$  were obvious in the case of exposure to DS-4, Lower Lias Clays and simulated clay pore solutions at 5°C. On the other hand, small wavebands at 660 and 756  $\text{cm}^{-1}$  were only detected in samples exposed to DS-2 sulfate solution and Coal Measures mudstone at 5° and 20°C, as shown in Figures 5.23 and 5.25, which suggested the formation of thaumasite in the concrete matrix, as XRD analysis showed the presence of thaumasite-ettringite solid solution. However, thaumasite was observed at 20°C in IR spectra of samples exposed to LLC and W-LLC solutions at a peak of 500  $\text{cm}^{-1}$ .

A small peak of ettringite was identified at peak 855  $\text{cm}^{-1}$  in the case of exposure to different concentrations of sulfate solutions and simulated clay pore solutions at both temperatures, while it was not observed in the case of exposure to clays, except for samples placed in Coal Measures mudstone at 20°C. Gypsum was identified in the case of exposure to DS-2, DS-4 and simulated

clay pore solutions at peaks around  $590$  and  $640\text{ cm}^{-1}$  at  $5^\circ$  and  $20^\circ\text{C}$ , while no peaks assigned to gypsum were found in the case of interaction with clays. In addition, a moderate peak at  $1100\text{ cm}^{-1}$  was identified, which refers to a sulfate-bearing phase in the form of thaumasite in DS-4 sulfate solution and Lower Lias Clays, as shown in Figures 5.23 to 5.26. In addition, the  $\text{SO}_4$  group, which might belong to sulfate-bearing minerals in the form of ettringite, was also identified at peak  $1087\text{ cm}^{-1}$  in sulfate solutions, simulated clay pore solutions and CM at  $20^\circ\text{C}$ . A carbonate phase in the form of calcite was present at  $712$ ,  $875$  and  $980\text{ cm}^{-1}$  and aragonite was identified at peaks  $694$  and  $1460.2\text{ cm}^{-1}$  in all exposure conditions. On the other hand, the C-O carbonate group, which contributed in the formation of thaumasite, was detected where thaumasite was formed at a peak around  $1390\text{ cm}^{-1}$ , as shown in Figures 5.29 to 5.32. It should also be mentioned that a peak at  $940\text{ cm}^{-1}$  which belonged to  $\text{SiO}_4$  was identified in IR spectra for samples interacting with clays and it was higher in LLC than that in CM. In this case this would indicate decomposition of C-S-H due to the reaction with carbonate and bicarbonate ions diffused from clay which release silica in the form of  $\text{SiO}_4$ , as reported by Suuzuki et al. (1985), Black et al. (2008) and Kobayashi et al. (1994).

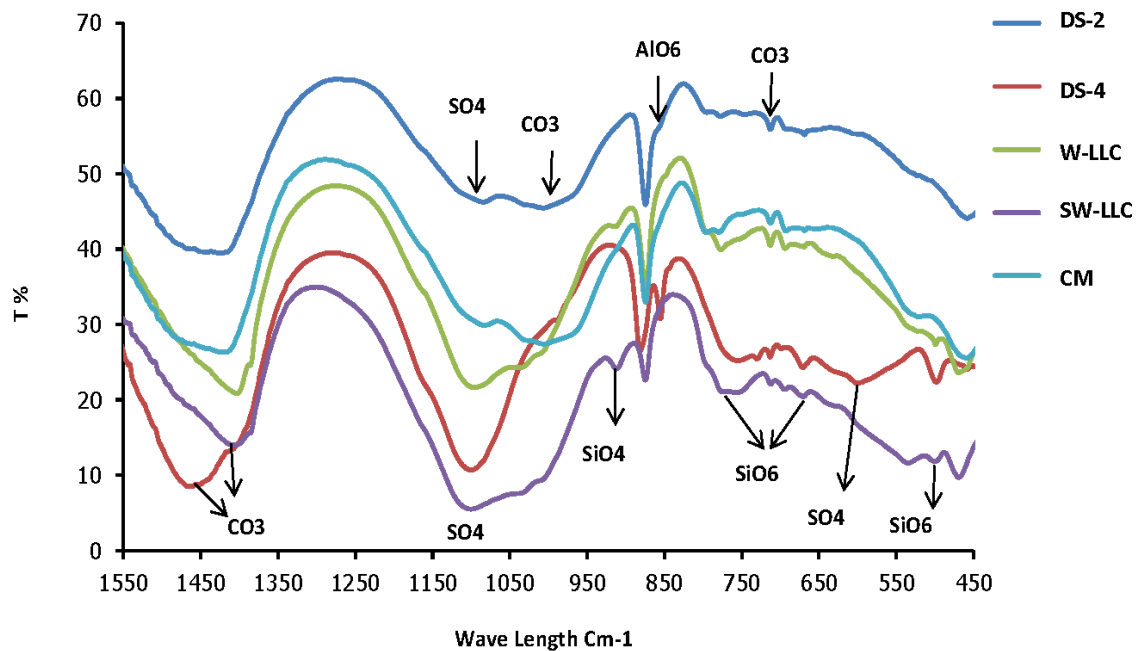


Figure 5.23 IR analysis of CEMI concrete exposed to different conditions at  $5^\circ\text{C}$

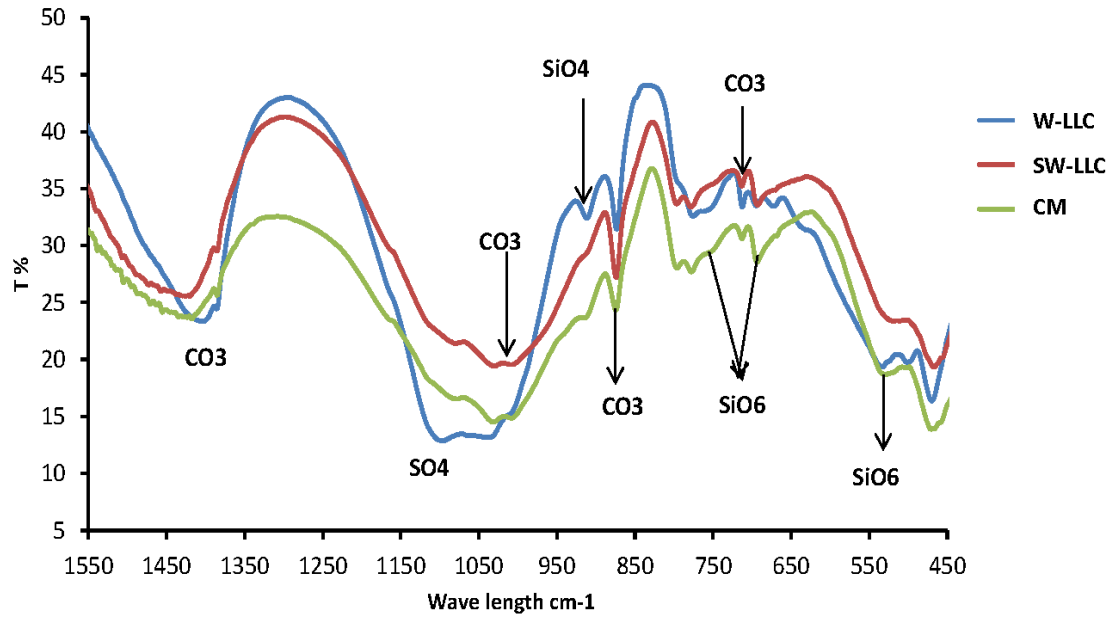


Figure 5.24 IR analysis of CEMI concrete exposed to clays in the presence of mobile ground water at 5°C

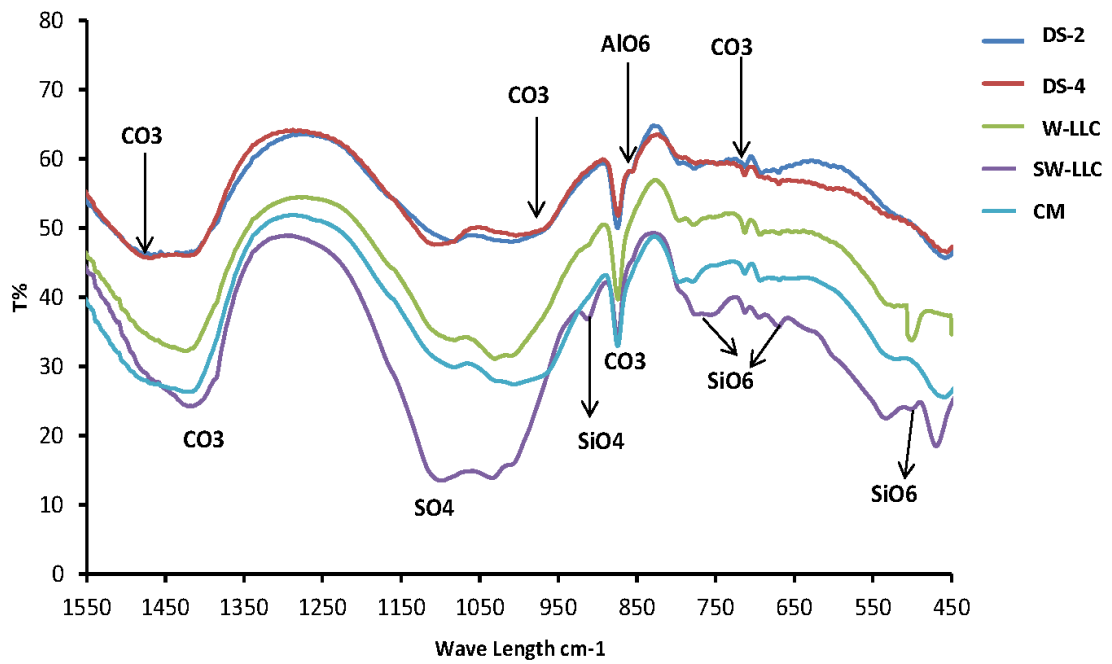


Figure 5.25 IR analysis of CEMI concrete exposed to different conditions at 20°C

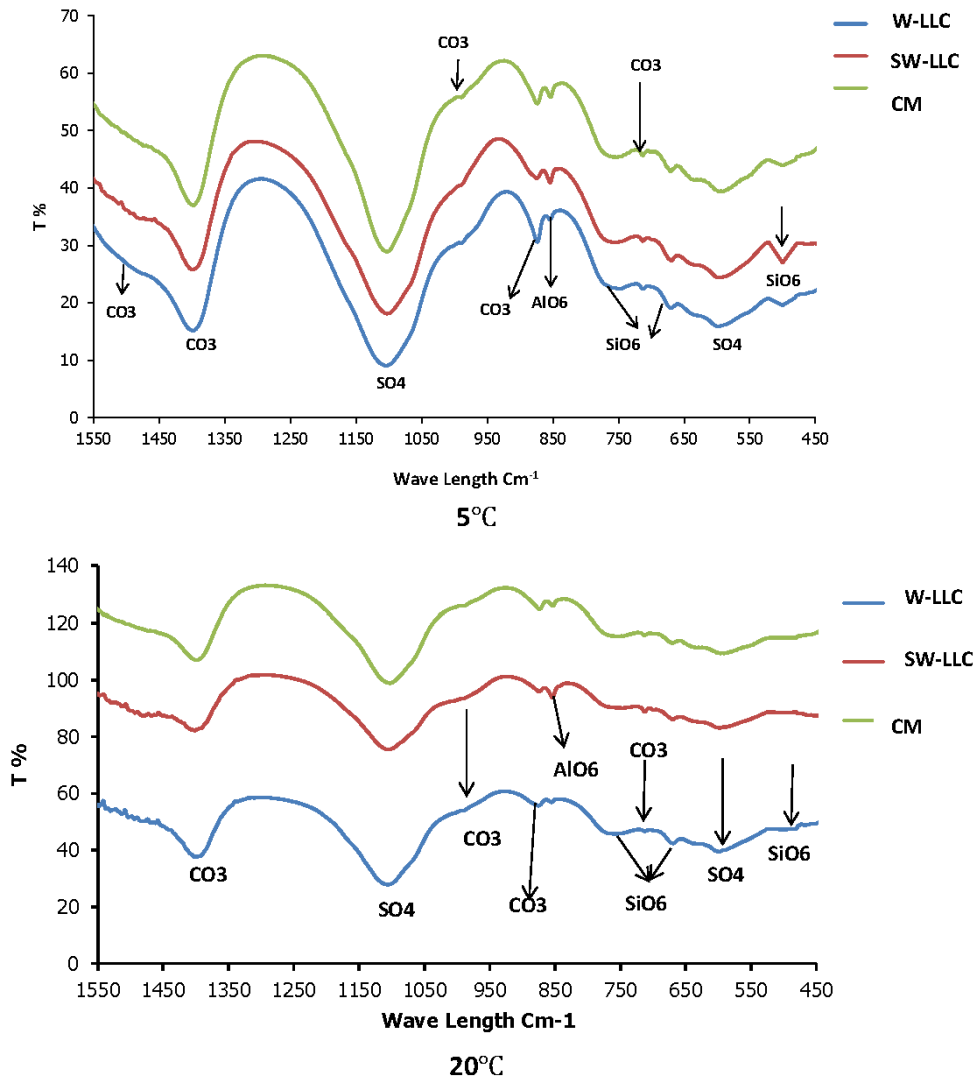


Figure 5.26: IR analysis of CEM I concrete exposed to simulated clay pore solutions at 5 and 20°C

### 5.5.2 IR analysis of CEMI- LF concrete exposed to different conditions at 5 and 20°C

FTIR spectra of deteriorated material and material from the surface of CEMI-LF concrete are shown in Figures 5.27 to 5.30. The IR spectra confirmed that the damage was caused by TSA in specimens exposed to DS-4 solution, LLC, CM and simulated clay pore solutions at 5° and 20°C. This can be clearly seen from the presence of peaks around 500, 660 and 756  $\text{cm}^{-1}$  which refer to the  $\text{SiO}_6$  group. However, in specimens placed in DS-2 and Coal Measures mudstone in

the presence of mobile groundwater,  $\text{SiO}_6$  group, indicated for the formation of thaumasite was only observed in small peaks at  $660$  and  $756\text{ cm}^{-1}$ . In addition, IR spectra confirmed the presence of ettringite, which  $\text{AlO}_6$  group peak was detected at  $855\text{ cm}^{-1}$  in concrete samples placed in DS-2, DS-4 and simulated clay pore solutions at both temperatures. However, it was not observed in specimens immersed in clays at  $5^\circ$  and  $20^\circ\text{C}$ , which confirms that the deterioration due to sulfate attack in samples exposed to pyritic clay was solely due to TSA. It should be mentioned that a peak belonging to ettringite in samples exposed to Coal Measures clay in the presence of mobile groundwater was not detected, although ettringite was identified in XRD results. This might be due to the small size of the sample examined in IR analysis, 2 mg, which might not represent the change in the concrete matrix due to exposure to this clay. An  $\text{SO}_4$  peak at  $590\text{ cm}^{-1}$  that was related to gypsum was identified in specimens placed in DS-2, DS-4 and simulated clay pore solutions at  $5^\circ$  and  $20^\circ\text{C}$ , while gypsum was absent in all concrete samples exposed to clays at  $5^\circ\text{C}$ , as shown in Figures 5.27 and 5.30.

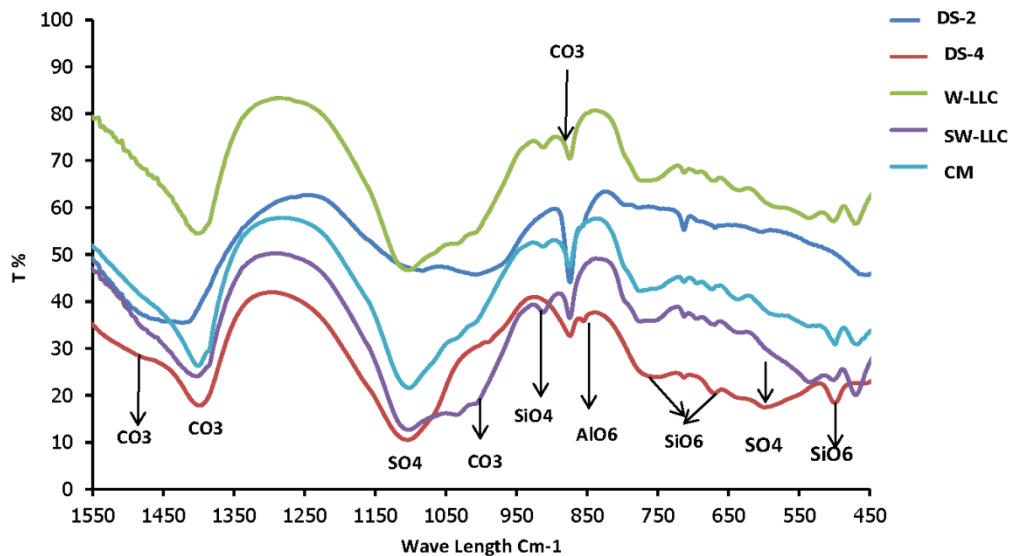


Figure 5.27 IR analysis of CEMI -LF concrete exposed to different conditions at  $5^\circ\text{C}$

However, at  $20^\circ\text{C}$  a peak belonging to gypsum was found in the case of exposure to different pyritic clays, although it was not detected in XRD analysis, which suggests that the presence of gypsum in IR spectra in the case of pyritic clay might come from gypsum available in clay, as the examined sample was collected from the concrete–clay interface. A sulfate-bearing phase that contributed to the structure of ettringite was detected at  $1082\text{ cm}^{-1}$  in the case of exposure to DS-2 and DS-4 sulfate solutions. A peak at around  $1100\text{ cm}^{-1}$  attributed to an  $\text{SO}_4$ -bearing phase



in the form of thaumasite was also detected in all exposure conditions, as shown in Figures 5.27 to 5.30. Carbonate phases such as calcite and aragonite were present in IR spectra at 694 and 1460  $\text{cm}^{-1}$  for aragonite and at 712,875 and 1476  $\text{cm}^{-1}$  for calcite in all concrete samples exposed to sulfate solutions and clays at both temperatures. In addition, a C-O group for carbonate involved in the structure of thaumasite was identified at peak 1390  $\text{cm}^{-1}$  where thaumasite was identified in all exposure conditions.

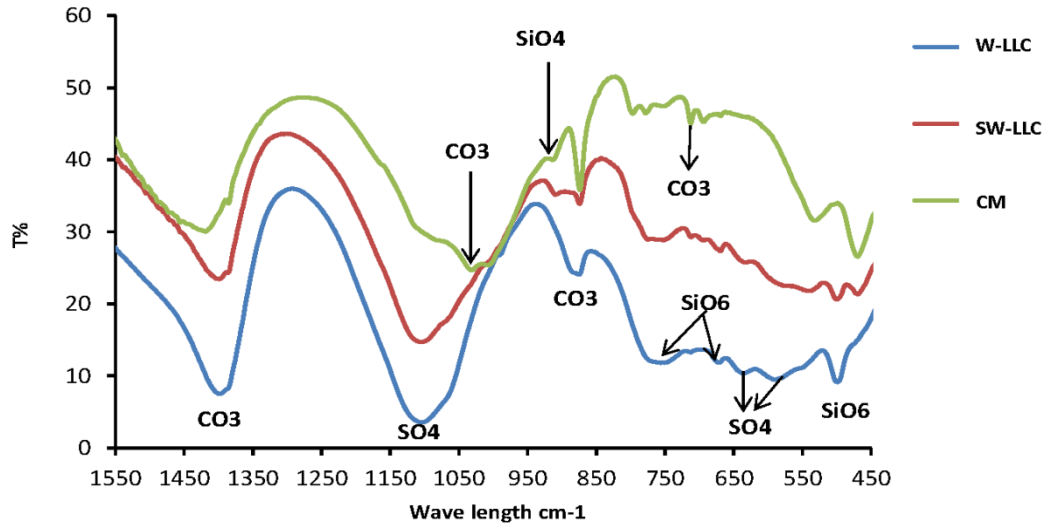


Figure 5.28 IR analysis of CEMI -LF concrete exposed to clays in the presence of mobile ground water at 5°C

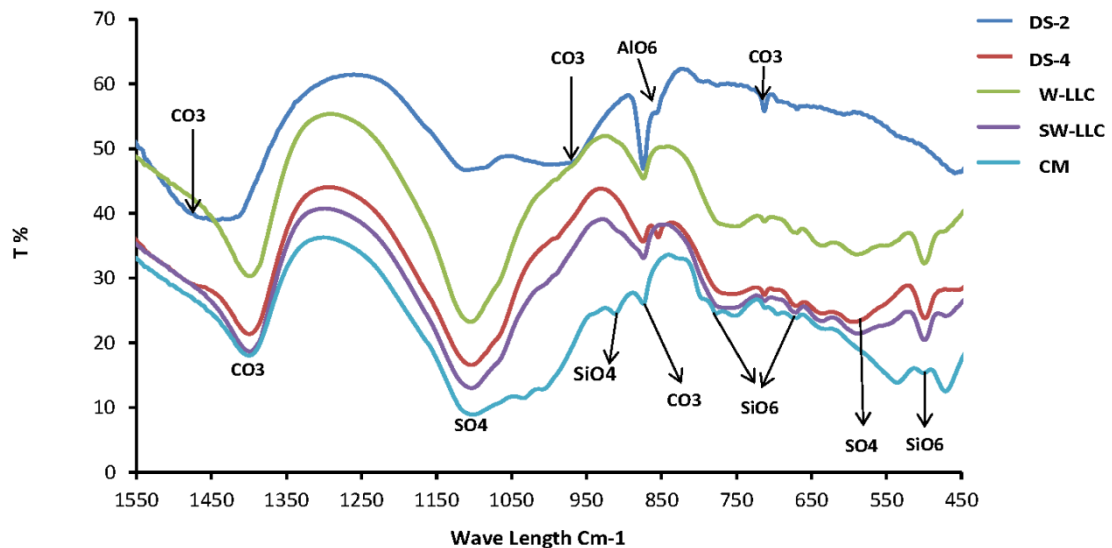


Figure 5.29 IR analysis of CEMI -LF concrete exposed to different conditions at 20°C

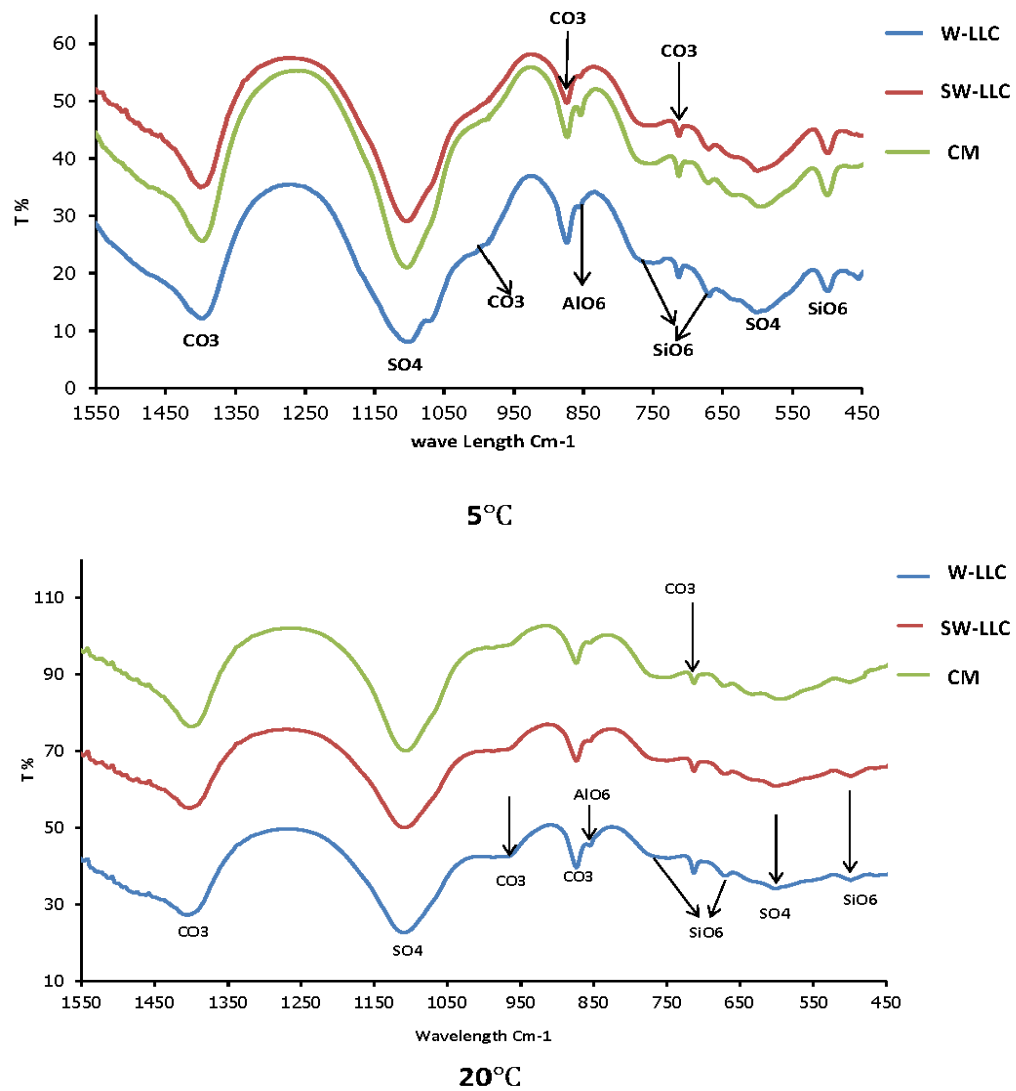


Figure 5.30 IR analysis of CEMI -LF concrete exposed to simulated clay pore solutions at 5 and 20°C

### 5.5.3 IR analysis of CEMI- PFA concrete exposed to different conditions at 5 and 20°C

Figures 5.31 to 5.33 illustrate the results of IR analysis for CEMI-PFA concrete. It can be seen that, in all concretes, the peak attributed to  $\text{SiO}_6$  at  $500 \text{ cm}^{-1}$  related to the formation of thaumasite was absent in all exposure conditions at 5° and 20°C. However,  $\text{SiO}_6$  peaks at 660 and  $756 \text{ cm}^{-1}$  were observed in all concretes exposed to different conditions and were clearly visible in samples exposed to clays at 5° and 20°C, which implies that thaumasite might be

formed. This indicates that thaumasite or thaumasite solid solution might form at both temperatures for PFA concrete.

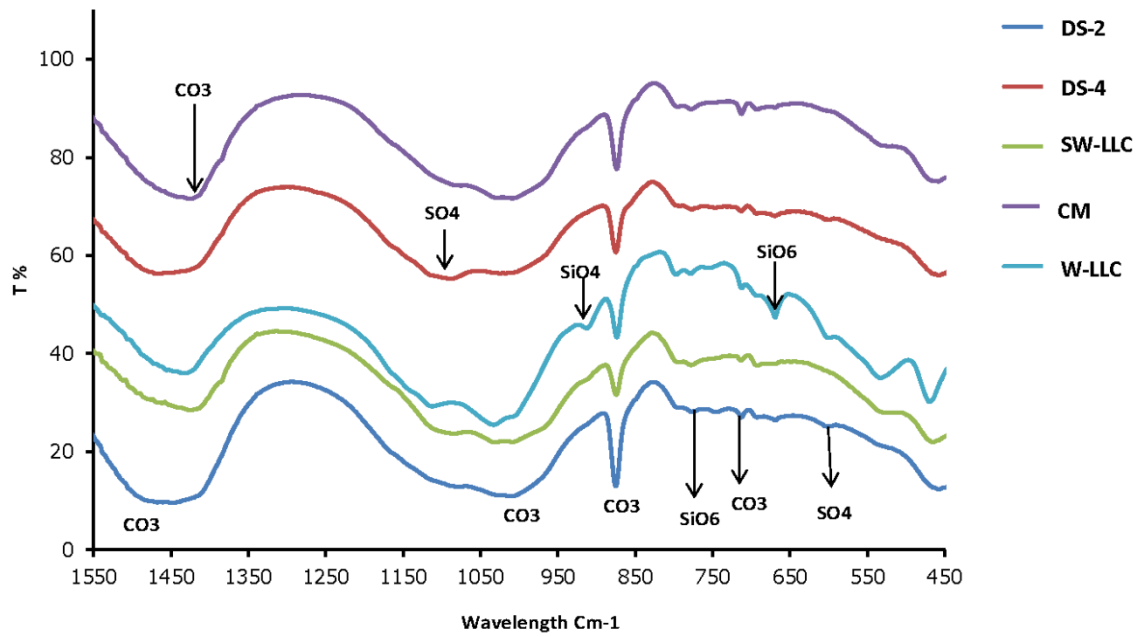


Figure 5.31 IR analysis of CEMI-PFA concrete exposed to different conditions at 5°C

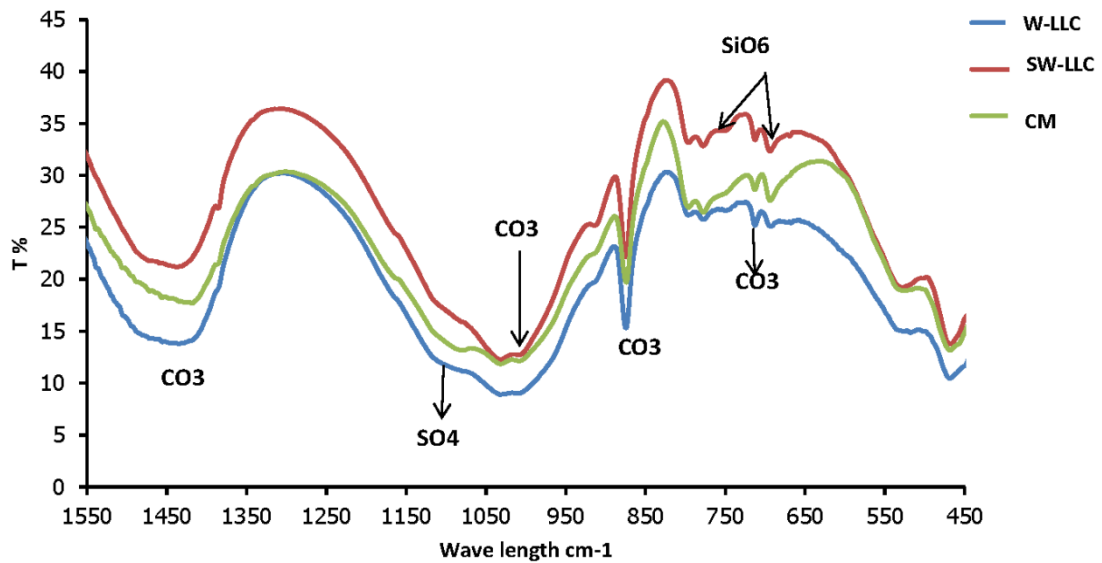


Figure 5.32 IR analysis of CEMI-PFA concrete exposed to clays in the presence of mobile ground water at 5°C

Small peaks attributed to the  $\text{AlO}_6$  group were observed at  $874.5 \text{ cm}^{-1}$  in the case of exposure to DS-2 at  $20^\circ$ , although the XRD results in Section 5.3.4 showed the presence of ettringite in all exposure conditions at both temperatures. An  $\text{SO}_4$  sulfate-bearing phase in the form of gypsum was identified at peak  $590 \text{ cm}^{-1}$  for samples immersed in DS-2 and DS-4 sulfate solutions at  $5^\circ$  and  $20^\circ\text{C}$ , while peaks at  $1100 \text{ cm}^{-1}$  associated with the  $\text{SO}_4$  group were identified and attributed to sulfate, which was involved where ettringite or thaumasite-ettringite solid solution was identified in all exposure conditions; this was clearly observed in the case of exposure to pyritic clays at  $5^\circ\text{C}$ . Peaks associated with the C-O group in the form of calcite were identified at  $713, 875$  and  $1426 \text{ cm}^{-1}$  in all exposure conditions. However, a C-O peak at  $1400 \text{ cm}^{-1}$  was observed in concrete exposed to aggressive clays, which refers to the carbonate ( $\text{CO}_3$ ) that contributes to thaumasite; this is evidence for the formation of thaumasite in the case of exposure to Lower Lias Clays.

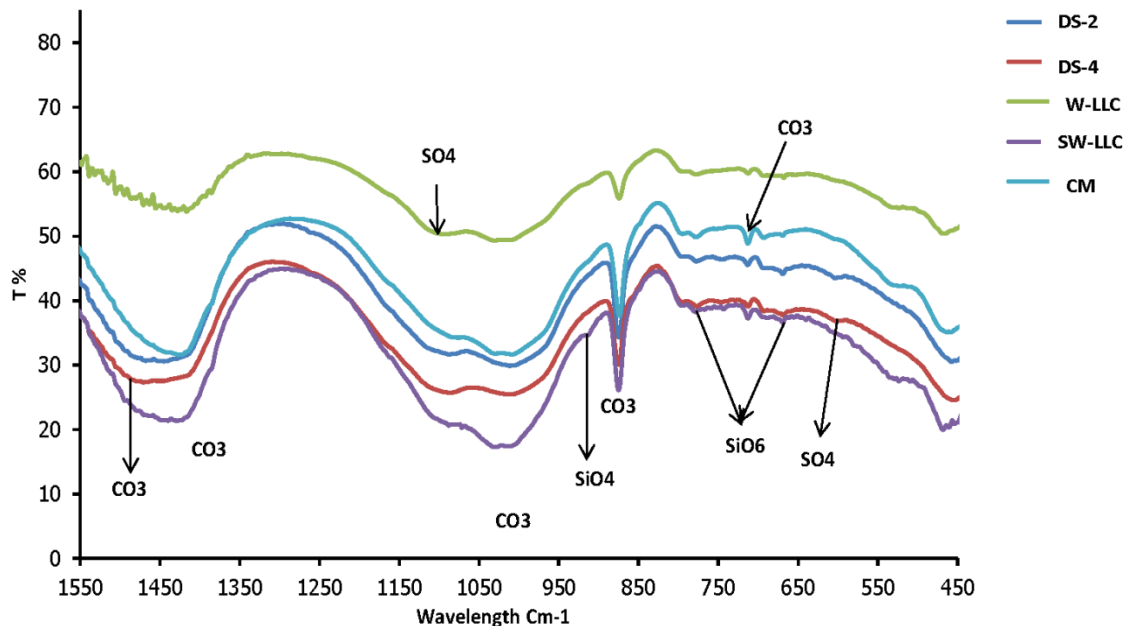


Figure 5.33 IR analysis of CEMI-PFA concrete exposed to different conditions at  $20^\circ\text{C}$

#### 5.5.4 IR analysis of CEMI- GGBS concrete exposed to different conditions at 5 and $20^\circ\text{C}$

Figures 5.34 to 5.36 show the IR spectra results for CEMI-GGBS concrete. There was no thaumasite peak detected at  $500 \text{ cm}^{-1}$  in any exposure conditions at  $5^\circ$  and  $20^\circ\text{C}$ . However,  $\text{SiO}_6$  stretched peaks observed at  $660$  and  $756 \text{ cm}^{-1}$  were identified in concretes placed in all exposure conditions at  $5^\circ$  and  $20^\circ\text{C}$ . These peaks were clearly identified in the case of exposure to clays at

5°C. Ettringite was detected at a waveband of  $855\text{ cm}^{-1}$  in specimens exposed to DS-2 and DS-4 sulfate solution at 5° and 20°C.

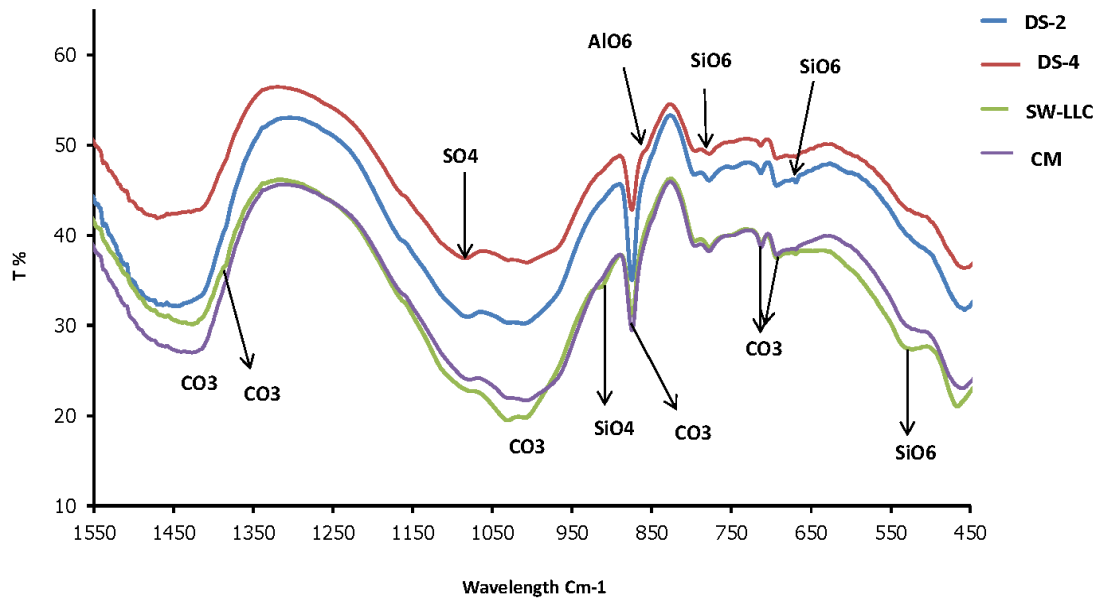


Figure 5.34 IR analysis of CEMI-GGBS concrete exposed to different conditions at 5°C

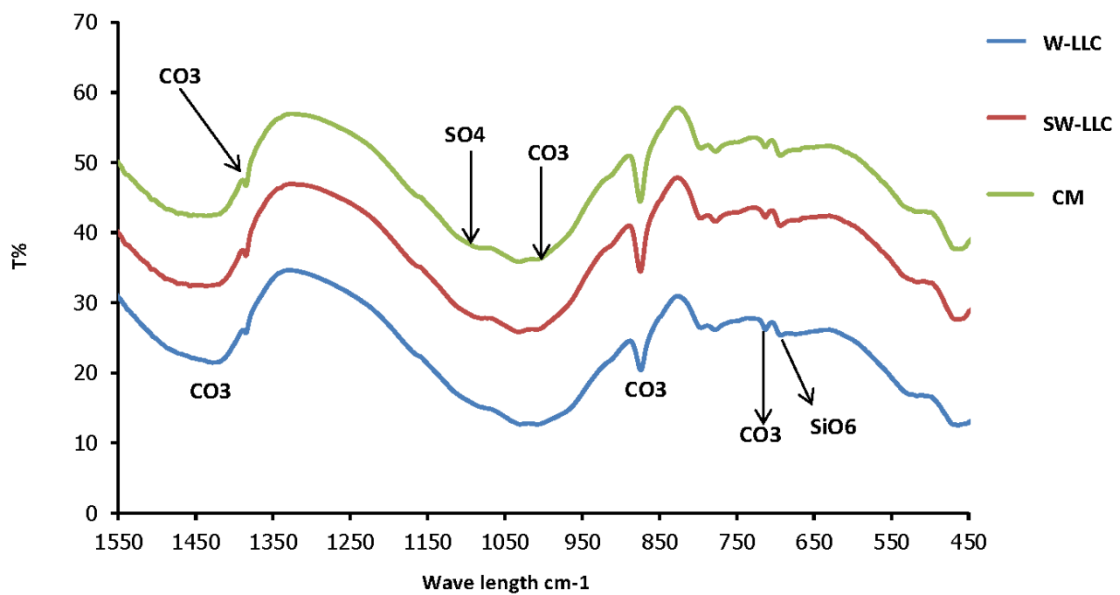


Figure 5.35 IR analysis of CEMI-GGBS concrete exposed to clays in the presence of mobile ground water at 5°C

However, IR spectra show the absence of ettringite in cases of interaction with clays, although the XRD analysis shows the formation of small quantities of ettringite, which might be formed as hydration product rather than sulfate attack. Gypsum was observed only in DS-2 and DS-4 sulfate solutions at peaks around  $590\text{ cm}^{-1}$  at  $5^\circ$  and  $20^\circ\text{C}$ , although the results of XRD analysis show the presence of high traces of gypsum in samples exposed to Coal Measures clay at  $5^\circ\text{C}$ . The sulfate-bearing phase that contributed to the formation of ettringite and thaumasite was detected in small amounts at peak  $1030\text{ cm}^{-1}$  for concrete exposed to LLC and CM clays, while it was found at peak  $1090\text{ cm}^{-1}$  in concrete exposed to sulfate solutions. Moreover, C-O carbonate mineral such as was observed at peaks  $714, 875$  and  $1438\text{ cm}^{-1}$  in all conditions, while aragonite was observed at about  $694$  and  $1470\text{ cm}^{-1}$  in all conditions. However, the C-O peak that may contribute to the structure of thaumasite or thaumasite solid solution was found at  $1380\text{ cm}^{-1}$  in concretes exposed to clays at  $5^\circ$  and  $20^\circ\text{C}$  and was higher at  $5^\circ\text{C}$  than  $20^\circ\text{C}$ .

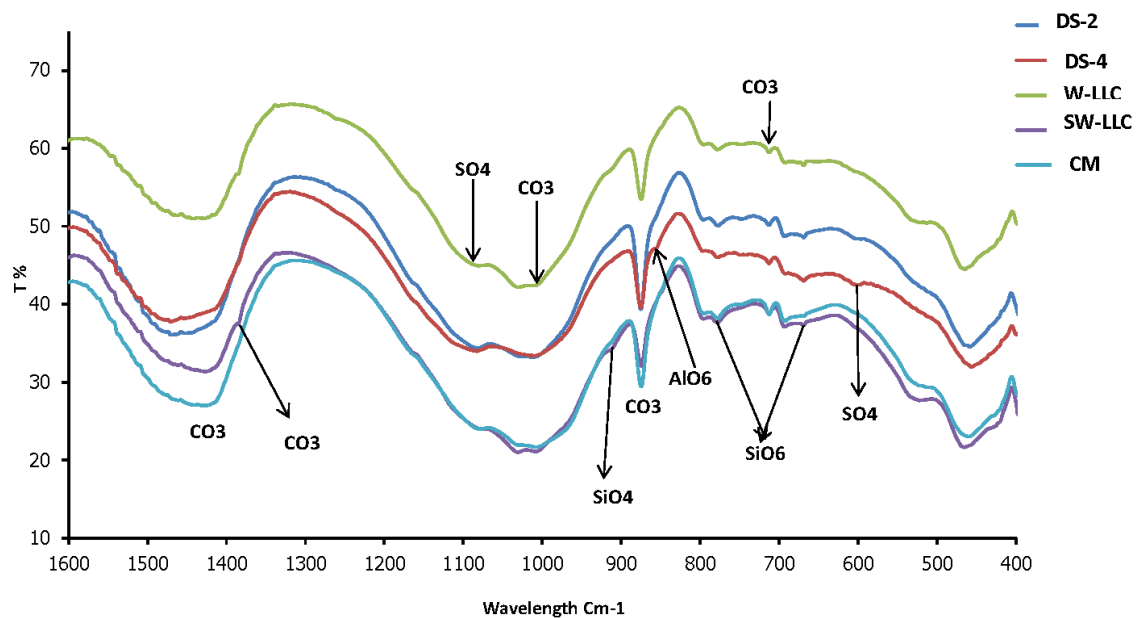


Figure 5.36 IR analysis of CEMI-GGBS concrete exposed to different conditions at  $20^\circ\text{C}$

## 5.6 Microstructural analysis of concrete by SEM

Changes in the microstructure of concrete provide evidence about the nature of reactions, deterioration mechanisms and chemical interactions between the sulfate solutions or clays and the concrete. This section presents the results of the investigation into the microstructural alteration of concrete made with different binders after 24 months of exposure to different conditions at  $5^\circ$  and  $20^\circ\text{C}$ . Only specimens where signs of deterioration were clearly obvious, as

well as PFA and GGBS specimens where XRD analysis showed formation of thaumasite, were examined. The analysis of phases within the microstructure of each sample was carried out by means of Energy Dispersive X-Ray analysis (EDX) linked to SEM. Sample preparation and test methods are described in Chapter 3. An effort was made in this research to **take account of** findings of other researchers in order to provide a clear assessment of the internal structure of the samples analysed.

### **5.6.1 CEMI concrete**

The microstructural analysis of CEMI concrete interacting with different exposure conditions is shown in Figures 5.37 to 5.40. Figures 5.37 and 5.38 show backscattered images and EDX analysis of specimens exposed to DS-4 sulfate solution at 5° and 20°C. The reaction zone at the surface of the specimen takes the form of the dark grey and grey layers. **On closer look inspection** in the dark grey zone was identified as consisting entirely of thaumasite at 5° and 20°C, which EDX analysis revealed the presence of only S, Si and Ca, which is characteristic of thaumasite. The magnified detail shows that the morphology of this thaumasite is dense needles, as shown in Figures 5.37 and 5.38. The distribution of thaumasite in the concrete matrix indicates that CEMI concrete has undergone TSA.

On the other hand, gypsum was identified in the grey zone, as EDX analysis showed the presence of S and Ca, which are attributed to gypsum, in smaller quantities at 20°C than at 5°C. Also, a general look at the sample at 20°C revealed that gypsum was formed around the aggregate within the dark grey regions identified as thaumasite. This suggests that the gypsum is the major source of sulfate that was involved in thaumasite formation. The decalcification of CSH due to magnesium was identified in the light dark grey region at 5°C, in which calcium was replaced with magnesium, as shown in EDX analysis in Figure 5.37. Cracking has developed around the aggregate at 20°C in the transition zone between cement paste and aggregate particles, as shown in Figure 5.38. This might be due to the formation of non-cementitious material, which leads to loss of binding with aggregate. Furthermore, large cracks appeared within the CEMI concrete matrix at 20°C due to the formation of ettringite, which is known to form more readily at high temperatures than at 5°C. However, thaumasite-ettringite solid solution was also present at 20°C, as Al was identified, along with S, Ca and Si, as shown in EDX analysis for spot A.



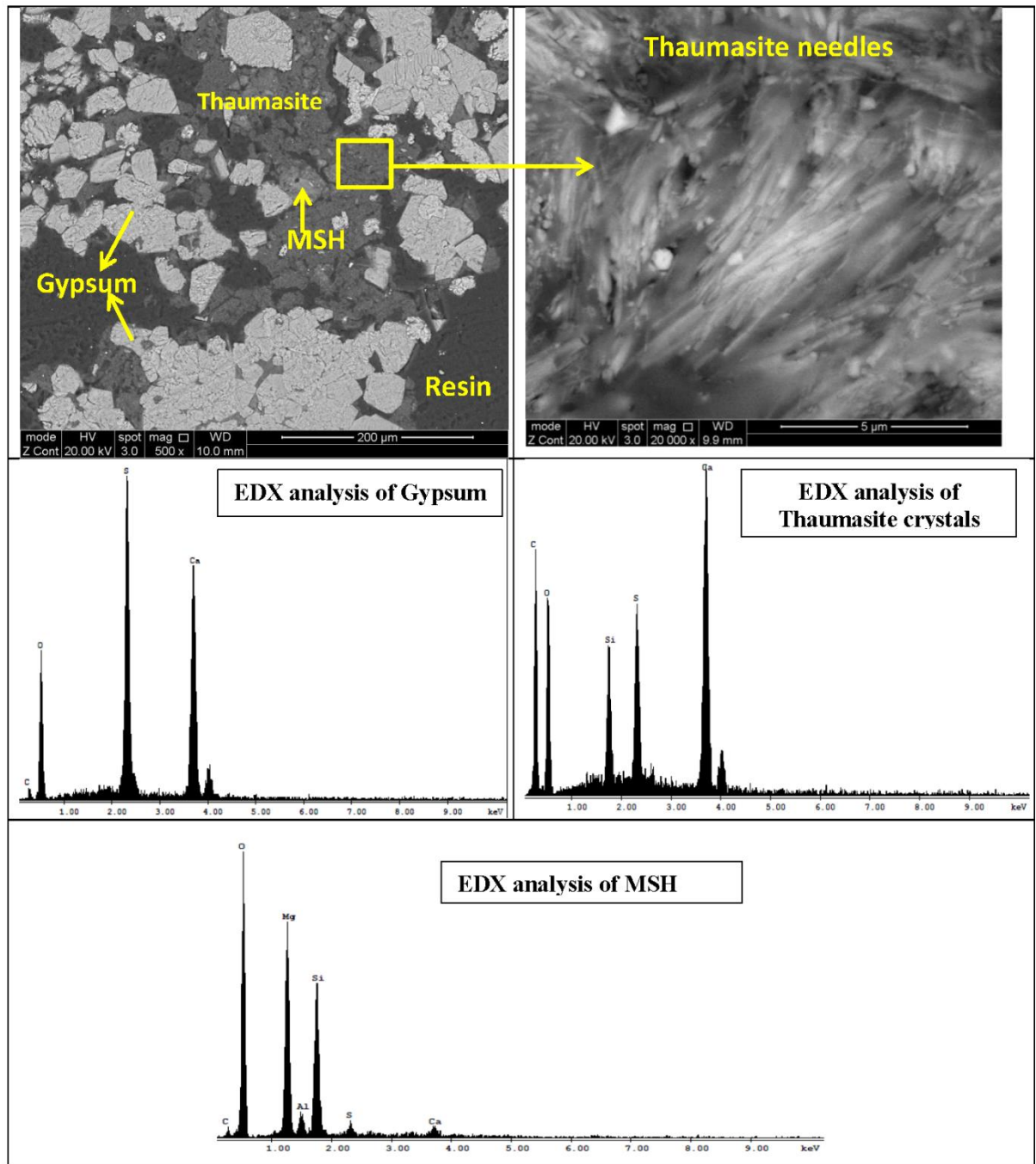


Figure 5.37 Microstructural analysis of CEMI concrete exposed to DS-4 sulfate solution at 5°C

The composition of thaumasite solid solution might be variable in **different areas** in the same sample, as reported previously by Torres (2004). Moreover, the presence of ettringite-thaumasite solid solution might be an indication for the formation of thaumasite from ettringite

by the replacement of the Al in ettringite with Si, as suggested by Torres (2004) and Torres et al. (2006). This, which is known as the woodfordite route of thaumasite formation, as reported by Bensted (2003, 1999), takes a long time to occur, which explains why fewer signs of deterioration appeared in CEMI concrete exposed to sulfate solution at a high temperature; with long-term exposure the signs of attack would develop fast. Overall assessment of CEMI microstructure exposed to the DS-4 solution revealed that different routes for thaumasite formation might be involved in similar samples at 5° and 20°C.

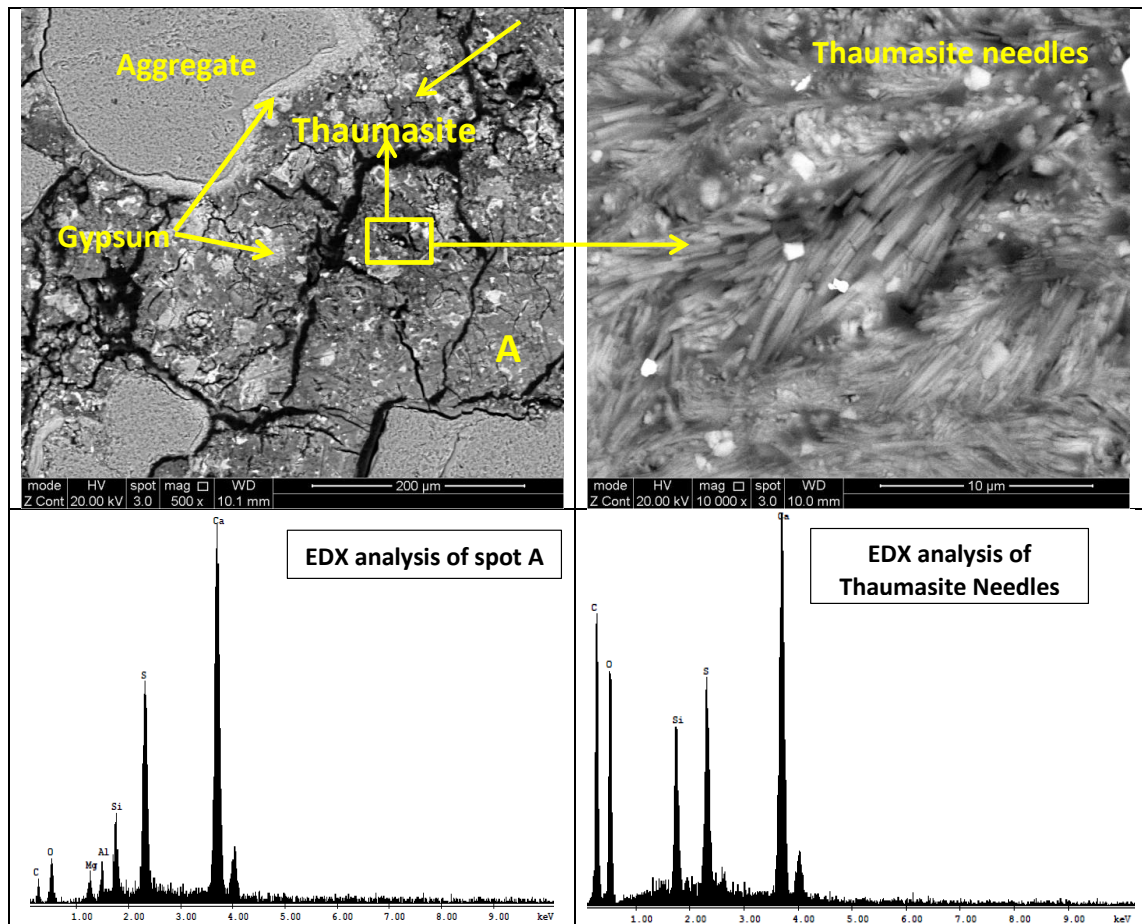


Figure 5.38 Microstructural analysis of CEMI concrete exposed to DS-4 sulfate solution at 20°C

Figures 5.39 and 5.40 present the microstructural alteration in CEMI concrete placed in clays at 5°C. The reaction zone at the surface cementitious matrix revealed the modification of the cement matrix due to attack. The main modification of the cement matrix was the formation of a

dark grey phase as the dominant deterioration product in the examined sample exposed to Lower Lias Clay and Coal Measures mudstone at 5°C. The formed phase seems to be non-cementitious material, as loss of binding with aggregate was observed. The magnified backscattered image shows needle-like bands which were identified as thaumasite by EDX analysis, while Si, Ca and S were only found in the chemical composition analysis.

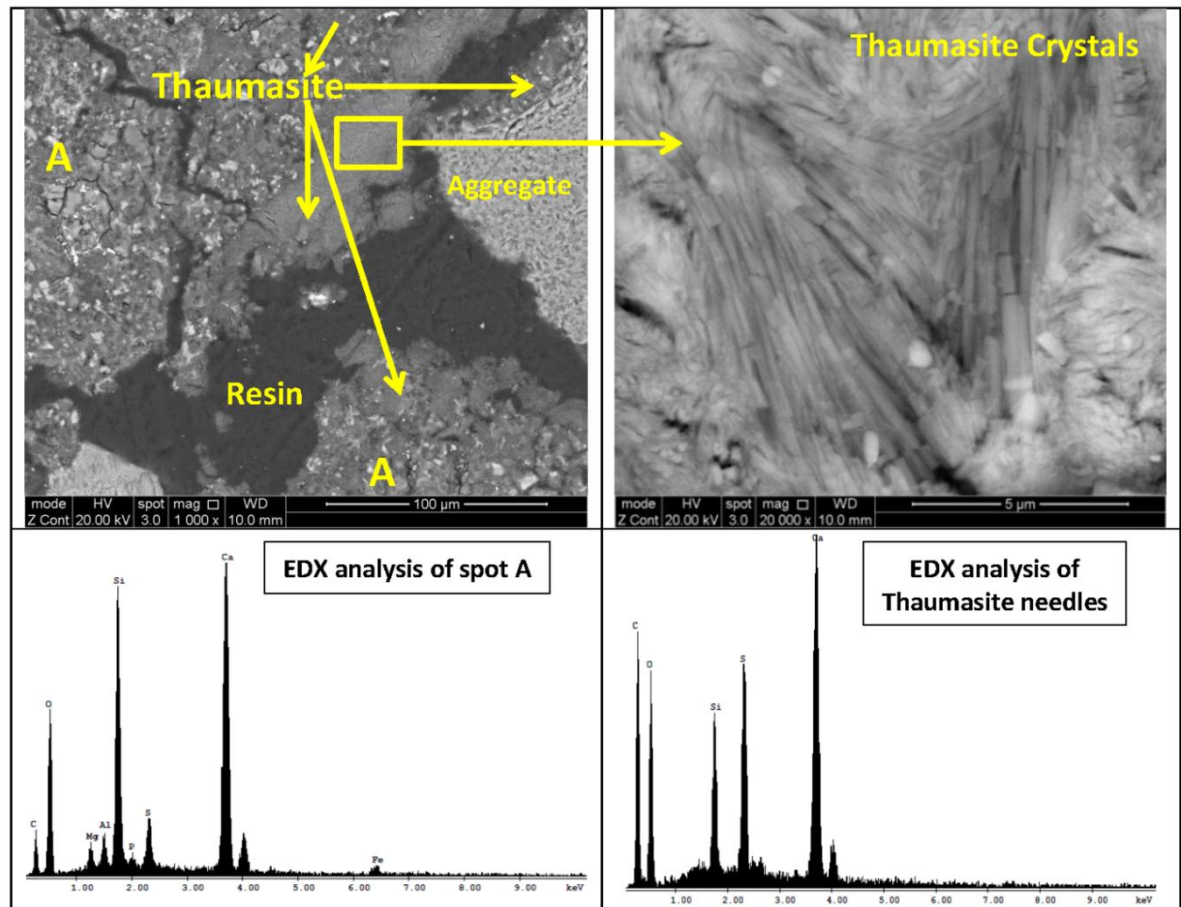


Figure 5.39 Microstructural analysis of CEMI concrete exposed to Lower Lias Clay at 5°C

Gypsum and ettringite were not found within the examined sample exposed to LLC and CM mudstone, unlike those exposed to sulfate solutions at both temperatures, which agrees with the XRD analysis in Section 5.3.4. Moreover, EDX analysis of the grey region showed the presence of low magnesium sulfate, aluminum and carbon, as shown in Figures 5.39 and 5.40. It is suggested that there could be a similarity between thaumasite and the above-mentioned phase which might accelerate and facilitate the formation of thaumasite.

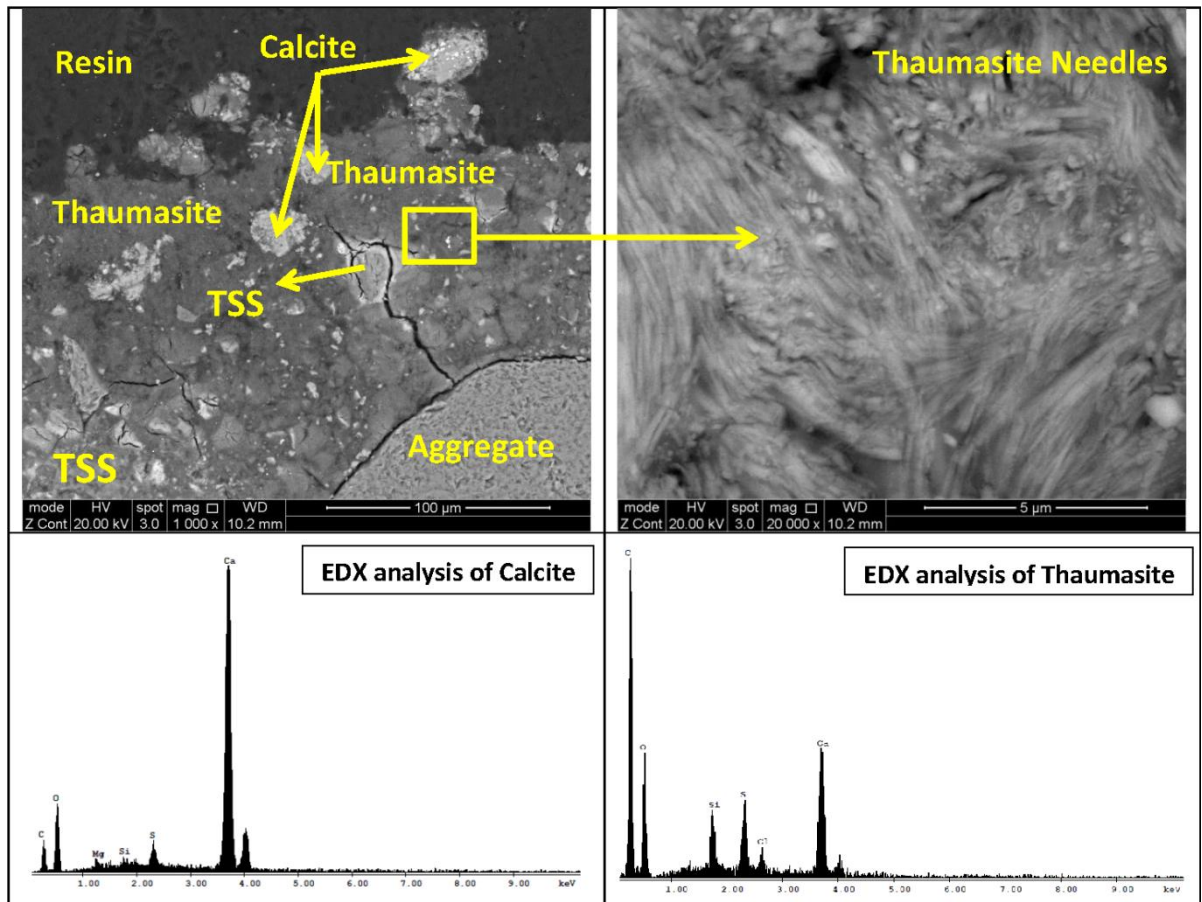


Figure 5.40 Microstructural analysis of CEMI concrete exposed to Coal Measures Clay at 5°C

In addition, the presence of magnesium and sulfate can be a result of diffusion from clay pore solution into concrete, while the presence of Al might indicate the presence of thaumasite solid solution, as ettringite was reported by Kunther et al. (2013) and Torres (2004) to be unstable in the presence of a high concentration of bicarbonate ions and relatively low pH of concrete pore solution. It should be mentioned that the decalcification of CSH in the case of exposure to aggressive clay was due to the high concentration of carbonate and bicarbonate ions present in the clay pore solution and catalysed by the relatively low pH of the surrounding environment, in comparison with the sulfate solution, in which decalcification was mainly due to a high concentration of magnesium. In the case of exposure to CM mudstone, chloride was identified within the thaumasite structure as the clay has a moderate concentration of chloride, suggesting the diffusion of chloride into concrete, and the results confirmed that thaumasite might have



chloride in its structure, as thaumasite found to be present in concrete samples was reported by Bensted (2003) to be a solid solution; it might therefore be possible for thaumasite to tolerate chloride and other species such as magnesium. The role of chloride in thaumasite formation was reported by Torres (2004), who pointed out that chloride might catalyse the formation of thaumasite at certain concentrations and might play an important role in enhancing the resistance of concrete to TSA at a high concentration of chloride. It is also highlighted that chloride can be found in the structure of thaumasite.

### **5.6.2 CEMI - LF concrete**

The microstructural changes of CEMI-LF concrete placed in different exposure conditions are shown in Figures 5.41 to 5.44. Specimens exposed to DS-4 sulfate solution at 5° and 20°C show modifications in the concrete microstructure. A non-cohesive bond has developed around the aggregate, resulting in loss of the bond between aggregate and cement matrices. Grey and dark grey colours were identified in the reaction zone at both temperatures. A magnified image of the dark grey area shows the presence of extensive needles, identified as thaumasite, as shown in Figures 5.41 and 5.42. Plates of gypsum were observed in the grey reaction zone. Hartshorn et al. (1999) stated that secondary gypsum would form along with thaumasite in case of attack resulted from exposure to magnesium sulfate, the formation of thaumasite is accompanied by the formation of secondary gypsum **which is in the line with this investigation**. However, the presence of magnesium in the composition of thaumasite as seen in the EDX analysis revealed that the formed phase is a solid solution in which magnesium and other ions might be present, as reported by Bensted (2003, 1999).

In Lower Lias Clay and Coal Measures mudstone at 5°C, the backscattered image of the microstructure also showed alterations in the concrete microstructure, in which a dark grey reaction zone was the main feature in the examined sample, as shown in Figures 5.43 and 5.44. The EDX analysis of the dark grey area (crystals) confirmed the presence of pure thaumasite. However, unlike the case of sulfate solution, gypsum and ettringite were not observed, which agrees with the XRD analysis in Section 5.3.4. Calcite was also observed in concrete exposed to CM mudstone. Moreover, Mg, Si, S, Al and carbon were observed in the EDX analysis of light dark grey zone that was observed close to the dark grey reaction zone of deteriorated cementitious matrix in all exposure conditions.

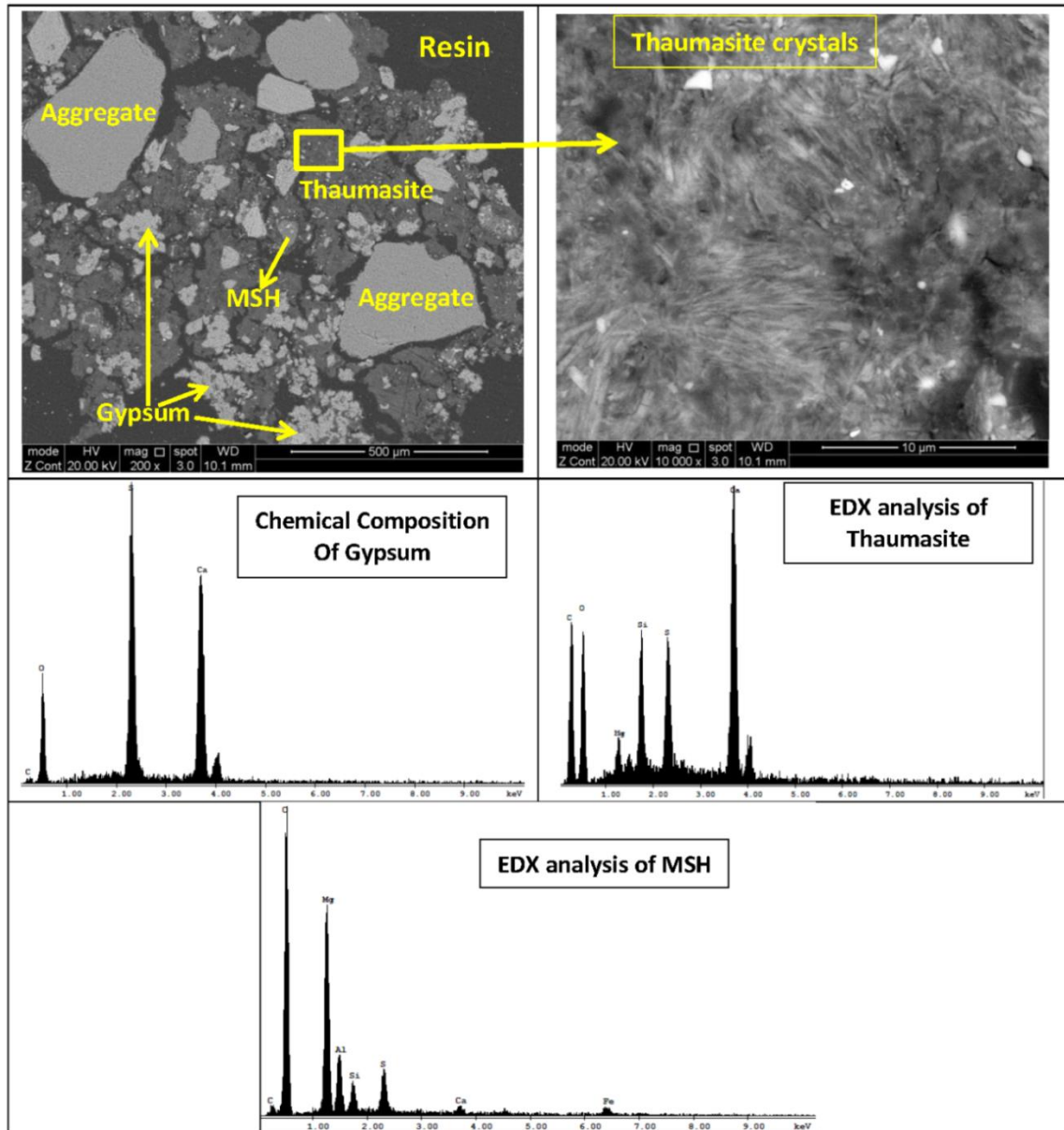


Figure 5.41 Microstructural analysis of CEMI-LF concrete exposed to DS-4 sulfate solution at 5°C

This complex compound might be due to the deterioration of CHS and other hydration products, and in the presence of sufficient carbonate and bicarbonate ions thaumasite solid solution might form. This might convert to thaumasite or accelerate and facilitate the formation of thaumasite, as discussed by Pouya (2007). The presence of a low Mg peak in its structure does not imply the

disintegration of CSH due to magnesium, as the clay contains a low Mg concentration compared to DS-4 sulfate solution.

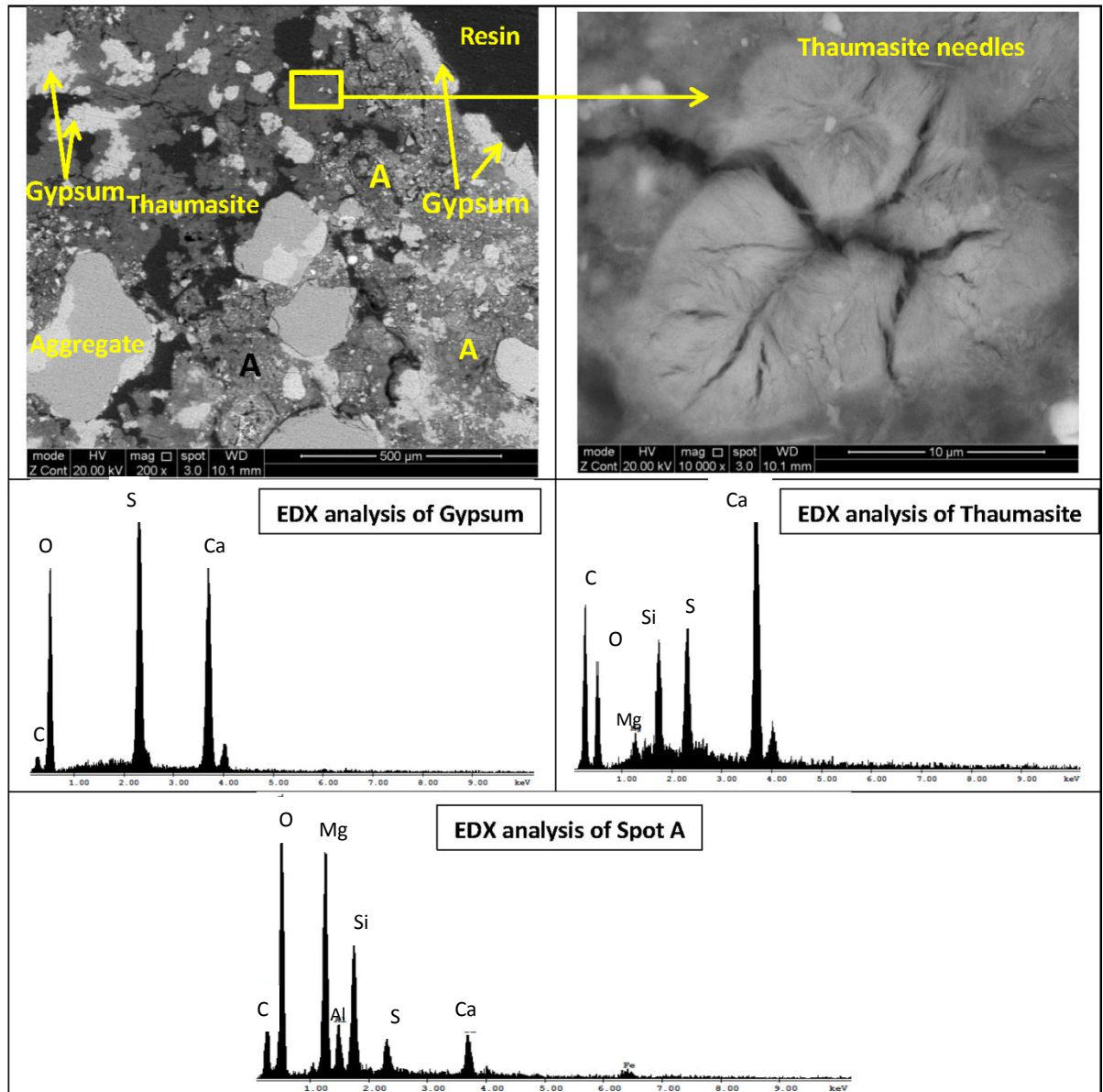


Figure 5.42 Microstructural analysis of CEMI-LF concrete exposed to DS-4 sulfate solution at 20°C

It is suggested that the high concentration bicarbonate ions in the clay pore solution and the relatively low pH of exposure conditions might accelerate the decalcification of CSH and the decomposition of other hydration products such as monosulfate and ettringite, leading to the



formation of a complex compound that may convert to thaumasite at a later stage of reaction, as sufficient sulfate and carbonate for thaumasite formation and progress of TSA become available. EDX analysis showed that a peak of chloride was identified within the thaumasite structure in the case of exposure to Coal Measures mudstone, where the clay has a moderate concentration of chloride. It is suggested that chloride is diffused into the concrete, and the results show the ability of thaumasite to accommodate chloride in its structure, as discussed previously in Section 5.6.1.

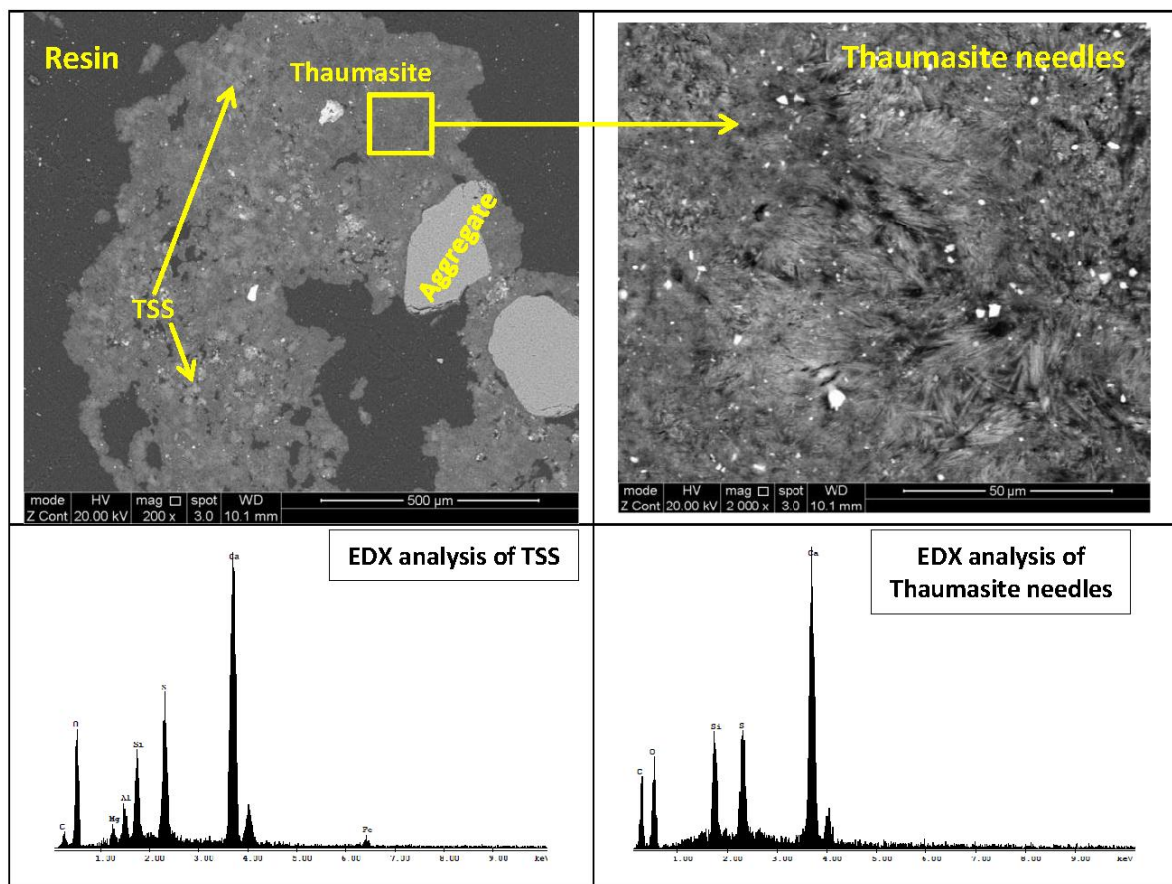


Figure 5.43 Microstructural analysis of CEMI-LF concrete exposed to Lower Lias Clay at 5°C

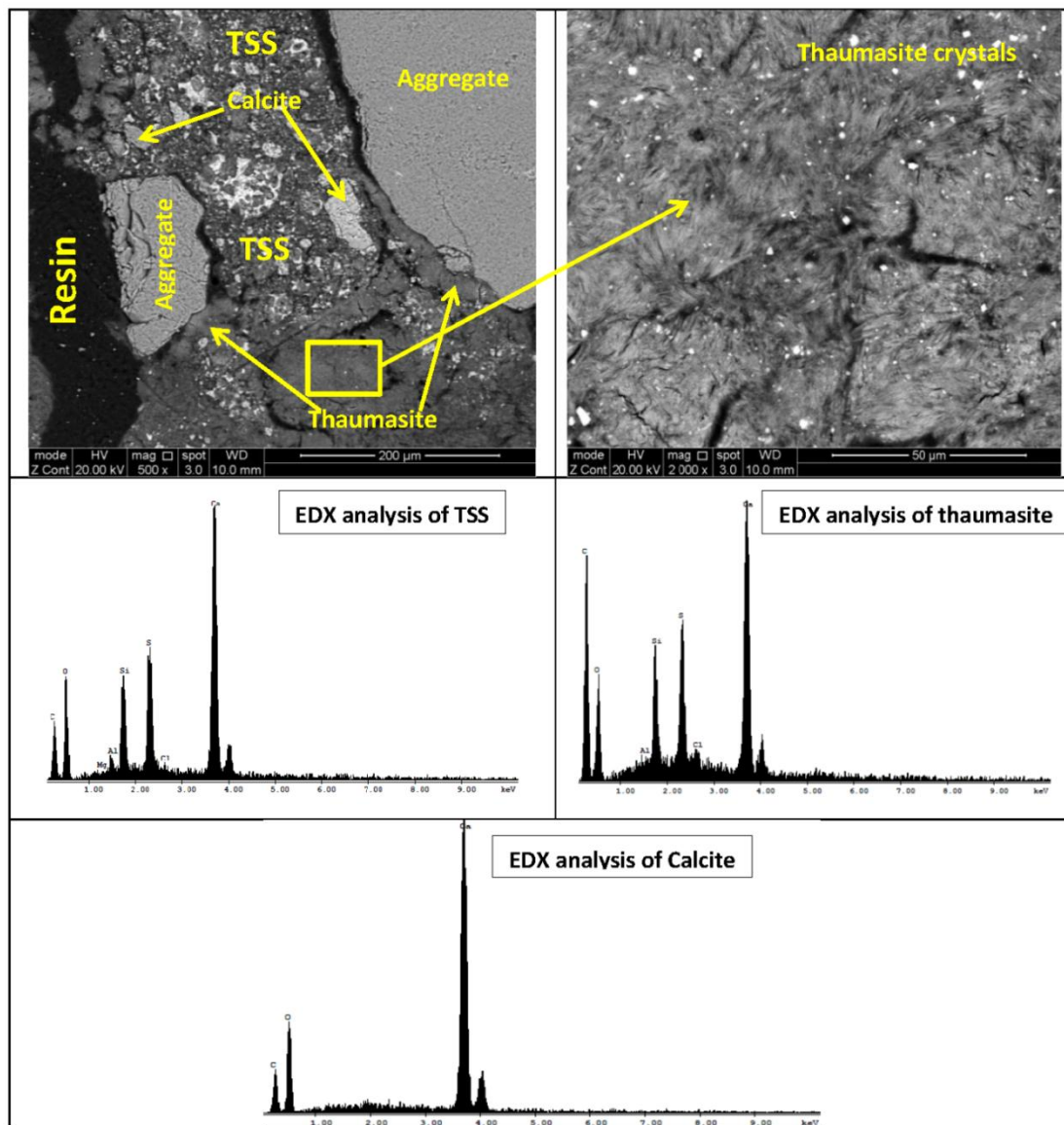


Figure 5.44 Microstructural analysis of CEMI-LF concrete exposed to Coal Measures at 5°C.

### 5.6.3 CEMI - PFA concrete

The performance of PFA concrete is **an uncertain** aspect of TSA, as the addition of PFA to concrete results in enhancement of the durability of the concrete in sulfate-bearing environments. The microstructural changes of CEMI-PFA concrete placed in different exposure conditions are shown in Figures 5.45 and 5.46. Figure 5.45 shows the microstructural alteration of PFA concrete after 24 months of exposure to DS-4 sulfate solution at 5°C. EDX analysis (spot A) reveals that the outer region was identified as M-S-Si-H-Al, as seen in Figure 5.45. This

is different from the known MSH phase owing to the presence of sulfate and aluminum in its structure, as reported by Pouya (2007). On the other hand, the presence of carbon in EDX analysis (spot A) within the M-S-Si-H-Al phase suggested the similarity between this phase and ettringite-thaumasite solid solution. This agrees with the XRD results in Section 5.3.4, as ettringite-thaumasite solid solution was found to be present in concrete exposed to DS-4 solution.

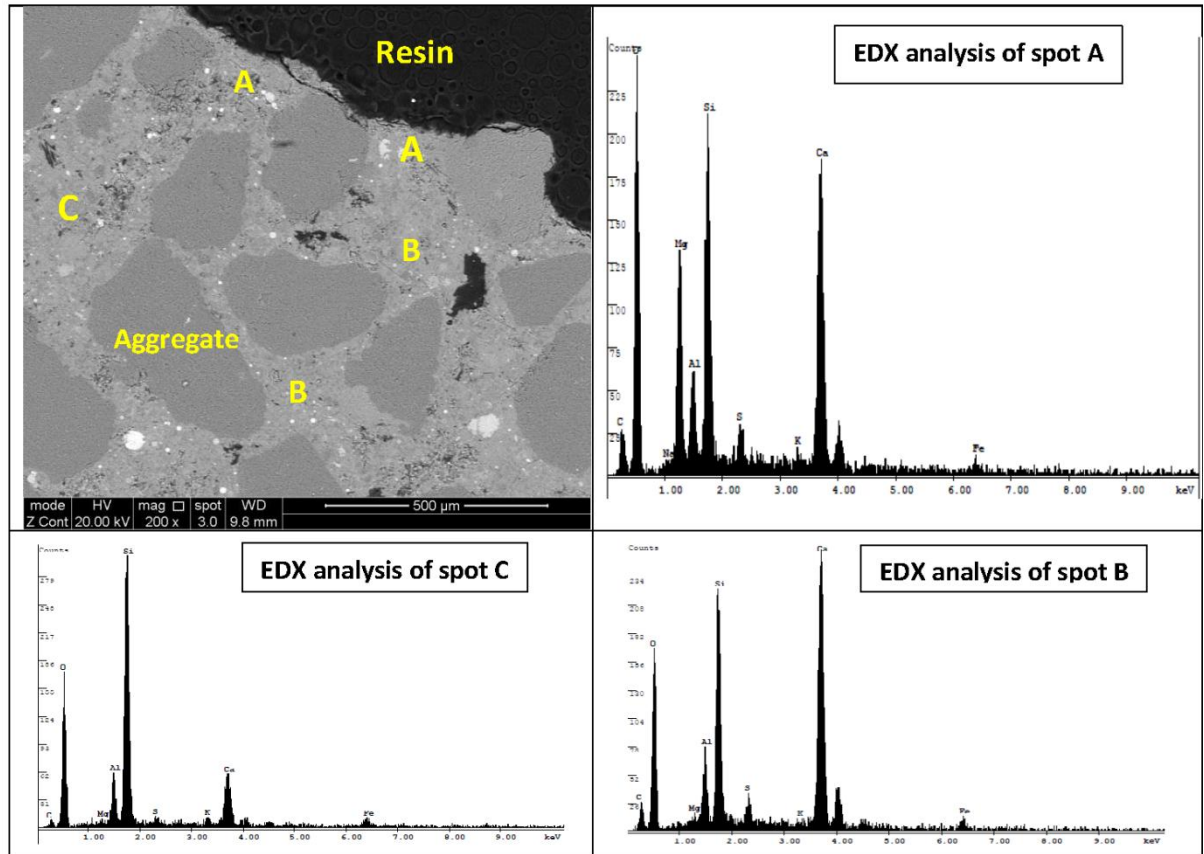


Figure 5.45 Microstructural analysis of CEMI-PFA concrete exposed to DS-4 sulfate solution at 5°C.

However, the composition of the phase at spot A consisted of Mg, Ca, Si and S, which could be a product of a reaction between magnesium sulfate and pozzolanic or ordinary CSH. The incorporation of sulfate and a slight amount of Al in this phase might be due to the lower Ca: Si ratio of pozzolanic CSH, which can accommodate other ions within its structure. The region beneath the M-Al-S-Si-H (spot B) layer was found to have less magnesium and to have incorporated Si in its structure as well as sulfate, as shown in Figure 5.45. This indicates the

transportation of magnesium and sulfate ions towards the inner cementitious matrix. In addition, the chemical composition of spot C revealed that the pozzolanic CSH contains more silica and less calcium. However, the presence of Al might be attributed to aluminates supplied by aluminum-bearing phases within the cementitious matrix. The PFA used in this investigation contains about 25%  $\text{AlO}_3$  and therefore the pozzolanic CSH can bear a significant amount of aluminum. Perhaps the aluminate present in the composition of PFA might have promoted the formation of ettringite. In addition, the high intensity of silicon in the micrograph shown in Figure 5.45 emphasizes the presence of a source of amorphous silica in the system, supplied through decalcification of ordinary and pozzolanic CSH, which was reported to have a higher Si/Ca ratio; PFA therefore acted as a source of amorphous silica in the system, as the solubility of quartz from aggregates in alkaline solution is not considerable (Taylor, 1997; Pouya, 2007). Also, the presence of ettringite solid solution in the cementitious matrix of PFA concrete implies that the incorporation of PFA in the concrete mixture did not totally prevent ettringite formation, which is in line with the findings of Hill et al. (2003) and Zhou et al. (2006). The SEM analysis revealed that it is not clear whether thaumasite was formed with the PFA concrete matrix, but ettringite-thaumasite solid solution was found, and incorporated Mg in its structure.

With reference to specimens placed in Lower Lias Clay at 5°C, modification in the concrete microstructure was observed. Figure 5.46 shows that the paste layer around aggregate particles did not consist of any distinctive deterioration layer. On the other hand, the dark grey region underneath the outer carbonated layer as well as at spot A showed the formation of crystals in concrete air voids as well as within the concrete matrix, where they appear as dense needles. EDX analysis of crystal needles showed the presence of Ca with relatively low Si as well as Al and S, suggesting the formation of thaumasite solid solution. This agrees with the XRD results in which thaumasite solid solution was detected along with small peaks of thaumasite. Within the inner layer of deterioration appearing in deeper regions (spot B), the layer comprised calcium aluminum silicate hydrate with low sulfate. This might refer to ettringite or ettringite solid solution. The formation of thaumasite solid solution within the cementitious matrix might be a result of a reaction between amorphous silica, resulting from decalcification of pozzolanic CSH due to interaction and the carbonate and bicarbonate ions diffused from clay into the inner part of the paste matrix. In addition, the outer carbonated layer which consists of calcite might serve thaumasite formation by providing more carbonate in order to initiate the formation reaction. However, TSA in PFA concrete proceeded at a lower rate than in CEMI and CEMI-LF.



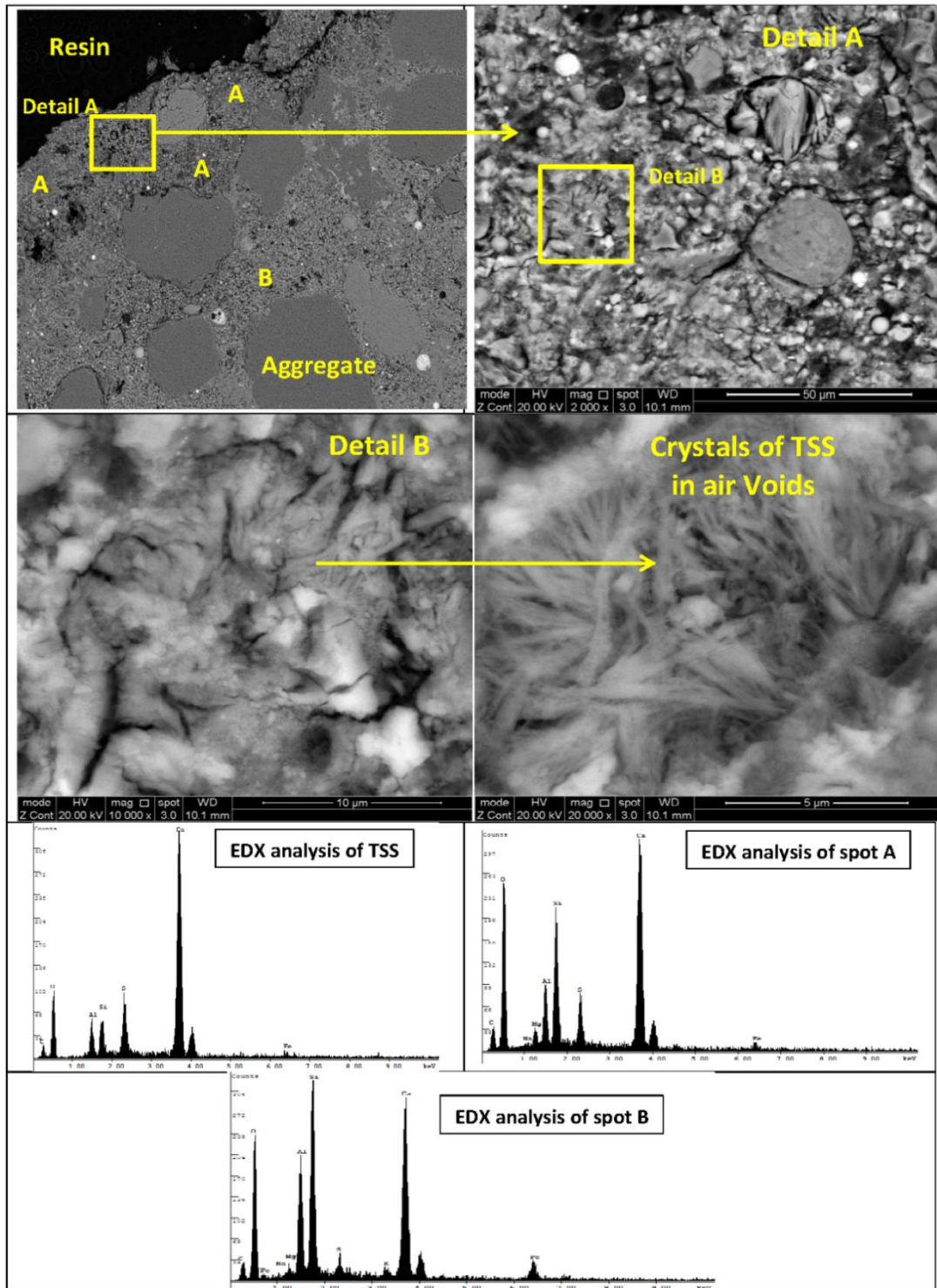


Figure 5.46 Microstructural analysis of CEMI-PFA concrete exposed to Lower Lias Clay at 5°C.

As far as the nucleation of thaumasite is concerned, the aluminum oxide content of fly ash seemed to play a role in the formation of ettringite, which has been reported to accelerate thaumasite attack (Bensted, 2003). However, the relative absence of portlandite from the system and the partial incorporation of aluminates within the pozzolanic CSH might reduce the amount of ettringite formed, it seems that the formation of thaumasite might have proceeded through a direct route from CSH or amorphous silica. The possibility of the formation of thaumasite from silica with respect to thermodynamic equilibrium was investigated by Bellman (2004). Therefore, regardless of the mechanism through which the thaumasite formed, the formation of a considerable amount of thaumasite solid solution showed that PFA concrete is susceptible to attack by thaumasite. The results of microstructural analysis show that PFA cannot prevent TSA formation in DS-4 sulfate solution and LLC at 5°C. Sulfate attack was delayed, probably because ettringite was less readily formed within the microstructure of PFA concrete. The enhancement of pore structure due to the consumption of portlandite by the pozzolanic reaction of PFA could be another possible explanation for delayed thaumasite attack. Overall, despite the absence of visual signs of TSA on the concrete surface, crystals of thaumasite solid solution were formed, and once they had grown to an advanced extent, signs of deterioration appeared on the surface.

#### **5.6.4 CEMI - GGBS concrete**

The microstructural changes of CEMI-GGBS concrete interacting with different exposure conditions is shown in Figures 5.47 to 5.50. Figure 5.47 shows the microstructural change in GGBS concrete immersed in DS-4 sulfate solution at 5°C. The presence of different layers of deterioration was confirmed by the backscattered SEM image. The reaction zone comprised two distinctive layers of which the outer was found to consist mainly of patches of calcite, as confirmed by EDX analysis. The dark grey matrix beneath the carbonated layer (spot A) was identified as MCSH, comprising high magnesium and less calcium, as shown in the EDX analysis in Figure 5.47. It is suggested that calcium was replaced with magnesium present in solution, which would accelerate the decomposition of the CSH phase in the cementitious matrix. However, the detected phase differed from the known MSH phase because of the incorporation of sulfate within its structure, from which brucite was absent, in the outer layer of concrete. Closer examination of the microstructure indicates that the layer beneath the M-C-S-Si-H layer (spots B and C) was found to have less magnesium, but incorporated the Ca in its structure. This indicates the transportation of magnesium ions towards the inner cementitious matrix.

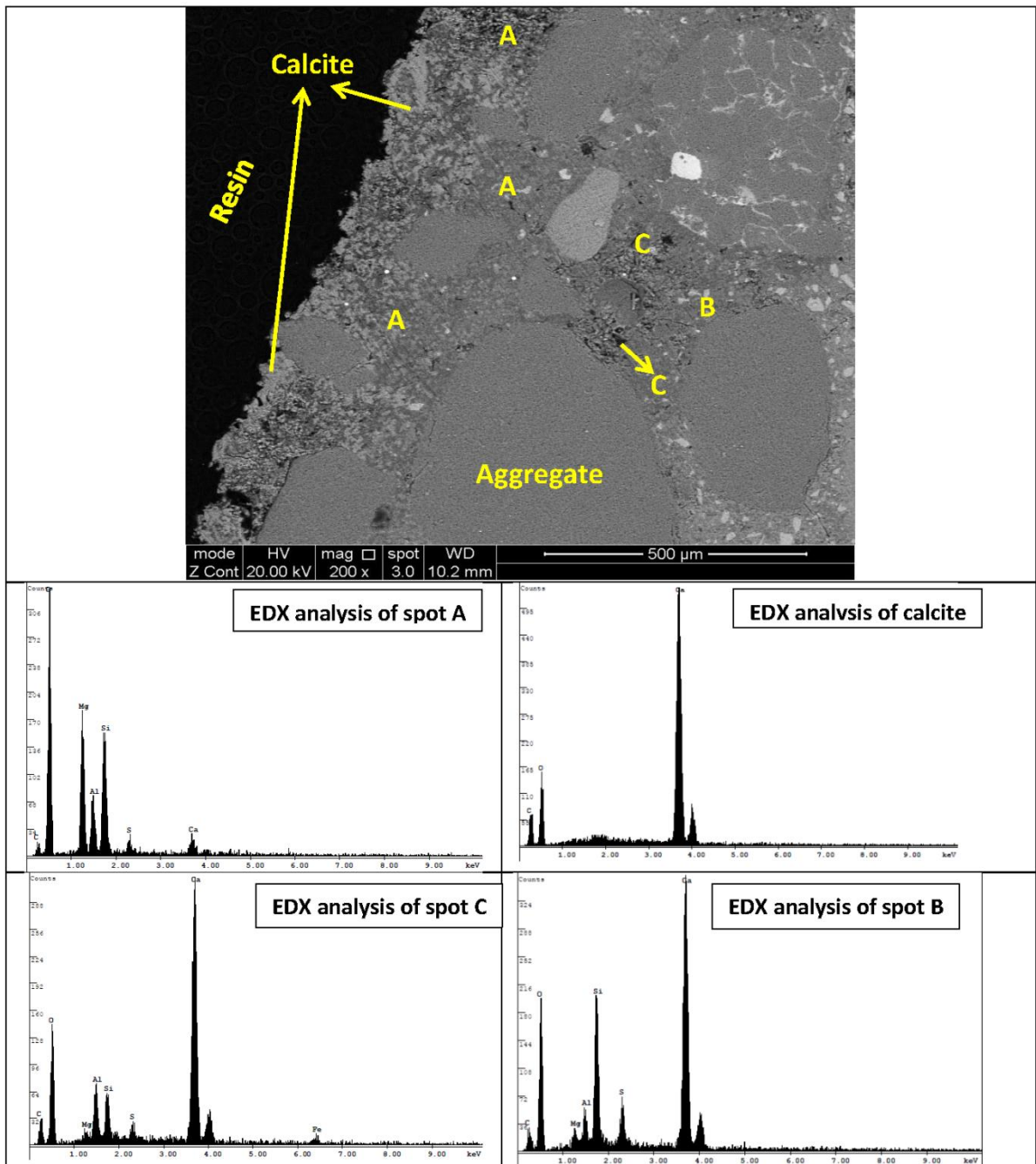


Figure 5.47 Microstructural analysis of CEMI-GGBS concrete exposed to DS-4 sulfate solution at 5°C.

The incorporation of aluminum and sulfate in the structure of the C-Si-Al-M-S phase might be related to the capability of pozzolanic CSH to accept external ions in its structure; similar findings were reported by Pouya (2007) and Bensted (2003). The incorporation of Mg and Al in



the hydration products of GGBS mixes, particularly within the confines of the original slag grains, was also reported by Escalanta and Sharp (2004). It should be mentioned that the MSH phase is a non-cementitious material; however, it has different features from thaumasite, resulting in loss of strength in concrete (Cohen and Bentur, 1988). In fact there was no sign of mushy material either on the surface or inside the sample. The presence of high magnesium and low calcium in the structure of the above phase indicates that the detected compound was not a solid solution of ettringite and thaumasite, although it has relatively low sulfate in its structure.

Thorough scanning of the matrix at different points showed no significant formation of ettringite. However, in regions (spot B and C) which were examined as shown in Figure 5.47, ettringite-thaumasite solid solution was detected, and the EDX analysis implies the presence of sulfate, aluminum and silica. Pouya (2007) reported that the incorporation of sulfate and aluminate in the structure of CSH might imply a slight deterioration of the main cementitious matrix towards phases like ettringite or thaumasite or a solid solution within air voids, which is the case in this investigation. The compositions of detected phases revealed the presence of elements required for thaumasite formation, of which sulfate was supplied from a magnesium sulfate solution and carbonate might have been supplied from the carbonated layer. The decomposition of CSH would serve as the source of silicate and calcium. Therefore, GGBS concrete in this research is susceptible to thaumasite formation, and deterioration due to TSA might progress with long-term exposure.

Specimens placed in Lower Lias Clay at 5°C also showed alteration in the microstructure, as seen in Figures 5.48 to 5.50. It can be seen that the outer layer of the matrix was distinctively different in its features from the inner area. The outer layer in Figure 5.48 consisted of carbonate minerals, namely calcite, as calcite crystals were clearly seen in the backscattered image. The formation of the calcite layer on the surface of the paste matrix might be due to reaction of carbonate and bicarbonate ions available in the clay pore solution with CSH, resulting in decalcification of CSH and the formation of more calcite and aragonite. In addition, it might form as a result of the initial carbonation of concrete after casting. The magnified backscattered image of the dark grey zone of the concrete matrix shows that air voids become filled with crystals.

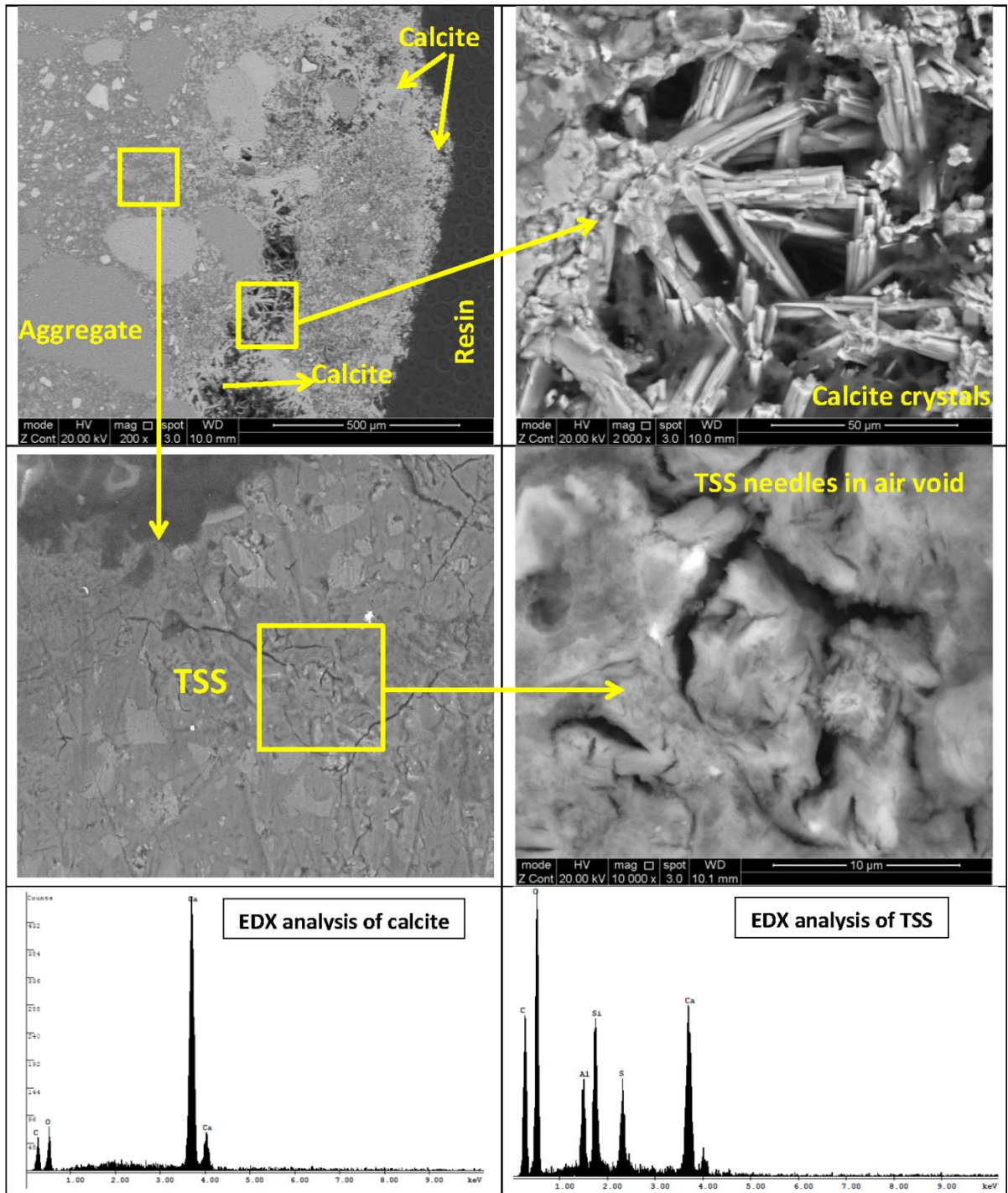


Figure 5.48 Microstructural analysis of CEMIGGBS concrete exposed to Lower Lias Clay at 5°C.

Similar observations were made at other parts of samples, as shown in Figures 5.49 and 5.50, providing more evidence of the formation of needles in air voids within the concrete matrix. The relevant EDX analysis of the crystals reveals the formation of thaumasite solid solution. Although no sign of attack was observed on the concrete surface, thaumasite might be present in the form of thaumasite-ettringite solid solution, which was detected in a few regions of the matrix. According to Brown et al. (2003), thaumasite and thaumasite solid solution can be formed even at room temperature and within any type of cementitious paste if a source of sulfate, carbonate, calcium and silicate is available. Clark (2002) stated that thaumasite formation (TF) is considered to be different from the growth of thaumasite resulting in severe progressive attack on concrete, which is referred to as TSA.

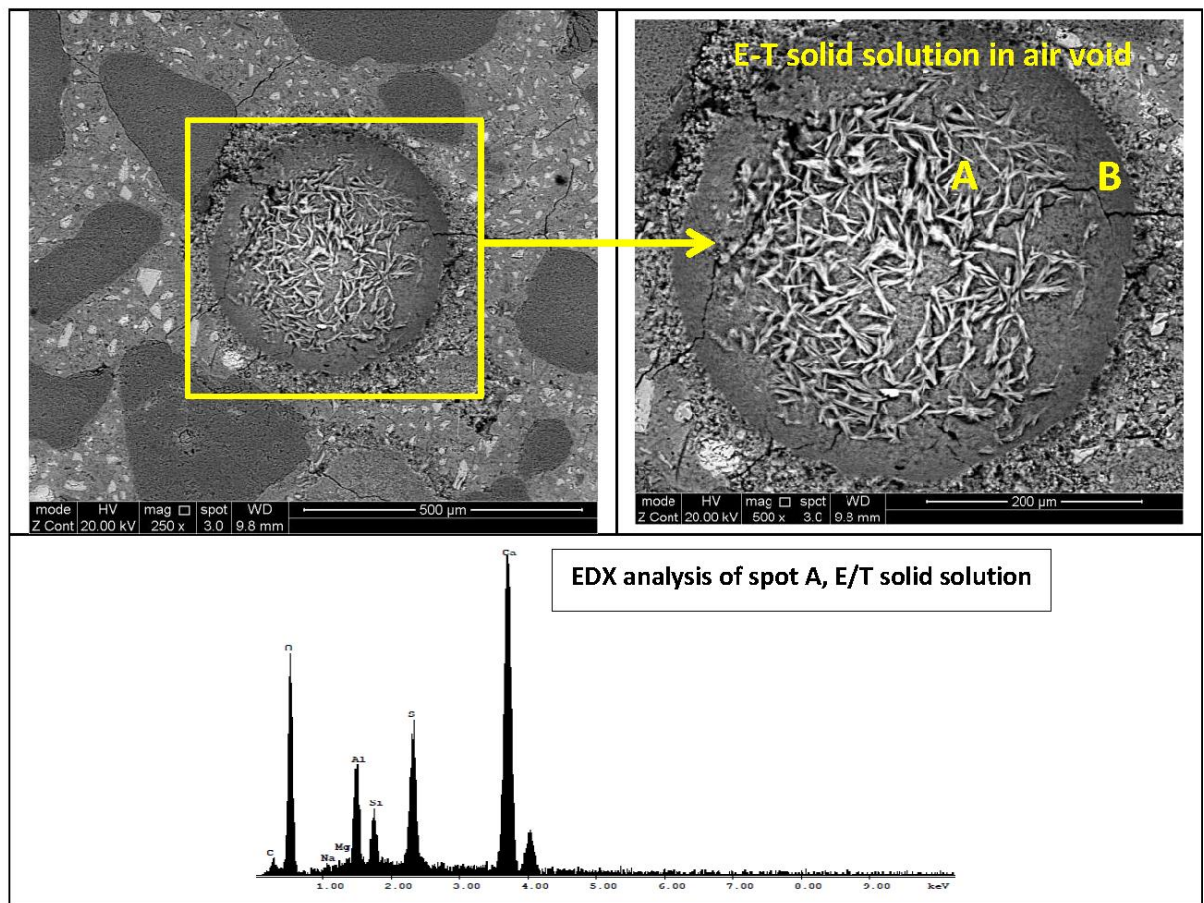


Figure 5.49 Microstructure analysis of CEMIGGBS concrete exposed to Lower Lias Clay at 5°C.

However, for the development of TSA in concrete, the same conditions are required as for TF, but the ingress of sulfates and carbonates has to be faster and the aggressive ions in the pore



solution have to be more concentrated to reach a supersaturation state such that thaumasite precipitates from the solution and a fast conversion of the matrix into thaumasite occurs.

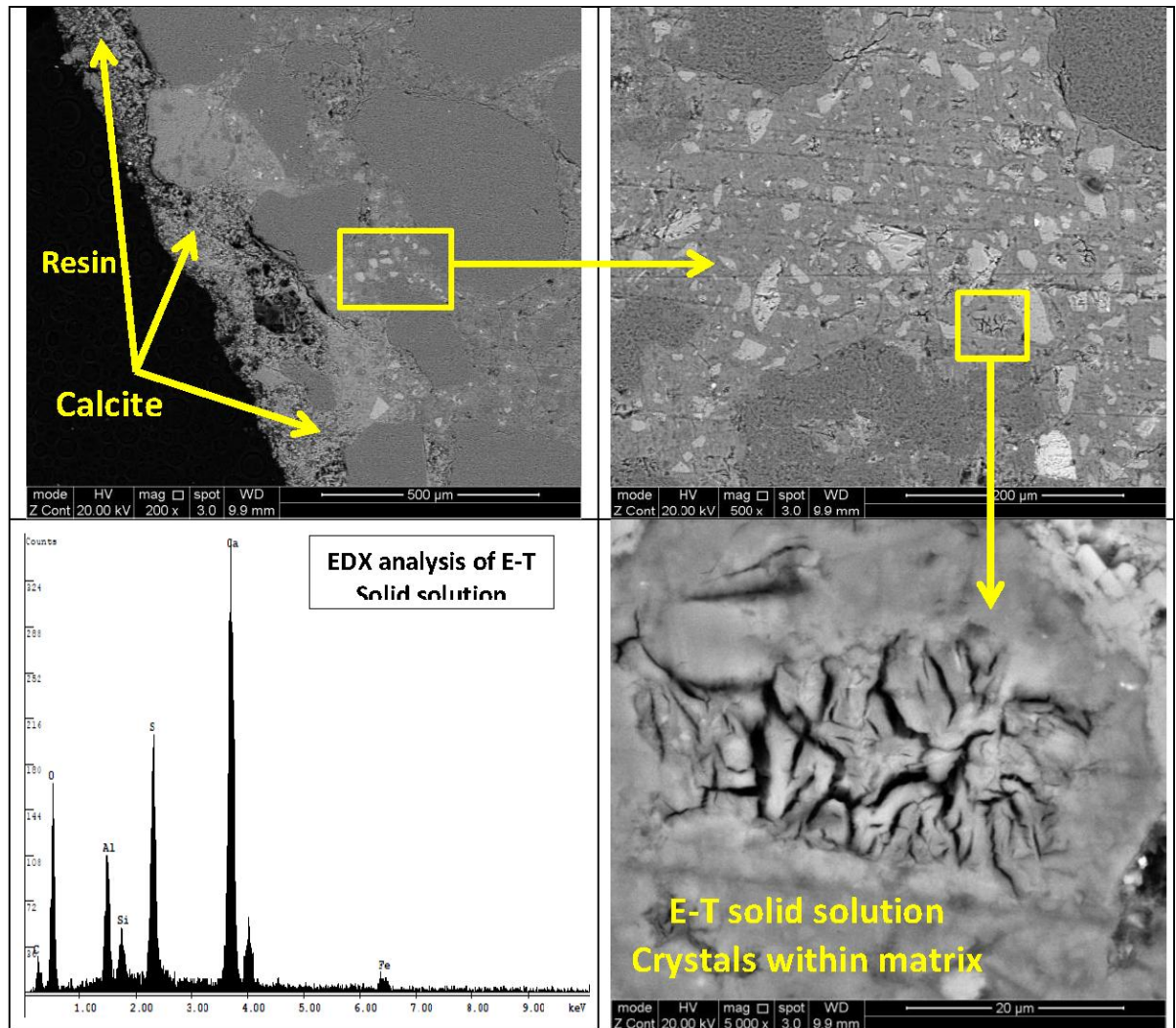


Figure 5.50 Microstructural analysis of CEMI-GGBS concrete exposed to Lower Lias Clay at 5°C.

Dissolution of calcite as bicarbonate, which is more soluble at pH below 10.33 (Collet, 2004), would deliver the source of carbonate to the reaction zone close to the intact layer of cement paste where the pH of clay is between 7 and 7.5; this would supply sufficient carbonate and bicarbonate ions to initiate a thaumasite formation, unlike exposure to sulfate solution. The presence of small amounts of sulfate and aluminum in the CSH structure may indicate the ability of pozzolanic CSH to incorporate external ions within its structure.

Gollop and Taylor (1996) stated that high GGBS levels increase the silica/calcium ratio of CSH, which results in more aluminum being bound up in the CSH and unavailable to form ettringite. Furthermore, the presence of a high concentration of bicarbonate ions in the clay pore solution influences the stability of ettringite, which might reduce its formation. In addition, the MCSH phase was not detected in the GGBS concrete matrix exposed to clays. This is attributed to the lower magnesium concentration available in the clay pore solution which would attack CSH and form the MCSH phase.

Overall, GGBS concrete was found to be less susceptible to all kinds of sulfate attack. As discussed previously, the lower cement content in such mixes reduces its susceptibility to TSA. Investigations carried out by Nobst and Stark (2003) reported that the susceptibility of cements to thaumasite formation is proportional to  $C_3A$  and  $Al_2O_3$  content. However, thaumasite was observed in their investigations on CEM III-B and -C cements containing more than 66% GGBS. It should be noted that these authors used ground cement pastes mixed with gypsum, calcite and water. Therefore, it might be postulated that the sulfate resistance of cement with a high slag content is due to restricting the ingress of sulfate by enhanced physical properties due to its low permeability. Lawrence (1992) noted that GGBS concretes suffered from disintegration and softening, rather than from expansion and cracking, because of the relative absence of ettringite from the system as the formation of ettringite in this condition would seem not to be predominant, which is the case in this investigation. In the case of exposure to magnesium sulfate solution, it seems that the formation of MCSH, which is a less complex compound, competes with the formation of thaumasite; as a result, TSA in GGBS concrete will not be the cause of damage, as reported by Pouya (2007). Instead, the disintegration of CSH gel and formation of non-hydraulic MSH will dominate the deterioration reactions.

However, in the case of exposure of pyritic clays where all conditions for thaumasite formation, such as a source of carbonate, sulfate, calcium and silicate, are available, GGBS is susceptible to thaumasite formation, and would worsen the performance of this type of binder in resisting TSA in long-term exposure. Therefore, from the engineering point of view, none of the pozzolanic cement replacements alone could provide total protection against thaumasite or conventional sulfate attack, particularly in buried concrete interacting with aggressive ground conditions.

## 5.7 Summary

The key findings of investigations into the durability of concrete exposed to different sulfate solutions, clays and simulated clay pore solutions at 5° and 20°C for 24 months, in terms of the thaumasite form of sulfate attack, are presented in this section. The types of concrete covered are CEMI, CEMI-10%LF, CEMI-50%PFA and CEMI-70%GGBS. An extensive search of the literature revealed very few studies into the interaction between buried concrete and pyrite-rich clays. It would appear that only one field investigation has yet been carried out to assess the performance of buried concrete, which was reported by Crammond et al. (2003). The recommendations contained in BRE SD1 (2005) and similar standards are based upon laboratory studies involving the immersion of concrete specimens in test sulfate solutions, which might be magnesium sulfate or sodium sulfate or a combination of both. Therefore, the study appears to be the first laboratory investigation to describe TSA deterioration in buried concrete in simulated field conditions. Accordingly, the influence of the chemical composition of clay on the extent of severity of the thaumasite form of sulfate attack at low and high temperature was evaluated in terms of visual observation, mineralogy of deteriorated materials and changes in concrete microstructure. The following conclusions can be drawn from the results:

- Signs of attack were observed in CEMI concrete cubes exposed to clays at both temperatures and were more severe in weathered and slightly weathered LLC than Coal Measures mudstone, whereas deterioration appeared only in concrete exposed to Lower Lias Clay in the presence of mobile groundwater at 5°C. However, in the case of exposure to solutions, signs of attack were observed in CEMI exposed to DS-4 sulfate solution and simulated clay pore solutions at 5°C and the deterioration was significant in concrete placed in simulated solutions.
- Intensive damage was found in CEMI-LF concrete; it was severe in the case of exposure to Lower Lias Clay at both temperatures, followed by specimens placed in DS-4 sulfate solutions and Coal Measures mudstone. In addition, deterioration was also observed in concrete columns interacting with LLC in the presence of mobile groundwater. However, no signs of deterioration were detected in cubes exposed to DS-2 sulfate solutions and Coal Measures mudstone in the presence of mobile groundwater. On the other hand, specimens placed in simulated clay pore solutions also showed deterioration but less than in pyritic clay.

- Replacement with 50% PFA and 70% GGBS revealed very good performance, as no deterioration was observed in all exposure conditions at low and high temperatures.
- The extent of attack was less in the case of exposure to Lower Lias Clays in the presence of mobile groundwater than in cubes buried without simulating mobile groundwater. In addition, the deterioration was more severe in weathered Lower Lias Clay, where more water-soluble sulfate was available and was transported into concrete by the groundwater. On the other hand, less deterioration was observed in slightly weathered Lower Lias Clay and Coal Measures Clay, in which less water-soluble sulfate and a high pyrite content are available. This might be due to the effect of mobile groundwater on the process of the oxidation of pyrite, as well as an incomplete neutralisation reaction of acid with carbonate available in clay to produce gypsum.
- The mode of deterioration of disintegrated concrete was different in all cases of exposure. Deterioration commenced in the edges and corners and was accompanied by cracks and spalling in the corners in the case of DS-4 sulfate solution and simulated clay pore solutions, while in Lower Lias Clay most of the concrete faces deteriorated and were converted to white mushy material, which implies that different routes of deterioration due to TSA occurred.
- The severity of deterioration regarding concrete type decreased as follows: CEMI-LF > CEMI > CEMI-PFA = CEMI-GGBS.
- The degree of deterioration of concrete exposed to various conditions decreased as follows: SW-LLC > W-LLC > DS-4 > CM mudstone > simulated solutions > DS-2. The degree of deterioration was less at a temperature of 20°C in all cases
- Maximum pH was observed in DS-4 after deterioration started. However, the pH of DS-2 sulfate solution was higher than that in DS-4 sulfate solution at an early age of exposure to all concrete types. This might be due to the brucite layer which was formed in DS-4 solution.
- In pyritic clays the pH value was found to be almost neutral; a maximum pH of 7.37 in weathered LLC was recorded after 24 months and in some cases pH was below 7. This is attributed to the presence of pyrite, which produces more acid, in the composition of



clay, as well as the presence of bicarbonate and carbonic acid in clay pore solutions due to the dissolution of calcite and the dissolving of CO<sub>2</sub> in water.

- In the case of exposure to clay, pH plays an important role in the extent of attack, as a low-pH environment results in destabilisation of CSH. This, together with the availability of sulfate and carbonate species in the clay, increases the propensity for the formation of thaumasite.
- With regard to the relation between increasing pH measurements and deterioration, pH values increased after 9 months in the case of DS-4 and after 6 months in the case of both pyritic clay and simulated clay pore solutions. This implies that the signs of attack due to TSA appeared after 9 months in the case of sulfate solutions and after 6 months in pyritic clays.
- Values of pH of sulfate solutions and simulated clay pore solutions in interaction with different concretes increased in the order CEMI-LF > CEMI > CEMI-PFA > CEMI-GGBS.
- XRD, IR and SEM analysis of deterioration products of CEMI and CEMI-LF replacement revealed that degradation was solely due to TSA at both temperatures in case of interaction with clays, while in DS-4 sulfate and simulated clay pore solutions, thaumasite along with ettringite and gypsum was the main deterioration product at 5°C. However, ettringite and gypsum were formed in DS-2 solution at both temperatures.
- In the case of exposure to clays, gypsum and ettringite were absent in the XRD patterns, IR and SEM images, which emphasises the fact that sulfate was engaged in the formation of thaumasite rather than gypsum and ettringite.
- Thaumasite solid solution was detected in the case of PFA and GGBS concrete exposed to pyritic clay at 5°C in XRD analysis, confirmed by SEM analysis, as needles of thaumasite solid solution were clearly found in the examined sample. This implies the susceptibility to TSA of those concretes that interacted with aggressive clays with long-term exposure. It is thought that the low permeability of those concretes is the main reason for the delay of deterioration, as low sulfate and carbonate ions would ingress

into concrete and precipitate more thaumasite in air voids to commence the disintegration of the concrete matrix.

- Gypsum was observed in GGBS concrete exposed to Coal Measures mudstone in which more aluminate involved in the formation of Friedel's salt and sulfate consumed in the reaction of gypsum and thaumasite solid solution.
- Friedel's salt was identified in all concretes exposed to Coal Measures Clay, due to the presence of a higher chloride concentration in CM mudstone in comparison to other exposure conditions.
- Using simulated clay pore solutions does not represent the actual conditions for clays; this was obvious from the analysis of XRD results, which suggested that the complex continued reactions in the aggressive clays used in the investigation lead to the differences in the deterioration products produced during the attack, which give them a unique mechanism of deterioration compared to sulfate and simulated solutions.
- It is suggested that there are two different routes for thaumasite formation and TSA. This was obvious from the difference in the deterioration products, among which only thaumasite was formed in concrete exposed to aggressive clays, while thaumasite along with gypsum and ettringite was identified in the case of exposure to sulfate solutions.
- The general findings revealed that, although Lower Lias Clay has water-soluble sulfates corresponding to the BRE sulfate class DS-2, concrete exposed to LLC with sulfate design class DS-2 deteriorated at a faster rate than corresponding specimens in DS-2 solution and at a similar rate to or faster than those exposed to the DS-4 sulfate solution at 5°C. This suggests that the aggressivity of clay and resulting concrete deterioration could exceed what might be observed in concrete exposed to equivalent standard test solutions, while the observations and mineralogical analysis provide further confirmation of the vulnerability of buried concrete to TSA.
- Based on the above, it would appear that clay composition which results in relatively low pH plays an important role in thaumasite formation and the severity of thaumasite sulfate attack. The attack may be enhanced by chemical reactions that occur during pyrite oxidation processes, which are absent in standard test solutions. In addition, the

presence of a high carbonate content in the form of calcite is considered to be the source of carbonate and bicarbonate ions required for thaumasite formation and TSA.

- Phases formed within concrete can be accurately identified using XRD and SEM techniques, especially where no signs of attack were clearly observed. However, using IR techniques might not give a clear analysis of all minerals formed. This might be due to the small size of the sample examined in IR analysis, 2 mg, which might not represent the change in the concrete matrix.

## CHAPTER 6

### 6. Changes in Clay and Ground water Chemistry During interaction with Concrete.

#### 6.1 Introduction

The change in sulfate content reported by Floyd et al. (2003) is attributed to the oxidation of pyrite within the soil, which in mudrocks such as the Lower Lias Clay can account for up to 5% of the sample mass, as reported by Czerewko et al. (2003). Aqueous, acidic, sulfate-rich solutions are produced. Reactions of these with other materials such as calcite or concrete produce sulfate minerals, the most common of which is gypsum. The solubility of gypsum is limited to 1.4 g/l  $\text{SO}_4$  and therefore it readily precipitates to form white patches of gypsum, observed within the weathered clay. Therefore, the weathering of pyrite might affect the buried concrete because of the change in the chemistry of the surrounding clay and chemical interaction at the concrete–clay interface.

**This chapter** presents the results of test designed to investigate the interaction between concrete and clays of different composition at 5 and 20°C. As explained in Chapter 3 tests were performed on weathered Lower Lias Clay (W-LLC), slightly weathered Lower Lias Clay (SW-LLC) and Coal Measures mudstone (CM) for twelve months at 5° and 20°C. The effect of mobile groundwater on changes in chemistry and the oxidation of pyrite in different clays in different exposure conditions were also investigated. The results presented include the assessment of changes in chemistry of pore solutions of clays that simulate groundwater at different burial depths. Therefore, two different sets of samples were investigated. The first set considered mobile groundwater by circulating water in tanks where concrete columns were immersed in clay, whereas in the second set, concrete cubes were placed in boxes containing clay. More details on the experimental design, methodology and characterisation of clays as well as the test method are reported in Chapter 3. The evaluations for clay were made by measuring changes in pH, water- and acid-soluble sulfate, total sulfur, pyrite oxidation, carbonate content and microstructure, while evaluations in groundwater were made by measuring the change in pH and water soluble  $\text{SO}_4$ , Ca, Mg, K, Na and Cl.

## 6.2 Changes in the chemistry of clay

The following sections detail the results of **changes in selected chemical aspects of the Lower Lias Clay** and Coal Measures mudstone after 12 months of interaction with different concrete types at 5° and 20°C in the presence and absence of the mobile groundwater. The evaluations for clay were made by measuring changes in pH, water- and acid-soluble sulfate, total sulfur, pyrite oxidation and carbonate content. Microstructural alterations of different clays were also evaluated.

### 6.2.1 Changes in pH

Tables 6.1 and 6.2 summarise the pH results over twelve months for different clays in different exposure conditions. The pH value of W-LLC was 7.8 before exposure to concretes. However, it decreased slightly to 7.41 during the experiment in the presence of mobile groundwater at 5°C, while a reduction in pH value to 7.2 and 7.12 was recorded in the absence of mobile groundwater at 5° and 20°C respectively. In addition, it was noticed that pH reached a maximum value at 9 months in the case of exposure to CEMI and at 6 months in case of exposure to CEMI-LF concretes at 5°C. Similar observations were made for SW-LLC.

Table 6.1 Changes in pH in the presence of mobile groundwater at 5°C

Clay Type	Concrete type	pH				
		Initial	3	6	9	12
W-LLC	CEMI	7.8	7.33	7.38	7.5	7.48
	CEMI-LF	7.8	7.45	7.78	7.5	7.51
	CEMI-PFA	7.8	6.88	6.93	7	7.21
	CEMI-GGBS	7.8	7.48	7.23	7.37	7.33
SW-LLC	CEMI	8.1	7.31	7.35	7.37	7.15
	CEMI-LF	8.1	7.24	7.4	7.36	7.24
	CEMI-PFA	8.1	7.28	7.32	7.27	6.97
	CEMI-GGBS	8.1	7.27	7.31	7.24	6.91
CM	CEMI	7.24	7.21	7.08	7.14	6.85
	CEMI-LF	7.24	7.18	6.94	7.04	6.99
	CEMI-PFA	7.24	6.79	6.72	6.85	6.79
	CEMI-GGBS	7.24	7.08	7.01	6.93	6.71

Table 6.2 Changes in pH in the absence of mobile groundwater at 5 and 20 °C

Clay Type	Concrete type	T, °C	pH					
			Initial	3	6	9	12	
W-LLC	CEMI	5	7.8	7.54	7.52	7.73	7.2	
		20	7.8	7.35	7.18	7.28	7.53	
	CEMI-LF	5	7.8	7.54	7.94	7.73	7.65	
		20	7.8	7.42	7.52	7.68	7.46	
	CEMI-PFA	5	7.8	7.58	7.40	7.32	7.24	
		20	7.8	7.43	7.31	7.19	7.17	
	CEMI-GGBS	5	7.8	7.48	7.38	7.27	7.17	
		20	7.8	7.4	7.31	7.22	7.12	
	SW-LLC	CEMI	5	8.1	7.46	7.47	7.54	7.48
			20	8.1	7.30	7.28	7.18	7.39
		CEMI-LF	5	8.1	7.45	7.70	7.56	7.60
			20	8.1	7.38	7.30	7.43	7.30
CEMI-PFA		5	8.1	7.54	7.36	7.23	7.10	
		20	8.1	7.53	7.40	7.28	6.97	
CEMI-GGBS		5	8.1	7.42	7.31	7.2	7.09	
		20	8.1	7.32	7.23	7.14	7.05	
CM		CEMI	5	7.24	7.18	7.09	6.99	6.93
			20	7.24	7.10	6.98	6.89	6.86
		CEMI-LF	5	7.24	7.16	7.10	7.2	7.18
			20	7.24	7.09	6.95	6.88	7.06
	CEMI-PFA	5	7.24	7.21	7.13	7.01	6.92	
		20	7.24	7.20	7.10	6.97	6.88	
	CEMI-GGBS	5	7.24	7.15	7.12	6.98	6.98	
		20	7.24	7.10	7.03	6.95	6.91	

The initial pH of SW-LLC was 8.1 and then reduced to 7.15 after 12 months of exposure to CEM I in the presence of mobile groundwater at 5°C, while the pH decreased to 7.1 and 6.97 at 5° and 20°C respectively in the absence of mobile water.

In Coal Measures mudstone, the initial pH was 7.24. There was a slight decrease in pH in the case of interaction with CEMI and CEMI-LF concretes. In addition, a slight decrease was also recorded where exposure to PFA and GGBS concrete, where the pH reached 6.79 and 6.71 for PFA and GGBS concretes respectively. The continuation of the pH reduction was observed in CM mudstone in contact with different concretes except CEMI-LF, which pH increased at 9 and 12 months in case of 5 and 20°C respectively.

Overall comparison of pH values of different clays revealed that they remained neutral with values between 7.05 and 7.94, except in a few samples in which the pH was slightly lower

than 7.0, which suggests that there was pyrite in regions in which calcite was absent or inaccessible. The reduction in the pH values of clays were ordered as follows: SW-LLC > W-LLC > CM mudstone. This might be due to the large amount of pyrite in SW-LLC and CM compared to W-LLC, resulting in production of more sulfuric acid. This would be buffered by calcium carbonate, clay minerals and calcium hydroxide from concrete in the interface region in the clay, which was reported by Czerewko and Cripps (2006) and Floyd et al. (2003) to have kept clay pH neutral in field observation in Gloucestershire, UK. In addition, the presence of bicarbonate and weak carbonic acid would also result in reduction of clay pH with age as carbonic acid and bicarbonate ions would be produced over time. On the other hand, the comparison showed that pH values at 20°C were slightly less than those at 5°C. This might be due to an increase in the rate of pyrite oxidation at 20°C, which would result in more acid, as reported by Czerewko and Cripps (2006). However, the slight reduction in pH of Coal Measures mudstone might be a result of the presence of a moderate concentration of sodium in its composition, which mitigates the reduction in pH due to the acid generated by pyrite oxidation. In addition, the pH measurements of SW-LLC and Cm mudstone in case of presence of mobile groundwater was slightly less than that in case of absences of groundwater, suggests that the acid-buffering reaction was incomplete in the presence of mobile groundwater.

The increase in pH values in the case of interaction with concrete revealed that more calcium hydroxide and other alkaline species such as K and Na were leached from concrete as signs of deterioration appeared in CEM I and CEM I-LF concretes. However, lower pH readings were observed in the case of interaction with PFA and GGBS concrete because of the high replacement values, 50% and 70% respectively so less hydroxyl was available. Furthermore, PFA and GGBS replacement reduce the permeability of the concrete. Therefore, fewer alkaline species would be leached from concrete. CEMI and CEMI-LF concretes suffered from TSA at the concrete–clay interface. This is in spite of the neutral pH of the interfacial clay. The explanation for the presence of thaumasite in near-neutral pH conditions, as discussed in Section 4.3.1, in which high pH at the concrete–clay interface might be leads to the formation of thaumasite, or that the neutral pH leads to decalcification of CSH, resulting in the formation of extensive thaumasite in the presence of sufficient sulfate and carbonate.

### **6.2.2 Water-soluble sulfate**

The variation in the concentration of water-soluble sulfate in the different clays up to 12 months is illustrated in Figures 6.1 to 6.3. The initial concentration of water-soluble sulfate was 2450, 1366 and 160.9 mg/l for W-LLC, SW-LLC and CM mudstone respectively. The concentration of water-soluble sulfate of W-LLC and SW-LLC clays decreased significantly



in the presence of the mobile groundwater at 3 months and then increased slightly after 9 months of exposure. However, the concentration of sulfate was much lower than the initial measurements. This implies that more soluble sulfate was leached into simulated groundwater. On the other hand, the water-soluble sulfate increased slightly with time in the case of CM mudstone, in which lower gypsum was presented before exposure. It is suggested that further gypsum was formed from the acid buffering reaction and dissolved in simulated groundwater. In addition, it was surprising that slight differences were noticed in the measurements of sulfate concentration in CM mudstone in contact with different concretes in the presence of mobile groundwater. This might be due to that less sulfate penetrated the concretes, as no signs of deterioration were observed in any of the concretes, as described in Section 5.2. Therefore, water might become saturated with sulfate ions and this might prevent the dissolution of more gypsum into water.

The concentration of water-soluble sulfate in the absence of the mobile groundwater at 5° and 20°C was higher than that in the presence of mobile water, in all clays. The water-soluble sulfate concentration of different clays revealed that water soluble sulfate in W-LLC significantly decreased up to 3 and then increased. In addition, the increase in the amount of water soluble sulfate was moderate as W-LLC contains a small amount of pyrite. However, sulfate concentration increase with time in SW-LLC and CM mudstone and it was significantly higher than that in W-LLC, which contained more pyrite to be oxidised with the potential to generate more sulfates. This was clearly obvious in the case of CM, as water-soluble sulfate increased by more than 15 times the value before exposure. It was also found that the water-soluble sulfate was higher at 20°C than at 5°C. This could be due to the oxidation of more pyrite at 20°C than 5°C, resulting in more water-soluble sulfate being formed.

With regard to the effect of concrete on changes in the chemistry of clay, it was noticed that the water-soluble sulfate concentration of all clays exposed to different concretes increased at 3 months in the absence of mobile groundwater. However, it decreased between 3 and 9 months in the case of interaction with CEMI and CEMI with 10% LF, as shown in Figures 6.1 to 6.3. It is postulated that more sulfate entered the concrete and engaged in thaumasite formation. It was also found that the concentration of water-soluble sulfate increased at 12 months. This might be due to the saturation of the concrete pore solution with sulfate, leading to precipitation of sulfate in the clays. However, more sulfates penetrated as concretes disintegrated. In the case of clays in contact with PFA and GGBS concretes at 5° and 20°C, the amount of soluble sulfate available in different clays rose significantly and was higher than in CEM I and CEM I-LF concretes. This might be attributed to the lower

permeability and porosity of those concretes. Therefore, sulfate would be precipitated in the clay.

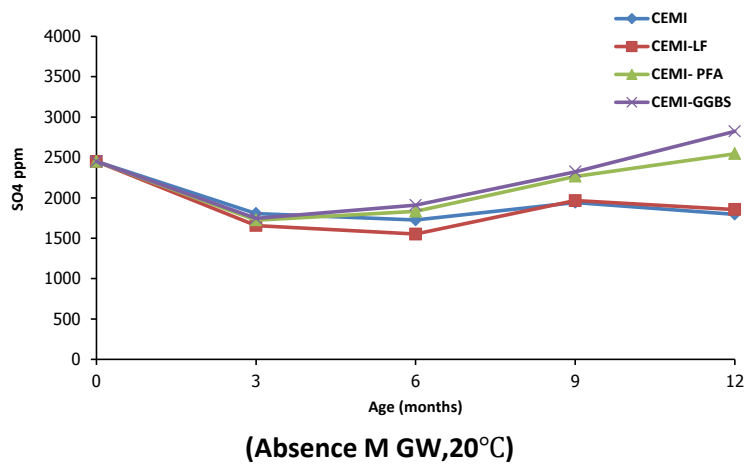
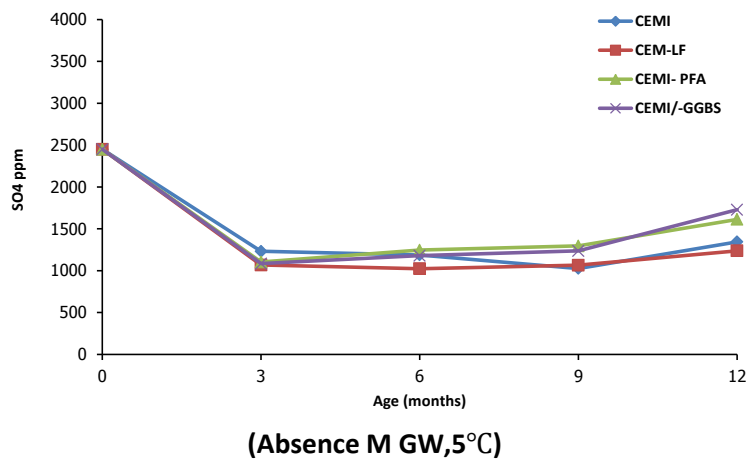
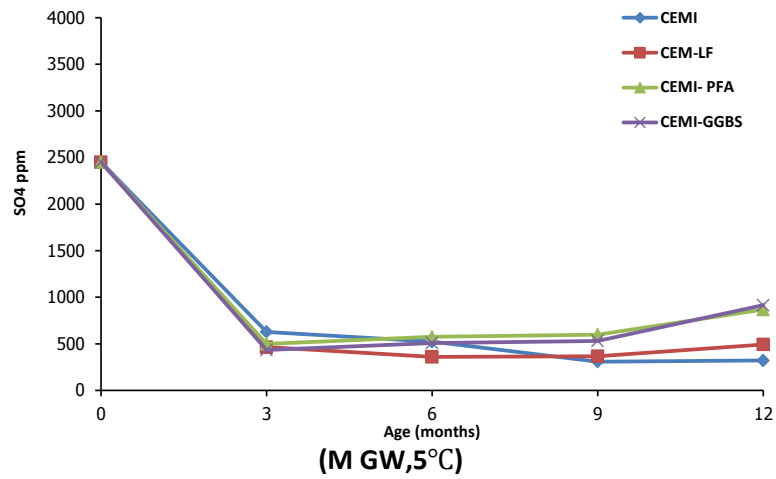


Figure 6.1 Water soluble sulfate of weathered Lower Lias Clay in different conditions

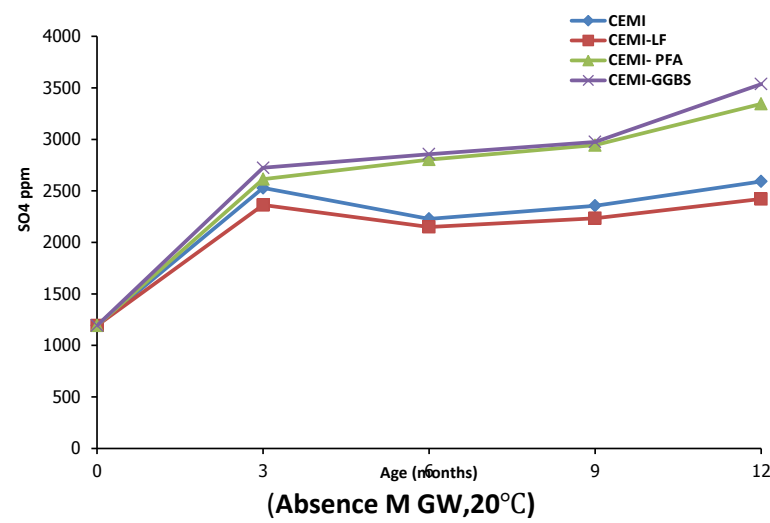
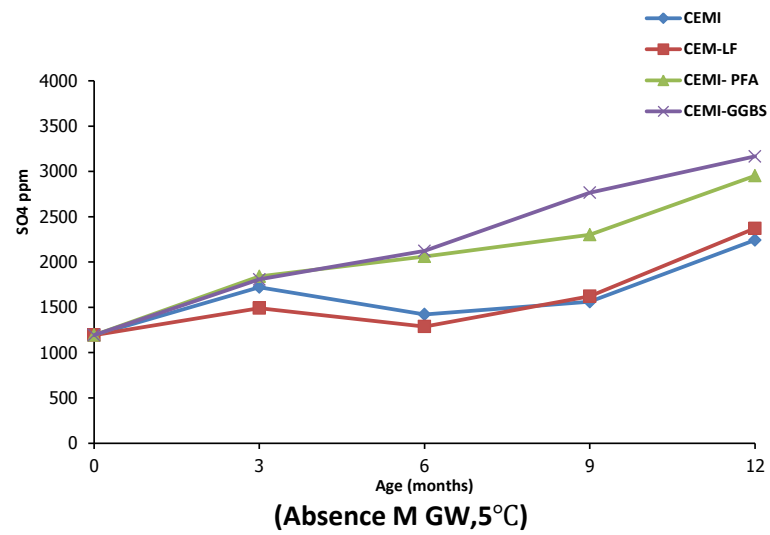
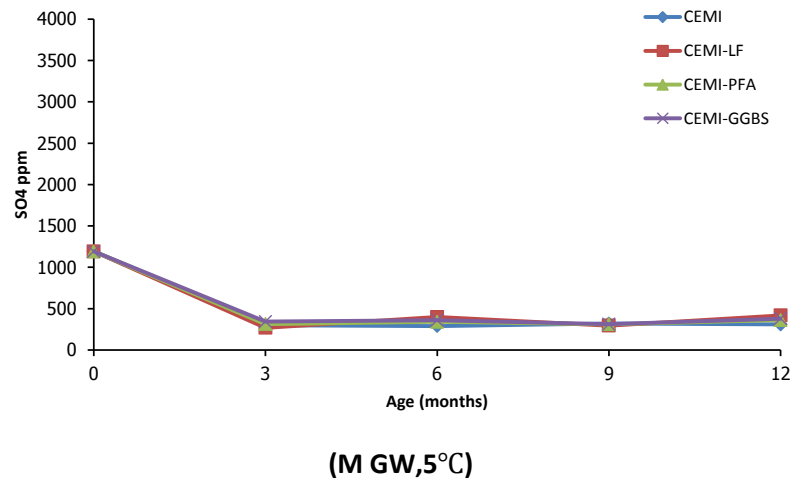


Figure 6.2 Water soluble sulfate of slightly weathered Lower Lias Clay in different conditions

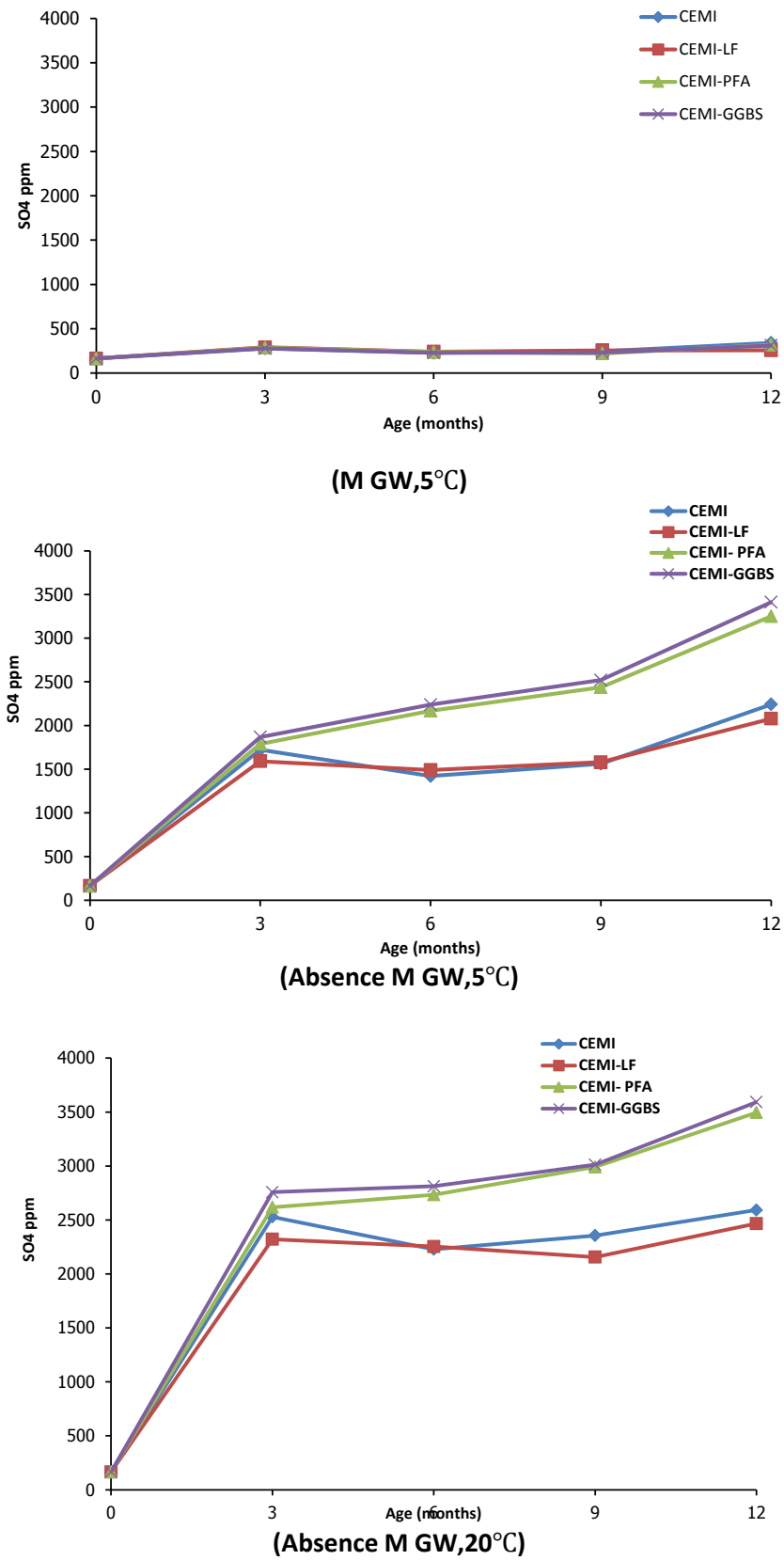


Figure 6.3 Water soluble sulfate of Coal Measures mudstone in different conditions

### **6.2.3 Acid soluble sulfate**

The variation in the acid-soluble sulfate (ASS) of different clays in different weathering conditions at 12 months is shown in Figures 6.4 to 6.6. It should be mentioned that the initial measurements of the acid-soluble sulfate before exposure were 0.82, 0.25 and 0.05 (% SO<sub>4</sub>) for W-LLC, SW-LLC and CM mudstone respectively. In mobile groundwater condition, the acid-soluble sulfate of W-LLC and SW-LLC clays was less at 3 months than in initial measurements, having decreased dramatically after exposure. ASS decreased slightly up to 9 months and then a slight increase was observed. This implies that more gypsum and water-soluble sulfate were dissolved in simulated groundwater. On the other hand, the acid-soluble sulfate increased slightly with time in the case of CM mudstone. This might be due to the formation of further gypsum from the acid buffering reaction, as less gypsum was available before exposure than in Lower Lias Clays. It might also be attributed to the fact that less sulfate penetrates the concretes, leading to precipitation of gypsum in the clay, as no signs of deterioration were observed in any of the concretes.

The acid-soluble sulfate in the absence of the simulated groundwater at 5° and 20°C was higher than mobile groundwater in all clays. The acid-soluble sulfate of different clays revealed that the increase in the amount of gypsum was lower in W-LLC than in SW-LLC and CM mudstone. It is suggested that more gypsum would form as SW-LLC and CM contain more pyrite, which oxidises and generates more sulfuric acid and is buffered by carbonate. It was also found that the concentration of acid-soluble sulfate was higher at 20°C than at 5°C. This was clearly obvious in the case of CM as acid-soluble sulfate increased by more than 25 times the value before exposure. This could be because more pyrite was oxidised at 20°C than 5°C. Generally, the acid-soluble sulfate increased with time in the case of SW-LLC and CM mudstone, while it decreased in W-LLC at 5°C up to 3 months and then gradually increased. However, a slight decrease in the acid-soluble sulfate was noticed where signs of deterioration were observed, leading to the penetration of more sulfate into deteriorated concretes.

With reference to the effect of concrete on chemical changes in clay, it was noticed that the acid-soluble sulfate of all clays was higher in the case of interaction with PFA and GGBS concretes than with CEMI and CEMI-LF concretes, as shown in Figures 6.4 to 6.6. It is postulated that in CEMI-LF and CEMI concretes more gypsum is dissolved in clay pore solution and simulated groundwater, and sulfate penetrated the concrete and engaged in thaumasite formation. However, the low permeability and porosity of PFA and GGBS would reduce the penetration of sulfate into those concretes. As a result, more acid-soluble sulfate would be precipitated and available in the clay.

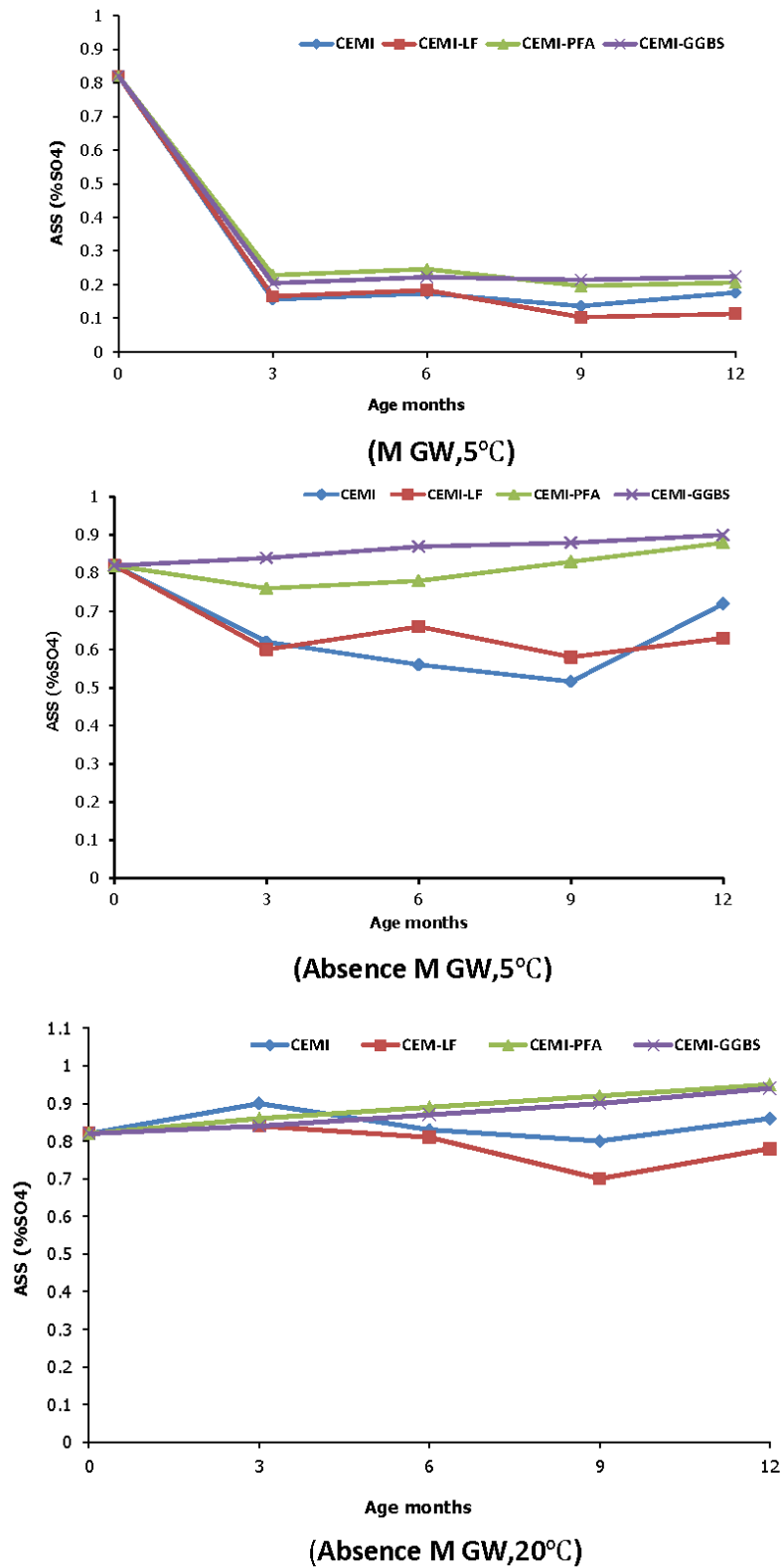


Figure 6.4 Acid soluble sulfate of weathered Lower Lias Clay in different conditions

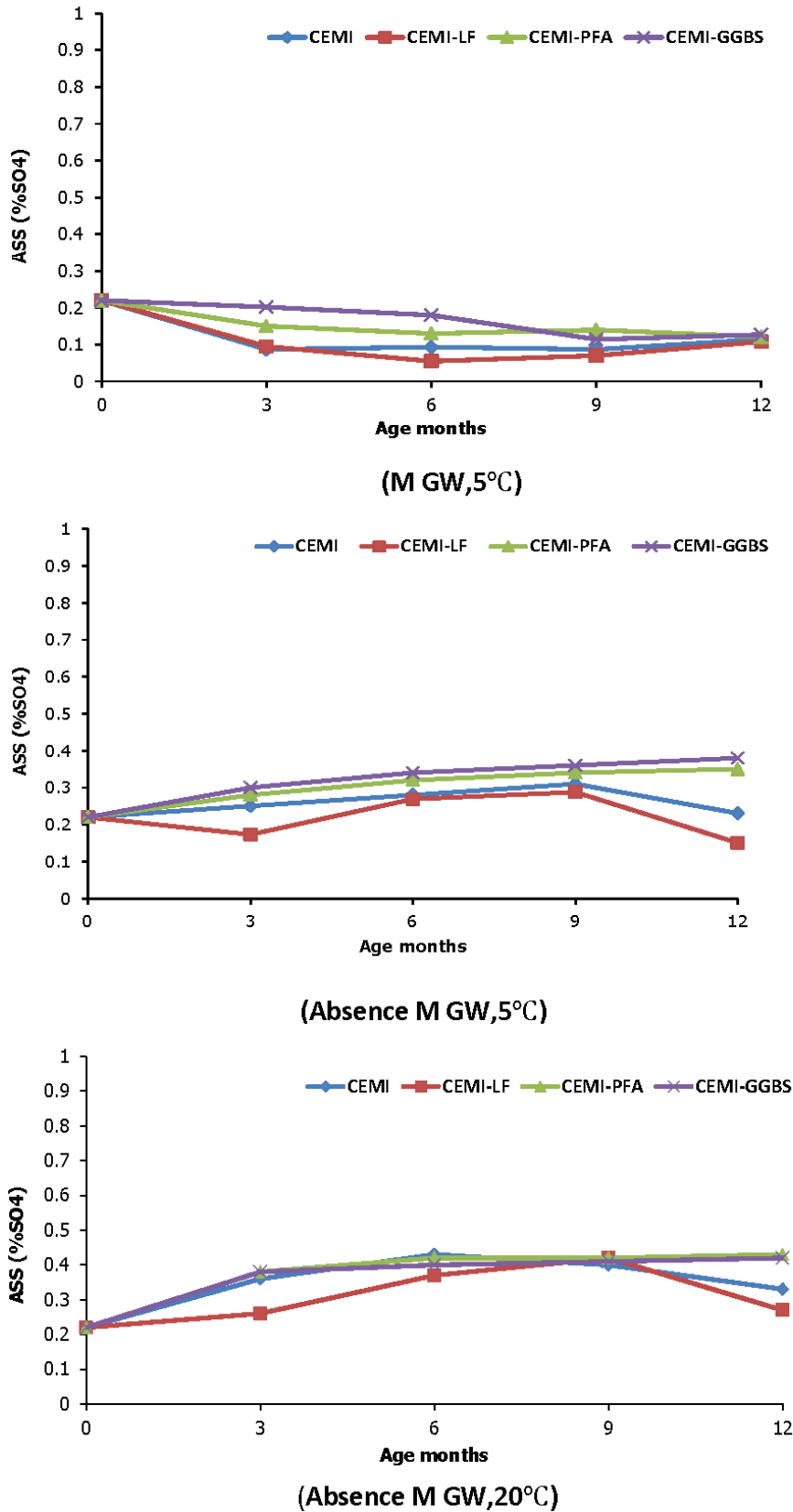


Figure 6.5 Acid soluble sulfate of slightly weathered Lower Lias Clay in different conditions



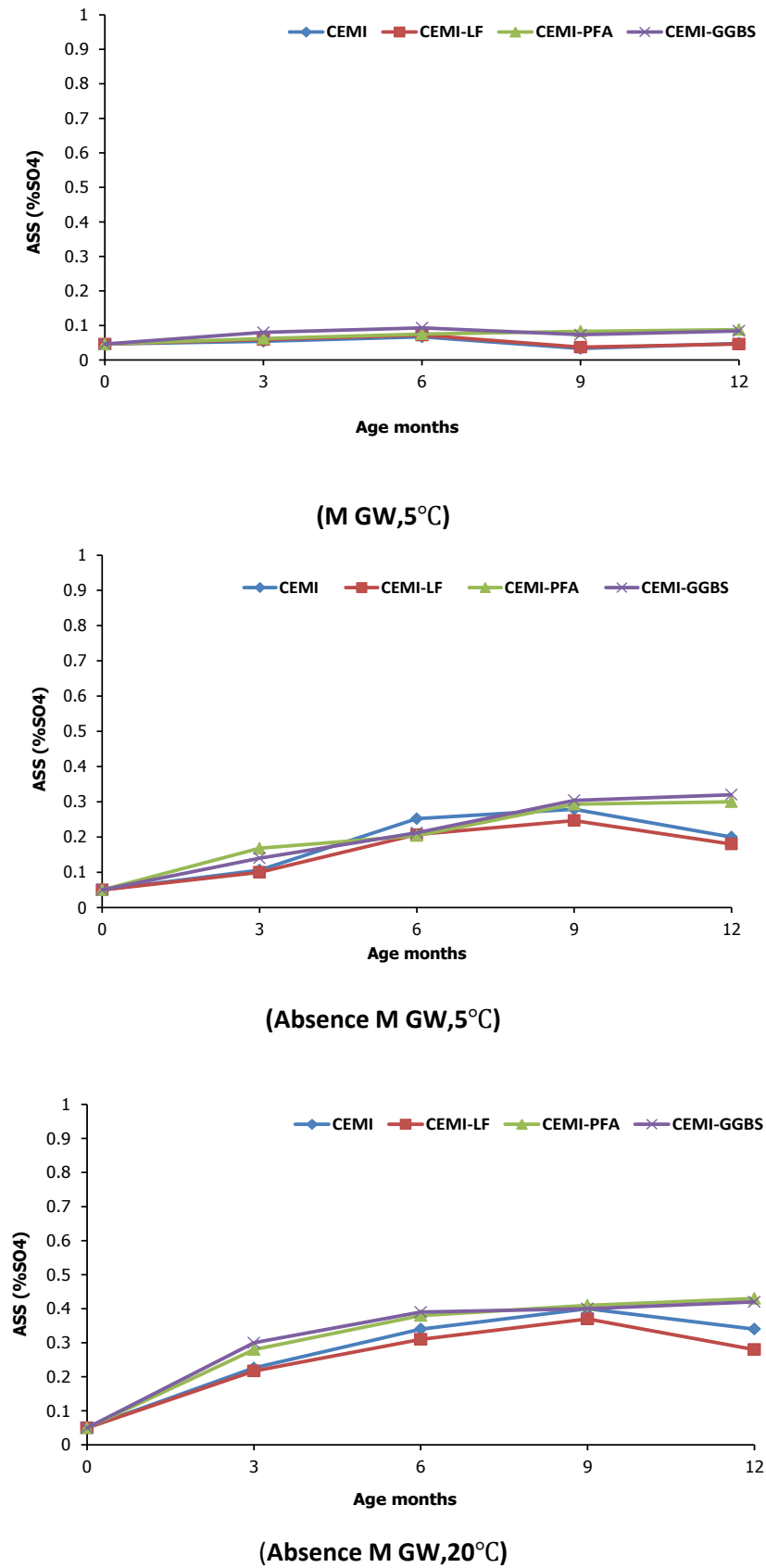


Figure 6.6 Acid soluble sulfate of Coal Measures mudstone in different conditions

#### **6.2.4 Total sulfur**

Total sulfur (TS) as described in Section 4.3.5, includes all forms of sulfur in the clay, such as epsomite, which is soluble in water, gypsum, partially soluble in water and soluble in acid, and pyrite, which is not soluble in either HCl acid or water. Figure 6.7 shows the results for total sulfur of different pyritic clays after 12 months of weathering in different conditions. The initial total sulfur of W-LLC, SW-LLC and CM mudstone was 0.6, 1.0 and 0.8 (%S) respectively. It can be seen from Figure 6.7 that the amount of total sulfur decreased gradually with time in all pyritic clays. The reduction in the total sulfur was higher for mobile groundwater. This was obvious in W-LLC, which had more gypsum than other clays. This implies that groundwater plays a role in the leaching out of water- and acid-soluble sulfate into the water, leading to a reduction in TS measurements over time. It was also found that the reduction in TS was more significant at 5°C than at 20°C. This might be because more sulfates penetrated into concretes and engaged in the deterioration reaction.

With regard to clay type, the reduction in total sulfur was ordered as follows: W-LLC > SW-LLC > CM. The maximum reductions of 0.3, 0.2 and 0.15 (%S) were recorded in W-LLC, SW-LLC and CM mudstone, as more deterioration was observed in SW-LLC and W-LLC than in CM. On the other hand, higher concentrations of Na and Cl ions in Coal Measures mudstone would penetrate into concrete and bind with the concrete matrix. This might influence the rate of sulfate penetration and lead all sulfates to precipitate in CM mudstone. Therefore, less reduction in TS would be found.

The influence of concrete type on the reduction of total sulfur was obvious, as shown in Figure 6.7. The amount of total sulfur in all clays in the case of interaction with CEMI and CEMI-LF was lower than that in the case of interaction with PFA and GGBS concretes. This may be due to the penetration of more sulfates into CEM I and CEM I-LF concretes and their participation in the formation of thaumasite, as more degradation was observed. On the other hand, the high resistance for ions penetration of PFA and GGBS concretes would lead the pore solution of clay to be saturated with sulfate, with the result that more gypsum would precipitate in clay. Because of this, the amount of total sulfur is almost constant and higher than in interaction with other concretes.

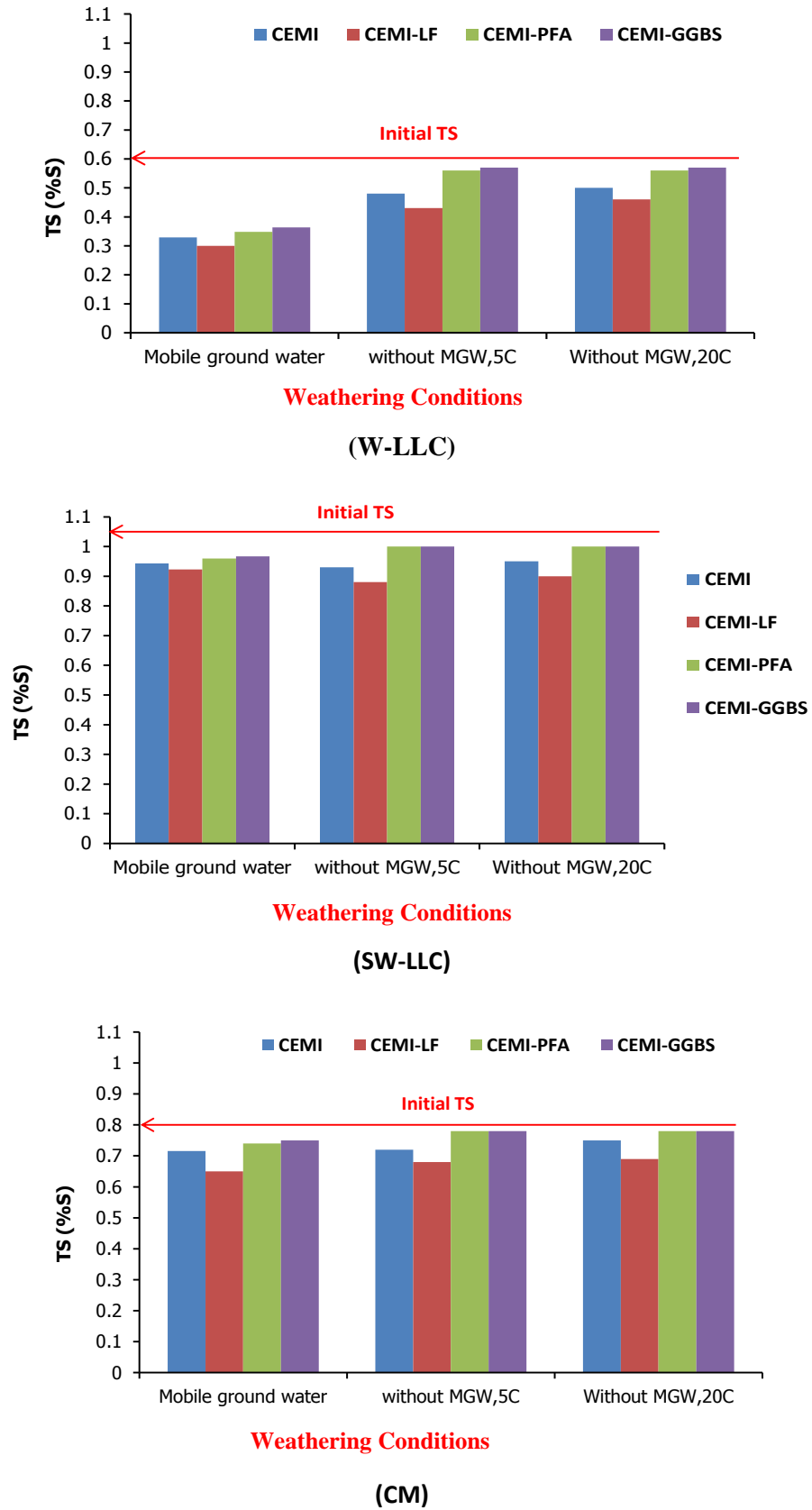


Figure 6.7 Total sulfur of different clays in different conditions after 12 months

### 6.2.5 Pyrite oxidation in different conditions

The results for the amount of oxidised pyrite in clays exposed to different conditions are presented in Table 6.3. The initial amount of pyrite in W-LLC, SW-LLC and CM mudstone before weathering was 0.6, 1.8 and 1.4 (% FeS<sub>2</sub>) respectively, so that the amount of pyrite decreased after 12 months in all clays. This was lower in the presence of the mobile groundwater than in the absence of simulated groundwater. It was also found that more pyrite was oxidised at 20°C than at 5°C. Schoonen et al. (2000) suggested that the rate of oxidation of pyrite is strongly dependent on temperature, since pyrite is thermodynamically unstable, and as the oxidation reaction is exothermal the increase in temperature leads to an increase in the rate of oxidation and catalyses the pyrite oxidation process.

Table 6.3 Pyrite oxidation in different clays in different exposure conditions

Clay Type	Concrete Type	Oxidised Pyrite (%FeS <sub>2</sub> )		
		Presence of Mobile GW 0-90 mm	Absence of Mobile GW	
		5°C	5°C	20°C
W-LLC	CEMI	0.09	0.15	0.20
	CEMI-LF	0.13	0.9	0.22
	CEMI-PFA	0.08	0.1	0.14
	CEMI-GGBS	0.06	0.09	0.12
SW-LLC	CEMI	0.12	0.21	0.24
	CEMI-LF	0.15	0.26	0.29
	CEMI-PFA	0.09	0.16	0.21
	CEMI-GGBS	0.08	0.18	0.20
CM	CEMI	0.16	0.24	0.28
	CEMI-LF	0.19	0.31	0.35
	CEMI-PFA	0.12	0.20	0.28
	CEMI-GGBS	0.11	0.21	0.25

With regard to clay type, the amount of oxidised pyrite was in the following order: CM > SW-LLC > W-LLC which maximum reductions of 0.15, 0.26 and 0.31 (%FeS<sub>2</sub>) were recorded in W-LLC, SW-LLC and CM mudstone respectively at 5°C. With reference to the influence of concrete types on pyrite oxidation, the amount of oxidised pyrite in all clays in interaction with CEM I and CEM I-LF was more than that for PFA and GGBS concretes, as shown in Table 6.3. In addition, more pyrite was oxidised where more deterioration occurred. This may be because the clay pore solution would not be saturated as more sulfate penetrated into CEM I and CEM I-LF. On the other hand, the high resistance of PFA and GGBS concretes to penetration of species derived from clay into concrete would cause the

pore solution of clay to be saturated. Therefore, it is believed that the supersaturation of the clay pore solution with sulfate ions might lead to a reduction in the rate of pyrite oxidation.

Overall, less pyrite was oxidised in the presence of the mobile groundwater. The mobility of water might lead to sulfate ions being leached into the groundwater, which might increase the rate of pyrite oxidation. However, it might result in an incomplete buffering reaction, as suggested by Czerewko and Cripps (2006). The failure to complete the buffering reaction might cause the variation of pH values within clays, and this would influence the rate of oxidation by restricting the oxidation of ferrous iron to ferric iron to oxidise more pyrite, as discussed by Calderia et al. (2003). This implies the low amount of oxidised pyrite in the presence of the mobile groundwater. On the other hand, more pyrite was oxidised in Coal Measures mudstone than in Lower Lias Clay, for which two reasons are suggested: firstly, the high amount of gypsum in weathered Lower Lias Clay might lead to the saturation of clay pore solution which would prevent more sulfate being leached from the clay, which might reduce the rate of pyrite oxidation. This was clearly seen in the results, in which more pyrite was oxidised as less gypsum was available before weathering. The second reason for the high amount of oxidised pyrite in Coal Measures mudstone is the presence of moderate concentrations of sodium and chloride, which would lead to an increase in the pH and might keep it constant. In addition, the sodium which is present might react with carbonate and form sodium carbonate, which accelerates the rate of pyrite oxidation by removal of the oxide coating produced by calcium carbonate that prevents further oxidation of pyrite, as reported by Calderia et al. (2003, 2010) and Descostes et al. (2002). Generally, as Calderia et al. (2003) and Descostes et al. (2000) report the difference between the pyrite oxidation in acidic and alkaline conditions is the precipitation of ferrous and ferric ions as pH increases. In addition, it was suggested that the formation of soluble ferrous carbonate in the presence of high concentrations of carbonate and bicarbonate ions enhances the oxidation of ferrous iron to ferric, which increases the overall rate of pyrite oxidation, even in high pH (>10) condition Overall, the compositions of clay, concrete type, saturation of the clay pore solution and temperature have a great influence on pyrite oxidation, and might control the process and rate of oxidation and even restrict oxidation.

### **6.2.6 Carbonate content**

The reduction in carbonate of the clays after 12 months of exposure are presented in Table 6.4, where the original calcite content of the clays was 30, 21.3 and 7.4 (% wt as  $\text{CaCO}_3$ ) for W-LLC, SW-LLC and CM mudstone respectively. Thus a reduction in carbonate content was noticed in all clays. With regard to exposure conditions, the reduction in calcite was lower in the presence of mobile groundwater than that in the absence of the mobile

groundwater in all clays. This might be due to incomplete acid buffering reaction by calcite as a result of water mobility. Czerewko and Cripps (2006) suggested that this may occur because of the effect of mobile groundwater. It was also found that the reduction in calcite was more significant at 20°C than at 5°C, which might be as a result of more acid was generated at 20° than at 5°C.

With regard to clay type, more calcite was consumed in the following order: CM > SW-LLC > W-LLC. This implies that more calcite would be consumed in the buffering reaction where more pyrite was oxidised, as discussed in Section 6.2.5. However, in the case of CM clay the presence of chloride in its composition might be another reason for the acceleration of the dissolution of calcite, as reported by Learson and Buswell (1984), who suggested that the solubility of calcite increases with an increase in the chloride concentration, and that maximum solubility was found in concentrations of 1 mole of NaCl.

According to Table 6.4, the amount of calcite in clays was affected by concrete type where higher consumption of calcite was observed in clays in contact with CEMI and CEM-LF than hat in PFA and GGBS concrete. As explained in Section 5.2.2, more deterioration was observed in CEMI-LF, leading to increased concrete permeability and porosity. Therefore, more carbonate ions would penetrate into concrete, which implies a higher reduction in calcite. On the other hand, the reduction in calcite was higher in the case of interaction with PFA concrete than with GGBS, although no signs of attack were observed in either concrete, which implies the susceptibility of PFA to carbonation, as explained in Section 4.3.3. With reference to the consumption of calcite in the acid buffering reaction, Table 6.4 also shows a comparison between the theoretical consumption of calcite from acid generated as a result of pyrite oxidation, and the experimental results. It can be seen that calcite consumption that theoretically calculated is lower than that measured values from the experiment in all clays. It is suggested that more calcite was dissolved in clay pore solutions and in simulated groundwater, where the solubility of calcite was increased in CM mudstone by the presence of chloride.

Table 6.4 Reductions in carbonate content in different clays in different exposure conditions

Clay	Concrete Type	Consumed Calcite					
		Presence of mobile groundwater (0-90 mm)		Absence of mobile groundwater			
		5°C		5°C		20°C	
		Experimental	Theoretical	Experimental	Theoretical	Experimental	Theoretical
W-LLC	CEMI	1.24	0.16	1.73	0.25	2.18	0.33
	CEMI-LF	1.45	0.17	2.15	0.32	2.35	0.37
	CEMI/-PFA	1.18	0.13	1.64	0.17	2.02	0.23
	CEMI-GGBS	0.95	0.09	1.36	0.15	1.95	0.2
SW-LLC	CEMI	1.31	0.19	1.87	0.35	2.05	0.4
	CEMI-LF	1.53	0.25	2.25	0.43	2.42	0.48
	CEMI/-PFA	1.16	0.15	1.69	0.27	1.78	0.35
	CEMI-GGBS	1.09	0.13	1.55	0.3	1.67	0.33
CM	CEMI	1.33	0.27	1.97	0.4	2.2	0.47
	CEMI-LF	1.35	0.33	2.1	0.52	2.35	0.58
	CEMI/-PFA	1.23	0.2	1.7	0.33	1.85	0.47
	CEMI-GGBS	1.15	0.19	1.54	0.35	1.6	0.42



In the case where more pyrite was oxidised and less calcite was consumed, the buffering reaction was not complete and therefore less calcite was consumed. The greater mobility of groundwater at a shallow depth may have led to incomplete neutralisation of acid, as suggested by Czerewko and Cripps (2006). However, in the case where more calcite is consumed and less acid is produced by pyrite oxidation, the dissolution of calcite in water is considered to be an additional factor in the consumption of more calcite. Although calcite solubility is low, it is increased by the presence of CO<sub>2</sub> and chloride. This would also be assisted at shallow burial depth by the presence of more dissolved CO<sub>2</sub>. Crammond (2003) and Torres (2004) reported that calcite was not decomposed at pH values less than 10.33, whereas the pH of the clay pore solution was in the range between 7 and 8. This might be responsible for the dissolution of more calcite.

### **6.3 Microstructural analysis of concrete**

It is difficult to recognize sulfur-bearing minerals in specimens, **even for an experienced microscopist**, especially when clay contains disseminated pyrite in the form of microscopic framboids up to 10 microns in size. Therefore, scanning electron microscopy (SEM) with energy dispersive X-ray analysis (EDX) was used in order to determine the microstructural features and morphology of sulfide minerals (pyrite). Both secondary images and backscattered images from polished sections were used for the range of different clays, namely W-LLC, SW-LLC and CM mudstone, which were weathered in different exposure conditions at 5° and 20°C. The methodology of sample preparation and the test procedures are described in Chapter 3.

#### **6.3.1 Weathered Lower Lias Clay (W-LLC)**

Figure 6.8 shows the backscattered image of W-LLC before weathering. It can be seen that the structural fabric consists of an ordered arrangement of clay minerals, predominantly illite and kaolinite. The EDX analysis shown in Figure 6.8 confirms kaolinite by the presence of Al, Si and O, while illite was confirmed by identifying Mg, K, Al, Si and O in EDX spectra. The fabric shows some clay minerals with a disordered end-face. This fabric becomes destroyed by weathering and gradually disappears as the state of weathering increases. Calcite was also identified; the relevant EDX micrograph is shown in Figure 6.8. Furthermore, framboids of pyrite were also observed, which was confirmed by EDX results. However, the pyrite surface was distorted by weathering and the progress of pyrite oxidation over time.

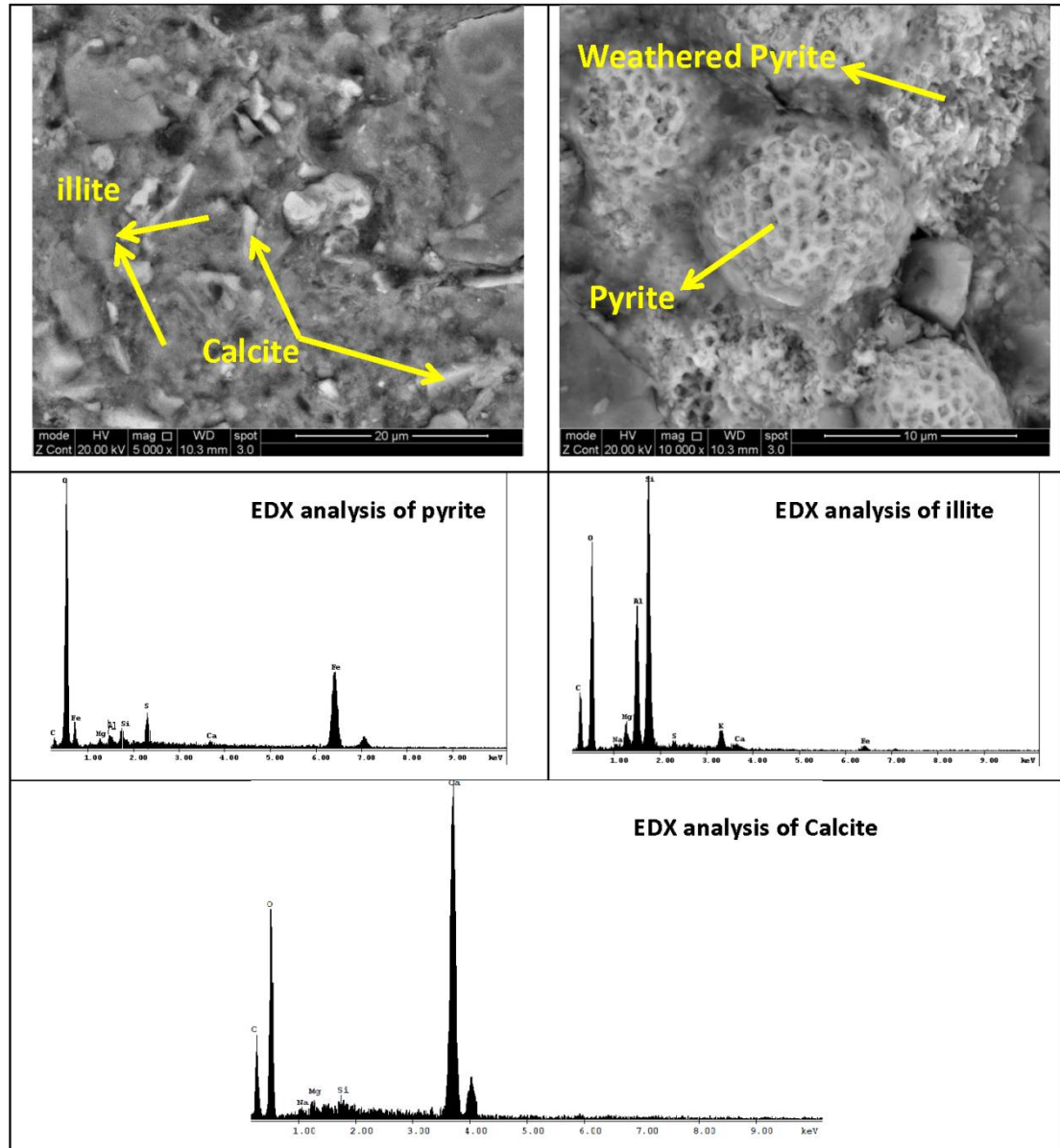


Figure 6.8 SEM analysis of W-LLC before exposure

The microstructural analysis of W-LLC after 12 months of weathering reveals the continuation of the destruction of the fabric at 5 and 20°C, as shown in Figure 6.9. It is suggested that oxidation of more pyrite generates more acid that might react with clay minerals and cause the destruction of the fabric. In addition, the fabric might disappear as the clay is weathered for a long time. It was also found that there was a change in the structure of illite and kaolinite. The attack caused by acid on clay fabric tissue led to the liberation of some cations such as Ca, Na and potassium. The reduction in the intensity of these cations after 12 months was noticed in the EDX results shown in Figure 6.9 when compared to those in Figure 6.8. Gypsum was identified in W-LLC samples in the case of immobile ground at

5° and 20°C, as shown in Figure 6.9. Pyrite was not observed after 12 months of weathering and this might be an indication of the progress of pyrite oxidation.

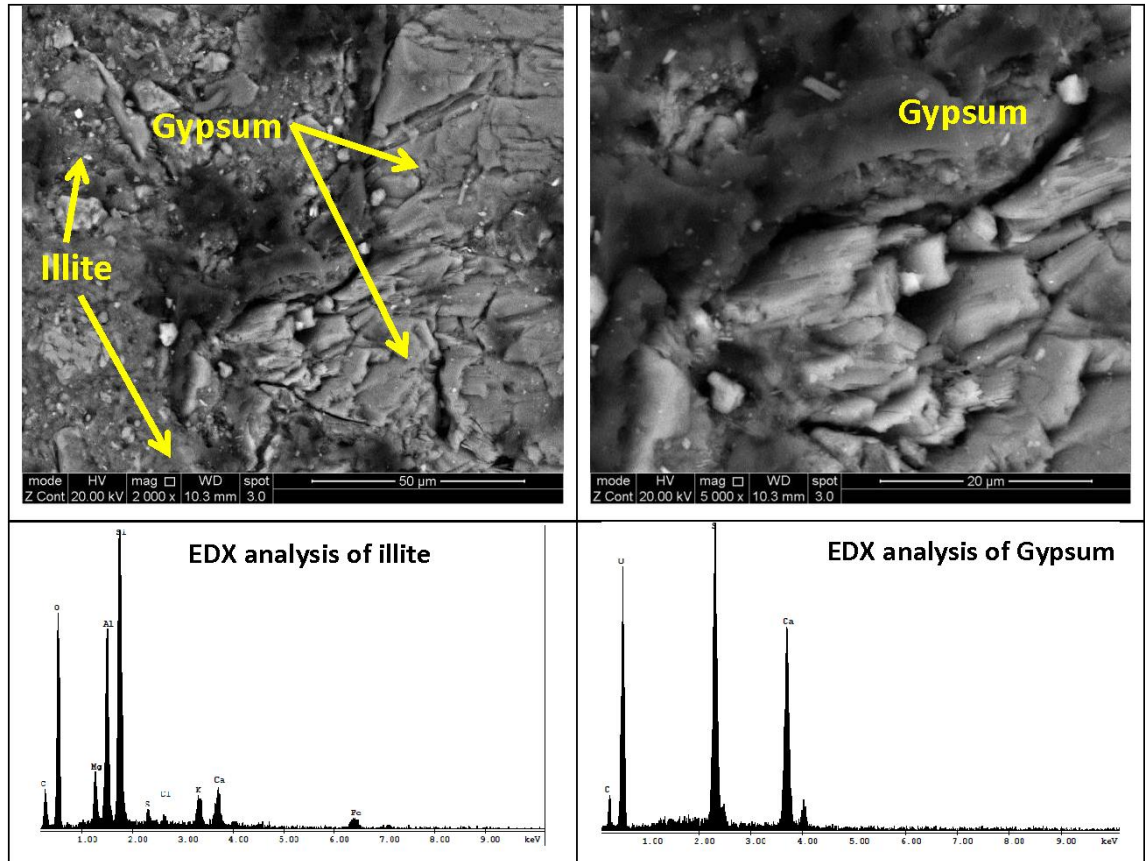


Figure 6.9 SEM analysis of W-LLC after exposure

### 6.3.2 Slightly weathered Lower Lias Clay (SW-LLC)

The microstructure of SW-LLC before weathering is shown in Figure 6.10. The layout of the phases within the clay sample was similar to that observed for W-LLC, in which illite, kaolinite and calcite were identified, as shown in the EDX analysis in Figure 6.10. In addition, the backscattered image showed the presence of pyrite, which was surrounded by calcite. However, the microstructural analysis of SW-LLC after 12 months revealed that there was alteration in the clay microstructure during weathering. This might be a consequence of the pyrite oxidation process, as explained in Section 6.3.1. It was found that gypsum appeared clearly, as shown in Figure 6.11, especially in clay samples at 20°C.

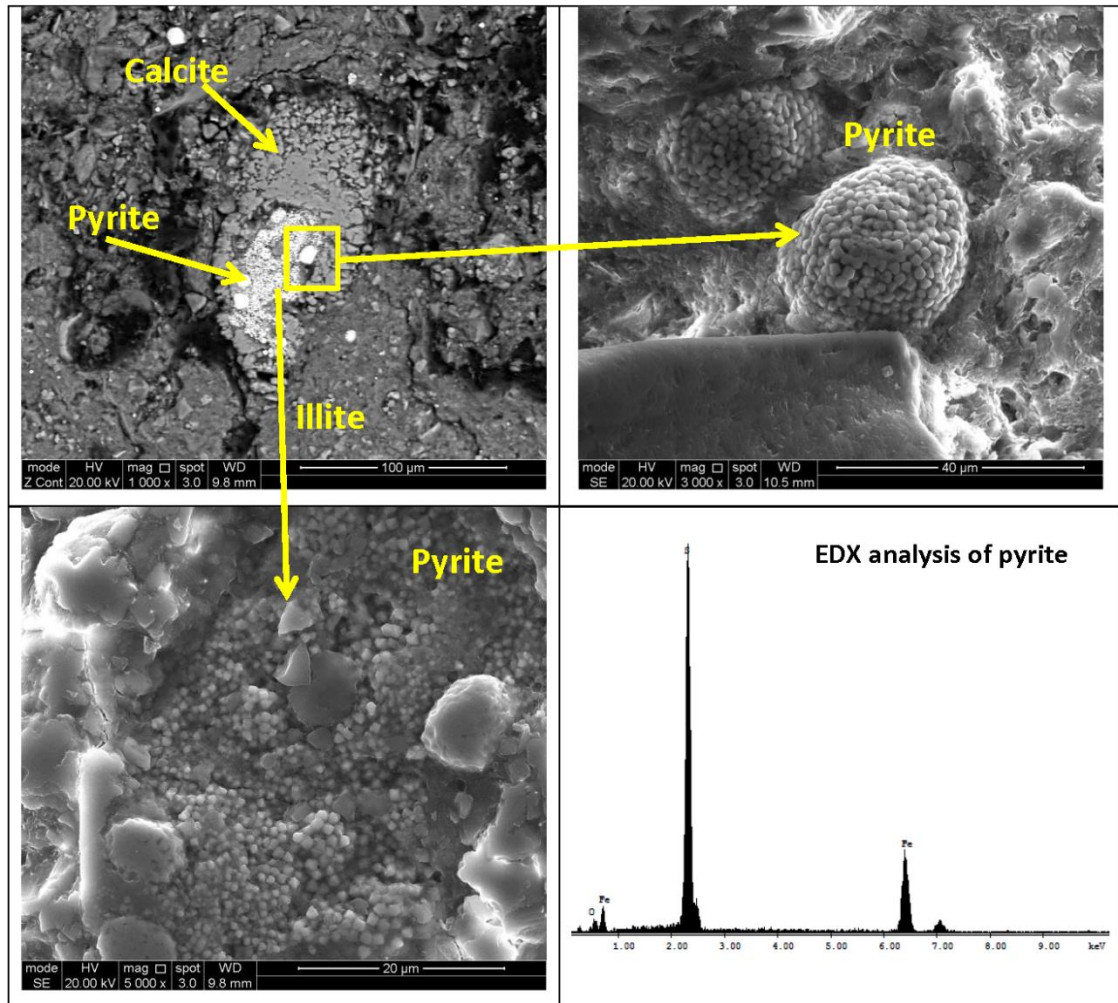


Figure 6.10 SEM analysis of SW-LLC before exposure

Moreover, more pyrite was easily identified on the backscattered image, although more pyrite was oxidised in SW-LLC, as discussed in Section 6.2.4, which confirms that SW-LLC contains a large amount of pyrite. However, some of the pyrite surface was destroyed, which suggests that an oxidation process might be in progress. Changes to clay minerals were also observed when compared to clay microstructure before exposure, as seen in Figures 6.10 and 6.11. In addition, alteration to the clay fabric also occurred, perhaps indicating engagement of clay minerals in acid buffering, as explained in Section 6.3.1. EDX analysis showed the presence of sulfur along with silica and Mg in the structure of calcite that was present around pyrite framboids, which might be due to the incompleteness of the buffering reaction with acid. On the other hand, gypsum was also observed in the back scattered image around pyrite, as shown in Figure 6.11, which implies that gypsum was formed as a result of the buffering reaction of the sulfuric acid with calcite that was present around pyrite.



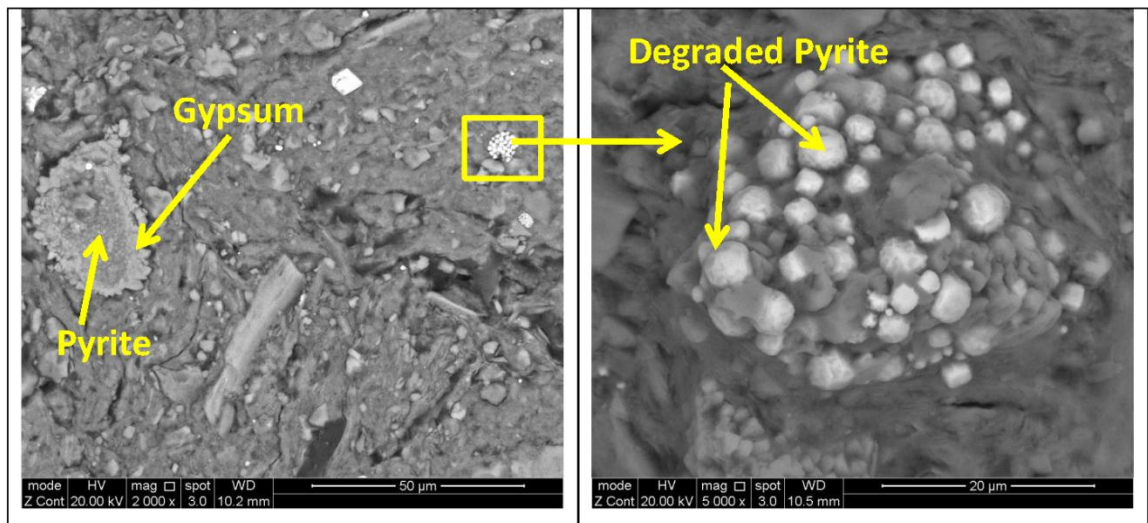


Figure 6.11 SEM analysis of SW-LLC after exposure

### 6.3.3 Coal Measures mudstone (CM)

Figure 6.12 shows the initial microstructural features of CM mudstone before exposure to different conditions. The backscattered image confirmed the presence of pyrite framboids and the structural fabric consists of an ordered arrangement of clay, which suggests that no changes occurred to the microstructure as a result of the pyrite oxidation process. EDX analysis showed the presence of different clay minerals such as illite and kaolinite, as shown in Figure 6.12 and confirmed the presence of chloride.

The microstructure changed after 12 months of exposure to different conditions is shown in Figure 6.13, which shows that weathering resulted in the reduction and alteration of pyrite and the degradation of the clay fabric. EDX analysis revealed that the structure of clay minerals was not pure as it was before weathering, as shown in Figure 6.13, which suggests some degradation of clay minerals. Replacement of mineral elements with other elements which are not in the structure of mineral composition was also detected, in particular iron and sulfur, which would be indicative of pyrite along with illite, indicated the attack of clay minerals by the pyrite oxidation process.

The backscattered image in Figure 6.13 reveals the formation of gypsum around some pyrite framboids, where there was obvious degradation of pyrite due to oxidation and the buffering reaction of acid produced during the pyrite oxidation process and calcite present around pyrite.

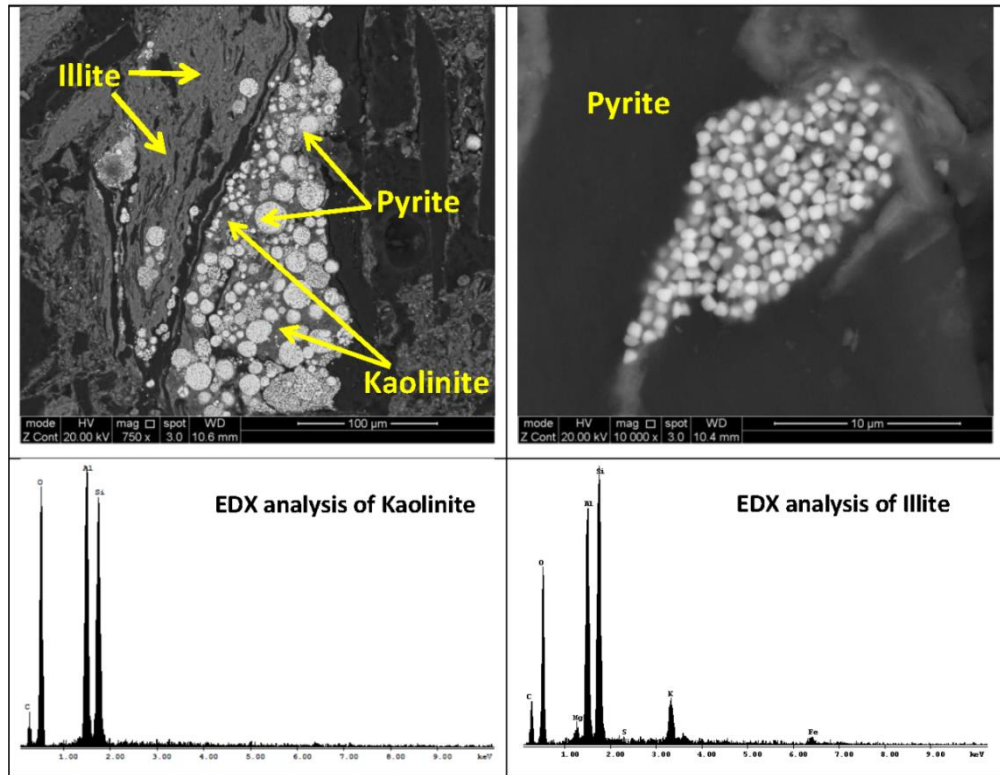


Figure 6.12 SEM analysis of CM before exposure

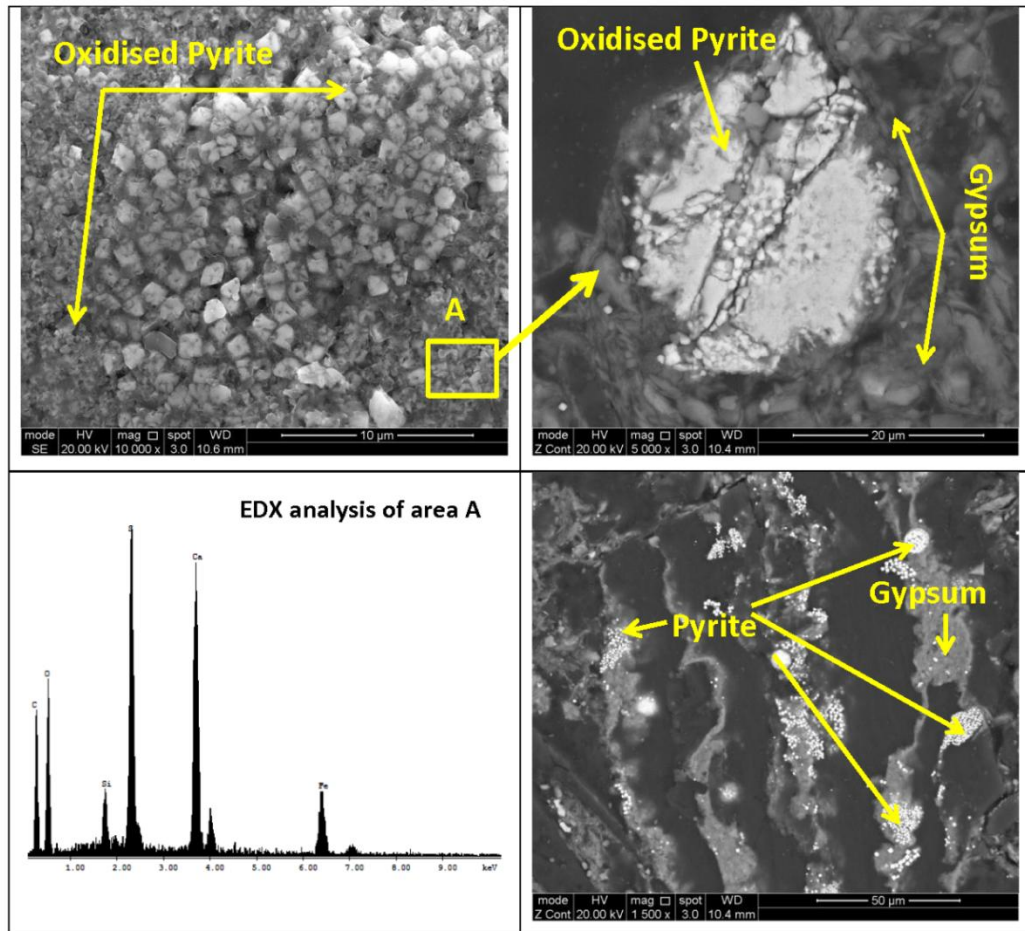


Figure 6.13 SEM analysis of CM after exposure

#### 6.4 Change in chemistry of simulated groundwater

This section presents the analysis of chemical change in simulated groundwater in the large-scale experiment (Series II) at various burial depths (0-200 mm, 200-400 mm and 400-600 mm). Three different clays were used, namely weathered Lower Lias Clay, slightly weathered Lower Lias Clay and Coal Measures mudstone, at 5°C. The presented results include the effect of burial depth and mobile groundwater on the chemical changes in the simulated groundwater. The methodology of clay pore solution extraction and test method are described in Chapter 3. Changes in groundwater chemistry were assessed by measuring pH, water-soluble sulfate, and determination of water-soluble species such as Ca, Mg, K and Na, Cl as well as concentration of carbonate ions (CO<sub>3</sub>).

##### 6.4.1 Change in pH

The results of pH change in the simulated groundwater over 18 months are shown in Table 6.5, where the initial pH was (8.27). The measurements of pH after 3 months were 7.13, 7.22 and 7.1 for W-LLC, SW-LLC and CM mudstone respectively at burial depth of 200 mm. The pH continued to decrease gradually, reaching 6.89, 6.83 and 6.85 at 9 months. However, a slight increase in pH was recorded at 12 months at burial depth (200mm) in all exposed conditions. It is suggested that more alkaline species were leached out from concrete into simulated groundwater, as signs of deterioration were clearly observed at 12 months, as described in Section 5.2. On the other hand, the pH values at burial depths of 400 and 600 mm are slightly higher than that at 200mm.

Table 6.5 Variation in pH of simulated groundwater up to 18 months

Clay Type	Burial Depth (mm)	pH Values - months						
		0	3	6	9	12	15	18
W-LLC	200	8.27	7.13	7.06	6.95	7.18	6.90	6.89
	400	8.27	7.27	7.20	7.11	6.98	6.95	6.69
	600	8.27	7.21	7.14	7.15	7.08	6.83	6.71
SW-LLC	200	8.27	7.22	7.22	6.98	7.21	6.86	6.79
	400	8.27	7.28	7.19	7.11	7.10	6.84	6.83
	600	8.27	7.31	7.28	7.23	7.18	7.02	6.82
CM	200	8.27	7.10	7.03	6.93	7.15	6.85	6.73
	400	8.27	7.22	7.14	7.11	6.89	6.85	6.78
	600	8.27	7.27	7.26	7.19	7.12	7.023	6.87

The results of pH at various depths revealed that slightly higher pH readings in all clays as burial depth increased. With reference to clay types, it was found that pH values were



slightly higher in the case of SW-LLC than in slightly weathered LLC and CM mudstone. In the case of CM mudstone the presence of sodium may raise the pH of pore solutions, although CM mudstone has a high pyrite content in which more acid would be produced due to pyrite oxidation.

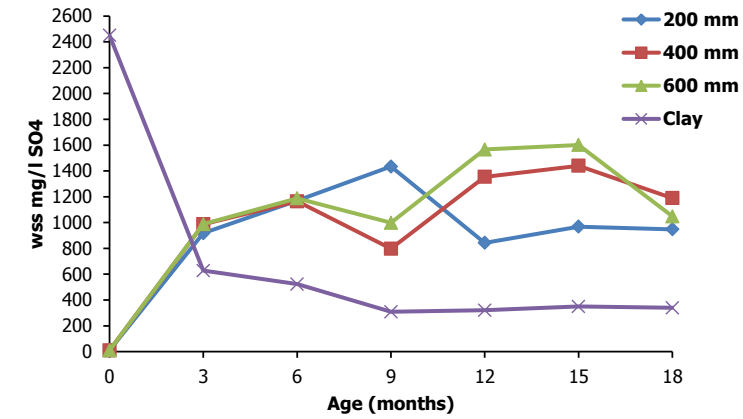
Overall, the reduction of pH of pore solutions might result from the incomplete buffering of acid in mobile water condition, as reported by Czerewko and Cripps (2006). As the clay pH was less than 10.33, calcite dissolution might be catalysed, as discussed by Torres (2004). This might produce more bicarbonate, which reduces the pH of the clay pore solution to less than 8.4. Furthermore, more CO<sub>2</sub> was probably dissolved at shallow burial depth, leading to the production of more bicarbonate and causing a reduction in the pH of groundwater. Therefore, it is suggested that pH would decrease over time, although less pyrite is oxidised. Leaching of magnesium from clay into groundwater might be considered an additional cause of further reduction in groundwater pH.

#### **6.4.2 Water-soluble sulfate**

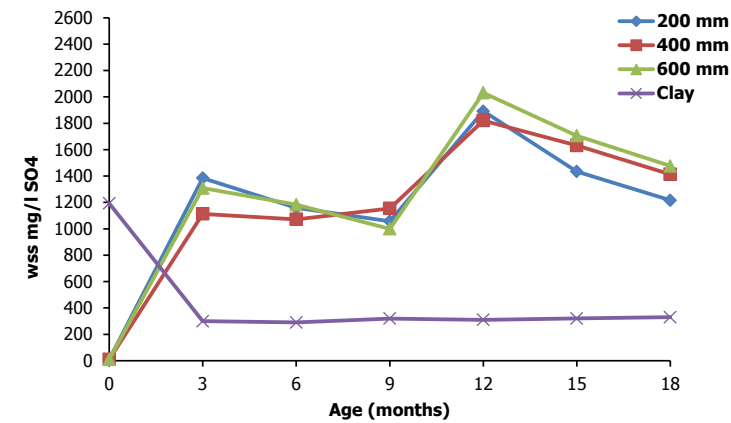
The measurement of sulfate concentration in the simulated groundwater up to 18 months is shown in Figure 6.14. It should be mentioned that the initial sulfate concentration of groundwater before interaction with clays was 85.4 mg/l. The sulfate concentration increased rapidly after 3 months, reaching 917, 1400 and 850 mg/l for W-LLC, SW-LLC and CM mudstone respectively. It continued to increase gradually up to 9 months and then decreased in the case of W-LLC, in which the reduction occurred only at a burial depth of 200 mm. On the other hand, the sulfate concentration decreased significantly in SW-LLC at 9 months and then increased to reach a maximum of 1800 mg/l at 12 months. The reductions at 9 and 12 months might be due to the penetration of more sulfate into concretes and its participation in the formation of thaumasite as more signs of deterioration were observed as seen in Section 5.2.2. These results agree with those for acid- and water-soluble sulfate, in which a significant decrease was recorded after 3 months, as seen in Figures 6.4 to 6.5. This could be an indication for the dissolution of gypsum and other water-soluble sulfates, available at the time of exposure and produced as a result of pyrite oxidation, into the simulated groundwater. It was also found that the concentration of sulfate at a burial depth of 600 mm was slightly higher than at 200 mm in the case of W-LLC and SW-LLC. It is suggested that less sulfate penetrates into concrete as burial depth increases.

The effect of burial depth on the ingress of sulfate into concrete was discussed in Section 4.2.2. However, in the case of CM mudstone, less sulfate was available at a burial depth of 600 mm than at shallow depths. This could be a result of the presence of less water and acid

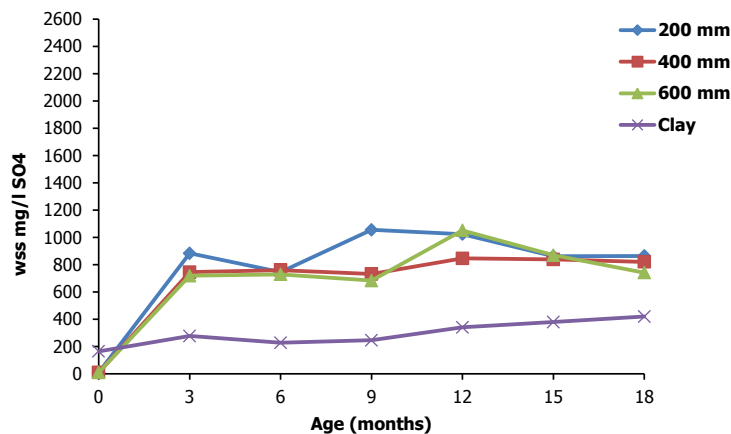
soluble sulfate in the clay before weathering (160 mg/l SO<sub>4</sub>) as well as a reduction in the rate of pyrite oxidation at deep burial depths because of the lower availability of oxygen.



W-LLC



SW-LLC



CM

Figure 6.14 Sulfate concentration of simulated ground water in different clays

With regard to clay types, the amount of available water-soluble sulfate in W-LLC and SW-LLC was 2450 and 1193 ppm respectively, while it was 160 ppm in CM mudstone. This would lead the concentration of sulfate in simulated groundwater to increase in the following order: SW-LLC > W-LLC > CM. This might be attributed to the dissolution of soluble sulfate available before exposure in the case of W-LLC and soluble sulfate produced from the pyrite oxidation process in the case of Lower Lias Clay, whereas in Coal Measures mudstone the sulfate level in groundwater was due to the sulfate generated from the pyrite oxidation process after weathering. The results also revealed that more sulfates were dissolved with time in the groundwater in the case of SW-LLC and W-LLC, while a gradual increase in sulfate concentration after three months was observed in CM mudstone, although more pyrite was oxidised, as shown in Section 6.3.3. This could be because sodium and chloride were available in high concentrations, which may dissolve in the groundwater, achieving saturation conditions in the simulated groundwater and reducing the probability of the dissolution of more sulfates.

#### **6.4.3 Water-soluble species**

The variation in water soluble composition of simulated groundwater in different clays is illustrated in Figures 6.15 to 6.19. The initial composition of simulated groundwater was 17.18, 15.7, 3.19, 4, 26.6 and 6 mg/l for Ca, Na, Mg, K, Cl and CO<sub>3</sub> respectively. In addition, the initial available water-soluble species in the clays are illustrated in Table 3.8. The calcium concentration was significantly increased in all simulated groundwater as shown in Figure 6.15, reaching 550, 420 and 126 mg/l for SW-LLC, W-LLC and CM mudstone respectively at a burial depth of 200 mm. It continued to increase to 579, 520 and 359 mg/l at 9 months for W-LLC, SW-LLC and CM mudstone respectively. However, a significant reduction was found at the age of 6 and 12 months in SW-LLC, while calcium concentration decreased by 50% in W-LLC and CM after 12 months. The concentration of calcium increased in the groundwater because of the dissolution of gypsum and calcite, both of which become more soluble at relatively low pH [7-7.5], as reported by Collete et al. (2004). Therefore, more calcium would dissolve into simulated groundwater. The remarkable reduction of calcium at 6 and 12 months for weathered and slightly weathered LLC might be due to the penetration of calcium into concrete after signs of deterioration appeared.

Figure 6.16 shows the variation in the magnesium concentration in simulated groundwater. It can be seen that the concentration of magnesium increased dramatically, which each maximum of 450 mg/l after 3 months of exposure to SW-LLC. Less magnesium was measured in W-LLC and CM.

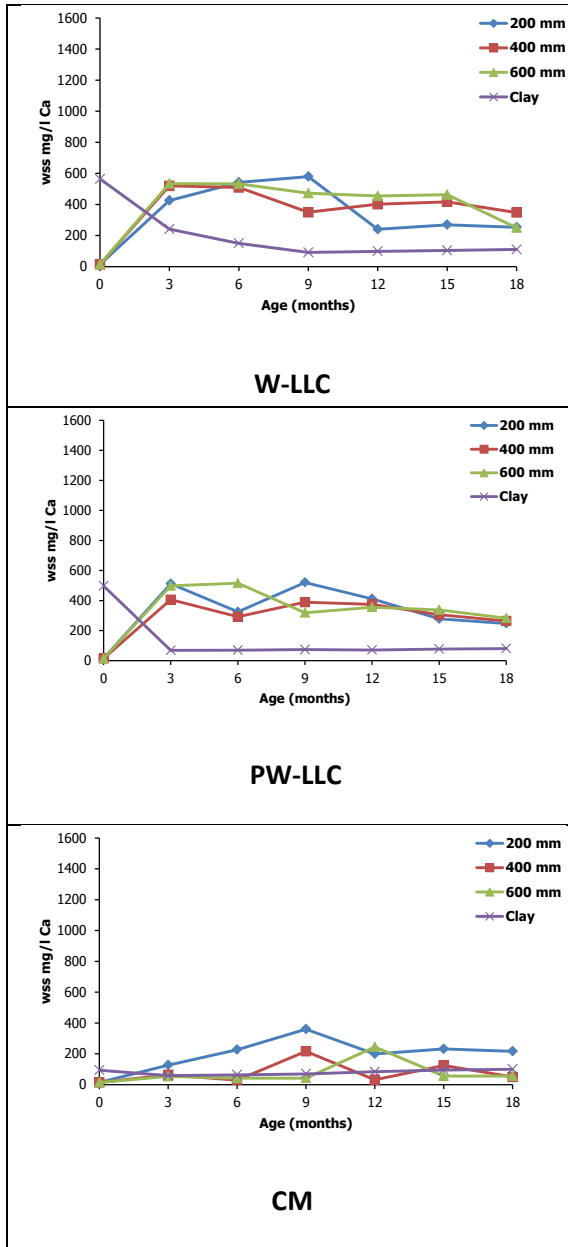


Figure 6.15 Calcium concentration of simulated ground water in different clays

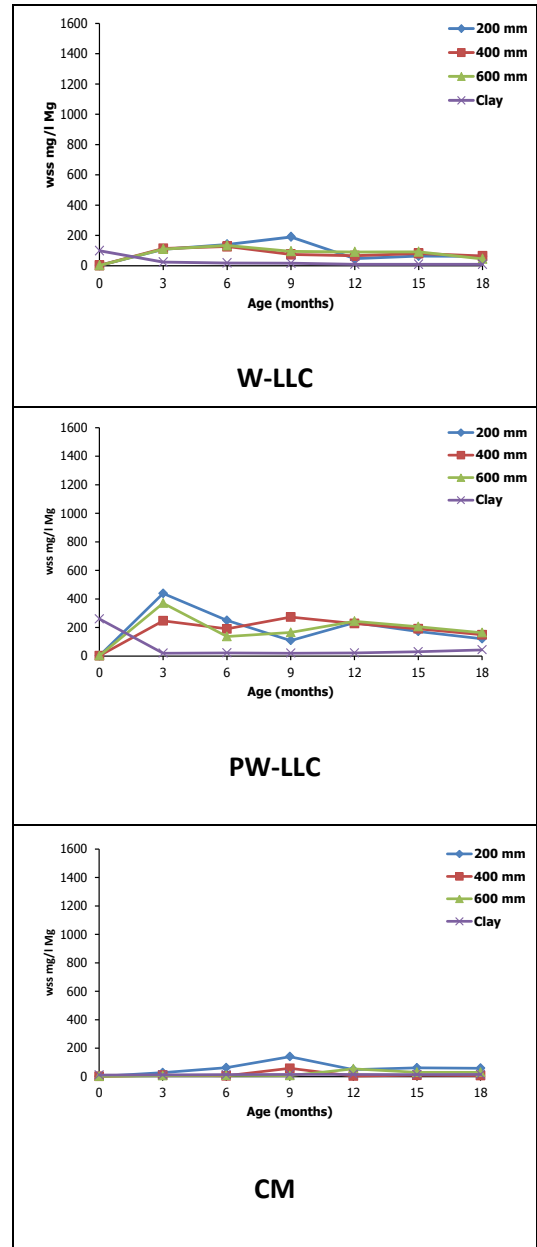


Figure 6.16 Magnesium concentration of simulated ground water in different clays

It was also found that the magnesium concentration in SW-LLC decreased significantly to 70 mg/l at 9 months and then gradually increased up to 12 months. On the other hand, it reached a maximum at 9 months in W-LLC before a significant reduction occurred at 12 months. The results also revealed that magnesium concentration was found to be high at a burial depth of 200 mm. An increase in the level of magnesium after 3 months implies that more available magnesium in the clays dissolved in the simulated groundwater. In addition, the continuation of the rise in magnesium concentration with time might be due to the reaction of acid produced during the pyrite oxidation process with clay minerals. This might be an additional source of magnesium as seen in CM clay. However, the reduction in the

concentration after 3 months in the SW-LLC, revealed that more magnesium penetrated into concrete before deterioration commenced and might contribute to the severity of deterioration in comparison to other concretes exposed to other clays, as shown in Section 5.2. Moreover, the reduction of magnesium concentration with burial depth might be because less pyrite was oxidised as burial depth increased, so less acid would react with clay minerals to release more magnesium and leach into the groundwater. In the case of CM mudstone, less magnesium was dissolved in groundwater, although more acid would be expected to be produced as a result of pyrite oxidation and to react with clay minerals and release Mg. However, the availability of the high concentration of chloride and sodium might cause saturation of groundwater, and other species would precipitate in CM mudstone clay.

A similar observation was made regarding the change of potassium concentration over time in all simulated groundwater, as shown in Figure 6.17. However, the maximum potassium concentration was 72, 70 mg/l and 50 mg/l at 9 months for W-LLC, SW-LLC and CM respectively.

The carbonate concentration was significantly increased in all simulated groundwater after 3 months as shown in Figure 6.18, reaching 230, 280 and 420 mg/l for W-LLC, SW-LLC and CM mudstone respectively at a burial depth of 200 mm. On the other hand, a significant reduction was found at the age of 9 months in SW-LLC and W-LLC, while carbonate concentration continued to increase with time in case of CM mudstone. It reached a maximum value of 623, 680 and 800 for W-LLC, SW-LLC and CM mudstone respectively at age of 18 months. There was slight difference in carbonate concentration at different burial depths. However, the concentration of carbonate was lower at burial depth (200 mm) at age of 9 months in case of Lower Lias Clay. This might be due to the ingress of carbonate ions into concrete, which contribute in the formation of thaumasite after signs of deterioration appeared at burial depth (200 mm) as seen in Section 5.2.2. The dissolution calcite in the groundwater might be an additional reason for increasing the concentration of calcium as seen in Figure 6.15, which calcite become more soluble at relatively low pH [7-7.5], as reported by Collete et al. (2004). In addition, calcite dissolution might increase due to dissolving of carbon dioxide from atmosphere and that produced from acid buffering reaction in ground water, which Collete et al. (2004) reported that the solubility of carbon dioxide increased by double at low temperature (5°C). Therefore, more carbonate and bicarbonate ions would dissolve in simulated groundwater. In the case of CM mudstone, the concentration of dissolved carbonate in simulated ground water was higher than that in W-LLC and SW-LLC. It suggested that the presence of high concentration of chloride in CM

mudstone that might be another reason for the acceleration the dissolution of calcite, as reported by Learson and Buswell (1984), who suggested that the solubility of calcite increased with increases in the chloride concentration, and the maximum solubility was found in concentrations of 1 mole of NaCl.

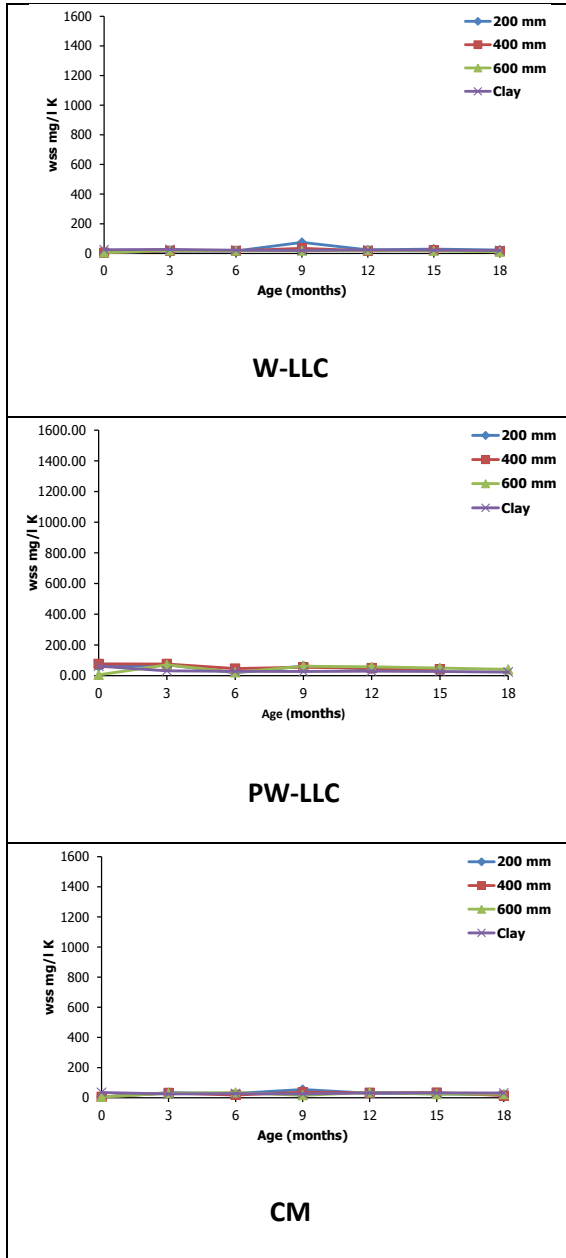


Figure 6.17 Potassium concentration of simulated ground water in different clays

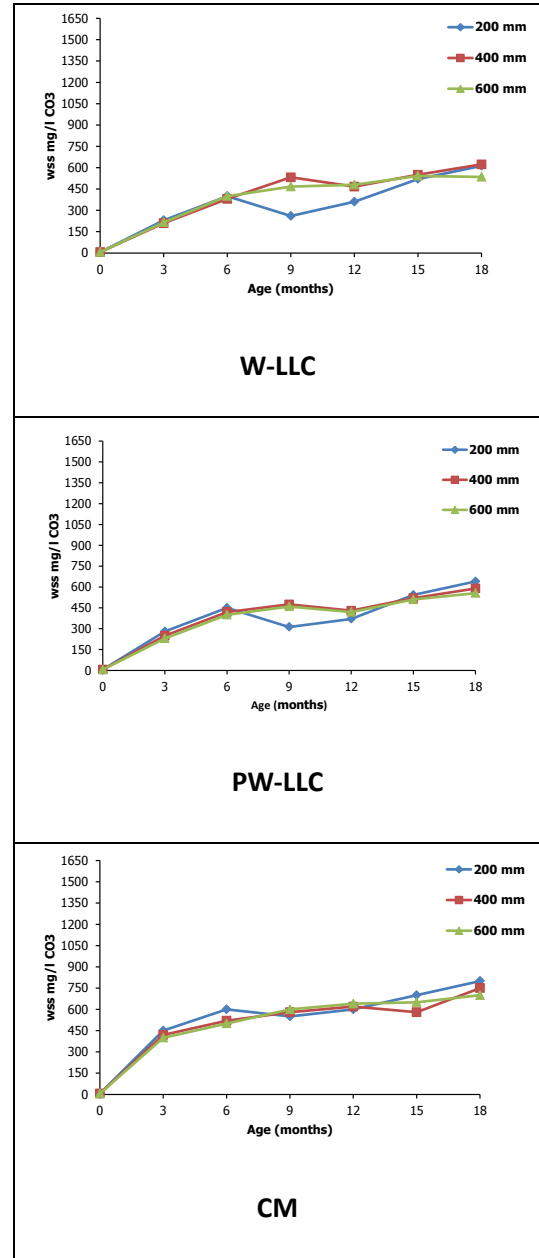


Figure 6.18 Carbonate concentration of simulated ground water in different clays

The concentrations of sodium and chloride are shown in Figures 6.18 and 6.19 which the concentration of sodium gradually increased in W-LLC and SW-LLC up to 12 months. On the other hand, a significant increase was noticed in CM clay, which reached a maximum of 1400 mg/l at 3 months and then significantly decreased, which suggests that more sodium

penetrates into concrete and reacts with the concrete matrix. In addition, it should be mentioned that sodium concentration after weathering of W-LLC and SW-LLC was 20 times higher than that before exposure, suggesting that sodium was released as a result of reaction of acid with clay minerals. It was found that the chloride level increased in all groundwater and was significant in CM mudstone. It reached a maximum of 700, 250 and 200 mg/l for CM, SW-LLC and W-LLC respectively after 3 months.

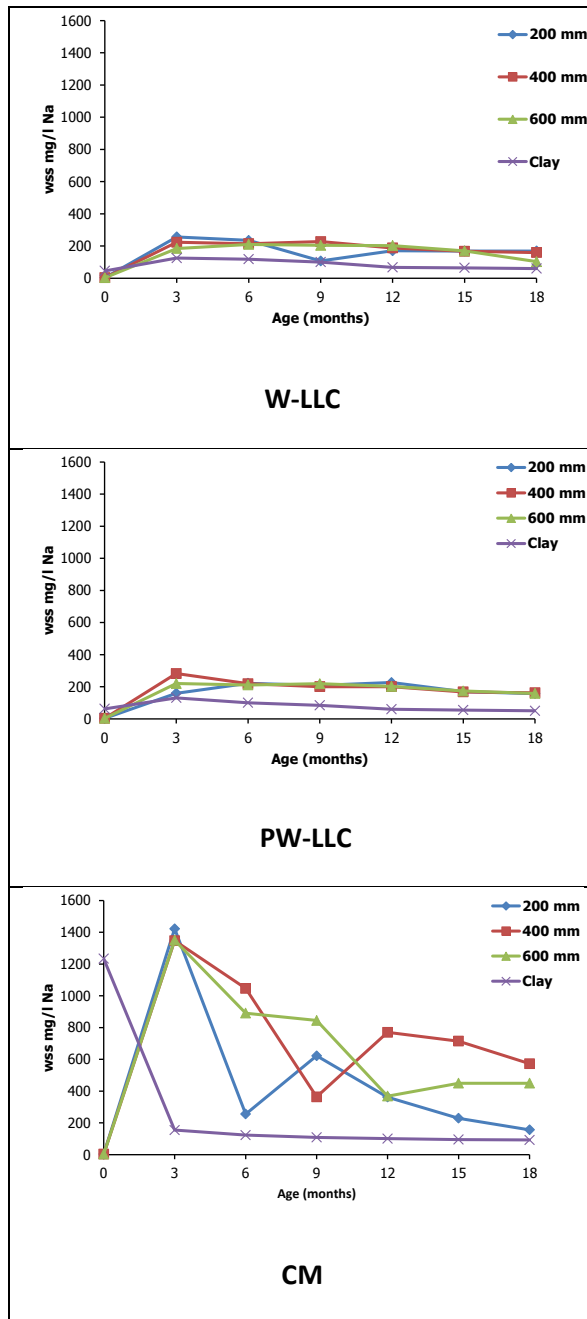


Figure 6.19 Sodium concentration of simulated ground water in different clays

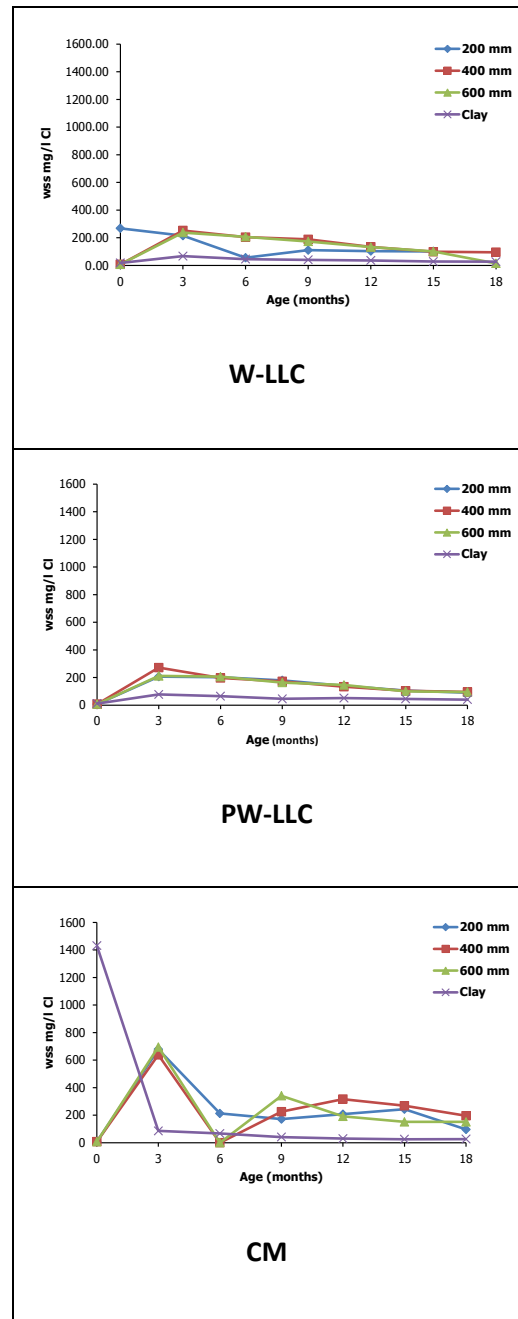


Figure 6.20 Chloride concentration of simulated ground water in different clays



However, it decreased after 3 months and continued to decrease, unlike Na, Mg and K. Furthermore, it should be mentioned that the concentration of chloride varied at different burial depths, and slight differences were noticed. The significant reduction in Cl concentration in CM mudstone indicated that Cl penetrated into concrete and reacted with  $C_3A$  to form Friedel's salts; this was confirmed in the XRD results in Section 5.4.

The overall comparison of different simulated groundwater compositions revealed that sulfate, calcium and carbonate were the main factors in W-LLC that might influence the severity of deterioration, while sulfate and carbonate along with calcium and magnesium were the main factors in SW-LLC that might play a role in the severity of deterioration, as more deterioration was observed in the case of slightly weathered LLC. However, in Coal Measures mudstone, the presence of high concentrations of chloride and sodium at the time of exposure led to the saturation of groundwater and the precipitation of other species in clays. In addition, sodium and chloride which leached into groundwater penetrated the concrete and reacted with the concrete matrix. This might prevent other species from penetrating to initiate the formation of thaumasite and might delay the progress of deterioration due to TSA. The groundwater plays an important role in leaching out species available in clay and transporting them to concrete. In addition, it might disturb the buffering reaction, leading to incompletely neutralised acid, so that the acid would react with clay minerals and release Na, Mg, K and Ca. This explains the increase in K, Mg and Na over time.

## **6.5 Summary**

The key findings of this investigation of the chemical changes in different Lower Lias Clays and Coal Measures mudstone, interacting with different concretes in the presence and absence of the mobile groundwater at 5° and 20°C for 12 months, are presented in this section. In addition, the findings in the changes of groundwater chemistry for 18 months are also presented. An extensive search of the literature revealed that few field investigations have yet been carried out to assess the changes in the chemistry of pyritic clay, making this study is thought to be the first systematic laboratory study of chemical change in different pyritic clays in simulated field conditions. The alterations in clay chemistry were evaluated by measuring changes in pH, water- and acid-soluble sulfate, total sulfur, pyrite oxidation, carbonate content and microstructure, while alterations in simulated groundwater were measured by the changes in pH and water-soluble species. The following conclusions can be drawn from these results:

- Overall comparison of pH values of Lower Lias Clays and Coal Measures mudstone showed a reduction in pH values of all clays in different exposure conditions compared to initial pH values before exposure, which were 7.8, 8.1 and 7.24 for W-LLC, SW-LLC and CM mudstone respectively. However, the pH values remained neutral, with values between 7.05 and 7.94, except for a few samples in which the pH was slightly lower than 7.0 in the case of Coal Measures mudstone.
- The pH values of Lower Lias Clays and Coal Measures mudstone after 12 months in the presence of the mobile groundwater were slightly lower than that in its absence, which suggests that the mobile groundwater might result in an incomplete acid buffering reaction with calcite and might cause a reduction in pH. However, the differences were not significant, which might be because sulfuric acid reacts with clay minerals and releases more alkaline species such as Na and K.
- The pH measurements of Lower Lias Clays and Coal Measures mudstone at 20°C were slightly lower than those at 5°C.
- The pH values of clays decreased as follows: W-LLC > SW-LLC > CM mudstone. This might be due to the high amount of pyrite in SW-LLC and CM compared to W-LLC, resulting in the production of more sulfuric acid.
- The slight reduction in pH of CM mudstone might be a result of the presence of a moderate concentration of sodium in its composition, which mitigates the reduction in pH due to the acid generated by pyrite oxidation.
- Although the acid generated from pyrite oxidation was buffered by calcium carbonate, clay minerals and calcium hydroxide from concrete in the interface region, the presence of bicarbonate and weak carbonic acid from the dissolution of calcite present in the clay as well as from the dissolution of CO<sub>2</sub> in the clay pore solution might be considered an additional reason for the reduction of clay pH with age as more would be produced over time.
- The pH values of all clays in contact with CEM I and CEM I-LF concretes were higher than those which interacted with PFA and GGBS concretes. It is postulated that more calcium hydroxide and other alkaline species such as K and Na were leached from concrete, which increase as signs of deterioration appeared in CEM I and CEM I-LF concretes, while the high replacement of cement with PFA and

GGBS concretes along with low permeability of those concretes resulted in fewer alkaline species being leached from concrete.

- The neutral pH might lead to decalcification of CSH, resulting in the formation of extensive thaumasite in the presence of sufficient sulfate and carbonate.
- A significant reduction in water-soluble sulfate was observed in Lower Lias Clays in the presence of the mobile groundwater, which suggests that more gypsum was dissolved in the groundwater. On the other hand, a slight increase in water-soluble sulfate was noticed in Coal Measures mudstone, which might be because less gypsum was available before exposure.
- In the presence of mobile groundwater, the measurements of sulfate concentration in Coal Measures mudstone in contact with different concretes were similar, which suggests that less sulfate penetrated into concrete, as no signs of attack were observed.
- The concentration of water-soluble sulfate in the absence of the mobile groundwater at 5° and 20°C was higher than in the presence of water mobility in all clays. In addition, the increase in the concentration of sulfate was higher in SW-LLC and CM than in W-LLC, which contains less pyrite than other clays. Moreover, the concentration of sulfate was higher at 20°C than at 5°C, as more pyrite is expected to oxidise at 20°C, and therefore more sulfate would be generated.
- Water-soluble sulfate in Coal Measures mudstone increased by more than 15 times its value before exposure. It is suggested that the presence of a high concentration of Na and Cl caused the clay pore solution to be saturated with these ions, so that more sulfate was precipitated.
- The concentration of water-soluble sulfate in Lower Lias Clays and Coal Measures mudstone was higher in the case of interaction with PFA and GGBS concretes than for CEMI and CEMI-LF concretes, which suggests that more sulfate was engaged in thaumasite formation in CEMI and CEMI-LF concretes, while the low permeability of PFA and GGBS concretes resulted in more sulfate being precipitated and being available in the clay.
- The results for acid-soluble sulfate revealed a remarkable reduction in gypsum in weathered and slightly weathered Lower Lias Clay in the **presence of mobile** groundwater, which implies that more gypsum and water-soluble sulfate were

dissolved in simulated groundwater. However, the amount of ASS in CM mudstone increased with time, which might be due to the formation of more gypsum from the acid buffering reaction, as less gypsum was available before exposure than in Lower Lias Clay.

- The acid-soluble sulfate concentration of all clays in the absence of mobile groundwater at 5° and 20°C was higher than in its presence. However, the measurements were higher at 20°C than at 5°C. In addition, the amount of gypsum formed in CM mudstone and SW-LLC was higher than that in W-LLC as the latter contained less pyrite. On the other hand, the presence of high concentrations of Na and Cl in CM mudstone might cause the clay pore solution to be saturated with these ions, so that more gypsum would precipitate in the clay.
- More gypsum was found in all clays in contact with PFA and GGBS concrete than in those which interacted with CEM I and CEM I-LF, as gypsum dissolved in the clay pore solution and contributed to TSA.
- The total sulfur decreased more in the presence of mobile groundwater than in its absence. In addition, a significant reduction in total sulfur was observed in W-LLC, which contained a high amount of gypsum, as it dissolved in the simulated groundwater.
- The reduction in total sulfur was more significant at 5°C than that at 20°C. This might be because more sulfates penetrated into concretes and engaged in the deterioration reaction.
- The reduction in total sulfur decreased in the following order: CM > SW-LLC > W-LLC, while maximum reductions of 0.3, 0.15 and 0.13 (%S) were recorded after 12 months in W-LLC, SW-LLC and CM mudstone. In addition, the lower reduction in CM mudstone might be due to the precipitation of gypsum in the clay as the clay pore solution became saturated with Na and Cl present in CM. In addition, more gypsum would precipitate as less deterioration was detected in all concretes exposed to CM mudstone.
- Total sulfur in all clays in contact with CEMI and CEMI-LF concretes was lower than that in contact with GGBS and PFA concretes. This may be due to the penetration of more sulfates into CEMI and CEMI-LF concretes and their participation in the formation of thaumasite, as more degradation was observed.

- The amount of pyrite decreased after 12 months in all clays in different exposure conditions. However, more pyrite was oxidised in the absence of mobile groundwater than in its presence. In addition, more pyrite was oxidised in Coal Measures mudstone than in Lower Lias Clays in all exposure conditions. Furthermore, the results revealed that high temperature increased the rate of pyrite oxidation in all clays. A similar observation was made regarding the effect of concrete type on the change of chemistry of clay, in which more pyrite was oxidised in interactions with CEMI and CEMI-LF than PFA and GGBS concretes.
- The amount of pyrite decreased in the following order: CM > SW-LLC > W-LLC. It is believed that the supersaturation of the clay pore solution with sulfate might reduce the rate of pyrite oxidation in the case of W-LLC, while the fact that less gypsum was available in clay and the presence of sodium were the main reasons for the higher rate of pyrite oxidation in case of CM mudstone.
- The results of pyrite oxidation showed that the mobile groundwater effect might control the process and rate of pyrite oxidation through the incompleteness of the buffering reaction, which might cause the variation of pH values within clays and thus influence the rate of oxidation by restricting the oxidation of ferrous iron to ferric iron to oxidise more pyrite. On the other hand, the composition of clay, concrete type, saturation of the clay pore solution and high temperature have a great influence on pyrite oxidation, and might accelerate the rate of oxidation.
- Less calcite was consumed in the presence of mobile groundwater in all clays. In addition, calcite consumption that was calculated theoretically was lower than that measured experimentally in all clays. It is suggested that more calcite was dissolved in clay pore solutions and in simulated groundwater, while the solubility of calcite was increased in CM mudstone by the presence of chloride.
- The weak correlation between the amounts of consumed pyrite and calcite revealed the incompleteness of the buffering reaction in the case where less calcite was consumed. However, in the case where more calcite is consumed and less acid is produced by pyrite oxidation, the dissolution of calcite in water is considered to be an additional factor in the consumption of more calcite.
- The microstructural analysis of different clays before and after weathering confirmed the oxidation of pyrite after 12 months by the presence of attacked pyrite

surface along with precipitated gypsum and change in the EDX analysis of clay minerals due to reaction with sulfuric acid generated from pyrite oxidation.

- The results of groundwater analysis showed a reduction in the pH of the pore solution, resulting from the incomplete acid buffering due to the presence of mobile groundwater. Furthermore, the high concentration of bicarbonate ions as a result of the dissolution of magnesium, calcite and CO<sub>2</sub> at shallow burial depth might cause a reduction in the pH of groundwater. Therefore, it is suggested that the pH of groundwater may decrease over time, although less pyrite is oxidised.
- The results for groundwater revealed that mobile groundwater plays a role in leaching out the water-soluble ions and cations from the clay. The concentrations of sulfate and calcium significantly increased in the groundwater of all clays. This could be due to the dissolution into the simulated groundwater of gypsum and other water-soluble sulfates available at the time of exposure and produced as a result of pyrite oxidation. In addition, the concentration of sulfate was higher at shallow burial depth than at shallow, where less pyrite is expected to oxidise and therefore less sulfate would be generated.
- The concentration of sulfate in simulated groundwater increased in the following order: SW-LLC > W-LLC > CM. This might be attributed to the dissolution of soluble sulfate available before exposure in the case of W-LLC and soluble sulfate produced from the pyrite oxidation process in the case of Lower Lias Clay, whereas in Coal Measures mudstone the sulfate level in groundwater was due to the soluble sulfate generated from the pyrite oxidation process after weathering.
- The concentration of calcium increased rapidly in the groundwater as a result of the dissolution of gypsum and calcite. In addition, the concentration of magnesium increased dramatically after 3 months in the case of SW-LLC, while less magnesium was measured in W-LLC and CM. On the other hand, high concentrations of sodium and chloride were observed after 3 months in groundwater in the case of CM mudstone, which contains high concentrations of Na and Cl dissolved in simulated groundwater. A similar observation for the increase in the level of potassium was observed, although the concentration was low compared to other ions and cations.
- The mobile groundwater might disturb the buffering reaction and lead to an incomplete acid buffering reaction, so that the acid would react with clay minerals and release Na, Mg, K and Ca; this explains the increase in these with time.

- The analysis of groundwater in different pyritic clays revealed that calcium, sulfate and carbonate were the dominant parameters in W-LLC that might influence the severity of deterioration, while sulfate, calcium, magnesium and carbonate were the main ion in SW-LLC which played a role in the severity of TSA, in which more deterioration was observed. However, in CM mudstone, the presence of high concentrations of chloride and sodium at the time of exposure led to the saturation of groundwater and precipitation of other species in clays. Moreover, sodium and chloride leached into groundwater penetrate concrete and react with the concrete matrix. This might prevent other species from penetrating the concrete to initiate the formation of thaumasite and delay the progress of deterioration due to TSA.



## CHAPTER 7

### 7. The Influence of Clay Composition on the Extent of TSA in Buried Concrete: Overall Discussion

#### 7.1 Introduction

The influence of the composition of Lower Lias Clay and Coal Measures mudstone on the severity of thaumasite sulfate attack (TSA) on concrete in the presence and absence of simulated groundwater at 5° and 20°C was investigated. Concrete mixes made with CEM I, CEM I blended with 10% Limestone Filler (LF), CEMI blended with 50%PFA and CEMI blended with 70 % GGBS were studied. In addition, the long term interaction of concrete with Lower Lias Clay as well as the long-term performance (nine years) of SRPC and PC-25%PFA were also investigated. The overall discussion addresses the objectives of this current work:

- to investigate the influence of clay composition on the extent of TSA.
- to investigate differences in thaumasite formation in different exposure conditions.
- to investigate the changes in the chemistry of pyritic clay and its aggressivity.
- to investigate the role of mobile groundwater on changes in the chemistry of clay and the extent of TSA.
- to review and assess the current guidance regarding the influence of aggressive ground conditions on TSA and to make recommendations for further consideration in guidance.

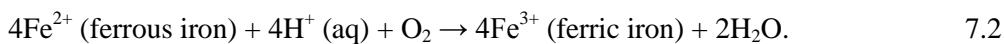
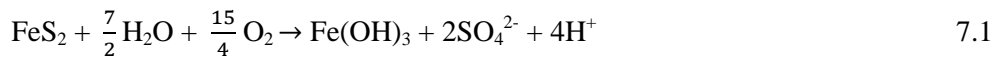
#### 7.2 Aggressivity due to changes in the chemistry of pyritic clays

The results in Chapter 6 for changes in the chemistry of different pyritic clays during the twelve months of the experiment confirmed that pyrite oxidation occurred, and that calcite and clay minerals were involved in reactions with the resulting acid. This resulted in an

increase in the level of sulfate in clay as well as the dissolution of calcite, which caused an increase in the level of carbonate and bicarbonate ions in the clay pore solution. In addition, other soluble ions and cations such as calcium, magnesium, sodium and chloride, increased as it leached out from clay in simulated groundwater. According to the results, the aggressivity of clay can be due to the following factors:

- the aggressivity resulting from pyrite oxidation
- the effect of calcite dissolution

Pyrite present in the clay oxidised and led to the formation of sulfate and sulfuric acid, as shown in Equation 7.1 (Czerewko and Cripps 2006). The process would result in raised acidity and sulfate levels in the groundwater.



The reaction of oxidation of ferrous iron in Equation 7.2 is considered to be the step which governs the rate of the process, which slows under acidic conditions, and which is influenced by the variation in pH, as reported by Czerewko and Cripps (2006).

The calcite present in the Lower Lias Clay and Coal Measures mudstone buffers the acidity, reacts with sulfuric acid and produces more gypsum, as illustrated in Equation 7.3. The solubility of gypsum is limited to 1.4 g/l  $\text{SO}_4$  and part of the gypsum is dissolved in the clay pore solution and groundwater. However, it readily precipitates to form white patches of gypsum observed within the weathered clay.



A low amount of pyrite was oxidised where groundwater was present (Section 6.2.5). The mobility of water might lead to the leaching of sulfate ions in the clay, which might increase the rate of pyrite oxidation. However, it could also result in the incompleteness of the acid buffering reaction, as reported by Czerewko and Cripps (2006). The results for carbonate in clay (Section 6.2.6) revealed that a low amount of calcite was consumed in the presence of mobile water in all clays, and this confirmed that the acid buffering reaction was incomplete. Therefore, this might cause variation in the pH values within clay and reduce the rate of

pyrite oxidation by restricting the oxidation of ferrous iron to ferric iron in Equation 7.2, as discussed by Calderia et al. (2003). In addition, Descostes et al. (2000) and Calderia et al. (2003), reported that carbonate ions play an important role on maintain pH of clay to be neutral or alkaline, in which the oxidation of Fe(II) to Fe(III) is slow in acidic condition, while it increase at pH above 4. It is suggested that the formation of soluble ferrous carbonate in the presence of high concentrations of carbonate and bicarbonate ions enhances the oxidation of ferrous iron to ferric, as shown in Figure 7.1; this shows the important role of carbonate in increasing the overall rate of pyrite oxidation.

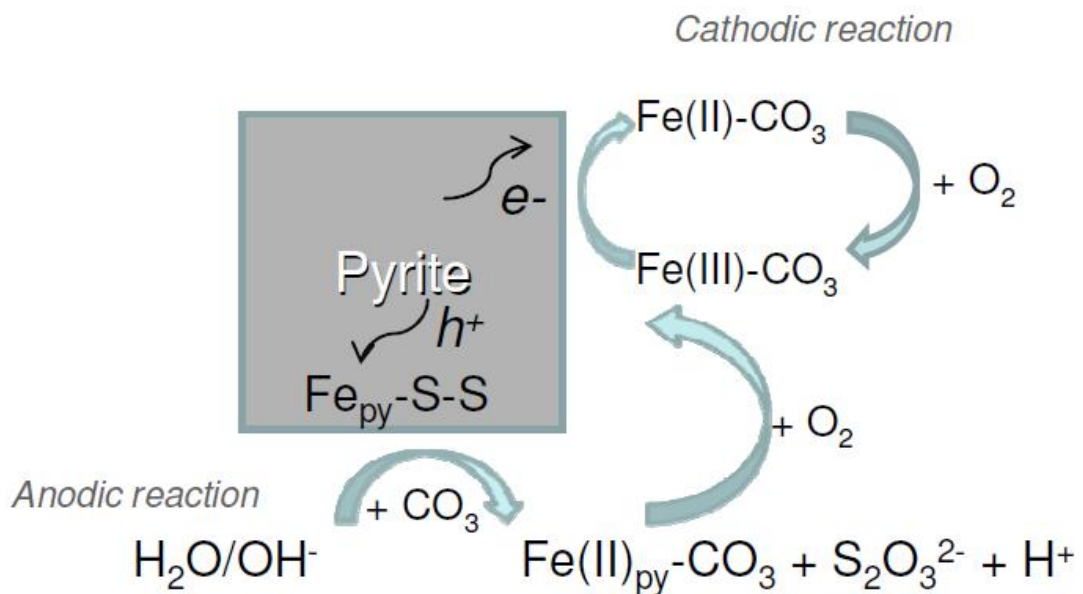


Figure 7.1: The oxidation of pyrite in the presence of carbonate (Calderia et al, 2010)

On the other hand, more pyrite was oxidised in Coal Measures mudstone than in Lower Lias Clay, as discussed in Section 6.2.5. The difference between Lower Lias Clay and Coal measures mudstone is that the latter has 1234 mg/l sodium, while Lower Lias Clay has a low concentration of sodium (42.13 mg/l), as described in Chapter 6. Therefore, it is suggested that the reason for the rapid rate of pyrite oxidation in Coal Measures mudstone is the presence of a moderate concentration of sodium, which increases the pH and maintains the pH at a constant level during the weathering process. In addition, the sodium present might react with carbonate and form sodium carbonate, which accelerates the rate of pyrite oxidation by removal of the oxide coating produced by calcium carbonate which prevents further oxidation of pyrite, as reported by Calderia et al. (2003) and Descostes et al. (2000).

An additional possible factor that might influence the rate of pyrite oxidation is the saturation of clay pore solutions with sulfate and other species such as calcium and carbonate ions. A low rate of pyrite oxidation was observed in the case of weathered Lower

Lias Clay (Section 6.2.5), which contains high amounts of gypsum (0.82 %  $\text{SO}_4$ ), calcium (580 mg/l) and carbonate (30%  $\text{CaCO}_3$ ), in contrast to Coal Measures mudstone (unweathered), which contains smaller amounts of gypsum (0.05 %  $\text{SO}_4$ ), calcium (90 mg/l) and carbonate (7.3%  $\text{CaCO}_3$ ). It is suggested that the high amounts of gypsum and other water-soluble ions in weathered Lower Lias Clay might lead the clay pore solution to be saturated with these species, as shown in Figure 7.2, which would prevent the sulfate being leached from the clay; this might reduce the rate of pyrite oxidation. On the other hand, the low concentrations of sulfate, calcium and carbonate available in Coal Measures mudstone before weathering, along with low ionic strength, result in a high activity coefficient that enhances the solubility of gypsum and carbonate. Thus sulfate ions would be leached from clay, and this would accelerate the rate of pyrite oxidation, as shown in Figure 7.2.

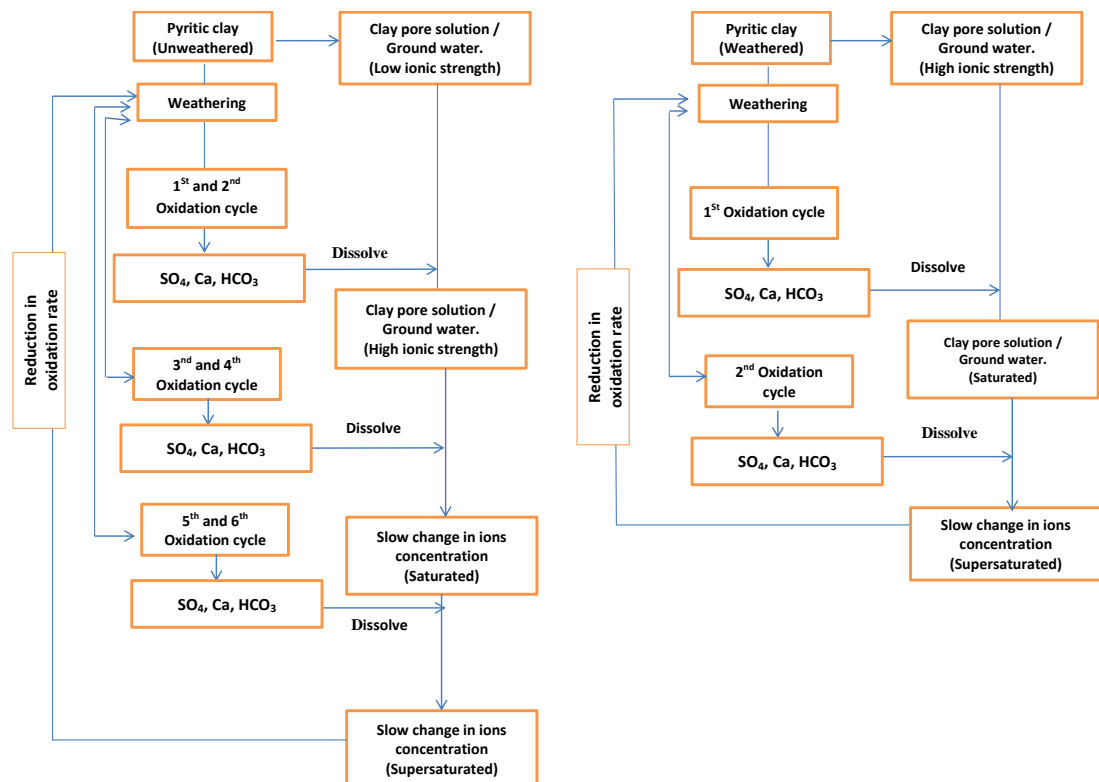


Figure 7.2 Flowchart showing the pyrite oxidation process in different clay condition

Overall, the saturation of the clay pore solution by the sulfate and the presence of a high concentration of carbonate and bicarbonate ions along with sodium can be considered important factors in controlling the rate of pyrite oxidation in this investigation.

With regard to calcite, the results in Section 6.2.6 showed that a reduction in calcite occurred in both Lower Lias Clay and Coal Measures mudstone. Part of the calcite would have been

consumed by the buffering reaction, as shown in Equation 7.2. However, since calcite is present in Lower Lias Clay and Coal Measures mudstone, dissolution of calcite in the clay pore solution and simulated groundwater (Section 6.4.3) would occur, as shown in Equation 7.4, and would result in availability of  $\text{CO}_3$  and  $\text{HCO}_3$  ions in the clay pore solution. On the other hand, atmospheric  $\text{CO}_2$  might also dissolve in the pore solution and groundwater, leading to an increase in the level of carbonic acid and bicarbonate ions in clay pore solutions, as illustrated in Equation 7.5. In addition, the  $\text{CO}_2$  resulting from the acid buffering reaction might dissolve in the clay pore solution and increase the solubility of calcite, as reported by Crammond (2003) and Torres (2004), who pointed out that the solubility of calcite increased as  $\text{CO}_2$  increased. Therefore, high concentrations of bicarbonate and carbonate ions become available in the clay pore solution and groundwater.



However, the amount of calcite consumed in Coal Measures mudstone was higher than in Lower Lias Clay (Section 6.2.6). In the case of CM mudstone, the presence of a moderate concentration of chloride (1420 mg/l = 0.1 mole NaCl) in its composition might be another reason for the acceleration of the dissolution of calcite, as reported by Learson and Buswell (1984), who suggested that the solubility of calcite increased with increases in the chloride concentration, and the maximum solubility was found in concentrations of 1 mole of NaCl.

The general findings in this study have revealed that, although Lower Lias Clay has water-soluble sulfate corresponding to BRE sulfate class DS-2, concrete exposed to LLC with sulfate design class DS-2 deteriorated at a faster rate than corresponding specimens in the DS-2 solution and at a similar rate to or faster than those exposed to the DS-4 sulfate solution at 5°C. This might be due to the series of reactions that raise the aggressivity of clay, as seen in Figure 7.3, which were absent in the DS-2 and DS-4 sulfate solutions.

Figure 7.3 summarises the aggressivity resulting from 1g of pyrite and 3g of calcite in Lower Lias Clay and Coal Measures mudstone, on the basis of Equations 7.1-7.5.

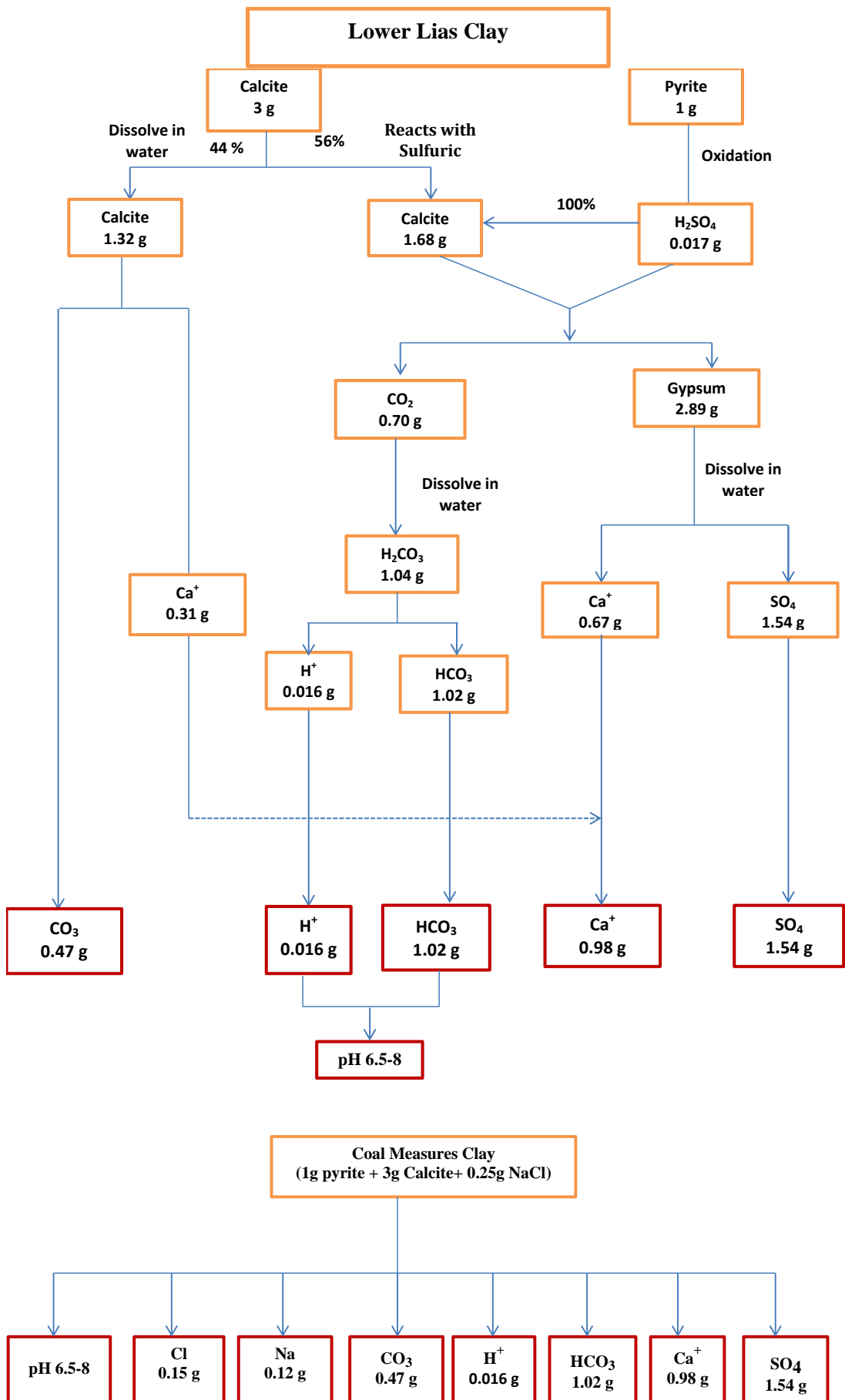


Figure 7.3 Flowchart showing the amount of aggressive species generated in different clays

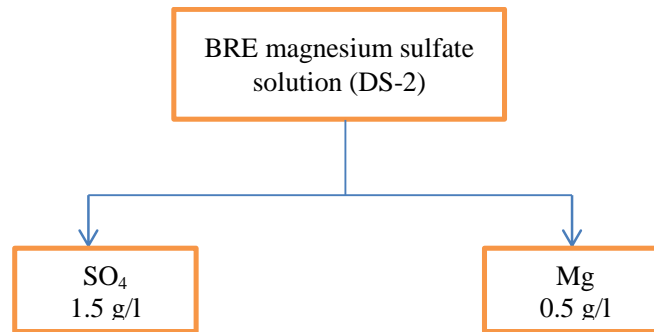


Figure 7.4 Flowchart showing aggressive species generated from the BRE, DS-2 sulfate solution

The flow diagram confirms that sulfate, carbonate, bicarbonate ions and calcium are the main factors in clay, along with chloride and sodium in the case of Coal Measures mudstone, that might influence the extent of deterioration due to TSA, and these species are absent in the BRE standard sulfate solution, as shown in Figure 7.4

Therefore, the continuation of pyrite oxidation, buffered reactions and calcite dissolution as explained in Equations 7.1 to 7.6 results in the generation of aggressive soluble sulfate,  $\text{CO}_3$  and  $\text{HCO}_3$  ions and acidity. The presence of bicarbonate and weak carbonic acid would also result in reduction of clay pH with age, as more bicarbonate and weak carbonic acid would be produced over time. This results in a clay pore solution of pH 7-8. In turn, this would affect the degree of solubility of calcite and gypsum, which is high at a pH of about 7-7.5, as reported by Collet et al. (2004); as a result more carbonate and sulfate ions would be available in the clay pore solution and groundwater than expected. In addition, Czerewko and Cripps (2006) reported that, under acidic conditions, the sulfuric acid may react with clay minerals and liberate exchangeable cations such as K, Na and Mg, increasing the level of magnesium sulfate, which is considered to increase the aggressivity of pyritic clay.

### 7.3 Thaumasite formation in different conditions

In this study, XRD, IR and SEM analysis of deterioration products of deteriorated concretes revealed that degradation was mainly due to TSA at both temperatures in the case of interaction with clays, while thaumasite along with ettringite and gypsum was the main deterioration product at 5°C in DS-4 sulfate and simulated clay pore solutions, and ettringite and gypsum were formed in the DS-2 solution at both temperatures. Therefore, the differences in the deterioration products formed imply that TSA occurs by different routes in the case of exposure to clays and to sulfate solutions.



The mechanism by which concrete becomes more vulnerable to TSA when it is in contact with clay rather than the equivalent solution is not well understood. It was suggested that, in the case of the foundations of the M5 motorway bridges, sulfuric acid, produced as in Equation 7.1, was the primary cause of deterioration (Hobbs and Taylor, 2000). However, a laboratory investigation by Hill et al. (2003) suggested that acid conditions do not promote thaumasite formation but that thaumasite formation was assisted because the acidic conditions give rise to increased sulfate concentrations. The suggested routes for TSA for both conditions are summarised below.

### 7.3.1 Exposure to sulfate solution

Figure 7.5 shows the schematic diagram for concrete attack due to magnesium sulfate solution. The mechanism of deterioration in the case of exposure to sulfate solution can be considered as following both the woodfordite and the direct route (Bensted, 2003), in which initial reactions result in the formation of gypsum and ettringite. Later, further interactions involving CSH result in thaumasite. It is suggested that thaumasite might form as a result of the conversion of ettringite as well as from reaction with CSH, gypsum in the presence of sufficient carbonate. However, formation of an insoluble brucite layer on the surface of the concrete could restrict the ingress of more sulfate ions into concrete, and the attack might be delayed. Therefore, the reaction for thaumasite formation commences in the reaction layer beneath the concrete surface covered by brucite. On the other hand, the progress of deterioration becomes visible as C-S-H starts to decalcify as calcium ions are replaced by magnesium ions and changes to M-S-H, which is not a cementitious binder. The decalcification of CSH has been reported to be much greater than that of sodium sulfate, which becomes metastable below pH of 12.5. Moreover, the decalcification of CSH begins when CH has been depleted by the reaction in order to form brucite. According to Schmidte et al. (2008), more gypsum is present in concrete where leaching has occurred and therefore thaumasite will form slowly. Furthermore, the formation of more gypsum might imply the decalcification of CSH in the case of sulfate solution. The reason thaumasite does not form in DS-2 sulfate solution is the low sulfate concentration and the amount of magnesium, which would not cause the decomposition of CSH; therefore, thaumasite formation would be slow and small in extent in DS-2 solution. On the basis of a thermodynamic calculation in which not all factors were considered, Bellman (2004) reported that a sulfate concentration as low as 5mg/l is required to initiate TF at pH 12.5 but that 100-300 mg/l would be required at higher pH. Therefore, in the case of a low magnesium sulfate solution, a high concentration is needed to initiate thaumasite, and this might be an additional reason for a delay in thaumasite formation in DS-2 sulfate solution compared to DS-4 solution.

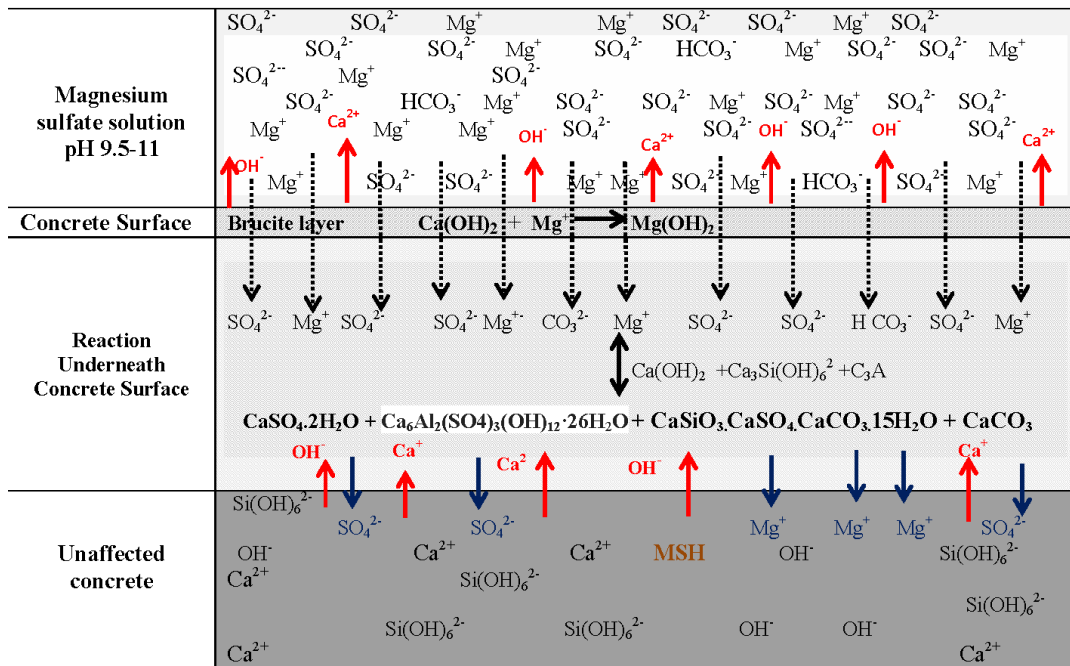


Figure 7.5: Schematic diagram of deterioration mechanism in sulfate solution

### 7.3.2 Exposure to pyritic clay

In the case of the clay used in this investigation, the continued oxidation of pyrite and the buffering reaction result in the generation of aggressive soluble sulfate and acidity, as explained in Equations 7.1 and 7.3. In addition, carbonic acid is available from the dissolution of atmospheric  $\text{CO}_2$  and from the buffering of sulfuric acid by calcite present in the clay. This results in a clay pore solution of pH 7-8. In turn, this would affect the degree of solubility of calcite and gypsum present in the clay, which would be high at pH of about 7-7.5 (as reported by Collette, 2003), and would result in increased availability of carbonate, bicarbonate and sulfate ions. In addition, sulfuric acid might react with clay minerals and liberate exchangeable cations such as K, Na and Mg, as reported by Czerewko and Cripps (2006). Under these conditions it is likely that the pH of pore waters in the concrete would be lowered to below 12.5 and as a consequence of CH and CSH would become unstable (Collins et al., 1987; He et al., 2011; Rasanen et al., 2003; McPolin et al., 2009). The high concentration of bicarbonate and carbonate ions and the pH environment would result in decalcification of CH and CSH, while the availability of sulfate and carbonate ions would create conditions for the formation of thaumasite by the direct route, as shown in the schematic diagram in Figure 7.6. In addition, the decomposition of C-S-H would increase the porosity of the concrete matrix and therefore allow more ions to penetrate into the concrete and extend the TSA, making the attack more severe.

This means that exposure to pyritic clay results in the formation of only thaumasite, and calcite, while gypsum and ettringite would be absent, which is a major difference between these tests and exposure to sulfate solutions (see Sections 4.3.1 and 5.3.2). Bellmann (2004) asserts that thaumasite might form directly from calcium hydroxide (CH) and C-S-H in the presence of sulfate and carbonate ions, which would limit gypsum production. Also, the high concentration of bicarbonate and carbonate ions derived from clay would affect the stability of ettringite and gypsum, resulting in their absence, as reported by Kunther et al. (2013) and Jenni et al. (2013). Therefore, the series of reactions in the clay–concrete interface increases the rate of deterioration in concrete exposed to the clay of design class DS-2, which was equivalent to or greater than the aggressivity of a DS-4 sulfate solution.

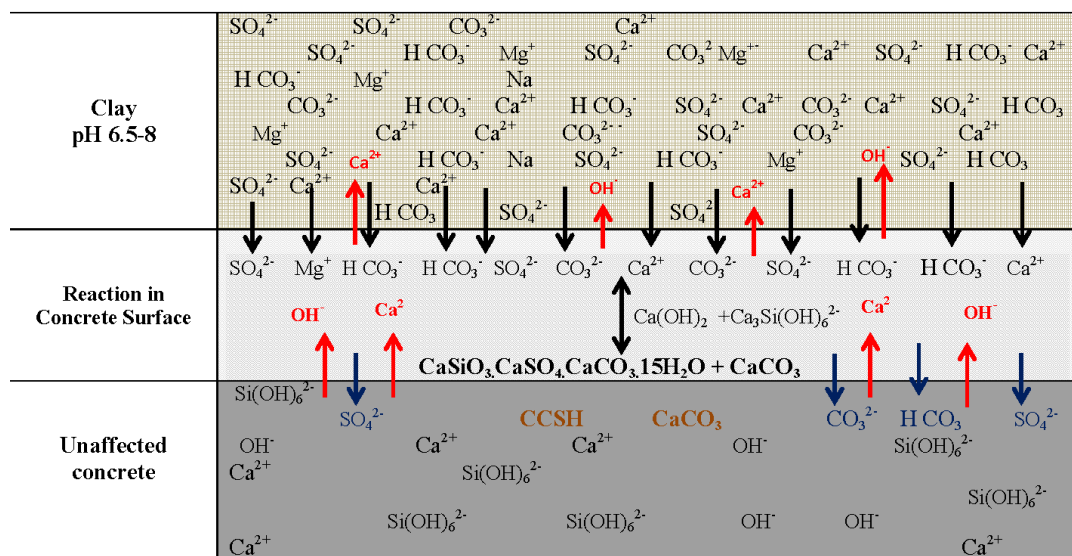


Figure 7.6: Schematic diagram of deterioration mechanism in Clay

The deterioration of concrete due to the formation of thaumasite via different routes in this study was confirmed by the visual observation of deteriorated cubes, as shown in Figure 7.7. The deterioration in cubes immersed in sulfate solution appears in the corners and edges, with thaumasite forming beneath the surface layer, which spalls over time. In contrast, all concrete skin was deteriorated and converted to mushy white material with exposure to clay and loss of bond to aggregate particles. Torres (2004) highlighted that in the presence of bicarbonate ions the deterioration readily forms in the surface concrete and forms a skin, while in its absence the thaumasite would form underneath the concrete surface. In addition, the attack in the case of exposure to clay was due solely to TSA, while thaumasite was found in the deteriorated material, whereas ettringite and gypsum were not detected. On the other hand, deterioration in the case of exposure to DS-4 sulfate solution was due to a combination of conventional and thaumasite forms of sulfate attack, in which thaumasite along with ettringite and gypsum were formed. This confirms that there are different routes of

thaumasite formation in sulfate solutions and clay, controlled by the presence of a high concentration of bicarbonate ions.

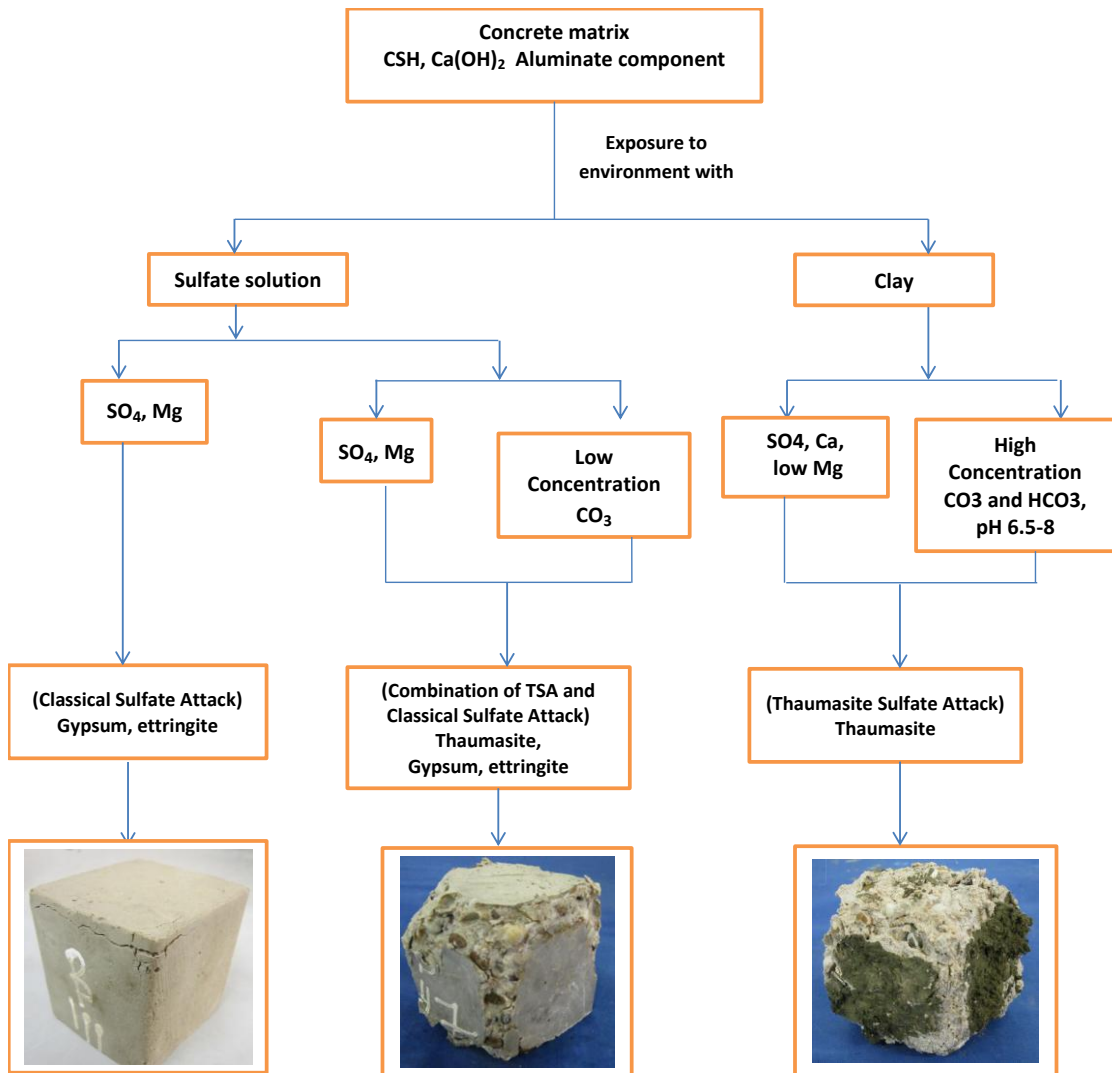


Figure 7.7: Flowchart of deterioration summarising deterioration products and deterioration modes in different exposure conditions

With reference to the role of pH in thaumasite formation and the stability of thaumasite, thaumasite is formed at pH higher than 10.5 and becomes metastable at pH below this value (Jalled, 2003). In this investigation, the pH of the Lower Lias Clay and Coal Measures mudstone was between 7 and 8, and severe attack due to thaumasite formation occurred. The effect of the pH of the surrounding environment results in lowering the pH of the concrete pore solution through the ingress of a high concentration of bicarbonate derived from clay or a high concentration of magnesium in the case of exposure to magnesium sulfate solution. This might accelerate the decomposition of CSH and make the attack severe. This supports the finding by Hartshorn et al. (1999), who suggested that thaumasite

can form below 10.5 when C-S-H is unstable. Liu et al. (2013) stated that low pH favours TF and high pH is an essential factor for TSA.

#### 7.4 UK guidance on assessment of aggressive ground

The reason why concrete is more vulnerable to TSA when it is in contact with clay rather than the equivalent solution is not clear, since most reported investigations are based upon laboratory studies involving the immersion of concrete specimens in test sulfate solutions, which might be magnesium sulfate or sodium sulfate or a combination of both. However, the Building Research Establishment (BRE) has introduced updated guidance for aggressive ground assessment in the form of BRE SD1:2005. Both this and the previous guidance, BRE SD1:2001, which are shown in Tables 7.1 and 7.2, base the assessment on water-soluble sulfate and the total potential sulfate (TPS) value. On the other hand, the effect of carbonate in the aggregate was considered in the 2001 version, while it was omitted from the 2005 version, because of the minimal effect it was thought to have on thaumasite formation. The British Standard for guidance in specifying concrete in aggressive conditions, BS 8500-1:2006, adopted the recommendations in BRE SD1:2005 for the assessment of aggressive ground conditions and specification of concrete designed to resist the attack. However, the effect of carbonate present in the clay as an external source of carbonate, as well as other species such as Ca, Na, Cl and K, was not included in the assessment of the aggressive chemical environment for concrete (ACEC) (BRE SD-1, 2005).

Table 7.1: Design sulfate classes in BRE SD1:2001 (BRE, 2001)

Design Sulfate Class for site	2:1 water/soil extraction		Ground water		Total Potential Sulfate SO4 %	Groundwater		ACEC Class For site
	SO4 Mg/l	Mg Mg/l	SO4 Mg/l	Mg Mg/l		Static Water	Mobile Water	
						pH	pH	
DS-1	<1200	-	<400	-	<0.24	All pH values		AC-1s
							>5.5	AC-1
							≤5.5	AC-2z
DS-2	1200-2300	-	400-1400	-	0.24-0.6	>3.5		AC-1s
							>5.5	AC-2
							≤3.5	AC-2s
DS-3	2400-3700	-	1500-3000	-	0.7-1.2		≤5.5	AC-3z
						>3.5		AC-2s
							>5.5	AC-3
DS-4	3800-6700	≤ 1200	3100-6000	≤ 1000	1.3-2.4		≤5.5	AC-3s
						>3.5		AC-4
							>5.5	AC-4
DS-5	>6700	≤ 1200	>6000	≤ 1000	>2.4		≤5.5	AC-4s
						>3.5		AC-5
							≤5.5	AC-5
						>3.5		AC-4s
						≤3.5	All pH values	AC-5

Table 7.2: Design sulfate classes in BRE SD-1:2005 (BRE 2005)

Sulfate				Groundwater		ACEC class for location
Design Sulfate Class for location	2:1 water/soil extract <sup>b</sup>	Groundwater	Total Potential sulfate <sup>a</sup>	Static water	Mobile water	
1	2	3	4	5	6	7
	SO <sub>4</sub> mg/l	SO <sub>4</sub> mg/l	SO <sub>4</sub> %	pH	pH	
DS-1	<500	<400	<0.24	≥2.5		AC-1s
					>5.5 <sup>d</sup>	AC-1 <sup>d</sup>
					2.5-5.5	AC-2z
DS-2	500 - 1500	400 - 1400	0.24-0.6	>3.5		AC-1s
					>5.5	AC-2
					2.5-3.5	AC-2s
					2.5-5.5	AC-3z
DS-3	1600 - 3000	1500 - 3000	0.7-1.2	>3.5		AC-2s
					>5.5	AC-3
					2.5-3.5	AC-3s
					2.5-5.5	AC-4
DS-4	3100 - 6000	3100 - 6000	1.3-2.4	>3.5		AC-3s
					>5.5	AC-4
					2.5-3.5	AC-4s
					2.5-5.5	AC-5
DS-5	>6000	>6000	>2.4	>3.5		AC-4s
				2.5-3.5	≥2.5	AC-5

The results given in Section 6.4.3 for the composition of pore water showed that a high concentration of carbonate ions, thought to be derived from the dissolution of calcite in the clay and to be a consequence of atmospheric CO<sub>2</sub> dissolution, led to a decrease in pH of the clay pore. It is likely that the increase in K, Mg and Na with time described in Section 6.4.3 would have been the result of the action of acid produced by pyrite oxidation on clay minerals, as reported by Czerewko and Cripps (2006). On the other hand, significant deterioration was observed in clay in which the analysis of pore water showed a high concentration of sulfate, calcium, and carbonate and bicarbonate ions. It is suggested that sulfate, calcium, and carbonate and bicarbonate ions were found to be the main species that might influence the severity of deterioration. Therefore, as shown in this work, it is not enough for the assessment of ground aggressivity in terms of TSA to consider only the total potential sulfate and magnesium. In addition, neglecting the effect of carbonate available in the clay as well as water-soluble calcium might lead to an underestimation of the aggressive chemical environment for concrete (ACEC) classification.

According to BRE SD-1 (2005), the highest value of water soluble sulfate of clay and groundwater is considered in the determination of design sulfate class. On the other hand, in case of clay that contains large amount of gypsum and small amount of pyrite in presence of ground water, significant reduction occurs in water-soluble sulfate and total sulfur, which total potential sulfate decreased accordingly. The results of water- and acid-soluble sulfate given in Sections 6.2.2, 6.2.3 and 6.4.2 showed the dissolution of gypsum and other soluble sulfate components in simulated groundwater, which would underestimate the design sulfate



class of Lower Lias Clay. For example, in weathered Lower Lias Clay, the design sulfate class before exposure to simulated groundwater was DS-3, while after exposure the water-soluble design sulfate class was reduced to DS-1 and the design sulfate class according to total potential sulfur was reduced to DS-2. On the other hand, the design sulfate class of simulated groundwater was found to be DS-3. Therefore, consideration of the highest concentration of sulfate from clay or groundwater would underestimate the actual design sulfate class required for the design of concrete to withstand aggressive conditions, which in this case should be DS-3. Therefore, it is suggested that the design sulfate class of clay that has a high amount of gypsum and a low amount of pyrite should be based on the water-soluble sulfate of clay plus the sulfate concentration of groundwater. Overall, on the basis of the arguments above, the UK guidance for the assessment of aggressive ground conditions with regard to the thaumasite form of sulfate attack should take into consideration the presence of a carbonate source in the clay, dissolved bicarbonate ions and calcium. The ACEC classification should be increased to a minimum of AC-3 where high concentrations of carbonate, bicarbonate and calcium are available in the ground.

According to the recommendations in BRE SD-1: 2005 and BS: 8500 (2006), both the SRPC concrete and the 25% PFA replacement concrete tested in nine years' exposure to clay of aggressivity (ACEC) AC-4 would be expected to resist attack, but as explained in Section 4.1.1 significant deterioration was observed. Furthermore, although the 50% PFA replacement and 70% GGBS concretes recommended for use in ground conditions of the aggressivity used in the tests were not affected by TSA after two years of exposure, thaumasite solid solution was detected, which suggests that attack could occur in long-term exposure to aggressive ground that has sufficient sulfate, carbonate and calcium. Although the Ca/Si ratio in these concretes is low, which is according to Pouya (2007) would reduce the possibility of thaumasite formation, the calcium required for thaumasite formation can be derived externally from clay. The findings in this study are supported by Abualgasem et al. (2013), who found that thaumasite formed in 70% GGBS cement powder, which implies that controlling permeability and porosity by using a high percentage replacement of GGBS, rather than cement chemistry, is the main factor in preventing TSA. In addition, controlling concrete quality by reducing the water-to-binder ratio or cement content may retard thaumasite formation but would not necessarily prevent it. However, by reducing the amount of water and aggressive species penetrating the concrete, using a bitumen coating, (even if damaged), was an effective barrier in protecting all concretes, including PLC concrete, from attack in the aggressive ground conditions created in this investigation. Therefore, providing surface protection by using a coating might protect concrete against TSA, regardless of concrete type.



According to the discussion on the review of the current UK guidance (BRE SD-1, (2005) and BS8500, (2006)) on the assessment of aggressive ground presented in this thesis (Chapter 7, pages 218 to 220), the results of this investigation suggest that the current guidance would underestimate ground aggressivity. This would imply that some concrete mixes made according to current specifications given in BRE SD-1, (2005) and BS8500, (2006), would be vulnerable to thaumasite formation and the thaumasite form of sulfate attack. Therefore, it is suggested that the current specifications given by BRE SD-1, (2005) and BS8500, (2006) should be modified or supplemented as shown in Tables 7.3 and 7.4. Furthermore, it would appear that there are important factors additional to those already considered that need to be considered in the classification of potentially chemically aggressive ground conditions.

Table 7.3: Review UK guidance for the classification of aggressive ground

Aspects	Guidance	Section	Current recommendations	Recommended Key Changes
<b>Classification of site location for chemical aggressive to</b>	<i>BRE SD-1, 2005.</i>	<i>Part C, C5 Table C1,C2</i>	<ul style="list-style-type: none"> <li>Classification is based on Mg and SO<sub>4</sub>. This would underestimate the assessment of ground aggressivity with regard to TSA.</li> </ul>	Concentration of carbonate (CO <sub>3</sub> ), bicarbonate (HCO <sub>3</sub> ) and calcium (Ca) derived externally from ground should be included in the classification of site aggressivity. In this work the aggressivity was probably underestimated by approximately one class whereas the corresponding amount of CO <sub>3</sub> 620 mg/l.
	<i>BS 8500, 2006</i>	<i>Section A.2 Table A.2</i>	<ul style="list-style-type: none"> <li>Classification according to water soluble is based on the higher of the concentrations of sulfate in either groundwater or clay. In case of clay that contains large amount of gypsum and small amount of pyrite in presence of ground water, significant reduction occurs in water-soluble sulfate and total sulfur, which total potential sulfate decreased accordingly. This would underestimate the design sulfate class.</li> </ul>	It is suggested that the design sulfate class of clay that has a high (> 0.8 %) amount of gypsum and a low amount of pyrite should be based on the water soluble sulfate of clay plus the sulfate concentration of groundwater, rather than using the acid soluble sulfate, which is in effect the gypsum content.

Table 7.4: Review the UK guidance for concrete in aggressive ground

Aspects	Guidance	Section	Current recommendations	Recommended Key Changes
<b>Specifying concrete for general cast – in-situ use</b>	<i>BRE SD-1,2005</i>	<i>Part D, D4 Table D1</i>	<ul style="list-style-type: none"> <li>• Design Chemical class (DC) and Aggressive Chemical Environment for Concrete (ACEC) are based on Tables C1 and C2.</li> </ul>	<p>Recommendations on these tables should be amended according to the changes in Tables C1 and C2 after considering carbonate and calcium supplied externally from clay. In addition, in case of DS-1 sulfate class in the presence of high concentration of carbonate the ACECE should be restricted to AC-3, rather than AC-1 in the present specification.</p>
	<i>BS 8500, 2006</i>	<i>Section A.4.4 Table A.9</i>		
	<i>BRE SD-1,2005</i>	<i>Table D2 and D3</i>	<ul style="list-style-type: none"> <li>• CEMI, CEM II (PLC), SRPC, CEMI-25%PFA are Recommended in case of exposure to aggressive ground conditions.</li> </ul>	<p>Unless additional protective measures are used CEMI, CEM II (PLC) and SRPC should be excluded from the recommended mixes for resistance of TSA as that are all vulnerable to severe thaumasite sulfate attack, . CEMI +25% PFA may also be subject to attack, but the rate of deterioration is slower.</p>
<i>BS 8500, 2006</i>	<i>Section A.4.2 Tables A.6, A.7 and A.11</i>			
<i>BRE SD-1,2005</i>	<i>Section D.6, Table D4</i>	<ul style="list-style-type: none"> <li>• coating as additional protection measures is only recommended for design sulfate class DS-5</li> </ul>	<p>The limited data on the use of coatings in this research suggest that current guidance should be changed to recommend consideration of coating as additional protection measures for all conditions including and more aggressive than DS-2. Only bitumen was investigated in this research whereas other different types of coating might be considered. Further research is required to assess the capabilities of different coating systems in typical ground conditions.</p>	
<i>BS 8500, 2006</i>	<i>Section A.4.4, Table A.10</i>			

## CHAPTER 8

### 8. Conclusions and Recommendations for Future Work

#### 8.1 Overall conclusions

A number of points have been raised in this laboratory investigation into the influence of clay composition on the extent of TSA in buried concrete. A number of issues regarding the long-term performance of concrete exposed to aggressive sulfate-rich ground conditions at low temperature, with and without pozzolanic materials, have also been investigated. The study examined the compositional changes of weathered and slightly weathered Lower Lias Clay and Coal Measures mudstone resulting from interaction with different concretes in the presence and absence of mobile groundwater at temperatures of 5° and 20°C, as well as changes in the groundwater chemistry with time. The main conclusions that can be drawn from the work carried out in the thesis are presented in this section.

From the literature review described in Chapter 2 the following conclusions can be drawn:

- An extensive search of the literature revealed very few studies into the interaction between buried concrete and pyrite-rich clays. This is in spite of the widespread occurrence of such clays, as noted by Czerewko and Cripps (2006), and the huge number of buried concrete structures. It would appear that only one field investigation has yet been carried out to assess the performance of buried concrete (Crammond et al, 2003).
- The mechanism by which concrete becomes more vulnerable to TSA when it is in contact with clay rather than the equivalent solution is not clear. Therefore, there is an urgent need to deepen our understanding of the mechanism of TSA in buried concrete exposed to pyritic ground.
- The recommendations contained in BRE SD1 (2005) and similar standards are based upon laboratory studies involving the immersion of concrete specimens in test sulfate solutions, which might be magnesium sulfate or sodium sulfate or a

combination of both. In addition, the current guidance and standards do not take into account the influence of carbonate from clay in the assessment of clay aggressivity with regard to TSA. However, there is no laboratory study of TSA in simulated field conditions in which the influence of the chemical composition of clay on thaumasite formation and the extent of TSA has been considered. Moreover, there is no technical investigation into the role of sulfuric acid produced by pyrite oxidation in pyritic clay containing calcite in its composition on thaumasite formation and the extent of TSA. Therefore, an investigation into these aspects is required.

- There is uncertainty about the performance of SRPC and PFA blended concrete in ground conditions conducive to TSA. No studies are currently reported into the long-term performance of BRE-recommended binders (SD-1, 2005) such as SRPC, PC with 25% and 50% PFA replacement, and PC with 70% GGBS.
- This laboratory study appears to be the first to describe TSA deterioration in buried concrete in simulated field conditions.

### **8.1.1 Long-term interaction between concrete and Lower Lias Clay**

The main aim of the long-term study into the interaction of concrete with Lower Lias Clay was to investigate the long-term performance of different buried concretes with regard to TSA and the effect of burial depth on the extent of TSA, and to assess the effectiveness of bitumen coating as a protective measure against TSA. The results from this study showed severe deterioration after nine years of exposure to clay. The major findings can be summarised as follows:

- Deterioration due to the thaumasite form of sulfate attack occurred in PC, PLC, SRPC, and PC-25% PFA concretes, with PLC concrete being the worst affected. The thickness of thaumasite deterioration in the concretes over the nine-year exposure period was as follows (in mm): PLC = 47; PC = 33; SRPC = 22; PC-PFA = 10. The study also affirmed the susceptibility to thaumasite sulfate attack (TSA) of both PC-25% PFA replacement and SRPC concretes. It seems that 25% PFA replacement would not prevent deterioration due to TSA, although it was observed that the attack occurred more slowly.
- The extent of concrete deterioration decreased with increased depth of burial below the clay surface; the most severe attack was in the upper 100 mm. This was probably due to increased access to air at shallow burial depth. In addition, less sulfate and

fewer carbonate ions were found to have penetrated the concrete as burial depth increased; this would also tend to reduce the extent of attack. This may be due to reduced concentration of ions in the pore water or to lower porosity of clay at greater depth, which would reduce both the severity of attack and the flow of ions between the clay and the concrete.

- Bitumen coating had been applied to certain faces of the samples, and it was found that only unprotected concrete faces in contact with clay suffered TSA. Thus, the bitumen coating, even if damaged, was an effective barrier in protecting all concretes, including the PLC concrete, from attack in the aggressive ground conditions created in this investigation. Therefore, surface protection using bitumen coating might protect concrete against TSA, regardless of concrete type.

### **8.1.2 Influence of clay aggressivity on the extent of TSA on different concretes**

Field conditions were simulated, while a relatively W/B ratio (0.6) was used for concrete in order to accelerate the penetration of species derived externally from clay and increase the reaction of thaumasite formation during the limited period of PhD investigation. The results of the investigation of the effect of the chemical composition of clay on the severity of TSA revealed that clay is more aggressive than a sulfate solution of a similar BRE design sulfate class. The following conclusions can be made:

- The degree of deterioration of concrete exposed to various conditions decreased as follows: slightly weathered Lower Lias Clay > weathered Lower Lias Clay > DS-4 sulfate solution > Coal Measures mudstone > simulated pore solutions >> DS-2 sulfate solution. The degree of deterioration was less at 20°C than that at 5°C in the case of exposure to sulfate solutions.
- Although Lower Lias Clay contains water-soluble sulfate corresponding to BRE sulfate class DS-2, it was found that concrete exposed to LLC with water-soluble design sulfate class DS-2 at 5° and 20°C deteriorated at a faster rate than corresponding specimens in DS-2 solution and at a similar rate to or faster than those exposed to the DS-4 sulfate solution. In addition, simulated solutions of equivalent aggressivity to the clays used in the study do not fully represent the exposure conditions. Therefore, clay compositions play an important role in thaumasite formation and severity of thaumasite sulfate attack. The attack could exceed what might be observed in concrete exposed to equivalent standard test

solutions and may be enhanced by chemical reactions that occur during pyrite oxidation processes, which are absent in standard test solutions.

- The form of deterioration of disintegrated concrete was different in the cases of exposure to clay and to sulfate solutions. Deterioration commenced at the edges and corners and was accompanied by cracks and spalling in the corners in the case of DS-4 sulfate solution and simulated clay pore solutions, while in Lower Lias Clay most of the concrete faces deteriorated and were converted to white mushy material. Moreover, XRD, IR and SEM analyses of deterioration products of CEMI and CEM-LF replacement concretes revealed that degradation was solely due to TSA in the case of interaction with clays at both temperatures, while thaumasite, ettringite and gypsum were the main deterioration products in DS-4 sulfate and simulated clay pore solutions at 5°C. However, ettringite and gypsum were formed in DS-2 solution at 5° and 20°C, which implies that different routes of deterioration due to TSA occurred.
- Although replacement with 50% PFA and 70% GGBS revealed very good performance, as no deterioration was observed in any of the exposure conditions used in the study, thaumasite solid solution was detected in 50% PFA and GGBS concrete exposed to pyritic clay at 5°C in the XRD and SEM analyses, which implies the susceptibility of those concretes to thaumasite formation if exposed to aggressive clays for longer periods.
- The sulfuric acid resulting from pyrite oxidation seems to play an important role in accelerating TSA in the presence of carbonate. It leads to lower pH of clay (between 7-8), which results in decomposition of CSH. This, together with the availability of sulfate and carbonate species in the clay, increases the propensity for the formation of thaumasite.

### 8.1.3 Mineralogical and chemical changes to clay

The main aim was to investigate the aggressivity resulted from chemical changes in different clays. The determination of the composition of different clays confirmed that pyrite oxidation occurred and that calcite and clay minerals were involved in reactions with the acid. The main findings are as follows:

- A reduction of pH occurred due to the oxidation of pyrite, which resulted in the production of sulfuric acid. In addition, the presence of bicarbonate and weak carbonic acid from the dissolution of calcite present in the clay as well as from

atmospheric CO<sub>2</sub> in the clay pore solution might be an additional reason for the reduction of clay pH over time. However, the pH values of clay were neutral (7-8) after weathering, as a result of the buffering of acid by calcite present in the clay.

- The concentrations of water- and acid-soluble sulfate in both Lower Lias Clays and Coal Measures mudstone after twelve months of weathering were higher at 20°C than at 5°C. However, significant reductions in water- and acid-soluble sulfate values were observed in Lower Lias Clays in the presence of mobile water, as a result of the dissolution of more gypsum in the groundwater.
- There is a relationship between the amount of oxidised pyrite, the reduction in total sulfur and the severity of attack due to TSA, in which the lower total sulfur and the high amount of oxidised pyrite found in clay where concrete has suffered from severe attack suggests that more sulfate penetrates into concrete and engages in thaumasite formation.
- The supersaturation of the clay pore solution with sulfate might reduce the rate of pyrite oxidation in the case of weathered Lower Lias Clay, while the lower amount of gypsum available in slightly weathered Lower Lias Clay and Coal Measures mudstone would explain why the higher rate of pyrite oxidation occurred. In addition, the presence of sodium in the case of Coal Measures mudstone was an additional reason for increased pyrite oxidation. However, incomplete buffering of acid due to mobile groundwater might cause a variation of pH values within the clays. This would reduce the rate of oxidation by restricting the oxidation of ferrous iron to ferric iron.
- The amount of calcite consumed in the buffering reaction derived from theoretical calculation is lower than that measured experimentally in all clays, which suggests that more calcite was dissolved in the clay pore solution and in simulated groundwater. Therefore, calcite in the clay is considered to be the external source of carbonate and bicarbonate ions required for thaumasite formation and TSA.
- The analysis of groundwater in different pyritic clays revealed that calcium, sulfate and carbonate ions were the dominant factors in weathered Lower Lias Clay, slightly weathered Lower Lias Clay and Coal Measures mudstone that might influence the severity of deterioration due to TSA. However, in Coal Measures mudstone, sodium and chloride leached into groundwater and penetrated the concrete, preventing other



species from penetrating to form thaumasite, and possibly delaying the progress of deterioration due to TSA.

- The results of this investigation reveal that, in the assessment of ground aggressivity in terms of TSA, it is not sufficient to consider only total potential sulfate and magnesium. In addition, neglecting the effect of carbonate available in the clay as well as water soluble calcium might lead to an underestimation of the ACEC (aggressive chemical environment for concrete) classification.

## 8.2 Implications of results for research and engineering

This research has provided new data on the long-term performance of SRPC concrete and concrete incorporating pozzolanic cementitious materials in aggressive ground conditions. The key implications of this research for engineering practice and for guidance on the assessment of aggressive ground in respect of TSA are as follows:

- According to BRE SD-1 (2005), SRPC concrete may be used in aggressive ground conditions to resist deterioration by TSA. However, the results of the long-term exposure to aggressive clay showed the vulnerability of buried SRPC concrete to TSA. The low  $C_3A$  formulation of SRPC is designed to control the formation of ettringite; however, CSH binder is susceptible to attack by TSA such that SRPC concrete is susceptible to TSA. Similarly, 25% PFA replacement of PC, as specified by recommendations in BRE SD-1 (2005), does not appear to provide protection against TSA in exposure to Lower Lias Clay, although TSA develops at a slower rate.
- High replacements of 50% PFA and 70% GGBS in concrete mixes provide very good performance in short-term exposure to Lower Lias Clay, but the presence of thaumasite solid solution products in the cement matrix suggests that these concretes may suffer from deterioration due to TSA after long-term exposure (over tens of years) to high concentrations of carbonate, bicarbonate and sulfate ions.
- According to the results from Long-term concrete-clay interaction with regard to the effect of burial depths on the extent of TSA, the degree of compaction and the permeability of landfill should be considered in the assessment of the vulnerability of buried concrete to TSA.
- The availability of a high concentration of dissolved carbonate from clay increases the possibility of thaumasite formation in comparison to a solution containing the

same level of sulfate. The external source of carbonate derived from the clay should be considered in the guidance for assessing the aggressivity of ground with regard to TSA, as deterioration due to TSA occurred in concretes without an internal source of carbonate.

- According to BRE SD-1 (2005) and BS 8500 (2006), the assessment of aggressive ground is based on soluble sulfate, the presence of magnesium and the total potential sulfate of the ground. This study shows the importance of sulfate, calcium and bicarbonate ions in the severity of deterioration. It is suggested that the assessment of ground aggressivity needs also to include the carbonate and water-soluble calcium contained in the clay as well as total potential sulfate and magnesium; therefore, the ACEC classification should be modified accordingly.
- Controlling concrete quality by the use of concrete with lower water-to-binder ratio or lower cement content may retard thaumasite formation but may not prevent it. In this study, thaumasite solid solution was found in concretes made with 50% PFA and 70% GGBS, which would indicate possible vulnerability to thaumasite formation and TSA in conditions of long-term exposure to aggressive ground conditions. Therefore, a combination of pozzolanic binder and surface protection may provide greater confidence in the performance of concrete in aggressive environments.
- According to BRE SD-1 (2005), the highest value of water soluble sulfate of clay and groundwater is considered in the determination of design sulfate class. On the other hand, in case of clay that contains large amount of gypsum and small amount of pyrite in presence of ground water, significant reduction occurs in water-soluble sulfate and total sulfur, which total potential sulfate decreased accordingly. However, this would underestimate the design sulfate class, as found in this study. Therefore, it is suggested that the design sulfate class of clay that has a high amount of gypsum and a low amount of pyrite should be based on the water-soluble sulfate of clay plus the sulfate concentration of groundwater.

### **8.3 Recommendations for further work**

The limitations of this study are associated with the limited time available for a PhD programme, especially when the long-term durability of concrete is examined in real environmental conditions. On the basis of the results obtained in this research, the following areas are suggested for further study:

- There is uncertainty about the long-term performance of 50% PFA and 70% GGBS blended concrete subject to aggressive clay. Therefore, it is recommended that a long-term investigation should be carried out, along with the application of thermodynamic modelling, for the assessment of a high percentage replacement of cement with PFA and GGBS, and to determine whether the resistance of these cements is due to their chemical or physical properties.
- Geochemical modelling based upon chemical equilibrium between the clay, concrete and pore fluids should be performed to estimate the concentrations of carbonate ions and calcium derived from clay that might contribute in the reaction of thaumasite formation and the progress of TSA.
- Using image analyses techniques as a method of deterioration quantification due to TSA.
- Study the effect of changes in clay minerals on the extent of thaumasite sulfate attack.
- An investigation is recommended into the formation of thaumasite in carbonated concrete exposed to pyritic clay with a high concentration of bicarbonate ions, in which decomposition of the carbonate layer might occur due to reduction in the pH of the concrete pore solution, and provides an additional source of carbonate for thaumasite formation.
- The guidance regarding the control of TSA should be developed on the basis of geochemical modelling and the results found in this investigation, in considering the carbonate, calcium and chloride source derived from clay and the effect of mobile groundwater and degree of backfill compaction.
- Surface protection was found to be an effective way to protect concrete in aggressive chemical conditions. Therefore, investigations on the durability of different coating systems in long-term exposure to various chemicals and also to probable physical damage are essential.
- The influence of chemical changes in pyritic clay on the physical properties of clay, which may affect the foundation design, should also be investigated

## REFERENCES

Abualgasem J.M., Cripps J.C. and Lynsdale C.J. (2013) Thaumasite formation in GGBS cement powders. 33rd Cement and Concrete Science Conference 2013 (pp 269-272). Portsmouth, UK, 2 September 2013 - 3 September 2013.

Abubaker F., Lynsdale, C.J. and Cripps, J.C. (2014) Laboratory Study of the Long-Term Durability of Buried Concrete Exposed to Lower Lias Clay. *Construction and Building Materials*, 64:120-130

Aguiar, J.B., Camoes, A. and Moreira, P.M. (2008) Coating for concrete protecting against aggressive environments. *Journal of Advanced Concrete Technology*, 6(1):243-250.

Almusallam A, Khan FM, and Maslehuddin, M. (2002) Performance of concrete coatings under varying exposure conditions. *Material and Structures*, 35:487-494.

Anstice, D.J., Page, C.L. and Page, M.M. (2005) The pore solution phase of carbonated cement pastes. *Cement and Concrete Research*, 35: 377- 383.

Ariyaratne. (2008) *Acid Sulfate Soil: Concrete structures-Advices for design and construction*. RTA Bridge Engineering- policy and specifications. Review Report, 3<sup>rd</sup> Edition (CC:BTD 2008/12). May 2008.

Arkesteyn, G.J. (1980) Pyrite oxidation in acid sulphate soils: the role of microorganisms. *Plant and Soil*, 54:119-134.

Barnett, S.I., Halliwell, M.A., Crammond, N.I., Adam, C.D. and Jackson, A. R. W. (2002) Study of thaumasite and ettringite phases formed in sulfate blast furnace slag slurries using XRD full pattern fitting. *Cement and Concrete Composites*, 24, (4):339-346

Bassuoni, M.T. and Nehdi, M.L. (2007) Resistance of self-consolidating concrete to sulfuric acid attack with consecutive pH reduction. *Cement and Concrete Research*, 37(7):1070-1084.

Belie N.D., Moneteny, A., Beeldens, A., Vincke, E., Gemert, D. and Verstraete, W. (2004) Experimental research and prediction of the effect of chemical and biogenic sulphuric acid on different types of commercially produced concrete sewer pipes. *Cement and Concrete Research*, 34(12):2223-236.

Bellmann, F. (2004) On the formation of thaumasite  $\text{CaSiO}_3 \cdot \text{CaSO}_4 \cdot \text{CaCO}_3 \cdot 15\text{H}_2\text{O}$ : Part I, *Advances in Cement Research*, 16 (2): 55-60.

Bellmann, F. (2007) "On the formation of thaumasite  $\text{CaSiO}_3 \cdot \text{CaSO}_4 \cdot \text{CaCO}_3 \cdot 15\text{H}_2\text{O}$ : Part III". *Advances in Cement Research*, 19 (4):139-146.

Bellmann and Strak, J. (2007) Prevention of thaumasite in concrete exposed to sulphate attack. *Cement and Concrete Research*, 37(8):1215-1222.

Bellmann, F. and Strak, J. (2008) The role of calcium hydroxide in the formation of thaumasite. *Cement and Concrete Research*, 38(10):1154-1161.

Bensted, J. (1998) Scientific background to thaumasite formation in concrete, *World Cement Research*, 29 (11): 102-105

## References

---

- Bensted, J. (1999) Thaumasite-direct, woodfordite and other possible formation routes. *Cement and Concrete Composites*, 25(3):873-877.
- Bensted, J. (2003) Thaumasite-direct, woodfordite and other possible formation routes. *Cement and Concrete Composites*, 25(3):873-877.
- Black, L., Garbev, K. and Gee, I. (2008) Surface carbonation of synthetic C-S-H samples: A comparison between fresh and aged C-S-H using X-ray photoelectron spectroscopy. *Cement and Concrete Research*, 48:735-740
- Blanco-Varela, M.T., Aguilera, J. and Martinez-Ramirez, S. (2006) Effect of cement C<sub>3</sub>A content, temperature and storage medium, on thaumasite formation in carbonated mortars. *Cement and Concrete Research*, 36:707-715.
- Borges, P.H.R., Costa, J. O., Milestone, N. B., Lynsdale, C.J. and Streatfield, R.E. (2010) Carbonation of CH and C-S-H in composite cement pastes containing high amounts of BFS. *Cement and Concrete Research*, 40(2): 284-292.
- British Standards Institution, (1988) BS 1881-124. *Testing concrete: Methods for analysis of hardened concrete*. London, UK.
- British Standards Institution, (1990) BS 1377-3. *Methods of test for soils for civil engineering purposes. Part 3: Chemical and electro-chemical tests*. London, UK.
- British Standards Institution, (2000) EN 197-1. *Cement-part 1: Composition specifications and conformity criteria for common cements*. London, UK
- British Standards Institution, (2002) BS EN 12620:2002+A1. *Aggregate for concrete*. London, UK
- British Standards Institution, (2005) *Fly ash for concrete: Definition, specifications and conformity criteria*. BS EN 450-1:2005+A1:2007.
- British Standards Institution, (2005) BS 4551:2005+A2:2013. *Mortar: Methods of test for mortar and screed: Chemical analysis and physical testing*. London, UK
- British Standards Institution, (2006) *Ground granulated blast furnace slag for use in concrete, mortar and grout: Definitions, specifications and conformity criteria*. BS EN 15167-1:2006
- British Standards Institution, (2006) BS 8500-1:2006+A1:2012. *Concrete – Complementary British Standard to BS EN 206-1 – Part 1: Method of specifying and guidance for the specifier*. London, UK
- British Standards Institution, (2011) BS EN 197-1:2011. *Cement: Composition, specifications and conformity criteria for common cements*. London, UK
- Brown, P.W. and Doerr, A. (2000) Chemical changes in concrete due to the ingress of aggressive species. *Cement and Concrete Research*, 30(3):411-418.
- Brown, P.W., Hooton, R.D., and Clark, B.A. (2003) The co-existence of thaumasite and ettringite in concrete exposed to magnesium sulfate at room temperature and the influence of blast-furnace slag substitution on sulfate resistance , *Cement and Concrete Composites*, 25 (8):939-945.

## References

---

Byars, E., Sharp, J., Lynsdale, C.J., and Cripps, J.C. (2003) *Thaumasite formation by combined acid and sulfate attack of concrete, Final Report*, Centre for Cement and Concrete, University of Sheffield, September 2003.

Building Research Establishment (2001) *Concrete in aggressive ground. Part I: assessing the aggressive chemical*. BRE Special Digest, CRC, 2001.

Building Research Establishment (2005) *BRE Special Digest I: Concrete in Aggressive Ground*. 3<sup>rd</sup> Edition, BRE, Watford. June 2005.

Brueckner, R. (2007) *Acceleration the Thaumasite Form of Sulfate Attack and an Investigation of its Effect on Skin Friction*. PhD thesis, Faculty of Engineering. The University of Birmingham, July, 2007, UK.

Brueckner R., Williamson, S.J. and Clark, L.A. (2012) Rate of the thaumasite form of sulfate attack under laboratory conditions. *Cement and Concrete composite*, 34:365-369.

Brueckner R., Williamson, S.J. and Clark L.A. (2012) The effects of the thaumasite form of sulfate attack on skin friction at the concrete/clay interface. *Cement and Concrete Research*, 42 :424-430.

Caldeira, C.L., Ciminelli, V.S.T., and Osseo-Asare, K. (2003) Pyrite oxidation in alkaline solutions: nature of the product layer. *International Journal of Miner Process*, 72: 373 – 386.

Caldeira, C.L., Ciminelli, V.S.T., and Osseo-Asare, K. (2010) The role of carbonate ions in pyrite oxidation in aqueous systems. *Geochimica et Cosmochimica Acta*, 74: 1777–1789.

Choi, C.S., Lee, S.T., Hobton, R.D., Jung, H.S. and Park, D.H. (2008) Effect of limestone filler on the deterioration of mortars and pastes exposed to sulphate solution at ambient temperature. *Cement and Concrete Research*, 38(1):68-76.

Clark, L.A. (1999) *Thaumasite Expert Group, The thaumasite form of sulfate attack: Risks, diagnosis, remedial works and guidance on new construction*, Department of the Environment, Transport and Regions: Rotherham, UK. 1999

Clark, L.A. (2002) *Thaumasite Expert Group Report: Review after Three Years Experience*. BRE Technical report, Building Research Establishment. Watford, UK, March 2002.

Clark, B. and Brown, P.W. (2000) The Formation of calcium sulfoaluminate hydrate compounds :Part II. *Cement and Concrete Research*, 30(2):233-240.

Cohen, M.D., (1984) Reply to discussion of " of expansion in sulfoaluminate - type expansion cements: Schools of thought", *Cement and Concrete Research*, 14: 610-612

Cohen, M.D. (1983) Theories of expansion of sulfoaluminate - type expansive cements: Schools of thought, *Cement and Concrete Research*, 13 (6): 809-818.

Collete, G., Crammond, J.N., Swamy, R.N. and Sharp, J. (2004) The role of carbon dioxide in the formation of thaumasite. *Cement and Concrete Research*, 34: 1599–1612.

Collins. R.J. (1987) Carbonation comparison of results for concretes containing PFA, cementitious slag ,or alternative aggregates, *Materials Science and Technology*, 3:986-992.

## References

---

Crammond, N.J. and Nixon, P.J. (1993) Deterioration of concrete foundation piles as a result of thaumasite formation. Proceedings of the 6th Durability Building of Materials Conference, Omiya Sonic Complex, Tokyo, Japan, 1993.

Crammond, N.J. and Halliwell, M.A. (1995) Assessment of the conditions required for the thaumasite form of sulfate attack, In: Scrivener, K.L., Young, J.F., editors. Proceedings of the MRS Symposium, Boston, USA, 1995.

Crammond, J.N. (2003) The thaumasite form of sulfate attack in the UK. *Cement and Concrete Composites*, 25: 809–818.

Crammond, N.J., Collette, G.W. and Longworth, T.I. (2003) Thaumasite field trial at Shipston-on-Stour: three-year preliminary assessment of buried concretes. *Cement and Concrete Composites*, 25(8):1035-1043.

Czerewko, M.A. and Cripps, J.C. (2006) Sulfate and sulfide minerals in the UK and their implications for the built environment. Proceeding of the 9<sup>th</sup> Conference of the IAEG, Paper number 121: 1-12.

Czerewko, M.A., Cripps, J.C., Duffell, C.G. and Reid J.M. (2003) The distribution and evaluation of Sulphur species in geological materials and manmade fills. *Cement and Concrete Composites*, 25(8):1025-1034.

Czerewko, M.A., Cripps, J.C., Duffell, C.G. and Reid J.M. (2003) Sulfur species in geological materials-sources and quantification. *Cement and Concrete Composites*, 25(7):657-671.

Delucchi, M., Barbucci, A. and Cerisola, G. (1997) Study of the physico-chemical properties organic coatings for concrete degradation control. *Construction and Building Material*, 11(7–8):365–71.

Descostes, M., Beaucaire, C., Mercier, F., Savoye, S., Sow, J. and Zuddas, P. (2002) Effect of carbonate ions on pyrite (FeS<sub>2</sub>) dissolution. *Bulletin Society Geologies- Franc*, 173(3):265-270.

Diamond, S. and Lee, R.J. (1999) Micro structural alterations associated with sulfate attack in permeable concretes, In: J. Skalny, J. Marchand (Eds.), Material Science of Concrete Sulfate Attack Mechanisms, *American Ceramic Society*, Westerville, D.H, 123-174.

Eden, M.A. (2003) The laboratory investigation of concrete affected by TSA in the UK. *Cement and Concrete Composites*, 25(8):847-850.

Emmanuel, K., Attiogbe, K. and Rizkalla, S.H. (1988) Response off Concrete to sulphuric acid attack. *ACI Material Journal*, 85-M46:481-488.

Erlin, B. and Stark, DC. (1965) *Identification and occurrence of thaumasite in concrete. Symposium on the effects of aggressive fluids in concrete.* Highway Research Record No 11: 108–113.

Escalante-Garcia, J.L. and Sharp, J.H., (2004) The chemical composition and microstructure of hydration products in blended cements. *Cement and Concrete Composites*, 26 (8): 967-976.

Fattuhi, N.I. and Hughes, B.P. (1983) Effect of acid attack on concrete with different admixtures or protective coating. *Cement and Concrete Research*, 13: 655-665.



## References

---

Floyd, M. and Wimpenny, D.E. (2003) Procedures for assessing thaumasite sulphate attack and adjacent ground conditions at buried concrete structures. *Cement and Concrete Composites*, 25(8):1077-1088.

Floyd, M., Czerewko, M.A., Cripps, J.C. and Spears, D.A. (2003) Pyrite oxidation in Lower Lias Clay at concrete highway structures affected by thaumasite, Gloucestershire, UK. *Cement and Concrete Composites*, 25(8):1015-1024.

Fountain, E.J. (2003) The Myth of TSA .BRE international Conference, Sheffield, UK.

Gaze, M.E. and Crammond, N.J. (2000) The formation of thaumasite in a cement: lime: sand mortar exposed to cold magnesium and potassium sulfate solutions. *Cement and Concrete Composites*, 22: 209-222.

Glasser, F.P., Machand, M. and Samson, E. (2008) Durability of Concrete-Degradation Phenomena Involving Detrimental Chemical Reactions, *Cement and Concrete Research*, 38: 226-246.

Gollop, R.S. and Taylor, HFW. (1996) Microstructural and microanalytical studies of sulfate attack Part IV Reactions of a slag cement paste with sodium and magnesium sulfate solutions. *Cement and Concrete Research*, 26 (7):1013-28.

Gorst and Clark. (2003) effect of thaumasite on bond strength of reinforcement in concrete, *cement and concrete composites*. 25: 1089 – 1094.

Grijalvo JA., Blanco-Varela MT., Maroto FP., Sanchez AP. and Moreno TV. (2000) "Thaumasite formation in hydraulic mortars and concretes, In: Malhotra VM, editor. Proceeding Fifth International Conference Durability of Concrete, Barcelona. Spain. *ACI SP*, 19: 1173- 1189.

Hagelia, P., Sibbick, R.G., Crammond, N.J. and Larsen, C.K. (2003) Thaumasite and secondary calcite in some Norwegian concretes. *Cement and Concrete Composites*, 25 (8):1131-1140.

Hagelia, P. and Sibbick, R.G. (2009) Thaumasite Sulfate Attack, Popcorn Calcite Deposition and acid attack in concrete stored at the «Blindtarmen» test site Oslo, from 1952 to 1982. *Material characterization*, 60 (7): 686-699.

Halliwell, M.A., Crammond, N.J. and Barker, A., (1996) *Thaumasite form of sulfate attack in limestone-filled cement mortars*, Building Research Establishment Laboratory Report BR307, Watford, UK, Construction Research Communications Ltd, 1996

Halliwell, M.A. and Crammond, N.J. (2000) *Avoiding the thaumasite form of sulfate attack: two year report* . Building Research Establishment Laboratory Report BR385, Watford, UK, construction Research Communication Ltd, 2000.

Hartshorn, S.A., Sharp, J.H. and Swamy, R.N., (1999) Thaumasite formation in Portland limestone cement pastes, *Cement and Concrete Research*, 29:1331-1340.

Hartshorn, S.A., Sharp, J.H. and Swamy, R.N. (2002) The thaumasite form of sulphate attack in Portland-limestone cement mortars stored in magnesium solution. *Cement and Concrete Composites*, 24(3-4):351-359.

He, R. and Jia, H. (2011) Carbonation Depth Prediction of Concrete Made with Fly Ash. *The Electronic Journal of e-Government*, 16:605-614.

## References

---

- Higgins, D.D. and Crammond, N.J. (2003) Resistance of concrete containing GGBS to the thaumasite form of sulfate attack. *Cement and Concrete Composites*, 25(8):921-929.
- Hill, J., Byars, E.W., Sharp, J.H., Cripps, J.C., Lynsdale, C.J. and Zhou, Q. (2003) An experimental study of combined acid and sulfate attack of concrete. *Cement and Concrete Composites*, 25: 997-1003.
- Hime, G. H., Mather, and Bryant, (1999) Sulfate attack or is it? , *Cement and Concrete Research*, 29:789-791.
- Hobbs, D.W. (2003) Thaumasite sulfate attack in field and laboratory concrete: Implications for specifications. *Cement and Concrete Composites*, 25(8): 921-929.
- Hobbs, D.W. and Taylor, M.G. (2000) Nature of the thaumasite sulphate attack mechanism in field concrete. *Cement and Concrete Research*, 30(4):529-533.
- Irassar, E.F., Maio., A.Di. and Batic, O.R. (1996) Sulfate attack on concrete with mineral admixtures. *Cement and Concrete Research*, 26(1): 113-123.
- Irassar, E.F., Bonavetti, V.L. and Gonzalez, M. (2003) Microstructural study of sulphate attack on ordinary and limestone Portland cements at ambient temperature. *Cement and Concrete Research*, 33(1):31-41.
- Irasser, E.F., Bonavetti, V.L., Trezaa, M.A. and Gonzalez, M.A. (2004) Thaumasite formation in limestone filler cements exposed to sodium sulfate at 20 °C, *Cement and Concrete Composites*, 27 (1):77-84
- Jallad, K.N., Santhanam, M., Menashi, D. and Cohen. (2003) Stability and reactivity of thaumasite at different pH levels. *Cement and Concrete Research*, 33(3):433-437.
- Jenni, A., Mader, U., Lerouge, C., Gaboreau. and Schwyn, B. (2013) In situ interaction between different concrete and Oplinus Clay. *Physics and Chemistry of the Earth*, In press available online 27 November 2013.
- Justnes, H.(2003) Thaumasite formed by sulphate attack on mortar with limestone filler. *Cement and Concrete Composites*, 25(8):955-959.
- Kalousek, G. L., Porter, L.C. and Benton, EJ. (1972) concrete for long-term service in sulfate environment, *Cement and Concrete Research*, 2(1): 79-89.
- Kim, J.P., Lee, S.T., Moon, H. and Hooton, R.D. (2005) Effect of solution concentration and replacement levels of metakaolin on the resistance of mortar exposed to magnesium sulphate solutions. *Cement and Concrete research*, 35(7):1314-1323.
- Kim, S. and Lee, S. (2010) Microstructural observation on deterioration of concrete structure for sewage water treatment. *KSCE Journal of Civil Engineering*, 14(5):753-758.
- Kobayashi, K., Suzuki, K. and Uno, Y. (1994) Carbonation of Concrete Structure and Decomposition of C-S-H. *Cement and Concrete Research*, 24:55-61.
- Kohler, S., Heinz, D. and Urbonas, L., (2006) Effect of ettringite on thaumasite formation. *Cement and Concrete Research*, 36 (4):697-706.
- Kawai, K., Yamaji, S. and Shinmi, T. (2005) Concrete deterioration caused by sulphuric acid attack. 10DMC International Conference on Durability of Building Materials and Components .Lyon, France.

## References

---

- Knights, D.S and Wimpenny, D.E. (2003) Sulfate and chloride profiles and the visual characteristics with depth from the face in buried concrete subject to TSA. BRE international conference, Sheffield.
- Kunther, W., Lothenbach, B. and Scrivener, K. (2013) Influence of bicarbonate ions on the deterioration of mortar bars in sulfate solutions. *Cement and Concrete Research*, 44: 77–86.
- Laboratory Methods Guidelines. (2004) *Appendix 15: Acid Sulfate Soils Laboratory: Methods Guidelines*. Version 2.1. Department of Natural Resources, Mines and Energy, Indooroopilly, Queensland, Australia, June 2004.
- Lawrence, C.D. (1992) The influence of binder type on sulphate resistance. *Cement and Concrete Research*, 22: 1047-58.
- Lea, F.M., (1971) *The chemistry of cement and concrete*, 3'd Edition, chemical publishing Co., New York,
- Lee, S.T., Hooton, R.D., Jung, H. and Choi, C.S. (2008) Effect of limestone filler on the deterioration of mortars and pastes exposed to sulfate solution at ambient temperature. *Cement and Concrete Research*, 38(1):68-76.
- Li, G., Xiong, G., Lu, Y. and Yin, Y. (2009) The physical and chemical effects of long-term sulphuric acid exposure on hybrid modified cement mortar. *Cement and Concrete Composites*, 31(5):325-330.
- Liu, Z., Dehua, D., Schutter, G.D. and Yu, Z. (2013) The effect of MgSO<sub>4</sub> on thaumasite formation. *Cement and Concrete research*, 35 (1): 102-108.
- Longworth, T.I. (2003) Contribution of construction activity to aggressive ground conditions causing the thaumasite form of sulfate attack to concrete in pyritic ground. *Cement and Concrete Composites*, 25(8):1005-1013.
- Loudon, N. (2003) A review of the experience of thaumasite sulphate attack by the UK Highways Agency. *Cement and Concrete Composites*, 25(8):1051-1058.
- Ma, B., Gao, X., Byars, E.A. and Zhou. (2006) Thaumasite formation in tunnel of Bapanixa dam in western China. *Cement and Concrete Research*, 36(4):716-722.
- Ma, B., Luo, Z., Li, X., Gao, X. and Wang, K. (2008) physical and chemical simulation of the thaumasite form of sulphate attack on concrete. 1<sup>st</sup> International Conference on Microstructure Related of Cementitious Composites, RILEM proceeding. 61: 1093-1101
- Marusin, S. L. (1987) Improvement of concrete durability against intrusion of chloride-laden water by using sealers, coatings and various admixtures. *ACI Special Publication*, 100: 599-620.
- Mather, K. (1980) Factors affecting sulfate resistance of mortars, Proceedings, 7<sup>th</sup> international Congress on chemistry of cement, Editions Septima, Paris, 4: 580-585
- Mather, B. (1969) *Sulfate soundness, sulfate attack and expansive cement*, Preliminary report, International symposium on durability of concrete, Technical University, Prague building research institute, 1969, Part 2: C-209-C-220.
- Mather, B. (1968) *Field and laboratory studies of the sulphate resistance of concrete*, Performance of concrete, University of Toronto press, 1968: 67-76
- Mather, B. (1966) *Effect of seawater on concrete*, Highway Research Board, No. 113: 33-42

## References

---

- Mather, B. (1984) Discussion of theories of expansion in sulfoaluminate - type expansion cements: Schools of thought, *Cement and Concrete Research*, 14: 603-609.
- McPolin, D.O., Basheer, P.A. and Long, A.E. (2009), Carbonation and pH in Mortars Manufactured with Supplementary Cementitious Materials. *Journal of Materials in Civil Engineering*, 21(5), 217–225.
- Monteny, J., Vincke, E., Beeldens, A., Belie, N.D., Taerwe, L., Gemert, D.V. and Verstraete, W. (2000) Chemical, microbiological, and in situ test method for biogenic sulphuric acid corrosion of concrete. *Cement and Concrete Research*, 30(4)623-634.
- Moradillo, M.K., Shekarchi, M. and Hoseini, M. (2012) Time-dependent performance of concrete surface coatings in tidal zone of marine environment. *Construction and Building Materials*. 30: 198–205.
- Mulenga, D. M., Stark, J. and Nobst, P. (2003) Thaumassite formation in concrete and mortars containing fly ash, *Cement and Concrete Composites*, 25: 907-9 12
- Newman, J. and Choo, B.S. (2003) *Advanced Concrete Technology*. Butterworth-Heinemann. An imprint of Elsevier,UK
- Nijad,I., Fattuhi. and Hughes, B.P. (1988) Ordinary Portland cement mixes with selected admixtures subjected to sulphuric acid attack. *ACI Material Journal*, 85-M50:512-518.
- Nixon, P.J., Longworth, T.I. and Matthwes, D.J. (2003) New UK guidance on the use of concrete in aggressive ground. *Cement and Concrete Composites*, 25(8):1177-1148.
- Nobst, P. and Strak, J. (2003) Investigation on the influence of cement type on thaumasite formation. *Cement and Concrete Composites*, 25(8):899-906.
- Pipilikaki, P., Papageorgiou, D., Teas, Ch., Chaniotakis, E. and Katsioti, M. (2008) The effect of temperature on thaumasite formation. *Cement and Concrete Composites*, 30(8): 964-969.
- Pouya, H.S. (2007) *Thaumasite Sulfate Attack (TSA) of Concrete in Aggressive Ground at Different Temperatures*, PhD Thesis, Faculty of Engineering. The University of Sheffield, July, 2007.
- Quispel,A., Harmsen, S.W. and Otzen, D. (1952) Contribution to the chemical and bacteriological oxidation of pyrite soil. *Plant and Soil*, IV (1):43-55.
- Rasanen, V. and Penttala, V. (2003) The pH measurement of concrete and smoothing mortar using a concrete powder suspension, *Cement and Concrete Research*, (34):813-820.
- Reid, J.M., Czerewko, M.A., and Cripps J.C. (2005) *Sulfate specification for structural backfills*. TRL Report 447, TRL Limited, Crowthorne.
- Rendell, F., Jauberthie, R. and Granthm. M. (2002) *Deteriorated concrete: Inspection and physicochemical analysis*. London: Thomas Telford.
- Rojas, M., Sotolongo, R., Frias, M., Marin, F., Julian, R. and Sabador, E. (2008) Decay of pavement mortar due to thaumasite formation. *Journal of Chemical Technology & Biotechnology*, 84(3):320-325.
- Romer, M., Holzer, L. and Pfiffner, M. (2003) Swiss tunnel structures: concrete damage by formation of thaumasite. *Cement and Concrete Composites*.25 (8):1111-1117

## References

---

- Sahu, S., Badger, S. and Thaulow. (2002) Mechanism of thaumasite formation in concrete", In: Firth International Conference on Thaumasite in Cementitious Materials, June, 2002, UK
- Saraswathy, V. and Rangaswamy, N. S. (1998) Adhesion of an acrylic pain coating to a concrete substrate - some observations, *Journal of Adhesion Science and Technology*, 12 (7): 681-694.
- Schmidt Th., Lothenbach B., Romer M., Scrivener K., Rentsch D. and Figi R. (2008) A thermodynamic and experimental study of the conditions of thaumasite formation. *Cement and Concrete Research*, 38: 337-349
- Schneider, S. (2011) *Collecting Fluorescent Minerals*, 2<sup>nd</sup> edition, Schiffer Pub Limited, Atglen, USA.
- Schoonen, M., Elsetinow, A., Borda, M. and Strongin, D. (2000) Effect of temperature and illumination on pyrite oxidation between pH 2 and 6. *Geochemical Transactions*, 1:23-33.
- Scrivener, K., Rentsch, D. and Figi, R. (2007) A thermodynamic and experimental study of the conditions of thaumasite formation. *Cement and Concrete Research*, 38(3):337-349.
- Sibbick, T., Fenn, D. and Crammond, N, (2003) The occurrence of thaumasite as a product of seawater attack. *Cement and Concrete Composites*, 25 (8):1059-1066
- Skalny, J., Marchand, J. and Odler, I. (2002) *Sulfate Attack on Concrete*. New York: Spoon press.
- Slater, D., Floyd, M. and Wimpenny, D.E. (2003) A summary of the Highway Agency thaumasite investigation in Gloucestershire: the scope of work and main findings. *Cement and Concrete Composites*, 25(8):1067-1076.
- Sotiriadis, K., Nikolopoulou, E. and Tsivilis, (2010) The effect of chloride on thaumasite form of sulphate attack in limestone cement concrete. *Material Science Forum*. 636-637: 1349-1354.
- Sotiriadis, K., Nikolopoulou, E. and Tsivilis. (2012) Sulfate resistance of limestone cement concrete exposed to combined chloride and sulfate environment at low temperature. *Cement and Concrete Composites*, 34(8): 903-910.
- Sotiriadis, K., Nikolopoulou, E., Tsivilis, S., Pavlou, A., Chaniotakis, E. and swamy, R.N. (2013) The effect of chlorides on thaumasite form of sulfate attack of limestone cement concrete containing mineral admixtures at low temperature. *Construction and Building Materials*, 43:156-164.
- Suzuki, K., Nishikawa, T. and ITO, S. (1985) Formation and carbonation of C-S-H. *Cement and Concrete Research*, 15:213-224.
- Suzuki, K., Kobayashi, K. and Uno, Y. (1994) Carbonation of concrete structure and decomposition of C-S-H. *Cement and Concrete Research*, 24:55-61.
- Swamy R.N. and Tanikawa, S. (1993) An external surface coating to protect concrete and steel from aggressive environments. *Material and Structures*, 26:465-78.
- Swamy, R.N., Suryavanshi, A.K. and Tanikawa, S. (1998) Protective ability of an acrylic-based surface coating system against chloride and carbonation penetration into concrete. *ACI Materials Journal*, 95: 101-112.

## References

---

- Taylor, H.F.W., *Cement Chemistry*. 2<sup>nd</sup> edition, Thomas Telford, New York, USA, pp.10-11, 1997
- Thomas, M.D.A., Bleszynski, R.F. and Scott CE. (2001) Sulfate attack in a marine environment .In J. Maracha and J. Skalny (eds) Materials Science of Concrete Special Volume Mechanisms of Sulfate Attack, *The American Ceramics Society*. Westerville, 301-313.
- Thomas, M.D.A., Rogers, CA. and Bleszynski, R.F. (2003) Occurrences of thaumasite in laboratory and field concrete, *Cement and Concrete Composites*, 25(8): 1045-1050.
- Tian, B. and Cohen M.D. (2000) Does gypsum formation during sulfate attack on concrete lead to expansion?, *Cement and Concrete Research*, 30: 117–123.
- Tsivilis,S., Kakali, A., Skaropolou, A., Sharp, J.H. and Swamy, R.N, (2003) Use of mineral admixtures to prevent thaumasite formation in limestone cement mortar. *Cement and Concrete Composites*, 25(8):969-976.
- Tsivilis S., Sortiriadis, K. and Skaropoulou, A. (2007) Thaumasite form of sulfate attack (TSA) in limestone cement pastes. *Journal of the European Ceramic Society*, 27 (2-3):1711-1714.
- Torres, S.M., Sharp, J.H., Swamy, R.N., Lynsdale, C.J. and Huntley, S.A. (2003) Long term durability in Portland-limestone cement mortars stored in magnesium sulfate solution, *Cement and Concrete Composites*, 25: 947– 954
- Torres, S.M. (2004) *The influence of chloride on thaumasite form of sulphate attack in mortar containing calcium carbonate*, PhD Thesis, Faculty of Engineering, The University of Sheffield, UK, 2004.
- Torres, S.M., Lynsdale, C.J., Swamy, R.N. and Sharp, J.H. (2006) Microstructure of 5-years-old mortars containing limestone filler damaged by thaumasite. *Cement and Concrete Research*, 36: 384 – 394.
- Tulliani, J.M., Montanaro., Negro, A. and Collepardi, M. (2002) Sulfate attack of concrete building foundations induced by sewage waters. *Cement and Concrete Research*, 32(6):843-849.
- Van A. and Visser, S. (1975) Thaumasite formation: a cause of deterioration of Portland cement and related substances, in the presence of sulfates, *Cement and Concrete Research*, 5:225-232.
- Varela, M.T., Aguilera, J. and Ramirez, S.M. (2006) Effect of cement C<sub>3</sub>A content, temperature and storage medium on thaumasite formation in carbonated mortars. *Cement and Concrete Research*, 36(8):707-715.
- Vera, R., Apablaza, J. and M. Vera, C.E. (2013) Effect of Surface Coatings in the Corrosion of Reinforced Concrete in Acid Environments. *International Journal of Electrochemical Science*, 8: 11832-11846.
- Wimpenny, D. and Slater, D. (2003) Evidence from the highways agency thaumasite investigation in Gloucestershire to support or contradict postulated mechanisms of thaumasite formation (TF) and thaumasite sulfate attack (TSA). *Cement and Concrete Composites*, 25(8):879-888.



## *References*

---

Zhou, Q., Hill, J., Byars, E.W., Lynsdale, C.J., Cripps, J.C. and Sharp, J.H. (2006) Relative resistance of Portland and pozzolanic cements to thaumasite form of sulfate attack (TSA). BRE international Conference, Sheffield, UK.

Zhou, Q., Hill, J., Byars, E.W., Lynsdale, C.J. and Sharp, J.H. (2006) The role of pH in thaumasite sulfate attack. *Cement and Concrete Research*, 36: 160 – 170.

Zivica, V. and Bajza, A. (2001) Acidic attack of cement based materials-A review. Part 1. Principle of acidic attack. *Construction and Building Materials*, 15(8):331-340